STUDIES IN

MARINE NATURAL PRODUCTS

A thesis

submitted in partial fulfilment

of the requirements for the degree

of

Doctor of Philosophy in Chemistry

at the

University of Canterbury

by

Warren J. MacLean

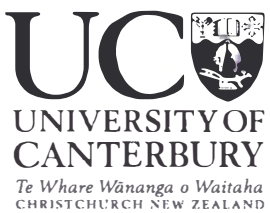

University of Canterbury

Christchurch, New Zealand

November 2005

ABSTRACT

The marine environment continues to be a prolific source of structurally diverse and biologically active natural products. Over the past few decades both macro- and micro-organisms have been extensively studied for such compounds. Annual reviews are dominated by novel compounds isolated from marine sponges, even though investigations have more recently been focused on micro-organisms. After decades of research into the development of marine natural products as potential pharmaceuticals, many marine compounds now feature prominently in current pre-clinical and clinical trials. This thesis represents a continuation of work in the area of isolation and structural elucidation of novel and/or biologically active natural products from both marine macro- and micro-organisms.

The four novel C_{31} polyacetylenic compounds **2.23**, **2.24**, **2.25** and **2.26** were isolated as the major components of the cytotoxic extract of the New Zealand marine sponge *Rhabderemia stelletta*, using bioassay-guided separation techniques. However, these structures were not unambiguously assigned due to the low resolution of the NMR signals associated with the long-chain alkyl protons and carbons. Elucidation was also hindered by compound degradation during structural analysis. The partial structures were identified *via* mass spectrometry and NMR spectroscopy and comparison of structural data for similar compounds reported in the literature.

The novel pteridines **3.13** and **3.15** were isolated as the major and minor components, respectively, from the cytotoxic organic extract of an as yet unidentified Antarctic marine sponge 02WM01-33. Identification was achieved using mass spectrometry and NMR spectroscopy, and comparison of these data to those published in the literature for similar structures. Although pteridines are distributed widely throughout nature, **3.13** and **3.15** represent a chemically interesting group of compounds as they possess a mono-oxygenated methyl side chain, which has not been previously reported among any of the naturally occurring pteridines.

The novel hydantoin compound **4.8** was isolated as the major biologically active component of the organic extract of the Antarctic marine sponge *Suberites* sp. using microtitre plate P388 assay guided fractionation. The relative stereochemistry of **4.8** was determined using 1D-NOESY experimental data. This work represents the first isolation of the hydantoin **4.8** as a natural product from a marine sponge. This compound has been reported previously in the literature, but only as a synthetic product.

The two novel anthraquinone compounds **5.35** and **5.41** were isolated as minor components of the cytotoxic organic extract of the Antarctic marine sponge-derived fungus *Aspergillus* sp., along with the three known anthraquinones **5.32**, **5.34** and **5.40**. This series of work revealed several areas in the literature that require revising: these include, (i) the compounds **5.31** and **5.41** were both reported as a new metabolites in 1985 and 2003, respectively, however, both compounds had been previously isolated and reported in 1966; (ii) the compound **5.36** requires the correct structural assignment in the literature; and finally, (iii) the compound **5.35** has two isomeric structures reported in the AntiMarin database, however, neither of these structures match the experimental ^{1}H NMR data supplied by the author of the database.

The three novel compounds **6.9**, **6.13** and **6.15** were isolated from the organic extract of an Antarctic marine sponge-derived fungus *Ulocladuim* sp., along with the previously reported compounds **6.6**, **6.7** and **6.16**. These compounds were

identified using NMR spectroscopy and mass spectrometry. This work highlights an inconsistency in the literature regarding the structural assignment of two carbons for the known compound **6.16**. The structural assignment of these carbons was confirmed by the independent isolation of **6.16** by another member of the Marine Group.

ACKNOWLEDGEMENTS

First and foremost I must extend my gratitude to my supervisors, Professors Murray Munro and John Blunt, for their guidance, support and encouragement throughout my years of study in the Marine Group.

Recognition must go to Gill Ellis for all of her expert help in sample identification and storage of samples collected in Antarctica, not to mention the hundreds of biological assays run on sample extracts.

Thanks to the technical staff of the Chemistry department which include; Bruce Clarke for mass spectrometry, the lads in the mechanical workshop for their help from time to time. Rob McGregor for his glassblowing skills and the multi talented attributes of Wayne Mackay.

Thanks must go to Nic Cummings of the School of Biological Sciences Department for work relating to the culturing of fungal samples.

Many thanks to the team at the Australian Institute of Marine Sciences (AIMS) and PharmaMar, for the opportunity to travel to Antarctica as a member of K059. To Nicole Webster, Andrew Negri, Carsten Wolff, Chris Battershill, Ren Naylor, James Monkovitch and Steve Mercer, thanks for the deep water sponge, fungal and bacterial samples that set me free and the chance to get naked and wet under the ice.

Thanks to the past and present members of the marine group, Scott Bringans, Tim Harwood, Annabel Murphy, Marie Squire, Sonia van der Sar, Dr Sylvia Urban, your help has been greatly appreciated, above all Dr Sean 'seabass' Devenish for his expert advice during many late night structural elucidation sessions, and for an

extra pair of hands when surgery was required on the HPLC. Also, for running additional mass spectrometry and of course most importantly, helping to develop the 'weapon of mass destruction' (patent pending) not to mention the high jinks that made life bearable. I could not have asked for a better lab buddy, you have helped me along through my PhD journey more than you can imagine.....cheers! A special thank you must also go to Sarah Hickford and her 'eagle eyes' for proof reading this thesis in preparation for its submission.

Thanks to PharmaMar for financial support through the first few years of my PhD, and to Southern Gas Services Ltd for financial support during the final years of my PhD.

Thanks to David Mcdonald, Nicolas Heaphy and all the other people that have long since left, this list would be far too long to write out in full, thank you for the opportunity of getting to know you.

To my dearly departed Grandma, who never quite understood what I did at University but took great pleasure at showing me off to her closest friends, sorry you didn't get to see me graduate, but I know you'll be watching from your lazy boy in the sky.

Finally, to my wife Melissa, your support, patience strength and understanding have made my long years of study at Canterbury University a pleasure. Your amazing adaptive ability never ceases to amaze me. Thank you for your continued love and support.

TABLE OF CONTENTS

LIST OF TABLES

LIST OF FIGURES

LIST OF ISOLATION SCHEMES

ABBREVIATIONS

1D	one dimensional
2D	two dimensional
AIDS	Aquired Immunodefficiency Syndrome
AIMS	Australian Institute of Marine Science
br	broad (spectral)
°C	degrees Celcius
C_{18}	octadecyl-phase (chromatography column packing)
calc	calculated
CD_3OD	deuterated Methanol
$CDCl_3$	deutrated chloroform
CH_3CN	acetonitrile
CI	chemical ionization (mass spectrometry)
CIGAR	constant time inverse-detected gradient accordion rescaled long-range heteronuclear multiple bond correlation (in NMR)
COSY	^1H-^1H correlation spectroscopy (in NMR)
CoV	Coronavirus
δ	chemical shift in parts per million from deuterated solvent
d	doublet (spectral)
DBE	double bond equivalents
DCM	dichloromethane
DIOL	dialcohol-phase (chromatography column packing)
DNA	deoxyribonucleic acid
DMSO	dimethyl sulfoxide
ELSD	evaporative light scattering detector
EtOAc	ethyl acetate
FDA	United States Food and Drug Administration
g	gram
H_2O	water (distilled)
HAART	highly active antiretroviral therapy

HIV	Human Immunodefficiency Virus
HMBC	heteronuclear multiple bond coherence (in NMR)
HPLC	high-performance liquid chromatography
HREIMS	high-resolution electron impact mass spectrometry
HRESMS	high-resolution electron spray mass spectrometry
HSQC	heteronuclear single quantum coherence (in NMR)
Hz	hertz
IC_{50}	concentration of sample required to inhibit the P388 cell growth by 50 %
J	coupling constant (in NMR)
L	litre(s)
LCESI	liquid chromatography electrospray ionization (mass spectrometry)
λ_{max}	maximum wavelength
m	multiplet (in NMR)
Me	methyl
MeOH	methanol
mg	milligram
MHz	megahertz
min	minute(s)
mL	milliliter(s)
MS	mass spectrometry
m/z	mass to charge ratio (mass spectrometry)
NCI	National Cancer Institute
ng	nanogram(s)
nm	nanometers (wavelength)
NMR	nuclear magnetic resonance
NOE	nuclear Overhauser effect
NOESY	nuclear Overhauser effect spectroscopy
P388 Assay	Murine leukaemia cells
PDA	photo diode array (in chromatography)
ppm	parts per million
q	quartet (spectral)
RAPD	random amplified polymorphic DNA
rDNA	ribosomal DNA

RFLP	restriction fragment length polymorphism
ROESY	rotating frame Overhauser enhancement spectroscopy
RT	retention time
s	singlet (spectral)
SARS	Severe Acute Respiratory Syndrome
SDY	Sabouraud Dextrose Yeast
t	triplet (in NMR)
TFA	trifluoroacetic acid
TLC	thin layer chromatography
TOCSY	total correlation spectroscopy
TMS	trimethylsilane
UV	ultra violet
μ	micro
WHO	World Health Organisation

CHAPTER 1

INTRODUCTION

1.1: Introduction

Ancient human civilizations relied on nature to provide the resources essential for survival. This is still as true now as it was thousands of years ago. Our continued existence has undoubtedly hinged on the ability to recognise that extracts from surrounding flora could be used to treat ailments that, if left untreated, would certainly prove fatal. It is upon this foundation that modern medicine has been built, and today we see that natural products still constitute a large portion of the drugs currently in use or undergoing clinical trials. Unfortunately, due to the stringent testing procedures, toxicity and supply requirements, most biologically active natural products do not see the inside of a medicine cabinet. However, many of these 'failed' compounds provide useful pharmacological information, especially if they have a novel mode of action, often resulting in their use as lead structures in the development of alternative compounds that may someday be used as medicinal agents.

1.2: What are Natural Products?

Naturally occurring compounds can be divided into two major classes: primary and secondary metabolites. Primary metabolic production pathways for

carbohydrates, proteins and nucleic acids are shared by all organisms. It is at the secondary metabolite, or natural product, production level that differences appear which are unique to a specific species. One such example is morphine (**1.1**), which occurs in just two species of poppy, *Papaver somniferum* and *P. setigerumoccurs.*[1]

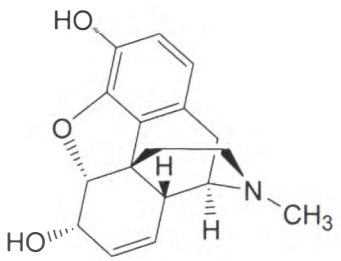

1.1

Williams *et al.*[2] defined a natural product as an organic compound that has "no explicit role in the internal economy of the organism that produces it." However, the argument was extended by noting that the existence of natural products in an organism serve to increase its survival fitness, and hence gain a competitive edge in its environment.

The biological activity of these natural products can be seen as having a protective role in the organism: protection from predation, overgrowth by fouling organisms and from infection by micro-organisms. This was supported by the observation that many organisms produce natural products under some kind of stress.[3] It was also noted by Williams *et al.* that biologically active natural products are sparse in organisms that possess an immune system and are common in those that do not.[2] This would imply that biologically active natural products play an important role in the chemical defense of organisms lacking a fully developed immune system (e.g. sponges). It also seems that natural products evolved under the pressure of natural selection as some of the biologically active natural products isolated to date interact directly with specific receptors unique to the predator/competitor. One such example is the family of cone snail venoms the conotoxins, which are highly selective peptide antagonists or agonists of ligand- or voltage-gated ion channels.[4]

1.3: Some Famous Natural Products

Uses for the bark of the willow tree (*Cortex salicis*), which was well known for its antipyretic and analgesic properties, date back to around 400 BC. It was used for thousands of years until the main bioactive principle, salicin (**1.2**), was identified. Degradation studies were undertaken in an effort to reduce the associated side effects of salicin (**1.2**). As a result of this research, both salicylic acid (**1.3**) and its acetyl derivative, acetylsalicylic acid (**1.4**), were discovered. Less than two years after its synthesis, acetylsalicylic acid (**1.4**) was marketed under the name Aspirin®, which without a doubt has to be one of the most famous and commonly available synthetic drugs worldwide.[5]

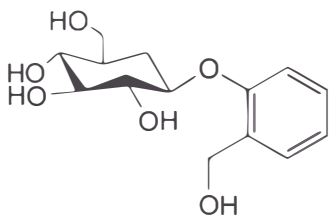

1.2

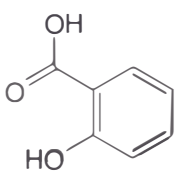

1.3

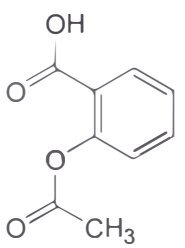

1.4

In sharp contrast, the natural product Taxol® (paclitaxel (**1.5**)), an anti-tumour agent currently in clinical use, was isolated from the bark of the yew tree *Taxus brevifolia* in 1971.[5] Unfortunately, its success was dependent upon securing enough of the active compound. It took years to develop a semi-synthetic analog (docetaxel (**1.6**)) which was derived from a renewable resource. In this case, this was the needles of the related yew tree *Taxus baccata*, which contained several precursors (the baccatins)[5] required for the total synthesis of docetaxel (**1.6**).

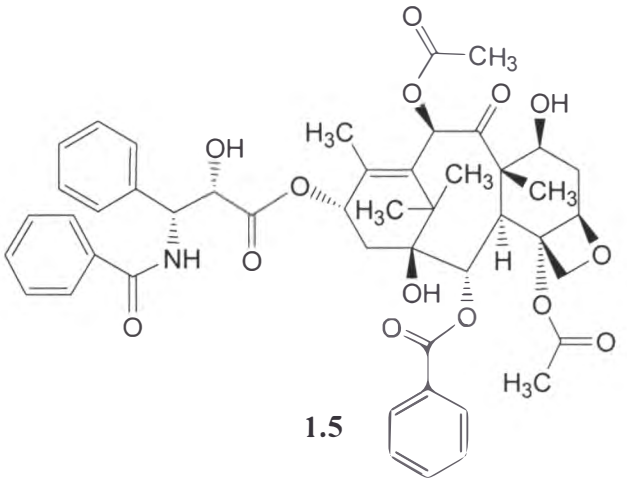

1.5

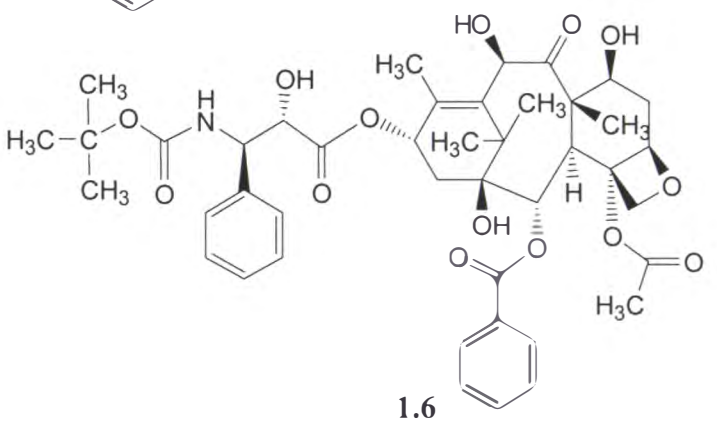

1.6

The antimalarial agent quinine (**1.7**) is obtained solely from the *Cinchona* tree, and was introduced into medicinal use in Europe in 1640.[6] However, it was not until 1824 that large-scale production started in Germany, and many more years passed before the total synthesis of quinine (**1.7**) was achieved by Woodward and Doering in 1945.[7] The disease malaria remains rampant in many countries despite many decades of research and development of antimalarial drugs. The World Health Organisation (WHO) estimates that approximately 40 % of the world's population are infected, with 300 to 500 million new cases reported each year.[6] Malaria claims between 1.5 and 2.7 million lives annually, mostly children.[6,8] Currently, the preferred treatment centres around the use of drugs that utilize a combined mode of action, in an attempt to inhibit the further emergence and spread of parasites resistant to one component of the combination.[8]

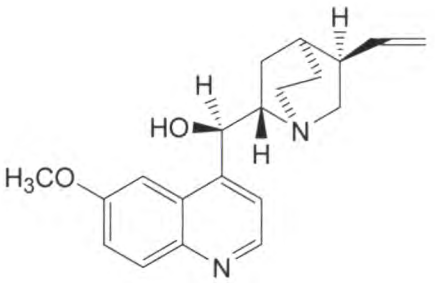

1.7

The earliest reported observation indicating that the fungus *Penicillium* sp. displayed antibacterial activity was described by Tyndall in 1896.[9] During that same year, small amounts of an antibacterial substance were isolated in crystalline form by Gosio.[10] This compound was subsequently confirmed to be mycophenolic acid (**1.8**).[10] Reports describing antibacterial properties of fungi continued to surface throughout the late 1800's and early 1900's, the pinnacle of which was the historical work published by Fleming in 1929 describing the effects of *Penicillium notatum* on bacteria.[11] It was not until the early 1940's, however, when a group of scientists at Oxford began investigating the use of penicillin (e.g. Penicillin G (**1.9**)) for human treatment, that the full potential of Sir Alexander Fleming's work was appreciated.[11]

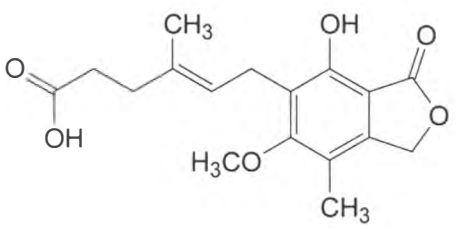

1.8

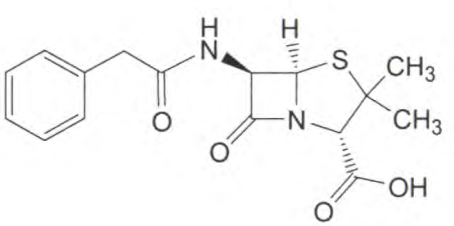

1.9

Fleming's work demonstrated the enormous potential that micro-organisms possessed. Their ability to biosynthesize antibacterial compounds that were suitable for incorporation into human therapeutics began a new era in drug discovery. The focus shifted from terrestrial fungi around 1945 in an effort to solve a serious clinical problem, the emergence of benzylpenicillin resistant S*taphylococci.* At this point, investigations into marine microbes began after it was observed that sewage outfalls displayed some degree of antibiotic activity as

they underwent a process of 'self purification'. As a direct result, a fungal isolate was obtained, yielding the penicillin related β-lactam antibiotic cephalosporin C (**1.10**).[11] Although actinomycetes remained the focus for several years, fungal isolates still remained a prolific source of antibiotics. The cyclic peptide cyclosporin A (**1.11**) was isolated from the fungus *Tolypocladium inflatum* in 1976.[10] Cyclosporin A (**1.11**) was initially isolated on the basis of its ability to inhibit fungal growth. However, it was also shown to have marked immunomodulatory properties, and is currently used as an immunosuppressant to prevent rejection of organs following transplant operations.[12]

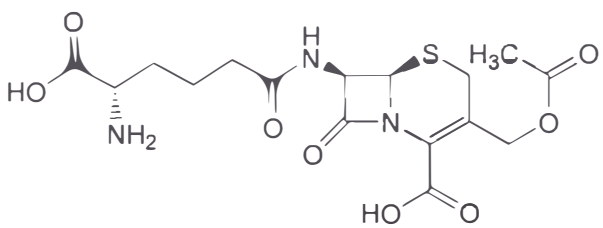

1.10

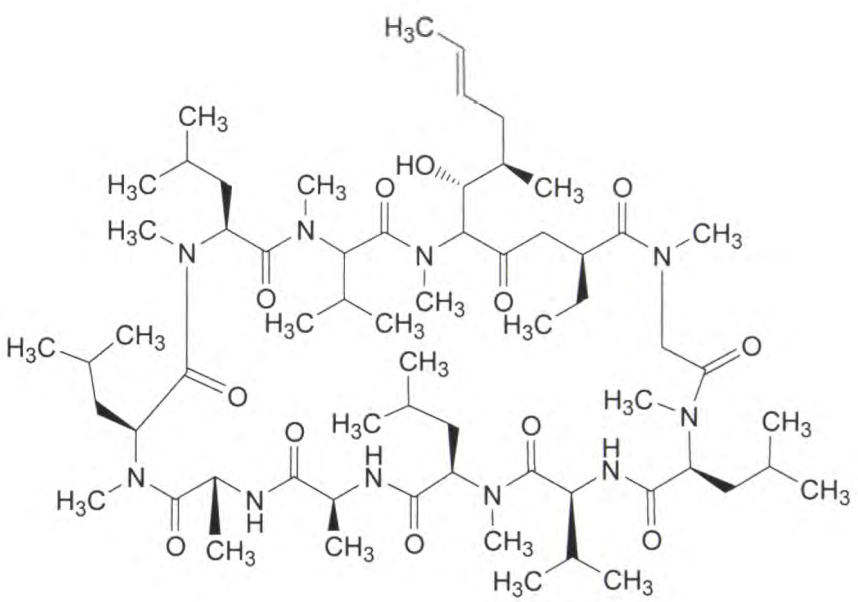

1.11

Today, the β-lactam antibiotics account for over 65 % of the world's antibiotic market and represent a $US 15 billion industry per annum.[13] The need for new β-lactam antibiotics remains set to continue, due to the ongoing emergence of resistant bacterial pathogens.

1.4: Why Search the Marine Environment?

The marine environment represents an enormously diverse ecosystem, covering more that 70 % of the planet's surface. Life has its origins in the oceans, and it is estimated that some of these ecosystems (coral reefs) have a biological diversity higher than that of a tropical rain forest. Current estimations predict the existence of 30 marine phyla, constituting 5,000,000 species of marine organisms.[14] Due to variations in environmental factors such as temperature, turbidity and nutrient flow, all marine animals, plants and micro-organisms are expected to produce entirely different metabolites to those observed in a terrestrial environment. The biomedical potential of the ocean has been known for thousands of years. Ancient civilizations from China, India and Japan have made use of seaweed, seashells and often parts of marine organisms for medicinal preparations. We are perhaps more aware of terrestrial plants and animals that have provided medicinally useful natural products, as this is the environment that mankind has evolved in, rather than those with marine origin. However, we must consider that the molecular physiology of eukaryotic cells evolved in our early marine ancestors.[4] Most of the marine natural products described to date possess unique chemical structures that have no terrestrial counterparts, and frequently exhibit interesting biological activity.[15]

The survival of an individual organism within this marine ecosystem is dependent upon the organism's ability to defend a unique niche in which they can thrive. This, combined with the fact that many of these marine organisms are soft bodied, slow moving or sessile, has most likely contributed to the organism's evolution towards the exceptional ability to either synthesize potent and structurally complex secondary metabolites, or form symbiotic relationships with bacteria or fungi that produce these toxic compounds, as a direct means of defense against spatial competition and predation.[4] The high potency of these compounds may be a direct consequence of the need to overcome rapid dilution on release into the water, in order to exert the desired effect, or be potent enough to deter pretators with minimum structural damage.[4]

Since the birth of marine chemistry in the mid-sixties, the number of reported metabolites isolated from the marine environment has steadily increased (**Figure 1.1**). This increase can be attributed to both improvements in technologies associated with sample collection and compound isolation/elucidation, and increased interest in this field of research.

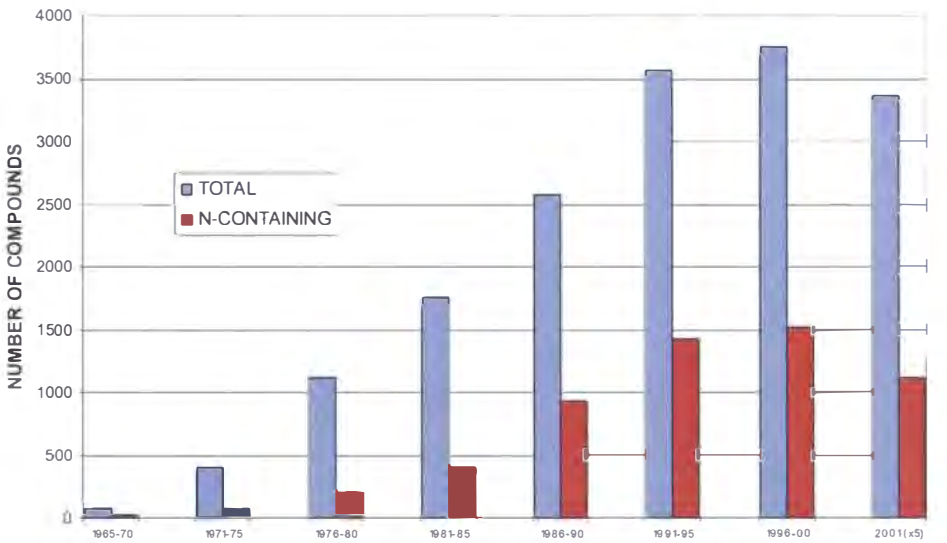

Figure 1.1: The total number of marine natural products isolated from 1965 onwards.[16]

Data presented by Dr Peter Murphy at the National Cancer Institute (NCI) revealed that, when the incidence of biological activity of all the known marine natural products isolated were compared across phyla, sponges were the most prevalent source.[17]

Data reviewing marine natural product isolations from 2000 to the present day indicates that this trend seems set to continue, as sponges still remain one of the most dominant sources of biologically active natural products (**Figure 1.2**), followed by coelenterates, when activity was compared across Phyla.[16,18-21] Sponge statistics may have been biased however, because of their prevalence, ease of collection, and ability to biosynthesize a variety of natural product structural classes. More recently, a greater interest in micro-organisms has seen an associated increase in the number of compounds isolated, and this phylum is proving to be a rich source of novel/biologically active natural products. This

phenomenon could also possibly be attributed to the accelerating advances in marine biotechnology.[21]

Sponge biodiversity is known to be at its highest in the tropical regions, concentrated in the region of Papua New Guinea and radiating concentrically outwards.[22] Generally, it has been accepted that species diversity differs with latitude. The polar regions are typically characterised by high abundance and low diversity, while tropical zones are characterised by low abundance but high diversity.[22] Tropical regions have predominantly been the focus of collection efforts, possibly due to high species diversity. It is widely accepted that species diversity infers chemical diversity.

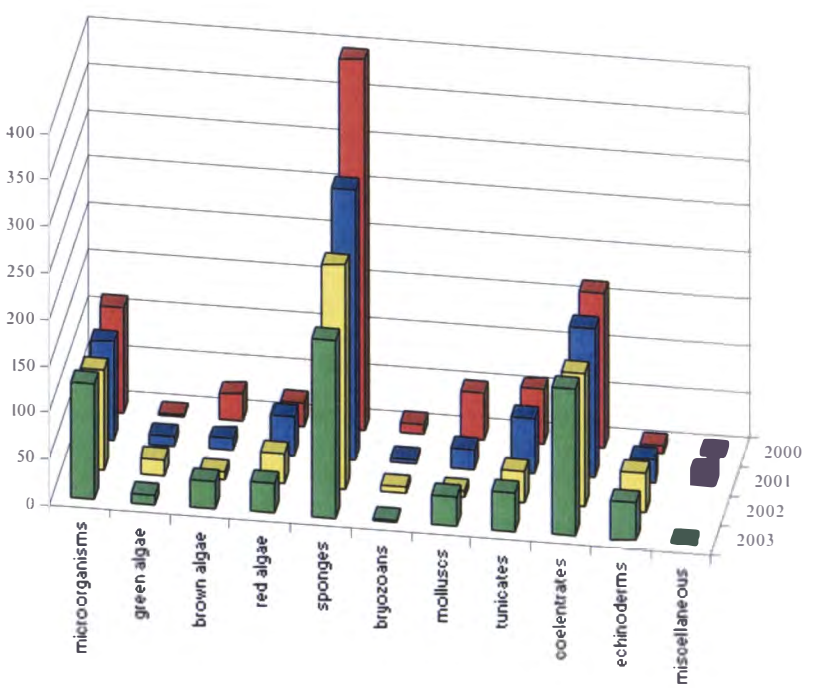

Figure 1.2: Distribution of novel active and non-active marine natural products by phylum for 2000 – 2003. Adapted from Faulkner *et al.*[20,21] and Blunt *et al.*[16,18,19]

1.5: Recent Advances in the Discovery of Biologically Active Natural Products

The main challenge for the natural product prospector is to be able to identify particular compounds containing desirable biological activity characteristics. This is necessary if a compound is to be considered as a potential candidate for pharmaceutical development. Historically, the biological activities of compounds from terrestrial sources were evaluated by a process of trial and error by native peoples. Compounds that possessed undesirable side effects or no longer displayed biological activity were discontinued from use in traditional medicines. More recently, during the 70's, compounds that were not antimicrobial were tested using animal models and cell-based assays. Today, elaborate high throughput screening programs have allowed tens of thousands of extracts to be routinely assessed for biological activity with the use of highly automated robotics. In industry, new assays are developed at a rate of one every six months, utilizing different target enzymes or receptors. When these assays are developed, all of the pure compounds held in the current library are evaluated. This process continues as new assays are developed. The high throughput assay is a mechanism-based assay system targeting drug candidates that display specific and selective activity. The need for excessive processing of the crude extract (solvent partitioning, semi-purification) is not necessary as the mechanism-based assay is more robust than the cell-based assays.[23] Ecological impacts are also reduced due to the need for a minimal quantity of extract as a result of increased sensitivity of the mechanism-based assay.[23] Although the high throughput assay system has its place in drug discovery, it is highly specific and restricts the selection of activity that a normal cell-based assay would identify. It is up to the natural product chemist to not only identify compounds that are structurally novel, but those that are mechanistically novel as well.

1.6: Why Continue Prospecting for Biologically Active Natural Products?

The need for new therapeutics is always expanding. Many diseases are becoming a growing health concern, as classical treatments are no longer effective with the development of multi-drug resistance.[24] This, combined with the emergence of new diseases, has resulted in an immense financial burden for both the individual and society. For the pharmaceutical and biotechnology industry, it represents a major market opportunity; for chemists it represents an enormous challenge. Therefore, the need for new drug leads that can be developed into new therapeutics is paramount.

Since the discovery of antibiotics in the first half of the twentieth century, the emergence of antibiotic resistant bacteria has left the scientific community ill prepared. This acquired resistance has spread rapidly, and treatment of infections caused by *Staphylococcus aureus* and other strains of resistant bacteria has become challenging. Vancomycin (**1.12**), the antibiotic of last resort for the treatment of *S. aureus* infections, has with increasing frequency also been rendered ineffective in recent years. Clearly, the continuing development of new and effective classes of antibiotic pharmaceuticals must keep pace with the ever-evolving antibiotic resistant bacteria. Daptomycin (**1.13**), a cyclic lipopeptide, is one such example, isolated from the fermentation broth of *Streptomyces roseosporus*.[24] The precise mechanism of action is not entirely understood, however calcium-dependent insertion of the 'lipid tail' into the cytoplasmic membrane plays an important role. Daptomycin (**1.13**) displays a wide spectrum of *in vitro* activity against a variety of Gram-positive organisms, including multi-drug resistant strains of *Staphylococcus*, *Streptococcus* and *Enterococcus*, and was released onto the market in mid 2004 after approval from the United States Food and Drug Administration (FDA). Daptomycin (**1.13**) represents the first lipopeptide approved for use in the treatment of complicated skin and soft tissue infections.[25]

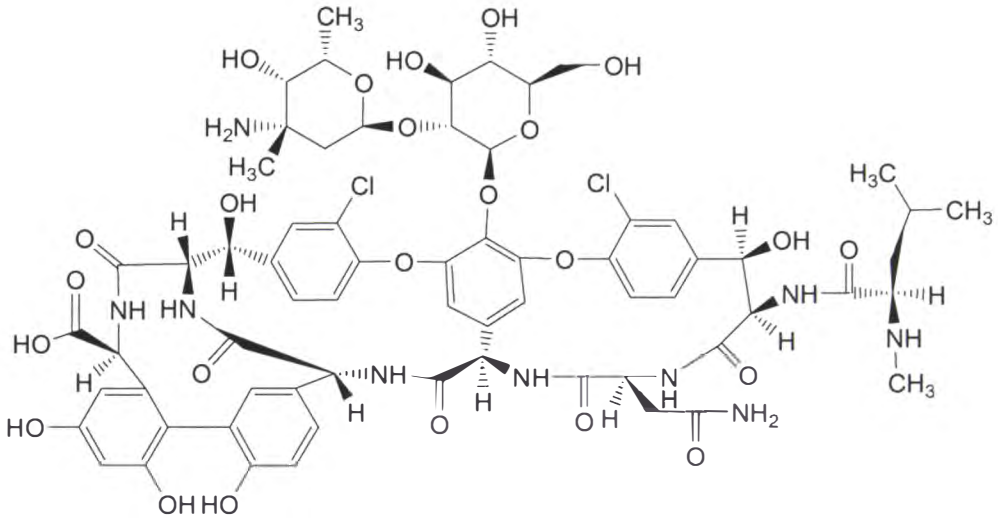

1.12

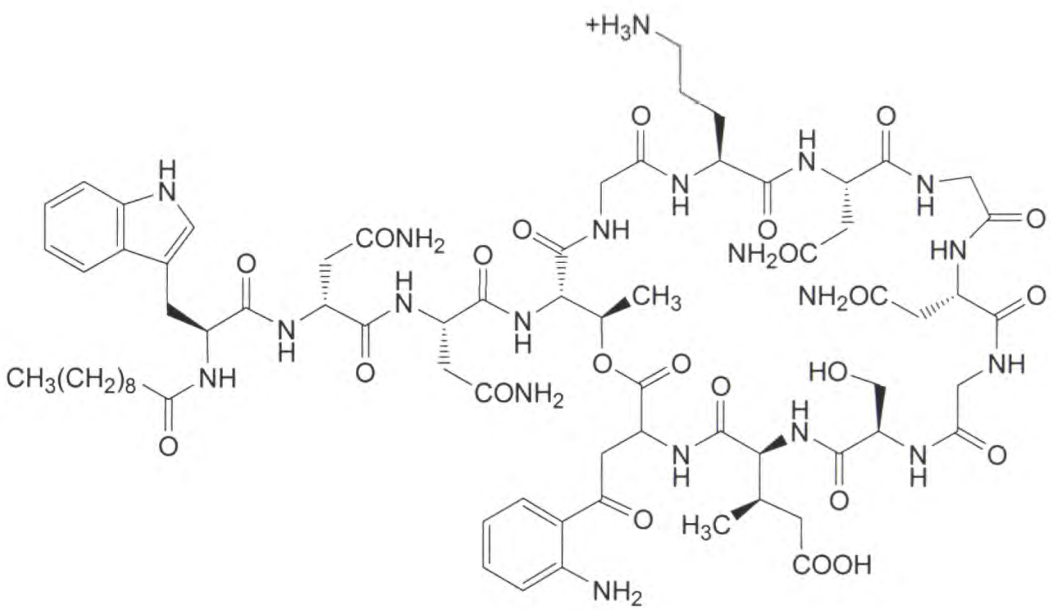

1.13

Cancer is a growing health concern for the worldwide population, with estimated new incidences reported to be 10 million cases per year (six million deaths), and is considered the second highest cause of mortality behind heart disease (16.7 million).[26,27] The World Health Organisation (WHO) predicts a rise in worldwide incidence to rise to 20 million cases per year (10 million deaths) by the year 2020.[27] Cancer develops after a cell accumulates mutations in several genes that control cell growth and survival. When a mutation seems irreparable, the affected cell usually enters apoptosis (cycle of cell death) rather than accumulate mutations that make it possible for the cell to divide uncontrollably and to metastasize

(break away from the original tumour) and establish tumours at different sites. Patients with many types of cancer may experience little or no significant response to even the best available combinations of surgery, radiation and drug therapy. These treatments possess a small degree of specificity for fast-growing cells, although damage still occurs to both normal and cancerous cells. When responses are obtained, the cancer cells can develop a level of resistance that often sees the subsequent treatments fail. To beat cancer, we need smarter therapies.

Once a tumour is diagnosed, a variety of treatment options are considered, depending on the tumour type, extent and location. Radiation and chemotherapy are the most commonly used therapies. Although these therapies have proven successful for some tumours, they are still highly toxic and nonspecific, since the primary mode of action is to damage deoxyribonucleic acid (DNA). Conventional chemotherapy is associated with drug resistance (both single and multi-drug) and systemic toxicity, thereby limiting therapeutic effectiveness. In order to reduce these effects, alternative therapies are being developed that are a combination of currently available treatments. These include chemotherapy combined with radiotherapy, immunotherapy, differentiation and angiogenesis inhibition therapy.[28,29] The objective of these approaches is to eliminate the problems associated with cancer cell resistance to a particular drug or class of drugs, and to diminish toxicity associated with high-dose chemotherapy. Unfortunately, the drugs currently used are not tumour specific, and are often associated with severe side effects.

The isolation of C-nucleosides from the Caribbean sponge *Cryptotheca crypta*[30] more than 50 years ago, led to the synthetic development of cytarabin (**1.14**, Ara-C)), the first marine-derived anti-cancer agent to be developed for clinical use. It is currently used for the treatment of patients with leukaemia and lymphoma.[31] Gemcitabine (**1.15**), one of its fluorinated derivatives, has also gained clinical approval for the treatment of pancreatic, breast, bladder and non-small cell lung cancer.

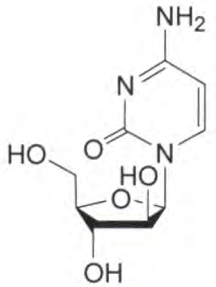

1.14

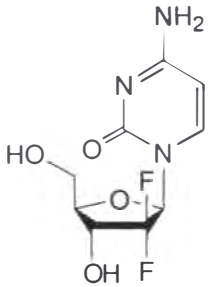

1.15

Numerous natural products have been approved for clinical use and are employed in anti-cancer therapies. Some examples of these include, doxorubicin (Adriamycin® (**1.16**) and the related compound daunorubicin (**1.17**)), vincristine (**1.18**), vinblastine (**1.19**) and mitomycin C (**1.20**).

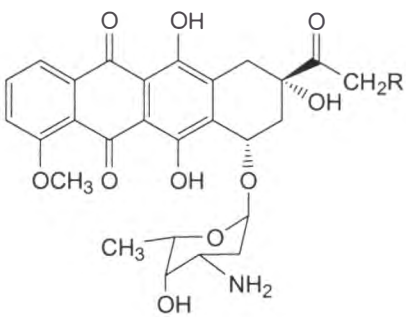

1.16 R = OH
1.17 R = H

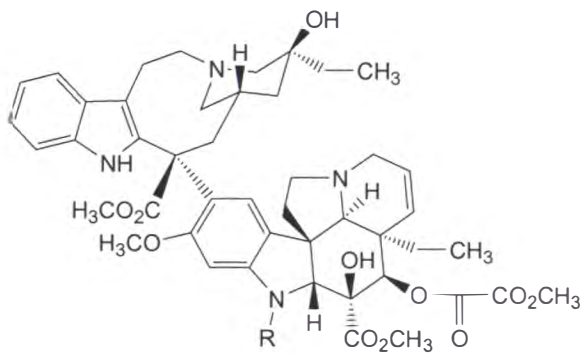

1.18 R = CHO
1.19 R = CH_3

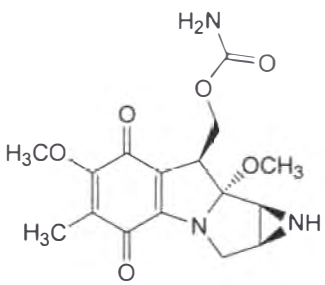

1.20

Doxorubicin (**1.16**) is an anthracycline-based antibiotic that has been of major importance in cancer chemotherapy since its clinical introduction in the early 1970's. Its main mode of action involves DNA strand breakage due to drug-mediated inhibition of DNA toperisomerase II, an essential cellular enzyme of

DNA synthesis and repair. However, considerations of toxicity, lack of effectiveness against a number of clinically common carcinomatous tumours (e.g. large cell lung, colorectal and bladder cancer) and development of drug resistance by tumours are among the reasons for the continuing search for compounds with improved therapeutic efficacy.

Since its first reported incidence in the United States in 1981, AIDS (Acquired Immunodefficiency Syndrome), like so many other diseases, has now become a worldwide problem. Current estimates (2004) suggest that 39.4 million people are living with the human immunodeficiency virus (HIV) that causes AIDS.[32] This number represents the highest recorded incidence to date. In New Zealand, figures remain relatively constant, with 157 people diagnosed in 2004 and 154 the previous year through HIV antibody testing.[33] HIV infection is primarily transmitted through blood to blood contact and sexual intercourse. The disease acts by killing the immune 'T-helper cells' that are an integral part of the human immune system's response to infection. When the level of T-cells has been significantly reduced, the patient often experiences secondary infections and the formation of cancers. This process is typical of AIDS, the final stages of the HIV viral infection. Initial treatment of the disease consisted of a single antiretroviral drug of nucleoside origin. This monotherapy improved the clinical status of infected patients by reducing the plasmid viral load, but quickly became ineffective due to rapid viral mutations. The 'triple cocktail' combination referred to as the 'highly active antiretroviral therapy' (HAART) was considered a major advancement in currently available treatments, possessing impressive *in vitro* activity against viral replication.

Currently, 37 licensed retroviral drugs are available for the treatment of HIV infections, however only 19 have been formally approved.[34] These belong to four families: (i) nucleoside reversed transcriptase inhibitors (NRTI), such as zidovudine (**1.21**) and didanosine (**1.22**); (ii) non-nucleoside reversed transcriptase inhibitors (NNRTI), including nevirapine (**1.23**) and delavirdine (**1.24**); (iii) nucleotide reversed transcriptase inhibitors (NtRTI), for example tenofovir disoproxil fumerate (**1.25**); and (iv) protease inhibitors (PI), such as saquinavir (**1.26**) and ritonavir (**1.27**). Unfortunately, even 'HAART' therapy,

although successful at reducing viral plasmid levels for many years, is not able to destroy residual viral populations that are residing within 'reservoir cells' in the lymphoid tissues. These are beyond the reach of any antiviral drugs available. This, combined with side effects associated with lifelong treatments including emergence of resistant mutations, accumulated toxicity and drug intolerance, has led to the review of therapeutic strategies.

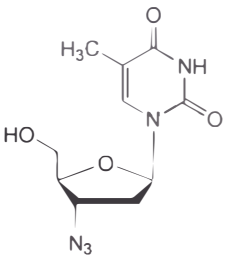

1.21

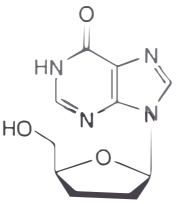

1.22

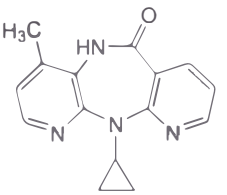

1.23

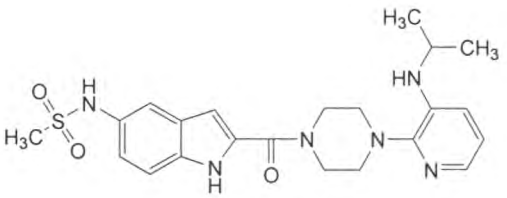

1.24

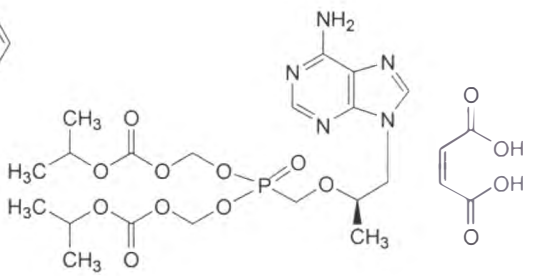

1.25

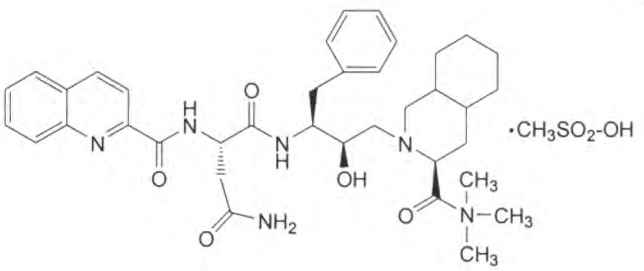

1.26

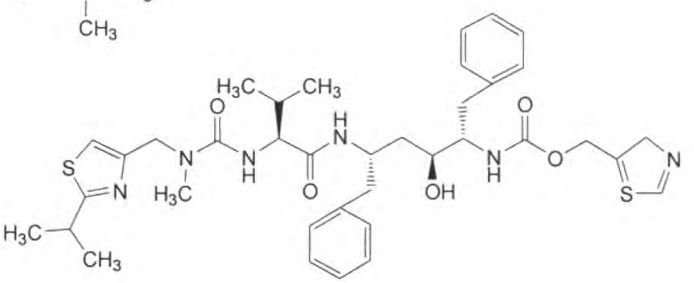

1.27

Like cancer and AIDS, tropical diseases affect a large proportion of the world's population (approximately 500 million people in Brazil, China, India and across the African continent) and include malaria, typhoid fever, leishmaniasis and

Chagas' disease.[35] Only a few natural and synthetic compounds have been effective at treating such diseases, however many of the currently available drugs come at a significant price and level of toxicity.

Typhoid fever is an illness following infection by the bacterium *Salmonella enterica serovar* Typhi. Chloramphenicol (**1.28**), isolated from the actinomycete *Streptomyces venezuelae*,[36] was introduced for the treatment of typhoid in 1948 and proved to be very effective both economically and clinically. However, by 1972 the first report of chloramphenicol-resistant *Salmonella enterica serovar* Typhi was described.[37] The transmission of resistance to *Escherichia coli* was also demonstrated *in vitro*. The focus of Western drug development centres on diseases such as cancer and those of the heart, and of the 1223 new drugs released onto the market between 1975 and 1996 only 11 new compounds (1 %), two of which were reformulations, were treatments for tropical diseases.[35] It is clear that effective funding and development of low-cost drugs is urgently needed if any impact is to be made in the fight against these tropical diseases.

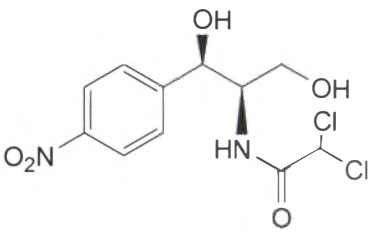

1.28

Clearly, the natural products that have been developed to date have played a pivotal role in controlling/treating human diseases. However, shortcomings in terms of drug toxicity, disease mutation, cost and availability can only be overcome if a multidisciplinary approach is employed. With the help of molecular biology technology, advances can be made in the identification of new molecular targets. This could not only revive 'old drugs', but may also provide targets for rational drug design.

What about the diseases that have yet to emerge? One such recent example is the Severe Acute Respiratory Syndrome (SARS) outbreak in Asia. Although conventional methods were used to contain further outbreaks of the SARS virus, the outbreak highlights the ongoing necessity for new drugs.

SARS, a previously unidentified disease, emerged from China as an untreatable and rapidly spreading respiratory illness. Between late 2002 and the first half of 2003 SARS outbreaks were reported in 32 countries. By July 5 2003, 8436 cases had been documented, 812 of which resulted in death.[38] The WHO responded by invoking traditional public health measures along with advanced technologies to control the illness and contain the cause. A novel coronavirus (CoV) was implicated, and its entire genome was sequenced by mid-April 2003. The major transmission mode of SARS-CoV is *via* close human contact, in particular, exposure to droplets of respiratory secretions from an infected person. A cluster of outbreaks within a Hong Kong apartment building were attributed to the persistence of SARS-CoV nucleic acid in excrements and wastewater, extended by lower temperatures. Fortunately, conventional methods proved effective in controlling the disease. Large amounts of chlorine-based disinfectants were used to treat hospital wastewater, and infected patients were kept in isolation once it was discovered that SARS-CoV can only persist as infectious particles for a very short period of time in *in vitro* environments.

1.7: The Phylum Porifera: An Overview

Sponges are noted in many texts as the simplest multicellular organisms and constitute the phylum Porifera of the animal kingdom, which includes about 10,000 described species.[3] They appeared on Earth over 600 million years ago, and have undergone little structural evolution over time. Sponges are sessile, and the majority are commonly found in locations where suitable substrates like coral and rocks are located. Their bodies contain no specific organs, but rather an organised mass of cells that exhibit a high degree of specialisation. Sponges obtain their food by filtering a high volume of water that is pumped through a

complex system of tissues, pores, canals and chambers. The flow of water is conducted from the inhalant surface to the exhalant apertures (pores).[3]

Sponges come in many colours, shapes and sizes, from millimeter thin encrustations, to branching ropes or to giant barrels more than 1.5 metres in height. They are ubiquitous, having been discovered in both fresh and salt water at all depths and latitudes.[3]

Soft tissue makes up the main mass of the sponge body. This tissue is supported by a framework of structures that are found in almost all sponges. These skeletal structures are of considerable importance in the classification of sponges, and may consist of calcareous spicules, siliceous spicules or spongin fibres (organic material). The classification (taxonomy) of sponges is extremely difficult as almost all of the identifying characteristics are variable. This has led to many reports in the literature of subsequent reclassifications of previously identified/classified specimens.[39]

Sponges contribute significantly to the biomass of marine ecosystems, and are distributed worldwide in a variety of habitats. This persistent ecological success has been attributed to the adaptive reproductive and physiological strategies, and an effective defence mechanism.[2]

Representatives from the phylum Porifera have a remarkable ability to synthesize a wide variety of secondary metabolites with potent biological activity. However, studies on metabolite production by sponge symbionts suggest that many compounds originally thought to be of sponge origin may well be of symbiont origin. One example that illustrates this particular point is the work by Faulkner and Bewley on Lithistid sponges,[40] where it was demonstrated that, after purification and analysis of the four cell types present in the *Theonella swinhoei* – eukaryotic sponge cells, unicellular heterotrophic bacteria, unicellular cyanobacteria and filamentous heterotrophic bacteria – the macrolide swinholide A (**1.29**) was limited to the population of unicellular heterotrophic bacteria and the β-amino acid containing cyclic peptides such as theonegramide (**1.30**) occurred only in the filamentous heterotrophic bacteria. Contrary to prior

speculation, no major metabolites were located in the cyanobacteria or sponge cells. A second example comes from PhD work being carried out at the University of Canterbury by Ms. Sarah Hickford on the origins of metabolites found in the sponge *Lamellomorpha strongylata*. Initial details were reported at the NZIC conference in Wellington November, 1999.[41] It has been established that the biologically active compounds swinolide H (isolated as the di-methylene acetal (**1.31**)) and theonellapeptolide IIIe (**1.32**) were localised within unicellular and filamentous heterotrophic bacteria, respectively, associated with the sponge.

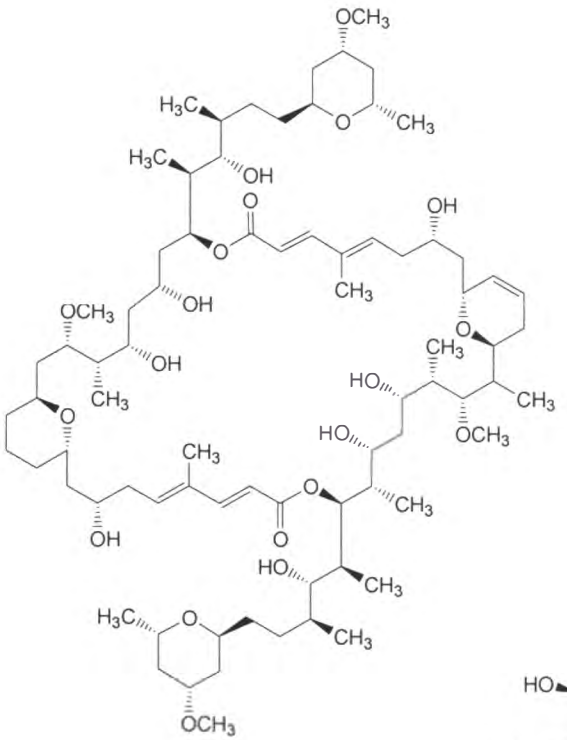

1.29

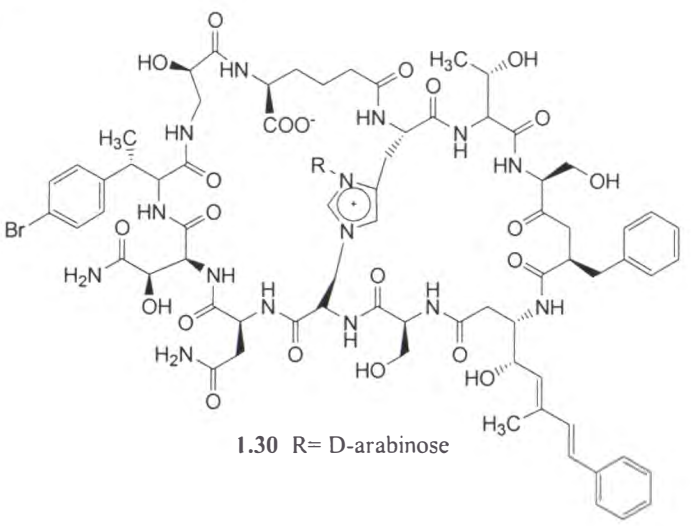

1.30 R= D-arabinose

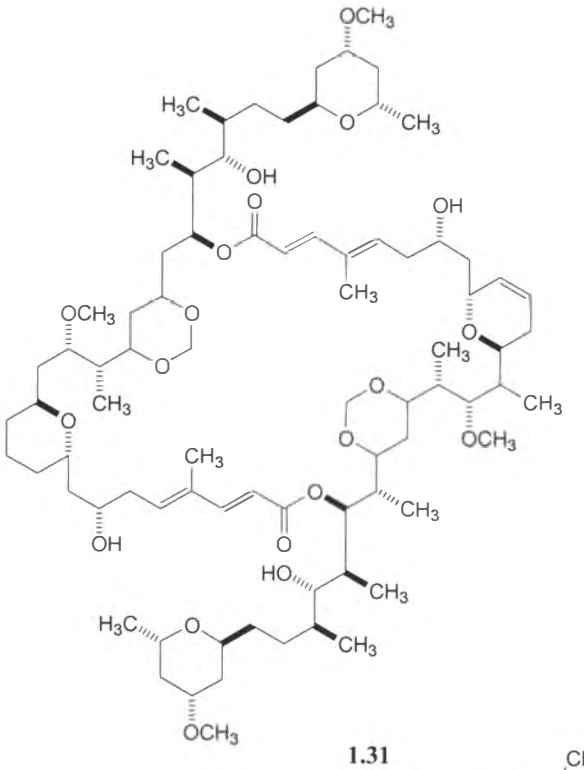

1.31

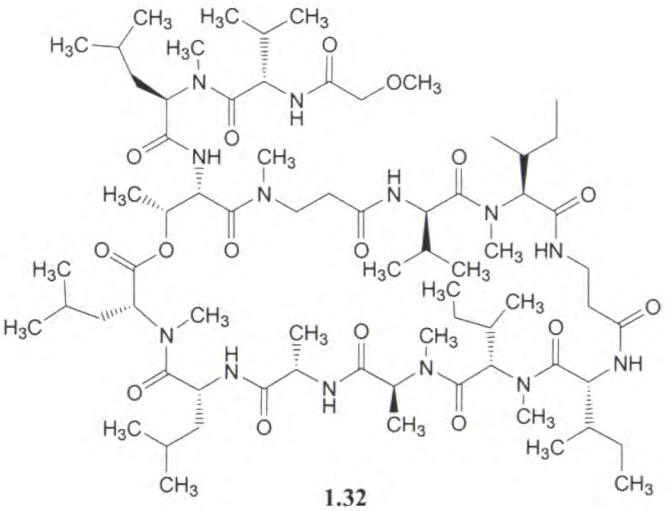

1.32

Finally, more recently Hill and Harmann[42] demonstrated that the microbe *Micromonospora* sp., isolated from a deep-water Indonesian sponge, produced the compounds manzamine A (**1.33**) and 8-hydroxymanzamine A (**1.34**) when grown under certain laboratory culture conditions with specific media. These compounds were originally isolated from the sponge itself.[43]

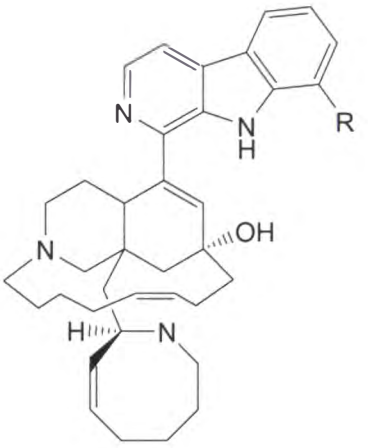

1.33 R = H
1.34 R = OH

The likelihood that a significant number of sponge-derived cytotoxic metabolites are in fact of microbial origin seems to be a real possibility as more literature is published confirming what many investigators have previously speculated.

1.8: Marine Fungi: An Overview

Marine fungi are ubiquitous. They are located in any environment that has a saline water source, including the oceans, river mouths and marshes. Even a few marine species have been isolated from great depths (>1500 ft).[44] The main factors that control the distribution of marine fungi are the availability of substrates, of hosts, temperature, hydrostatic pressure and oxygen. There is still debate as to what the properties are that define a fungi as marine. The most obvious is that the fungus requires sodium for survival at a concentration that defines it as a macronutrient,[45] while others claim that it is the absence or presence of certain enzyme activity.[46] However, the generally accepted definitions that are used to divide marine fungi into two groups are *obligate* and *facultative*. *Obligate* marine fungi are those that grow and sporulate exclusively in a marine or estuarine habitat, while *facultative* marine fungi are those that originate from the land or freshwater but can grow and possibly sporulate in a marine environment.[47] Many species of fungi were reclassified according to this definition, reducing the number of true marine fungi. To date there is no direct

method to identify whether or not an isolate is truly marine, other than to observe *in vivo* the ability to grow in the marine environment. Species identification has become more rapid with the use of molecular data such as deoxyribonucleic acid (DNA), ribosomal DNA (rDNA), random amplified polymorphic DNA (RAPD) and restriction fragment length polymorphism (RFLP) fingerprints. These techniques combined with searchable databases, have made identification more consistent, faster and easier for the non-specialist.[10] The processes of classification, identification and preservation of fungal isolates are very important procedures in natural product research. An inaccurate account of any one of these techniques would make experimental reproducibility impossible. Literature reports also provide chemical/biological information describing structural types and biological activities that mycologists can use to help in the profiling and classification process.

Fungal isolates investigated in this thesis were derived from sponge tissue collected from the frigid waters of Antarctica. Studies on fungi in Antarctica have been largely concerned with terrestrial specimens involved with the decomposition of organic matter.[48] It has only been in recent times that systematic collections have been made from the marine environment, although these have generally been limited to sea borne materials such as drift wood.[49]

For more detailed information regarding biologically active/novel compounds isolated from marine fungi, see **Sections 5.1** and **6.1**.

1.9: Antarctic Sponges

Marine sponges continue to be a rich source of biologically active metabolites with a wide range of activity. The main attention, however, has been focused on the investigation of specimens that inhabit temperate or tropical areas, due to the increased biodiversity and ease of collection. The Antarctic marine environment has been considered to be harsh; however, below the line where the bottom is scoured by anchor ice, the benthic community is remarkably rich and stable.

Although vertebrate predators, predominantly fish, which browse on sessile invertebrates (sponges) are rare at these latitudes, there is a high incidence of predation by macroinvertebrates such as sea stars. This phenomenon could explain why a plethora of novel and/or biologically active secondary metabolites have been isolated from sponges of widely distributed genera. Approximately twenty-one species of conspicuous Antarctic sponges have been identified, most of which have been investigated for novel/biologically interesting compounds.[22] Examples of these include sponges of the genera *Artemisina*,[50,51] *Cinachyra*,[52] *Dendrilla*,[52-57] *Homaxinella*,[58,59] *Isodictya*,[60,61] *Phorbas*,[50] *Psammopemma*,[62] *Leucetta*,[50,63] *Suberites*,[64-67] *Latrunculia*,[68,69] *Negombata*[68] and *Kirkpatrickia*.[50,52,70-72]

The two sponges *Latrunculia* sp. and *Kirkpatrickia varialosa* have significant importance for the Marine Chemistry Group at the University of Canterbury.

The genus *Latrunculia* (Order Hadromerida, Family Latrunculiidae) has had at least 2 species described, *L. apicalis* and *L. biformis*, in Antarctica. A major feature of this genus is the characteristic discorhabd microscleres, from which they were originally named. It was from this genus that the first reported marine isolation of the 1,3,4,5–tetrahydropyrrolo[4,3,2-*de*]quinoline ring system was achieved, with the discovery of the discorhabdins (**1.35-1.55**).[73]

Discorhabdin C (**1.37**) was first described in 1986 by Perry *et al.* as a highly toxic pigment isolated from the New Zealand sponge *Latrunculia* sp. at the University of Canterbury.[73] Between 1986 and 2004, 22 compounds in the discorhabdin family were isolated and described in the literature from the genus *Latrunculia*.[68,69,73-78] More recently the 23rd example, discorhabdin W (**1.56**), was isolated from a New Zealand species collected from Fiordland.[79] Discorhabdin W (**1.56**) is the first example of a dimeric compound in this series. However, of these isolated compounds, only discorhabdins C (**1.37**) and G (**1.41**)[69] and discorhabdins B (**1.36**) and R (**1.52**)[68] have been isolated from Antarctic waters.

The discorhabdin series is characterised by a range of biological activities against a variety of assays, but especially note worthy are the high levels of *in vitro*

cytotoxic activity against a variety of cell lines (P388, L1210, L5178, HCT-116 and KB). In subsequent *in vivo* testing, only discorhabdin D (**1.38**) showed results that could be defined as important.

In mechanism-based assays, discorhabdin P (**1.50**) was found to be an inhibitor of two key peptides, calicneurin and CPP32 (a member of the caspase family), at levels that were considered to be highly significant. Interestingly, discorhabdin P (**1.50**) is *N*-methyldiscorhabdin C (**1.37**) and in distinct contrast, discorhabdin C (**1.35**) showed no activity against either enzyme.[73]

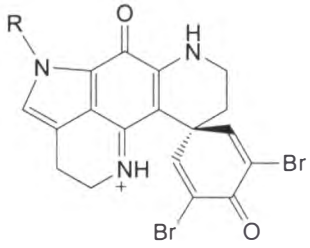

1.35 R = H
1.50 R =CH_3

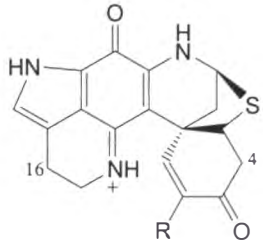

1.36 R = Br
1.37 R = Br, Δ^4
1.51 R = Br, Δ^{16},Δ^4

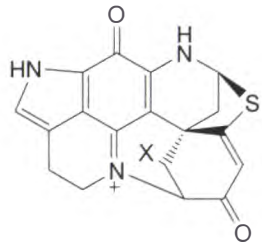

1.38 X = H
1.42 X = **a**
1.48* X =$NHCH_2COOH$

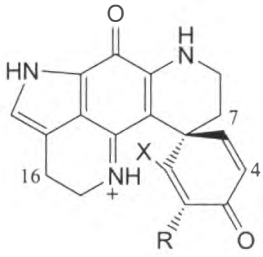

1.39 R = Br, X= H
1.40 R = Br, Δ^{16}, Δ^4, X = H
1.41 R = Br, Δ^7, X = H
1.43 R = X = H,
1.45* X = **a**, R = H

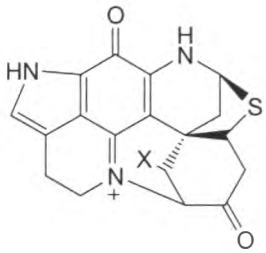

1.46* X = OH
1.44 X = **a**

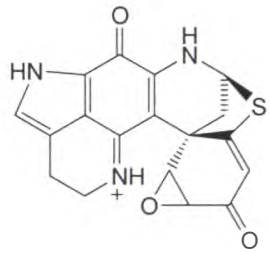

1.52

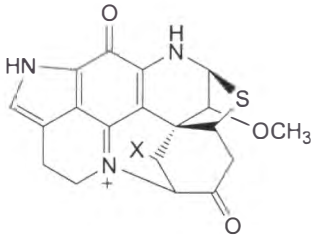

1.47* X = **a**

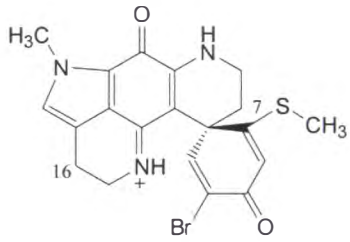

1.53 Δ^{16}
1.54 Δ^7, Δ^{16}
1.55 Δ^7

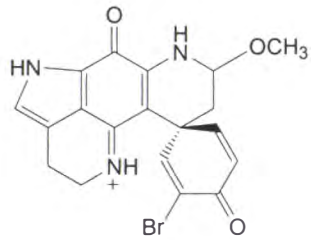

1.49*

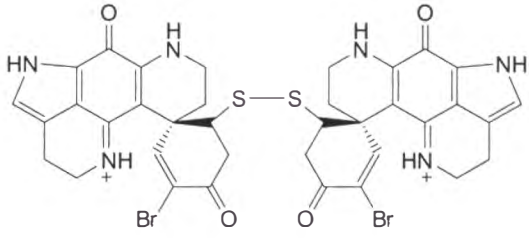

1.56*

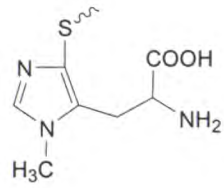

a

*Discorhabdins that have been isolated but are as yet unpublished.[17]

The second of the two genera, *Kirkpatrickia varialosa*, yielded the variolin (**1.57-1.60**) group of compounds. They were isolated in 1994 by Blunt, Munro and coworkers,[71,72] using P388 bioassay-guided isolation techniques, from sponge material collected in the Antarctic. The variolins represented a new class of marine alkaloid, possessing a novel fused tricyclic heteroaromatic core structure (a pyrido[3',2',4,5]pyrrolo[1,2-c]pyrimidine) that was unlike any terrestrial or marine natural product that had been isolated previously.

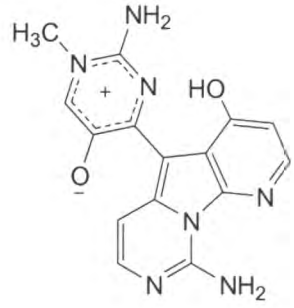

1.57

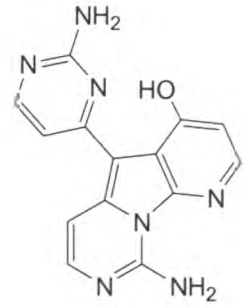

1.58

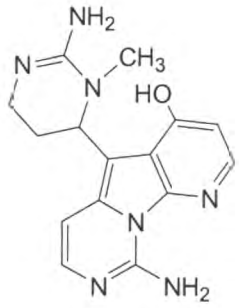

1.59

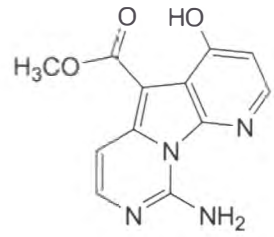

1.60

Pharmacological evaluations of these compounds involved testing against a variety of cell lines and micro-organisms. Activity in the P388 (murine leukaemia) cell line assay (*in vitro*) varied across the compounds. Variolin B (**1.58**) was identified as being the most potent against the P388 cell line (IC_{50} 210 ng/mL), as well as having moderate antiviral activity. PharmaMar (Spain) undertook further development of these compounds as synthetic targets because of their high potential as anti-tumour agents. In structure activity studies oxidation of the isolated D ring in the molecule as in variolin A (**1.58**) or *N*-3'-methyl-3',4',5',6'-tetrahydrovariolin B (**1.59**), was found to reduce activity.[80] The activity of these compounds seems to be associated with the presence of the aminopyrimidine ring,

as variolin D (**1.60**), which lacks this ring, possesses no appreciable activity. Due to insufficient quantities of variolin B (**1.58**), and the inability to re-collect the original sponge, interest was stimulated in the total synthesis. The first total synthesis was published by Anderson and Morris[81] (Chemistry Department, University of Canterbury), followed closely by Álvarez and coworkers,[80] in 2003. The total synthesis provided access to sufficient material suitable for the preparation of analogues. At present, the variolin analogues are undergoing preclinical trials at PharmaMar.[42]

1.10: The Current State of Play

Currently, there are many marine-derived compounds that have just entered, or are about to enter, into clinical and pre-clinical trials (**Table 1.1**) for the treatment of various diseases.[42] A brief overview is given below for a few selected compounds in an attempt to acquaint the reader with the significance that natural products are likely to play in the future of modern medicine for the treatment of diseases such as cancer.

Investigations into potential anti-cancer drugs from the marine environment led to the isolation of a plethora of chemical compounds. These include didemnin B (**1.61**) from the tunicate *Tridemnum solidum* (Rinehart *et al.*),[82] dolastatin 10 (**1.62**) from the Indian Ocean mollusk *Dolabella auricularia* (Pettit *et al.*),[83] the simple compound girolline (**1.63**) from the sponge *Pseudaxinyssa cantharella* (workers at Rhone-Poulenc Rorer),[42] the bengamides A (**1.64**) and B (**1.65**) from a marine sponge (Crews *et al.*),[84] and finally the cryptophycins (for example cryptophycin 52 (**1.66**)) which was initially reported from a blue-green alga (Merck)[85] but was subsequently isolated from a non-marine cyanophyte (Moore *et al.*)[86] and then from an Okinawan sponge (Kobayashi *et al.*).[87] However, all of these compounds have been withdrawn from anti-tumour trials. Didemnin B (**1.61**) proved too toxic in Phase II trials. Dolastatin 10 (**1.62**) did not demonstrate any significant *in vivo* anti-tumour activity (Phase II), while girolline (**1.63**) administration caused substantial hypertensive side effects in patients (Phase I).

Problems with the intrinsic biological properties of the bengamides A (**1.64**) and B (**1.65**) and cryptophycin 52 (**1.66**) led to the development of synthetic derivatives, however, unfortunately all of the natural and synthetic compounds were withdrawn from further clinical trials (Phase I and Phase II respectively).[42]

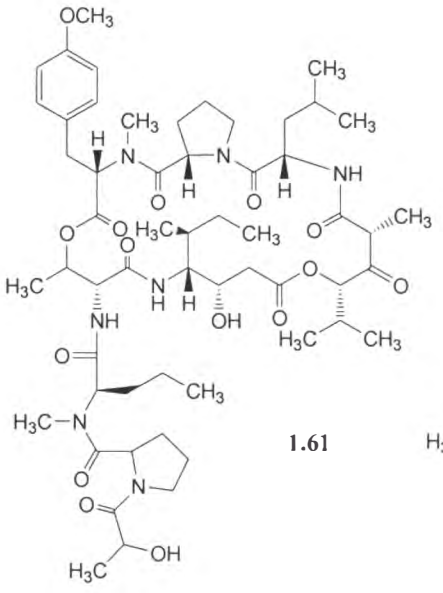

1.61

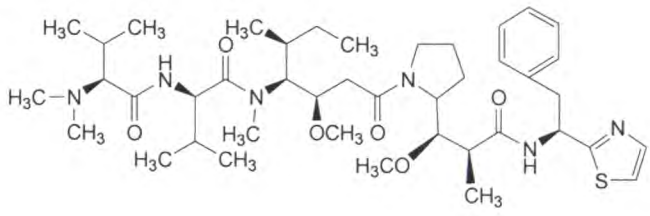

1.62

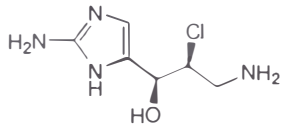

1.63

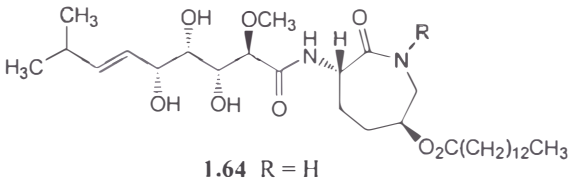

1.64 R = H
1.65 R = CH3

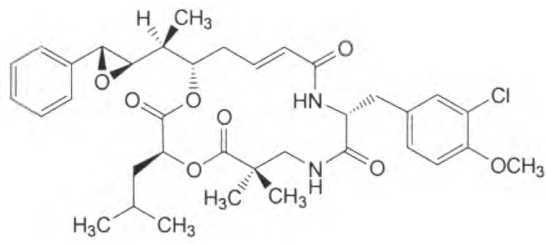

1.66

The marine alkaloid ecteinascidin 743 (**1.67**, ET-743), isolated from the ascidian *Ecteinascidia turbinata*, along with the shark cartilage-derived compound neovastat (which is not a true compound but rather a "defined mixture" of >500kDa compounds), are currently the most clinically advanced anticancer agents, with both compounds having reached phase III trials in Europe.[42]

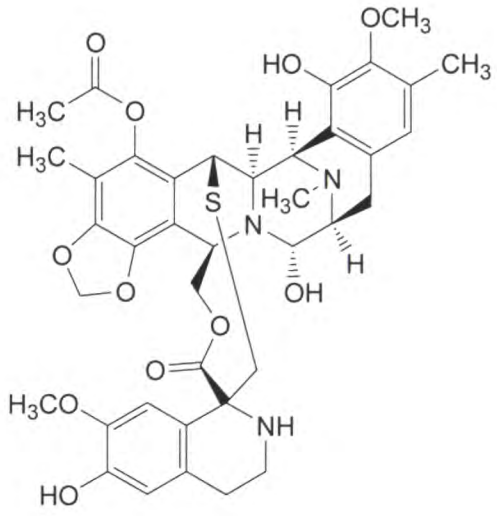

1.67

Additional promising anti-cancer agents (that have been selected for preclinical trials) include compounds that possess quite different biological modes of action. These include the tubulin interactive agents, enzyme and DNA inhibitory compounds and actin-active agents.

After the mechanism of paclitaxel (**1.5**) was discovered, a systematic study of marine organisms began, using bioassay guided separation (tubulin interactive assay), in an attempt to identify other compounds which acted via the same mechanism. As a result, a variety of compounds were isolated.

Compounds that are described as tubulin interactive agents include laulimalide (**1.68**) and isolaulimalide (**1.69**), isolated by Mooberry *et al.*,[88] and peloruside A (**1.70**), isolated by Northcote's group,[89] from the marine sponges *Cacospongia mycofijiensis* and *Mycale hentscheli*, respectively. The compound curacin A (**1.71**) was isolated from the cyanobacterium *Lyngbya majuscula* (Gerwick *et al.*),[90] while the compounds vitilevuamide (**1.72**), and diazonamide (**1.73**), by Ireland's group[91] and Fenical's group,[92] respectively, were isolated from the ascidians *Didemnum cuculiferum* and *Diazona angulata*, respectively. Fenical's group[93] also isolated, from the Australian octacoral *Eleutherobia* sp., the compound eleutherobin (**1.74**). Pietra's group[94,95] identified sarcodictyin (**1.75**) from both of the Mediterranean corals *Sarcodictyon roseum* and *Eleutherobia aurea*.

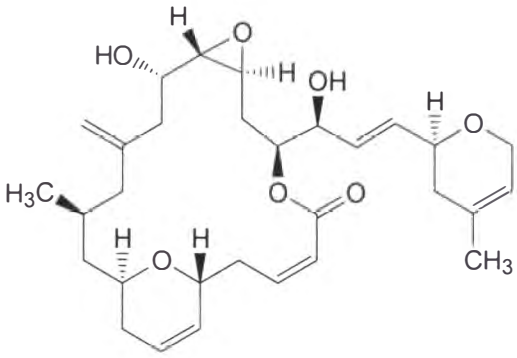

1.68

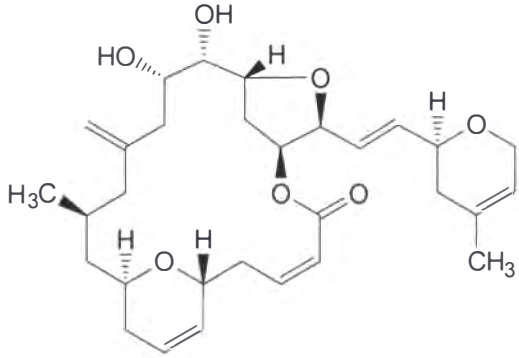

1.69

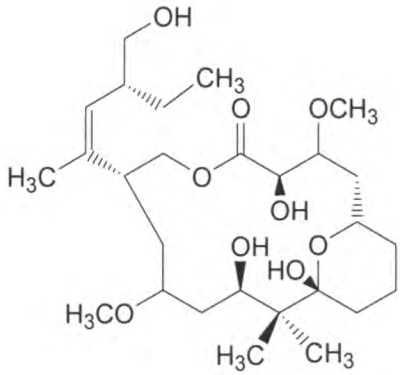

1.70

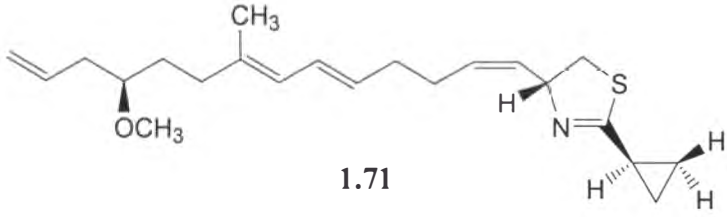

1.71

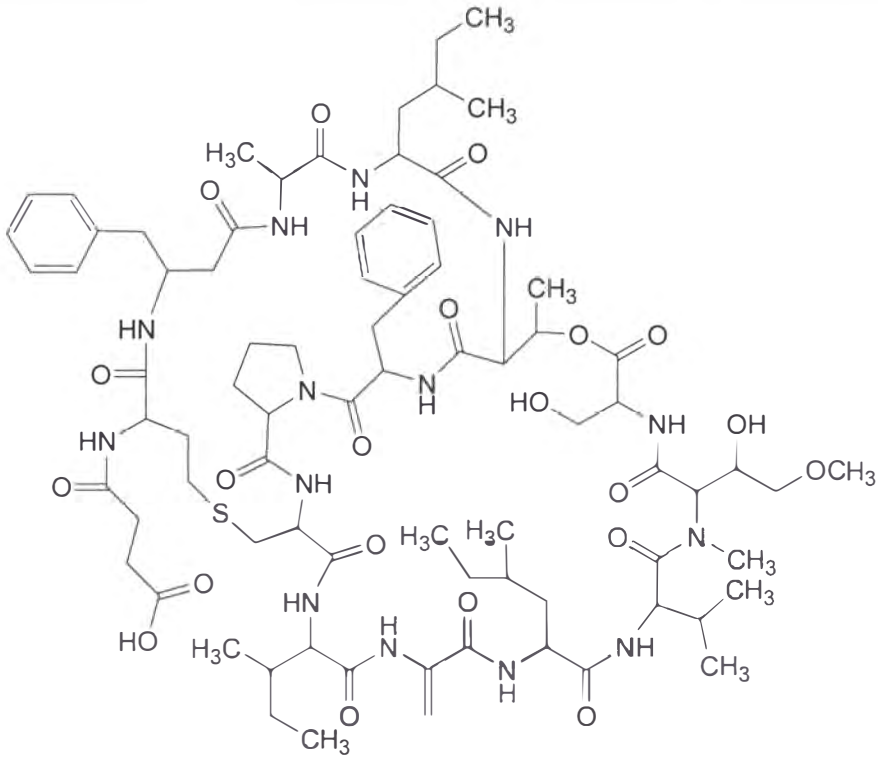

1.72

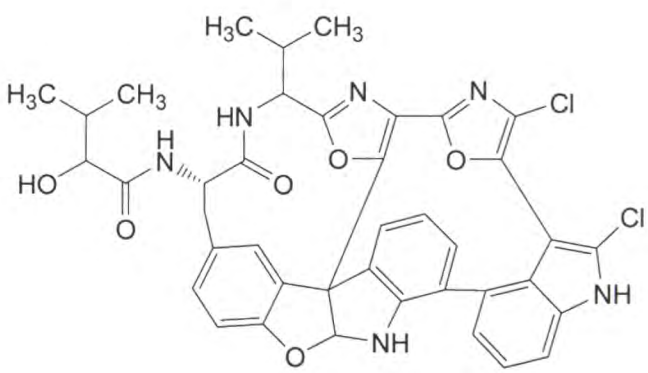

1.73

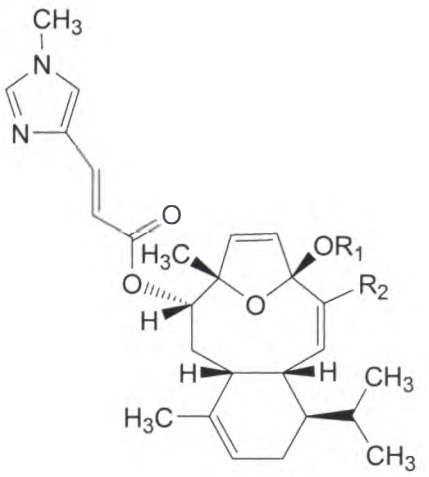

1.74 $R_1 = H$ $R_2 =$ 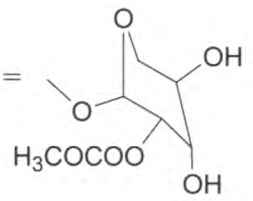

1.75 $R_1 = H$, $R_2 = CO_2CH_3$

In addition, natural products displaying activity as anti-Alzheimer's, anti-inflammatory, analgesic, anti-microbial, anti-malarial and anti-HIV agents have also been reported as entering preclinical trials.[42]

All of these compounds demonstrate the ability that marine natural products possess to invoke a variety of pharmacological effects. However, the problem of supply is one of the major obstacles for the development of a natural product currently undergoing clinical trials. In most cases, the compound of interest is only isolated in milligram quantities from large collections, often accounting for only 10^{-6} of the wet weight of the organism, especially in the case of invertebrates.[96] Several tonnes of sponge biomass would be required annually to meet market requirements. Therefore careful account must be taken regarding the source of the active compounds. Synthetic or semi-synthetic routes will reduce the need for large-scale collections of the organism, although these strategies need to be economically feasible and the yield optimised. The cellular location of the compound is also important. Is it the sponge, tunicate or bryzoan that is producing the biologically active compounds, or are they of microbial origin? This question, when answered, may have significant consequences, especially if

microbes are found to be the source. Entirely new approaches for the production of the 'drugs' are then opened up, especially given biotechnological advances in the area of gene cloning.[97,98]

The biologically active compounds discussed in this section are only a small representation of the drug candidates currently undergoing trials. A more exhaustive list of compounds derived from the marine environment currently in preclinical, phase I, II or III trials is shown in **Table 1.1**. These examples also illustrate the structural diversity that marine natural products possess.

Table 1.1: Marine Natural Products and their synthetic derivatives in various stages of clinical development.[42]

Name	Source	Status (disease)	Status
didemnin B	*Trididemnum solidum* (Tunicate)	Phase II (cancer)	*
aplidine	dehydrodidemnin B (total synthesis)	Phase II (cancer)	
dolostatin 10	*Dolabella auricularia* (cyanophyte)	Phase I/II (cancer)	*
TZT-1027	synthetic dolastatin	Phase II (cancer)	
cematodin	synthetic derivative of dolastatin 15	Phase I/II (cancer)	
ILX 651, synthatodin	synthetic derivative of dolastatin 16	Phase I/II (cancer)	
girolline	*Pseudaxinyssa cantharella* (sponge)	Phase I (cancer)	*
bengamide derivative	*Jaspis* sp. (sponge)	Phase I (cancer)	*
cryptophycins	*Nostoc* sp. and *Dysidea arenaria* (terrestrial cyanophyte and sponge)	Phase I (cancer)	*
bryostatin 1	*Bugula neritina* (bryozoan)	Phase II (cancer)	
ecteinascidin 743	*Ecteinascidia turbinata* (ascidian)	Phase II/III (cancer)	
E7389	*Lissodendoryx* sp. (sponge)	Phase I (cancer)	
discodermalide	*Discodermia dissoluta* (sponge)	Phase I (cancer)	
kahalalide F	*Eylsia rufescens/Bryopsis* sp. (mollusk/green microalga)	Phase II (cancer)	
ES-285 (spisulosine)	*Spisula polynyma* (clam)	Phase I (cancer)	
HTI-286 (derivative)	*Hemiasterella minor* (sponge)	Phase II (cancer)	
KRN-7000	*Agelas mauritianus* (sponge)	Phase I (cancer)	
squalamine	*Squalus acanthias* (dogfish shark)	Phase II (cancer)	
Æ-941 (defined mixture)		Phase II/III (cancer)	
NVP-LAQ824	Synthetic	Phase I (cancer)	
laulimalide	*Cacospongia mycofijiensis* (sponge)	preclinical (cancer)	
curacin A	*Lyngbya majuscula* (cyanobacterium)	preclinical (cancer)	
vitilevuamide	*Didemnum cucliferum* and *Polysyncraton lithostrotum* (ascidians)	preclinical (cancer)	
diazonamide	*Diazona angulata* (ascidian)	preclinical (cancer)	
eleutherobin	*Eleutherobia* sp. (octacoral)	preclinical (cancer)	
sarcodictyin	*Sarcodictyon roseum* (coral)	preclinical (cancer)	
peloruside A	*Mycale hentscheli* (sponge)	preclinical (cancer)	
salicylihalimides A	*Haliclona* sp. (sponge)	preclinical (cancer)	
thiocoraline	*Micromonospora marina* (actinomycete)	preclinical (cancer)	
variolins	*Kirkpatrickia variolosa* (sponge)	preclinical (cancer)	
dictodendrins	*Dictyodendrilla verongiformis* (sponge)	preclinical (cancer)	
GTS-21 (DMBX)	synthetic	Phase I (Alzheimer's)	
manoalide	*Luffariella variabilis* (sponge)	Phase II (antipsoriatic)	*
IPL-576,092	*Petrosia contignata* (sponge)	Phase II (antiasthmatic)	
IPL-512,602	derivative of 576,092	Phase I (antiasthmatic)	
IPL-550,260	derivative of 576,093	Phase II (antiasthmatic)	
ziconotide (Prialt)	*Conus magnus* (cone snail)	Phase III (pain)	
CGX-1160	*Conus geographus* (cone snail)	Phase I (pain)	
CGX-1007	*Conus geographus* (cone snail)	Phase I (pain and epilepsy)	*
AMM336	*Conus catus* (cone snail)	preclinical (pain)	
χ-conotoxin	*Conus* sp. (cone snail)	preclinical (pain)	
CGX-1063	Synthetic	preclinical (pain)	
ACV1	*Conus victoriae* (cone snail)	preclinical (pain)	

*Denotes compounds that have been reported as discontinued from clinical and preclinical trials.

It is clear that marine invertebrates and micro-organisms represent a source of biologically active marine natural products that are as structurally diverse as they are biologically active. Although investigation into the marine environment began many decades ago, few biologically active compounds have made it through the drug development process into commercial use, due to their potency and lack of target specificity. However, synthetic chemical derivatives hold new hope for those compounds that do not possess favorable pharmacological properties. In order to increase the number of natural products potentially useful as pharmaceuticals, a multidisciplinary approach is needed especially in the areas of microbiology and synthetic chemistry. Technology has also allowed for rapid advances in drug discovery research, by allowing collections in habitats previously inaccessible to humans, genetic fingerprinting of sponges and micro-organisms, the culturing of previously "unculturable" bacteria and fungi that are host specific, rapid throughput screening that is mechanism-based, and finally, the development of techniques used in the isolation and structural elucidation of potential drug candidates. We can only wonder at what prospects the next few decades will hold.

1.11: The Aim of this Thesis

To investigate the biological activity of the chemical constituents of New Zealand and Antarctic marine invertebrates, combined with micro-organisms cultured from the tissues of Antarctic sponges (fungi), using the assays available in-house at the University of Canterbury.

Isolation and characterization of the active compounds will be achieved using combinations of chromatographic techniques, while structural elucidation will utilize mass spectrometry, ^{1}H, ^{13}C and 2D NMR spectroscopic techniques.

CHAPTER 2

ISOLATION OF COMPOUNDS FROM THE NEW ZEALAND MARINE SPONGE *Rhabderemia stelletta* (01MNP0729)

2.1: General Introduction

Long-chain acetylenic compounds are unsaturated fatty acid derivatives that are commonly characterised by unbranched long alkyl chains. They are structurally simple yet display a high degree of diversity in relation to their chain length and functionalities. The most abundant naturally occurring saturated fatty acids have the general formula $CH_3(CH_2)_nCO_2H$ (n=12, 14, 16 and 18) and are vital components of natural waxes, seed oils and glycerides. Glycerides typically have polar head groups and lipophilic tails and are commonly encountered as constituents of cell membranes, playing an important role in the structural integrity and selective permeability of the cell membrane structure.

In addition to their structural role, (poly)unsaturated fatty acids act as precursors for biologically active metabolites. Oleic acid (**2.1**) is the biosynthetic precursor for polyacetylenes like crepenynic acid (**2.2**), a compound produced by many species of Compositae (daisy) which has anti-microbial activity, and wyerone (**2.3**) produced by the broad bean under stress which displays anti-fungal activity.[99]

Fatty acid synthases are enzymes that control the biosynthesis of fatty acids. Bacterial synthases comprise six or seven discrete enzymes, whilst plants and mammals contain more sophisticated synthases comprising two identical multifunctional proteins that posses seven different catalytic activities. Each protein reacts with the acyl carrier protein (ACP), which acts as a cofactor carrying the growing fatty acid on phosphopantetheine attached to its thiol group during most of the assembly process.

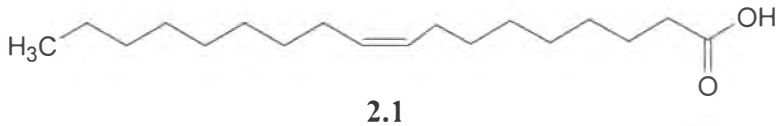

2.1

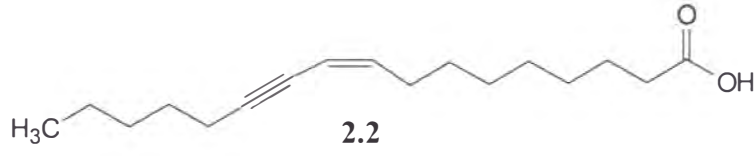

2.2

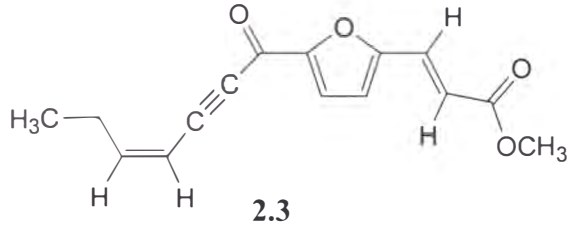

2.3

Historically the isolation of polyacetylenic compounds from plants has been prevalent, and terrestrial sources still provide an abundant source of novel polyacetylenic compounds. Recently the novel polyacetylenic compound dendrotrifidic acid (**2.4**) (9*Z*, 16*S*)-16-hydroxy-9,17-octadecadiene-12,14-diynoic acid was isolated from the leaves of the *Dendropanax morbifera*, a plant whose extract was reported to display anti-fungal activity.[99] Extracts from the *Dendropanax* genus display cytotoxic activity and have been used extensively in

traditional medicine for the treatment of migraines and other ailments. Although dendrotrifidic acid (**2.4**) possesses no significant *in vitro* anti-fungal activities, it does display a high degree of anti-complement activity when tested *in vitro*.[100] Aciphyall (**2.5**), a novel C_{34} polyacetylene, was identified from the methanolic extract of the subalpine giant spear grass *Aciphylla scott-thomsonii*, representing the first instance of a chain length exceeding C_{18} from a higher plant.[101] Aciphyall (**2.5**) exhibited both weak cytotoxic activity in the P388 assay (IC_{50} > 25 μg/mL) and antifungal activity against *Trichophyton mentagrophytes* (60 μg/mL).

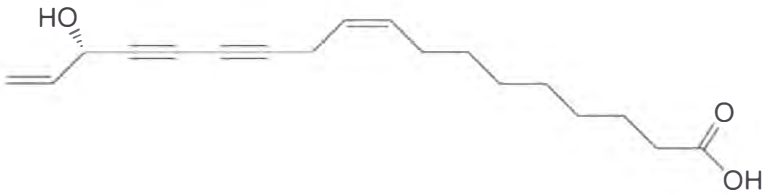

2.4

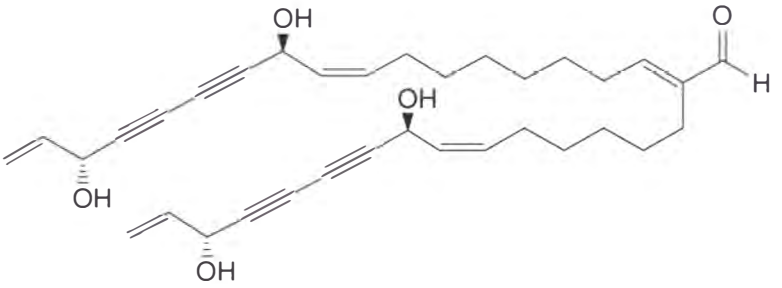

2.5

It has only been within the last 30 years that biologically active acetylenes have been reported from the marine environment, with over 100 compounds currently described. Distribution seems ubiquitous, with acetylenes isolated from algae,[102] sea hares,[103] stony corals,[104] nudibranchs[105] and sponges.[105-129]

The nonterpenoid C_{15}-halogenated compounds (*Z*)-maneonene A (**2.6**) and B (**2.7**), (*E*)-maneonene B (**2.8**) along with iso-maneonene A (**2.9**) iso-maneonene B (**2.10**) and (*Z*)-maneonene C (**2.11**) were isolated from the red marine alga *Laurencia nidifica*.[102]

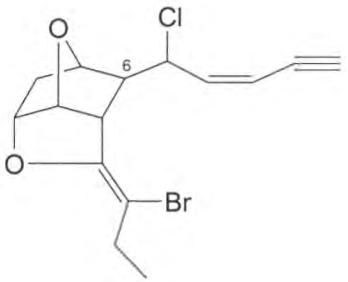

2.6
2.11 C_6 - endo isomer

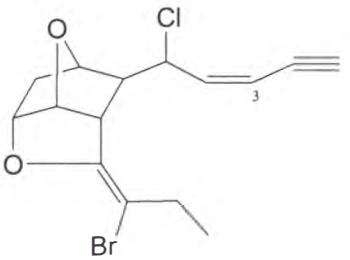

2.7 3(*Z*)
2.8 3(*E*)

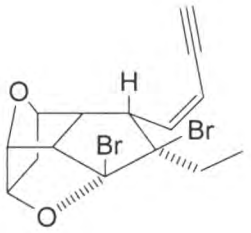

2.9

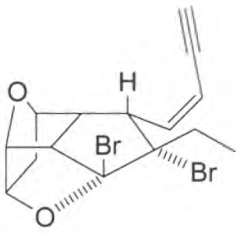

2.10

Two halogenated acetylenic ethers, dactylyne (**2.12**) and its isomeric analogue isodactylyne (**2.13**), were reported from the sea hare *Aplysia dactylomela*.[103] These two compounds are members of a group of similar nonterpenoid C_{15} ethers isolated from red algae.[102]

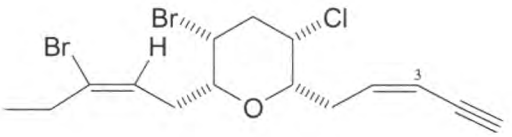

2.12 3(*Z*)
2.13 3(*E*)

C_{46} to C_{49} (**2.14-2.18**) straight chain polyacetylenes have been isolated from both the nudibranch *Peltodoris atromaculata*[105] and the marine sponge *Petrosia ficiformis*.[108,109,112,114-116,119,120]

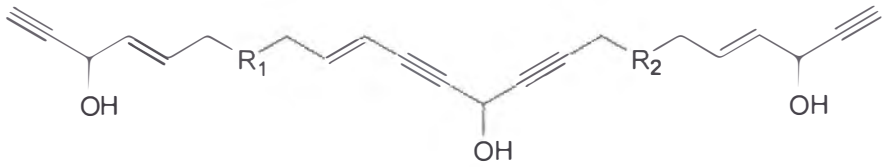

$R_1 + R_2 = C_nH_{2n-6}$

2.14 n = 25
2.15 n = 28

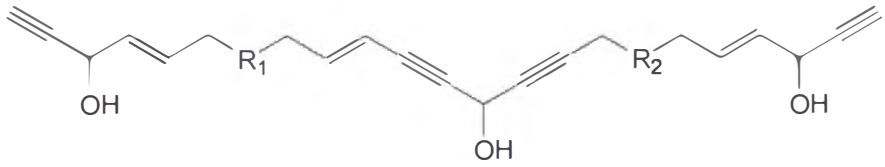

$R_1 + R_2 = C_nH_{2n-4}$

2.16 n = 28
2.17 n = 31
2.18 n = 34

Polyacetylenes isolated from three species of hermatypic corals *Montipora sp*, *M. mollis*, and *Pectinia lactuca* inhibited the growth of some bacteria and fungi.[104] Hard corals consist mainly of calcareous skeleton and it was assumed that these animals would not produce any significant secondary metabolites, thus they had been previously overlooked as a source of novel biologically active compounds. However, the polyacetylenic alcohols **2.19** and **2.20** along with the associated esters **2.21**, **2.22** were isolated from all three species of hard corals. All of the compounds displayed ichthyotoxicity against guppies at concentration levels of 1-5 ppm. Compounds **2.19** and **2.20** were active at 10 μg/disc against *Bacillus subtilis*, *Staphylococcus aureus*, *Aspergillus* sp., and *Cladosporium* sp., while **2.21** and **2.22** displayed no antimicrobial activity at a concentration of 10-100 μg/disc.

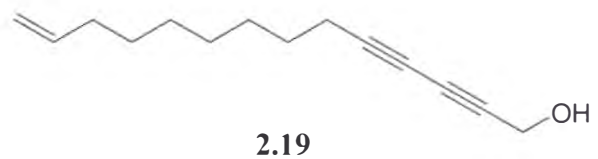

2.19

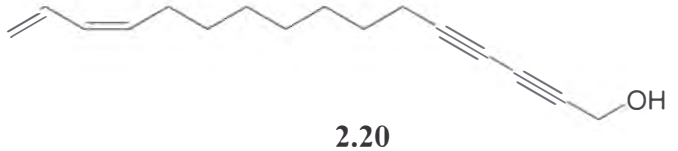

2.20

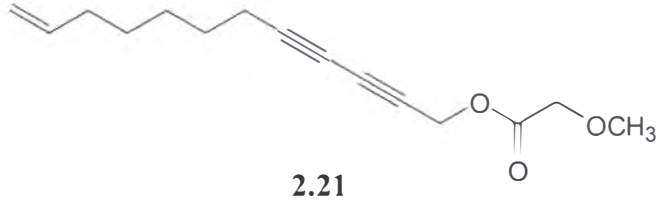

2.21

2.22

Despite the fact that polyacetylenes continue to be isolated from various terrestrial and marine flora and fauna, marine sponges, in particular sponges from the order Haplosclerida, dominate as a source of novel biologically active acetylenes/polyacteylenes.[117]

Haplosclerida have proven a rich source of straight chain polyacetylenic compounds that exhibit a variety of different chain lengths and oxygenation patterns. From this order, 88 compounds have been reported, with the bulk of these originating from five families, consisting of eight genera; specifically *Adocia*, *Callyspongia*, *Cribrochalina*, *Haliclona*, *Pallina*, *Petrosia*, *Siphonochalina* and *Xestospongia*.[109,112] However, a series of C_{32}-C_{35} hydroxylated polyacetylenes have also been isolated recently from the marine sponge *Theonella* sp. (order Astrophoridae).[117]

The genera *Petrosia* and *Xestospongia* are characterised by the presence of hydroxylated C_{30} and C_{46} polyacetylenes as well as brominated C_{18} acetylenic

acids, while the *Haliclona* and *Adocia* are represented by the highly hydroxylated C_{47} acetylenic acids and hydroxylated C_{30} polyacetylenes. Hydroxylated C_{23}-C_{41} and C_{32}-C_{33} polyacetylenic acids were reported from the genus *Pellina*. Hydroxylated C_{20}-C_{22} polyacetylenes were found in the genus *Cribrochalina*. The polyacetylenic hydrocarbons C_{21}-C_{22} are also characteristic of the genera *Callyspongia* along with C_{23} sulfonated and C_{22}-C_{23} hydroxylated polyacetylenes in addition to a C_{25} polyacetylenic amide.[123]

These secondary metabolites exhibit a variety of biological activities including antifungal, antimicrobial, HIV protease inhibitory, HIV reversed transcriptase inhibitory, antifouling, immunosuppressant and anti-tumour activity.[117]

In order to rationalize the distribution of these compounds throughout the marine environment, and explain their diverse biological activity, the ecological chemistry of the predator-prey and symbiotic relationships must be considered. There is little doubt that the plethora of secondary metabolites that have been identified have arisen in direct response to the continually changing interactions between species. The nudibranch *P. atromaculata*[105] is able to find its prey, the sponge *P. ficiformis*,[108,109,112,114-116,119,120] by chemotaxis and store metabolites taken up during predation while the sea hare *A. dactylomela*[103] feeds upon the red alga *L. nidifica*.[102] Isolation of biologically active compounds from three of the chemically "ordinary" species of hard coral would be highly suggestive that these are metabolites from a common symbiotic organism, the activity of which implies that they play a significant role in the coral's defensive mechanism.

2.2: Introduction

The marine sponge *Rhabderemia stelletta* was collected and identified by the National Institute of Water and Atmosphere (NIWA) at an unknown depth, Spirits Bay, North Island, New Zealand. A voucher sample of 01MNP0729 is held at NIWA Wellington, New Zealand. The material was kept frozen until chemical/biological assessment could be performed at the University of Canterbury. Subsequent analysis of the organic extract in-house utilizing the P388 assay revealed that the extract displayed significant anti-tumour activity with an IC_{50} < 975 ng/mL. An extensive literature search revealed that chemical studies on the marine sponge genus *Rhabderemia* are limited; with no literature reported for this genus.[130,131] For this reason, the biologically active *R. stelleta* species was selected for further chemical investigation.

2.3: Extraction of Marine Sponge Rhabderemia stelletta *(01MNP0729)*

The frozen sponge material was thawed in MeOH and homogenised until the specimen was completely macerated. After filtering through celite under vacuum, the residue was re-suspended and re-extracted using combinations of MeOH and DCM. All filtrates were combined and the solvent was removed under vacuum. The crude organic extract was partitioned between EtOAc and H_2O, the organic layer was collected and the solvent was removed under reduced pressure to yield a thick yellow/brown gum. Both the organic and aqueous fractions were analysed to locate the biological activity observed in the initial extract. P388 activity was present in the organic fraction only (IC_{50} < 975 ng/mL, 2.45 g). The aqueous layer contained no significant cytotoxic activity (IC_{50} > 12500 ng/mL).

The organic extract was subjected to analytical reversed phase (C_{18}) HPLC microtitre plate chromatography (see **Experimental**, **Section 7.1.6.2**) and P388 assay to locate the compounds responsible for the observed activity (**Figure 2.1**).

Well 88, corresponding to compounds eluting between 26-32.5 minutes, was found to contain the compounds responsible for the observed activity. The two major components eluting at 28.5 and 29.5 minutes displayed similar ultra violet (UV) profiles (λ_{max} (CH_3CN/H_2O) 230 nm, **Figure 2.2**), which suggested that the molecule contained conjugated bonds that were not aromatic in nature. Electrospray mass spectrometric analysis by direct injection of the active well was inconclusive as an abundance of mass peaks observed in both positive and negative modes made the identification any parent ions or any patterns corresponding to sodium or potassium adducts impossible. Due to the lack of structural information it was unlikely that a positive identification of these compounds would be achieved by interpretation of the UV spectra and retention time alone, therefore it was necessary to proceed with further purification.

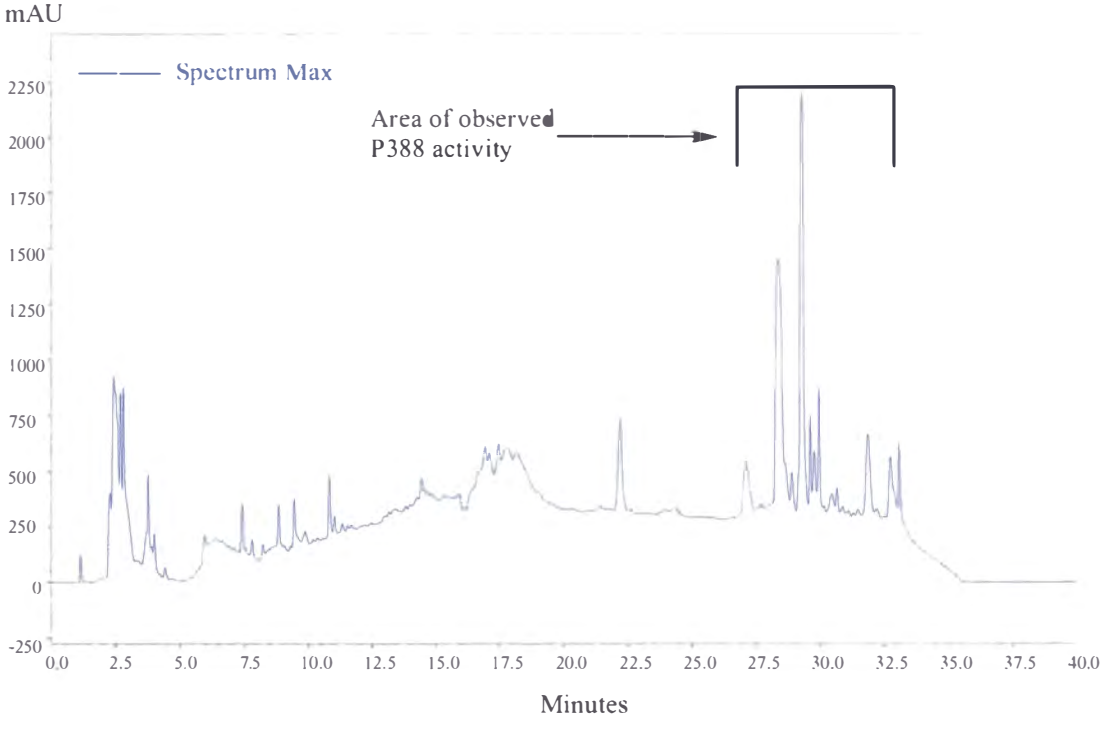

Figure 2.1: HPLC trace of DCM/MeOH crude extract (blue). Region of biological activity indicated between 26–32.5 minutes (black) as obtained from microtitre plate analysis.

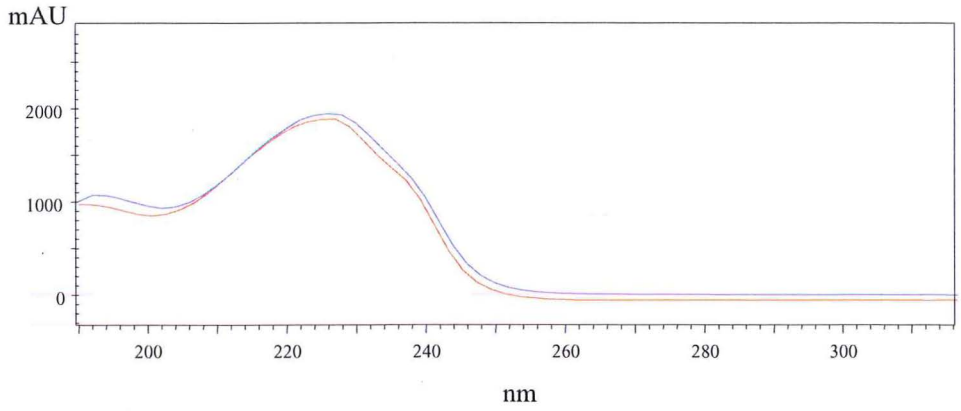

Figure 2.2: UV profiles of the two major compounds observed in the region of biological activity (26-32.5 minutes) as determined by microtitre plate assay (P388).

2.4: Chromatography of the Organic Extract

2.4.1: Reversed Phase (C_{18}) Flash Chromatography of the Organic Extract

The organic extract was dissolved in a minimum volume of solvent (MeOH and DCM) and adsorbed onto C_{18}. The solvent was removed under reduced pressure and the dry pellet was loaded on the top of a reversed phase C_{18} flash chromatography column equilibrated to 100 % H_2O. The column was eluted using stepped solvent gradient concentrations of H_2O, MeOH and DCM. Any remaining material was washed from the column with MeOH and DCM (0.1 % TFA). Seventeen fractions were collected and all fractions were submitted for biological assay in the P388 assay. The biological activity was found to be localised in fraction 12, which eluted with 2:1 DCM/MeOH (wjm12-312, IC_{50} 2001 ng/mL, 79.4 mg). This fraction was analysed by reversed phase (C_{18}) analytical HPLC, using the standard gradient elution method (see **Experimental, Section 7.1.3.2**), and it was confirmed that this fraction contained the peaks responsible for the activity observed in the initial microtitre plate analysis in **Figure 2.1**.

2.4.2: Normal Phase (DIOL) Flash Chromatography of Fraction wjm12-312

The next stage of purification consisted of a normal phase (DIOL) flash chromatography column as the compounds contained within fraction wjm12-312 were very non-polar. Fraction wjm12-312 was dissolved in a minimum volume of pet. ether, and loaded onto the DIOL column. Fractions were eluted from the column using a stepped solvent gradient from 100 % pet. ether through DCM to EtOAc and finally MeOH, with 12 fractions collected in total. Odd numbered fractions were submitted for biological assay with fractions wjm12-701 and wjm12-703 containing all of the biological activity (IC_{50} 938 and 1205 ng/mL respectively). On the basis of these results, it was assumed that fraction wjm12-702 would also be suitably active in the P388 assay; therefore these three fractions were combined.

At this point of the isolation it was observed that fraction wjm12-704 had begun to crystallize. Closer inspection of the 'crystal' like material using a polarized filter microscope showed that no polarization of light was observed. Further inspection revealed that a gelatinous gum-like substance that would not dissolve had formed. This lack of solubility prevented any further investigation into the type of compounds contained within this fraction.

2.4.3: Reversed Phase (C_{18}) Semi-preparative HPLC Chromatography of Fractions wjm12-701 to wjm12-703

Fractions wjm12-701 to wjm12-703 were combined and purified *via* semi-preparative reversed phase (C_{18}) HPLC chromatography, using an isocratic method developed for maximum resolution on the analytical reversed phase (C_{18}) HPLC. Fractions were collected as peaks eluted. Four fractions were collected (**Figure 2.6**); purity was confirmed by re-injection onto the analytical reversed phase (C_{18}) HPLC column. These fractions were subsequently examined by one

dimensional (1D) and two dimensional (2D) NMR spectroscopy. Structural elucidation of these pure compounds is discussed in **Section 2.5**.

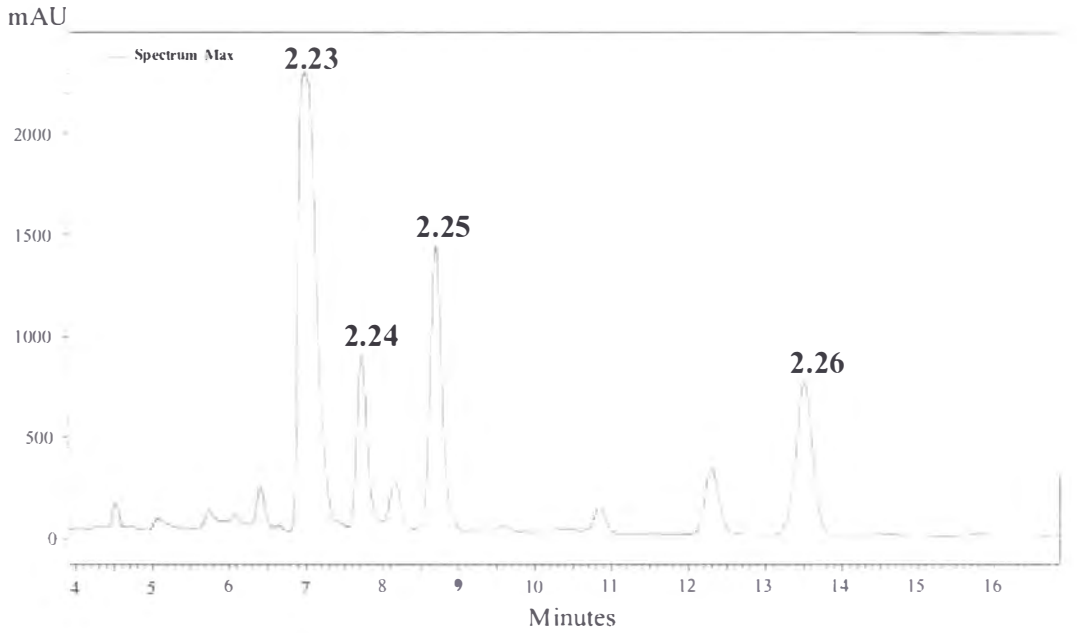

Figure 2.3: HPLC trace of the combined fractions wjm12-701 to 12-703 indicating the four compounds (peaks) of interest (**2.23**, **2.24**, **2.25** and **2.26**).

2.5: Structural Elucidation of Compounds Isolated from Rhabderemia stelletta

*2.5.1: Structural Elucidation of **2.23***

The first compound (**2.23**) was isolated as a pale yellow oil (6.5 mg). High resolution electrospray mass spectrometry (HRESIMS) identified a $[M+Cs]^+$ ion at *m/z* 583.2549 (calc 583.2552) which led to the molecular formula $C_{31}H_{46}O_2$. The ^{13}C nuclear magnetic resonance (NMR) spectrum (**Figure 2.4**) combined with the heteronuclear single quantum coherence (HSQC) spectrum identified 14 well-defined carbon signals corresponding to: six olefinic carbons (δ_C 146.2 (δ_H 5.99), 134.4 (δ_H 5.86), 133.5 (δ_H 5.86), 129.5 (δ_H 5.57), 128.4 (δ_H 5.58) and 107.0 (δ_H 5.42)), two oxymethine carbons (δ_C 63.2 (δ_H 4.80) and 62.7 (δ_H 4.82)), and 6

acetylenic carbons, two of which were protonated (δ_C 86.9, 83.3, 81.1 (δ_H 3.05), 80.1, 79.6 and 73.8 (δ_H 2.54)). The 10 remaining carbon signals left to satisfy the molecular formula were largely unresolved (δ_C 27.8-29.0). These signals corresponded to protons at δ_H 1.26-1.39 which dominated the ^{1}H NMR spectrum (**Figure 2.5**) and were subsequently assigned as methylene units of a long alkyl chain.

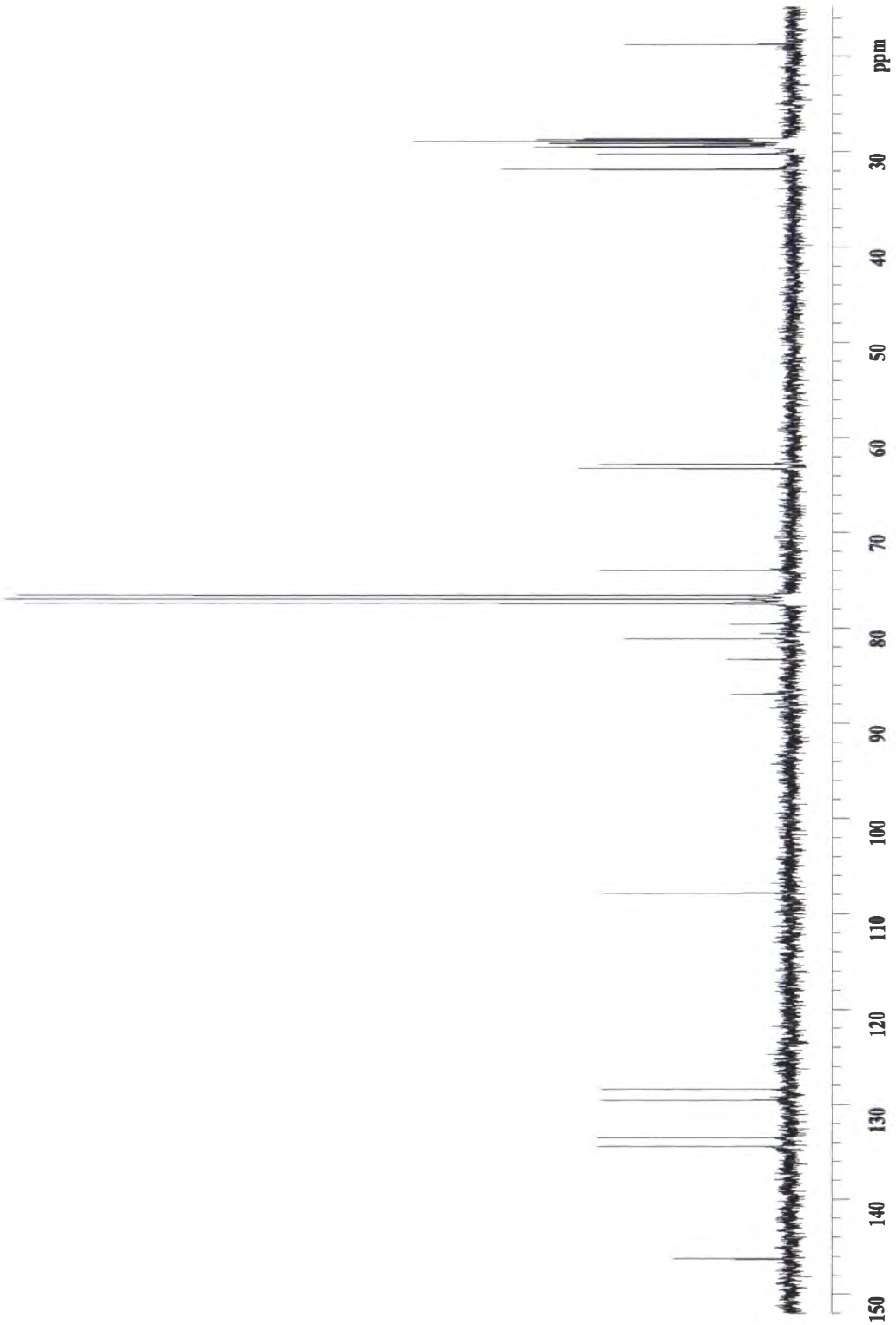

Figure 2.4: The ^{13}C NMR spectrum of **2.23** ($CDCl_3$).

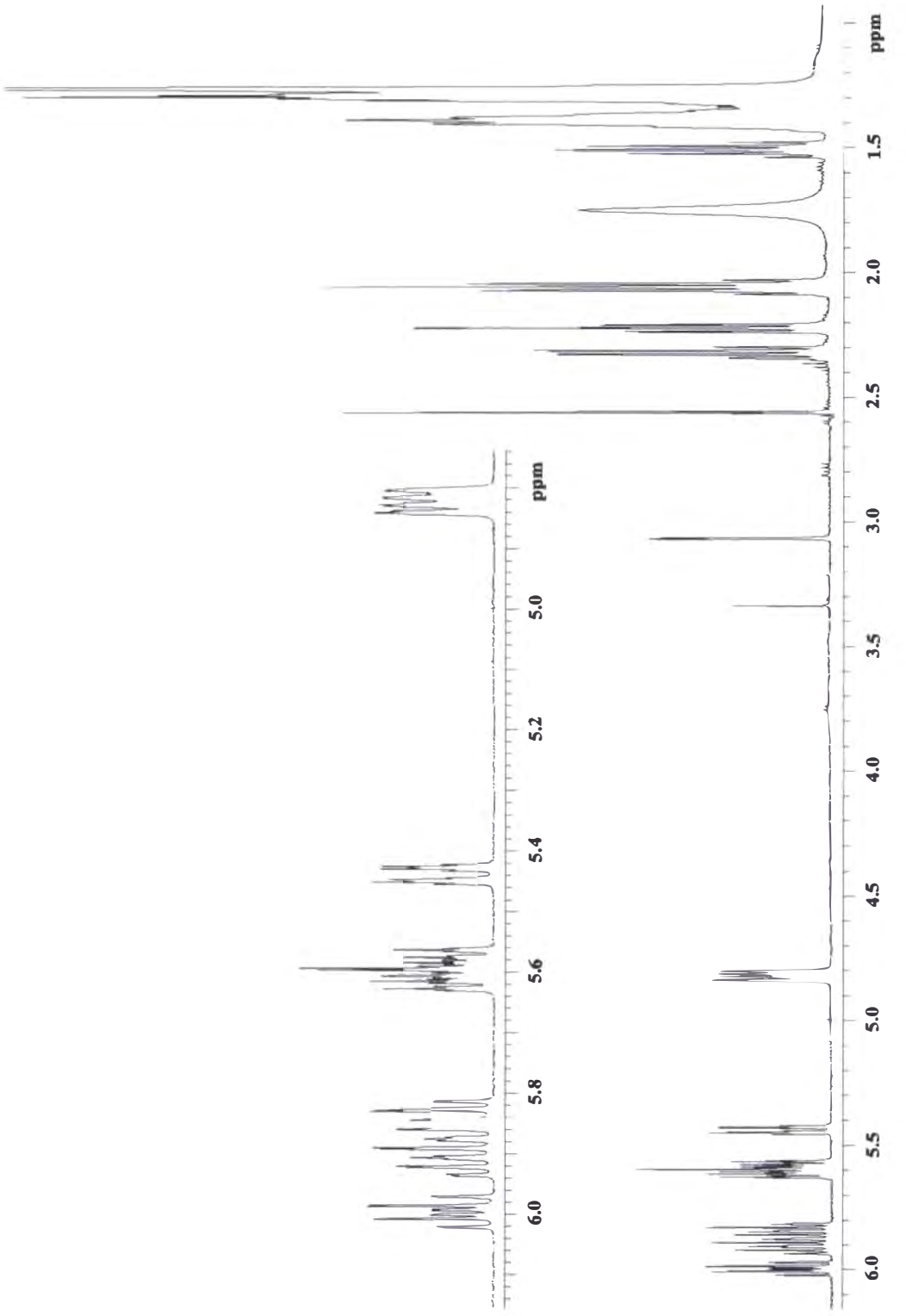

Figure 2.5: The ^{1}H NMR spectrum of **2.23** ($CDCl_3$).

Analysis of the ^{1}H-^{1}H correlation spectroscopy (COSY) spectrum (see **Figure 2.11**, page 57) revealed cross peak correlations from both the H-4 and H-5 (δ_H 5.58 and 5.86, respectively) olefinic protons to the H-3 (δ_H 4.82) oxymethine and H-6 (2.05) methylene protons. The H-3 (δ_H 4.82) oxymethine proton was also COSY correlated to the H-1 (δ_H 2.54) terminal acetylene proton *via* long range coupling ($J_{1,3}$ = 2.0 Hz); the position of the terminal acetylenic proton was confirmed with the constant time inverse-detected gradient accordion rescaled long-range heteronuclear multiple bond correlation (CIGAR) experimental correlations from the H-1 (δ_H 2.54) terminal acetylenic proton to the C-2 (δ_C 83.3) acetylenic carbon, and from the H-3 (δ_H 4.82) oxymethine proton to the C-2 (δ_C 83.3) acetylenic carbon and the C-4 and C-5 (δ_C 128.4 and 134.4, respectively) olefinic carbons. Connectivity from carbon C-1 to C-6 was established providing the partial structure **A** (**Figure 2.6**). The geometric configuration of the double bond positioned at C-4/C-5 was assigned as (*E*) based on the vicinal coupling constant between the H-4 and H-5 (δ_H 5.58 and 5.86, respectively, $J_{4,5}$=16.5 Hz) olefinic protons. For structural clarity, only the key NMR correlations discussed in the text are depicted in the structural figures.

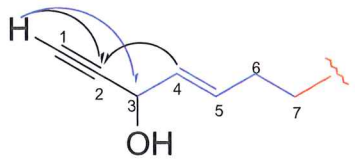

A

Figure 2.6: Partial structure **A**, with key COSY (blue) and CIGAR (black) NMR correlations.

The long-range COSY correlation from the H-29 (δ_H 5.42) proton to the H-31 (δ_H 3.05, $J_{29,31}$ = 2.0 Hz) terminal acetylene proton combined with the CIGAR correlations from the H-28 (δ_H 5.99) olefinic proton to C-26, C-27, C-29 and C-30 (δ_C 28.7, 30.2, 107.9 and 80.1, respectively) carbons defined the connectivity from C-26 to C-31, validating partial structure **B** (**Figure 2.7**). The geometry of the double bond C-28/C-29 was assigned as (*Z*) based upon the comparison of the experimental ^{13}C NMR chemical shifts to published data for the C-28/C-29

olefinic carbons[109,132] of similar compounds, and the coupling constant between the H-28/H-29 ($J_{28,29}$=10.5 Hz) protons extracted from the ^{1}H NMR spectrum.

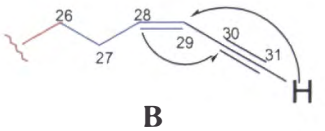

B

Figure 2.7: Partial structure **B** with key COSY (blue) and CIGAR (black) NMR correlations.

The partial structure **C** (**Figure 2.8**) was tentatively determined to be similar to that of partial structure **A** (**Figure 2.6**) on the basis of the ^{1}H NMR chemical shift comparisons. However, the triple bond contained within this partial structure was found to be internal based on the fact that both the C-15 and C-16 carbons were *sp* quaternary. The orientation of the C-15 and C-16 carbons was determined by the CIGAR correlation from the H-18 (δ_H 5.57) olefinic proton to the C-16 (δ_H 79.6) acetylenic carbon. The connectivity from C-12 to C-21 was achieved *via* a combination of both COSY and CIGAR NMR data. COSY correlations from the H-13 (δ_H 1.50) methylene protons to the H-14 and H-12 (δ_H 2.22 and 1.26-1.39, respectively) methylene protons secured C-12 to C-14, while the CIGAR correlations from the H-14 (δ_H 2.22) methylene protons to the C-13, C-15 and C-16 (δ_C 28.9, 86.9 and 79.2 respectively) carbons established C-13 to C-16 connectivity. The CIGAR correlation from the δ_H 4.80 (H-17) oxymethine proton signal to both C-15 and C-16 (δ_C 86.9 and 79.2, respectively) acetylenic carbons established that the oxymethine proton was located on the C-17 carbon position. The COSY cross peak correlations from the H-18 (δ_H 5.57) olefinic proton to both H-17 and H-19 (δ_H 4.80 and 5.89, respectively) protons, defined C-17 to C-19, while COSY correlations from the H-20 (δ_H 2.05) methylene protons to the H-19 (δ_H 5.89) olefinic proton and the H-21 (δ_H 1.26-1.29) methylene protons completed connectivity from C-19 to C-21, as shown in partial structure **C** (**Figure 2.8**). The configuration of the double bond C-18/C-19 was assigned as (*E*) based on the coupling constant between the H-18 and H-19 (δ_H 5.57 and 5.89, respectively, $J_{18,19}$=16.5 Hz) olefinic protons and comparison of their ^{13}C NMR chemical shifts with similar compounds previously isolated.[109]

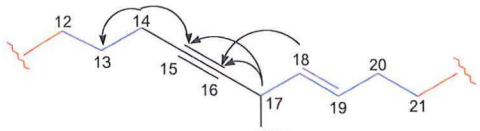

C

Figure 2.8: Partial structure **C** with key COSY (blue) and CIGAR (black) NMR correlations.

The remaining atoms ($C_{10}H_{20}$) satisfying the molecular formula were designated as long-chain methylene units connecting the partial structures **A** to **C** and **B** to **C**. Elucidation of the long-chain methylene units was performed by careful examination of the COSY, HSQC and CIGAR data. Due to the nature of the overlapping signals, no conclusive assignment could be made. The total correlation spectroscopy (TOCSY) experiment was utilized. In the TOCSY experiment, magnetization is propagated along a spin system by successive scalar coupling and all protons that sit within the same spin-system are correlated, regardless of whether they are directly coupled to one another. It is well known that in a linear molecule the deshielding effect of a substituent diminishes as the distance between it and the proton increases.[133] The H-28 (δ_H 5.99) proton was selected for irradiation based upon the fact that it possessed a well defined chemical shift. Various mixing times were selected to enhance relayed coherence transfer through the upfield protons, in an attempt to observe the long-range ^{1}H-^{1}H correlations through the alkyl chain to either the H-14 (δ_H 2.22) or H-19 (δ_H 5.89) protons, depending upon the orientation of the central unit. Correlations from the H-28 (δ_H 5.99) proton would determine the number of methylene groups connecting partial structures **B** and **C** and the orientation of the central unit **C**. This would also allow the remaining methylene units linking **A** to **C** to be assigned by default. No TOCSY correlations to either H-14 or H-19 (δ_H 2.22 and 5.86, respectively) protons were observed when H-28 (δ_H 5.99) was irradiated, as displayed in **Figure 2.9**.

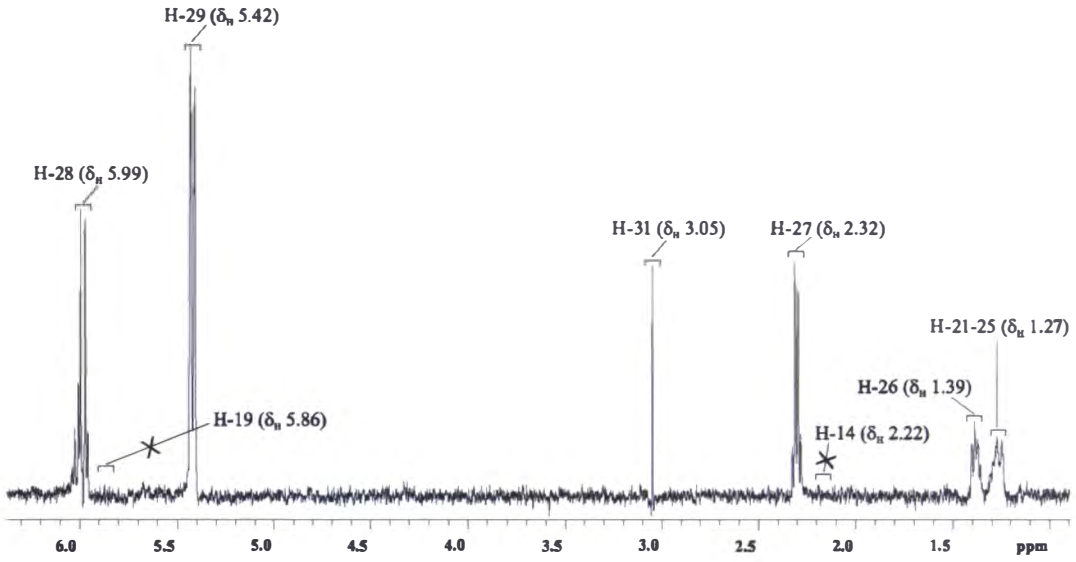

Figure 2.9: TOCSY correlations observed for irradiated proton H-28 (δ_H 5.99) (mixing time=0.08 ms).

Therefore, the overall gross structure could not be unambiguously determined by TOCSY NMR experiments. Both alkyl subunits (X and Y, **Figure 2.10**) contain protons and carbons with similar chemical shifts and it would not be unreasonable to suggest that the alkyl chains have similar lengths, however, this data would also support a variety of lengths assigned to each linking 'section' between subunits **A** to **C** and **C** to **B** where X+Y=10 ($C_{10}H_{20}$), for the methylene subunits.

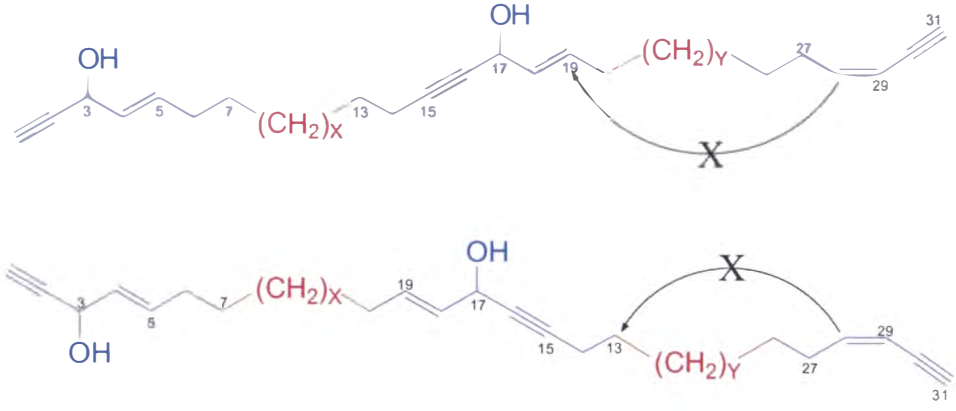

Figure 2.10: Diagnostic TOCSY correlations (black) for **2.23**, two possible orientations of substructure **C**. Confirmed portions of structure are in blue, while unconfirmed in red.

EI mass spectrometry was employed as an indirect method to fix the location of the double bonds by the identification of conspicuous mass fragments. Unfortunately no significant fragments were observed to aid in the assignment of the overall structure.

The absolute configuration of compound **2.23** could not be determined by any chemical method due to the compound's subsequent degradation while undergoing NMR experimental analysis.

Experimental ^{1}H, ^{13}C and 2D NMR data for **2.23** are shown in **Table 2.1**.

Table 2.1: The ^{1}H, ^{13}C, COSY and CIGAR NMR data for **2.23** ($CDCl_3$).

position†	$^{13}C\ \delta_C$§	$^{1}H\ \delta$ ξ	COSY	CIGAR
1	73.8 (CH)	2.54 (d, 2.0)	H-3	C-3, C-2
2	83.3 (C)			
3	62.7 (CH)	4.82 (br d, 5.5)	H-4, H-1	C-5, C-4, C-2
4	128.4 (CH)	5.58 (dd, 16.5, 6.0)	H-5, H-3	C-6, C-3, C-2
5	134.4 (CH)	5.86 (dt, 16.5, 6.5)	H-6, H-4	C-6, C-3
6	31.8 (CH_2)	2.05 (m)	H-7, H-5	C-7, C-5, C-4
7	29.0 (CH_2)	1.40 (m)		C-6, C-5
8-12‡	27.8-29.0 (CH_2)	1.26-1.39 (m)		
13	28.9 (CH_2)	1.50 (q, 7.0)	H-14, H-12	C-15, C-14
14	18.7 (CH_2)	2.22 (td, 6.5, 2.0)	H-13	C-17, C-16, C-15, C-13
15	86.9 (C)			
16	79.2 (C)			
17	63.2 (CH)	4.80 (br d, 6.0)	H-19	C-19, C-18, C-16, C-15
18	129.5 (CH)	5.57 (dd, 16.5, 6.0)	H-20, H-19	C-20, C-19, C-17, C-16
19	133.5 (CH)	5.86 (dt, 16.5, 6.5)	H-20, H-18	C-21, C-20, C-18, C-17
20	31.8 (CH_2)	2.05 (m)	H-21, H-19	C-22, C-21, C-19
21-25‡	27.8-29.0 (CH_2)	1.26-1.39 (m)		
26	28.7	1.39 (m)	H-27	
27	30.2 (CH_2)	2.32 (q, 6.5)	H-28, H-26	C-29, C-28, C-26
28	146.2 (CH)	5.99 (dt, 10.5, 7.0)	H29, H-27	C-30, C-29, C-26
29	107.9 (CH)	5.42 (br d, 10.5)	H-31, H-28	C-30, C-28
30	80.1 (C)			
31	81.1 (CH)	3.05 (d, 2.0)	H-29	C-30, C-29

† Numbering defined as the two primary alcohols in (**2.23**) at C-3 and C-17 and the terminal acetylenes at C-1 and C-31. § ^{13}C NMR chemical shift values (δ ppm from $CDCl_3$ at 77.0) obtained on Unity 300 (75 MHz). ξ ^{1}H NMR spectrum recorded at 500 MHz in $CDCl_3$ (δ ppm from $CDCl_3$ at 7.25) followed by multiplicity and coupling constant(s) (*J*/Hz). ‡Inconclusive chemical shift assignment and coupling constants ($J_{H\text{-}H}$), due to signals being overlapped.

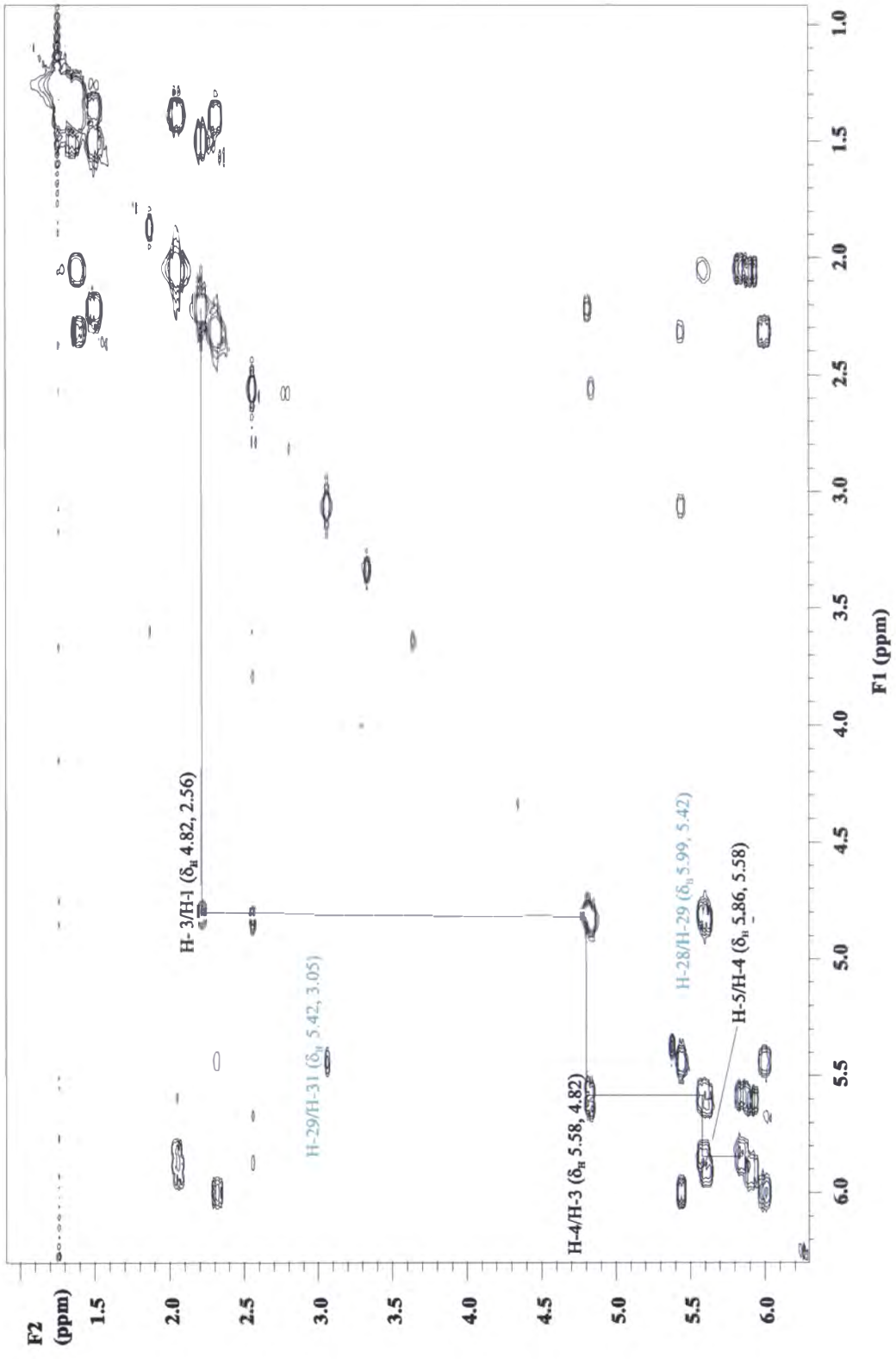

Figure 2.11: The COSY NMR spectrum indicating H-1 (black) and H-31 (blue) correlations from the terminal acetylene protons of **2.23**.

2.5.2: Structural Elucidation of **2.24**

The second compound to elute was **2.24**, which was isolated as a pale yellow oil (4.5 mg). HRESIMS identified a $[M+Cs]^+$ ion at *m/z* 581.2396 (calc. 581.2396) which led to a molecular formula of $C_{31}H_{44}O_2$, two mass units less than the previously isolated compond **2.23**. Both the ^1H and ^{13}C NMR spectra (**Figures 2.12** and **2.13** respectively) were reminiscent of **2.23**, with some significant differences. The loss of a proton signal at δ_H 4.80 (H-3 or H-17), the downfield shift of the two olefinic protons at δ_H 5.57 (H-18) and 5.89 (H-19) to δ_H 7.10 and 6.14 respectively, and the appearance of a new signal at δ_H 2.28 were noted. These changes strongly suggest that this compound may be the oxidation product of **2.23**, thus satisfying the requirements of the mass spectral data.

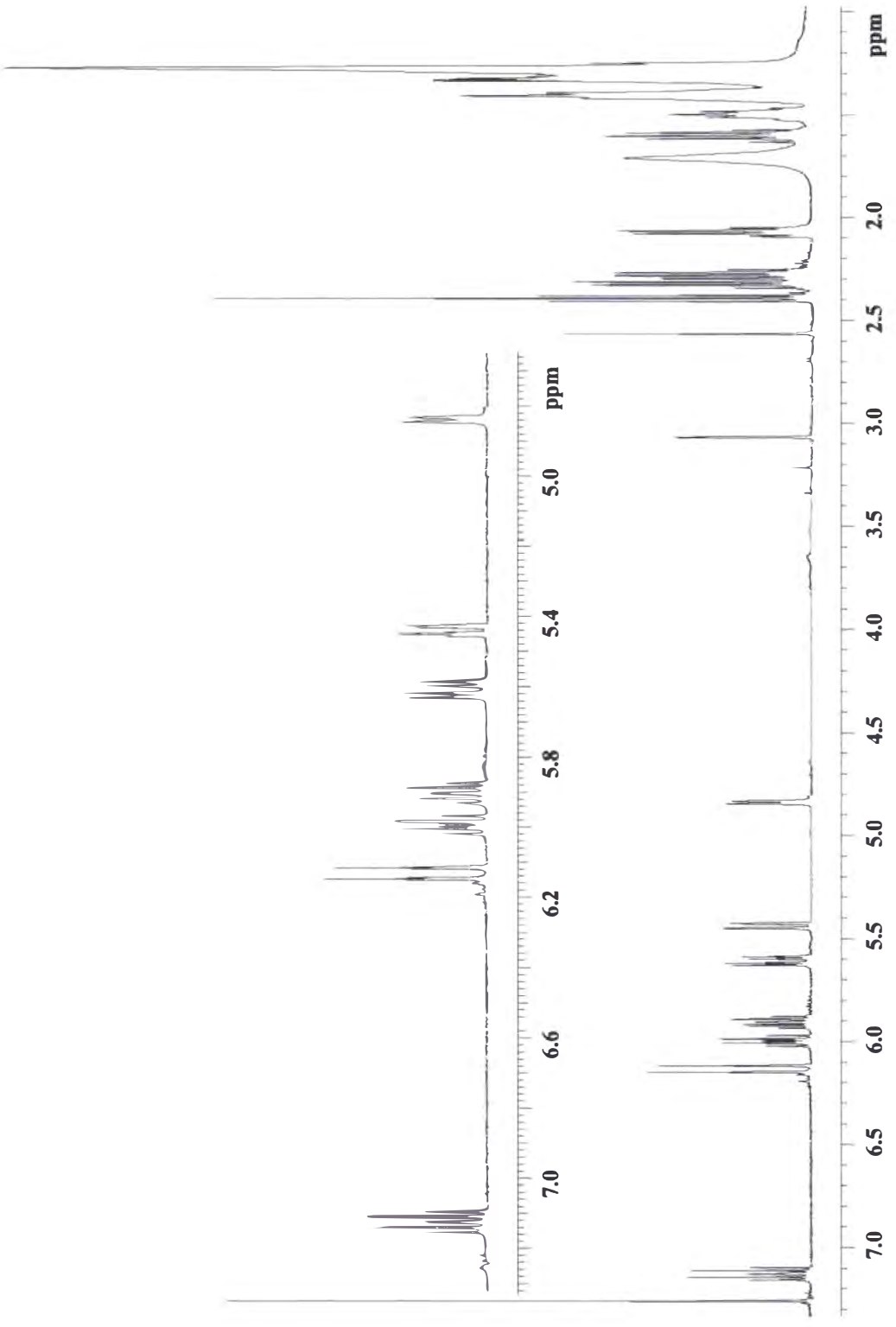

Figure 2.12: The ^{1}H NMR spectrum of **2.24** ($CDCl_3$).

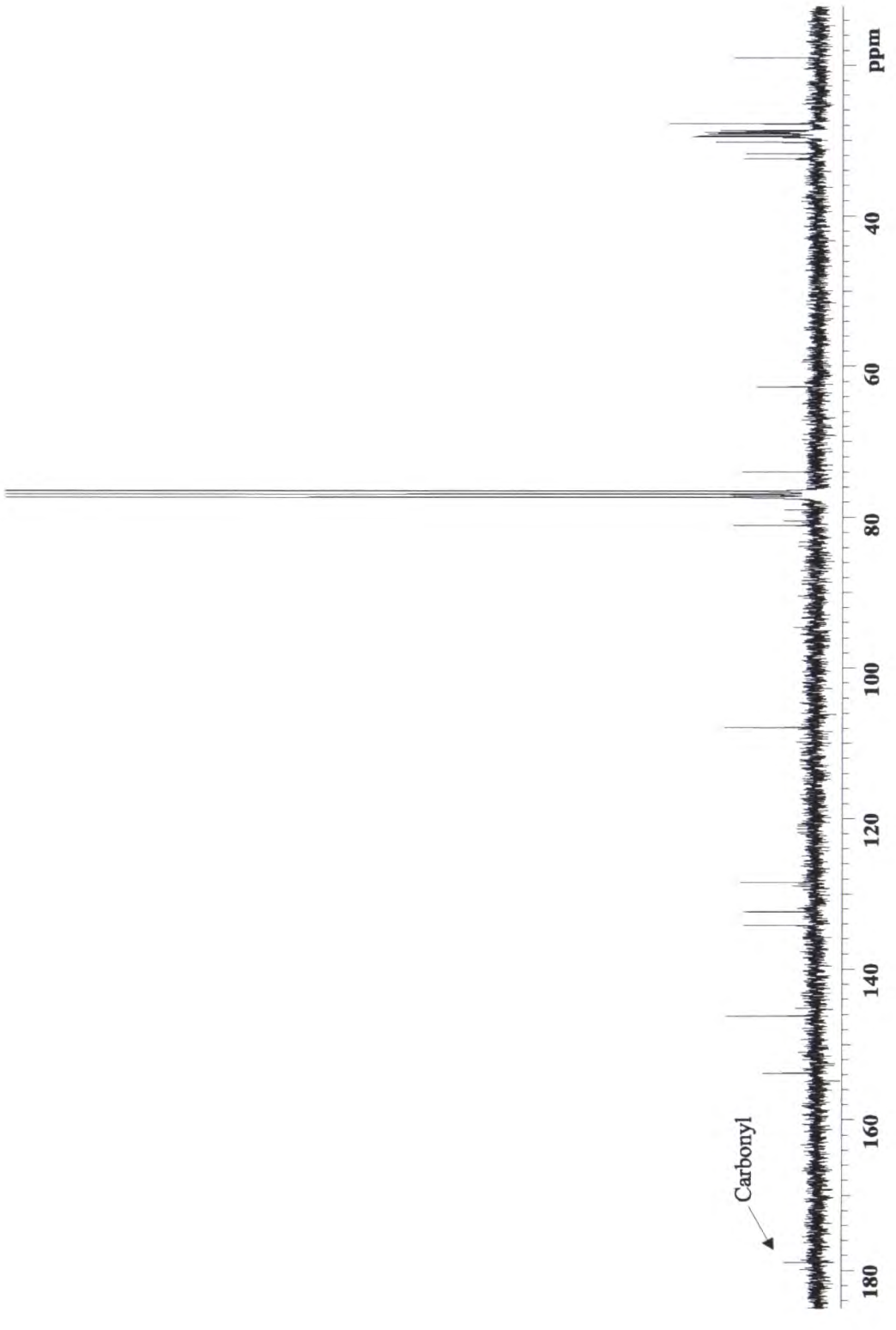

Figure 2.13: The ^{13}C NMR spectrum of **2.24** indicating the addition of a carbonyl peak at δ_C 179.0 ($CDCl_3$).

The ^{13}C NMR spectrum revealed an additional signal at δ_C 179.0 suggesting the presence of a carbonyl group at C-17 as a downfield shift of the C-18 (from δ_C 129.5 (**2.23**) to δ_C 153.9) olefinic carbon was observed. The COSY (see **Figure 2.17**, page 65) cross peak correlation from the H-18 (δ_H 7.10) olefinic proton to the H-19 (δ_H 6.14) olefinic proton, combined with the CIGAR correlations from the H-18 (δ_H 7.10) olefinic proton to the C-15, C-16 and C-17 (δ_C 94.6, 79.2 and 179.0, respectively) carbons indicated that the carbonyl group was conjugated with both the alkyne and the olefin groups, suggesting an *α, β*-unsaturated ketone with the carbonyl α to the acetylene moiety. Consecutive COSY correlations from the H-11 (δ_H 1.27) alkyl methylene protons to H-12, H-13 and H-14 at (δ_H 1.41, 1.60 and 2.22, respectively), combined with the H-18 (δ_H 7.10) olefinic proton to H-19, H-20, H-21 and H-22 (δ_H 6.14, 2.28, 1.50 and 1.32, respectively), defined the partial structure **D** (**Figure 2.14**) from carbons C-11 to C-22. Due to the deshielding effect of the carbonyl functionality, a greater number of methylene units could be defined. The geometry of the double bond was determined to be (*E*) based on the H-18/H-19 proton coupling constants extracted from the ^1H NMR spectrum ($J_{18,19}$ = 15.5 Hz) and chemical shift comparison with those from partial structure **C** (**Figure 2.8**).

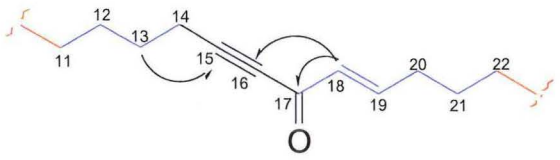

D

Figure 2.14: Proposed partial structure **D** with key COSY (blue) and CIGAR (black) NMR correlations.

Analysis of the NMR data, including ^1H, ^{13}C, COSY, HSQC and CIGAR NMR spectra also led to the conclusion that **2.24** contained the same partial structures **A** and **B** (**Figure 2.15**) as determined for compound **2.23**. The geometry of the double bonds was confirmed by ^{13}C NMR chemical shift data and coupling

constants and assigned as (*E*) for the C-4/C-5 ($J_{4,5}$ = 16.5 Hz) carbons and (*Z*) for the C-28/C-29 ($J_{28,29}$ = 10.5) carbons.

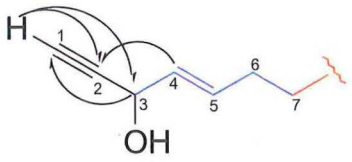

A

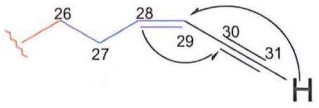

B

Figure 2.15: Partial structures **A** and **B** with key COSY (blue) and CIGAR (black) NMR correlations.

No TOCSY NMR data was obtained for **2.24**, due to subsequent compound degradation. Although a greater number of methylene units could be defined for partial structure D, the molecular formula still required C_6H_{12} to be assigned. Because of the overlapping nature of the chemical shifts for the remaining carbons (δ_C 28.0-29.0) and protons (δ_H 1.26-1.39), it was concluded that the number of methylenes linking partial structures **A** to **D** and **D** to **B** would be similar. However, to satisfy the mass requirements X+Y had to equal six methylene units. No information regarding the orientation of the central partial structure **D** was available; therefore, no unambiguous assignment of **2.24** could be made. **Figure 2.16** is a representation of the possible orientations and connectivities of the proposed subunits.

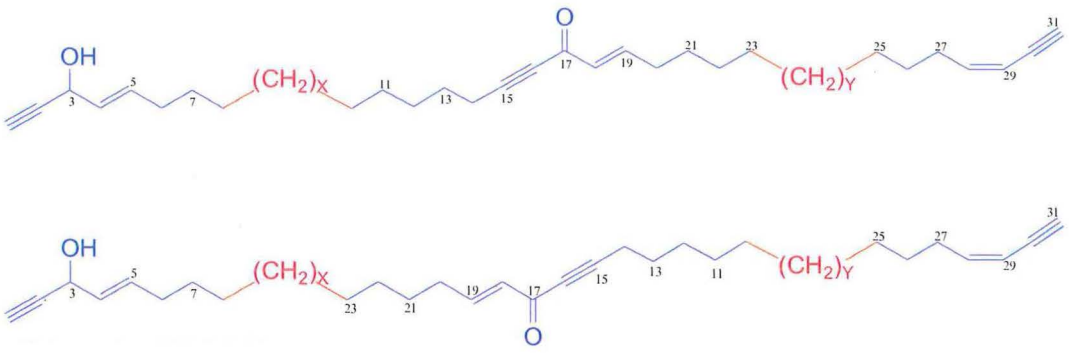

Figure 2.16: Proposed connectivity for subunits **A**, **B** and **D** where X+Y=6, confirmed partial structures in blue, unassigned methylene portions in red.

The subsequent degradation of compound **2.24** meant that no further mass spectrometric, NMR or chemical experiments could be carried out to obtain additional structural information for the unambiguous assignment of **2.24**.

The NMR data for compound **2.24** is shown in **Table 2.2**.

Table 2.2: The ^{1}H, ^{13}C, COSY and CIGAR NMR data for **2.24** ($CDCl_3$).

Position[†]	^{13}C δ[§]	^{1}H δ [ζ]	COSY	CIGAR
1	74.2 (CH)	2.54 (d, 2.0)	H-3	C-3, C-2
2	83.6 (C)			
3	62.7 (CH)	4.82 (br d, 5.5)	H-4, H-1	C-5, C-4, C-2, C-1
4	128.3 (CH)	5.58 (dd, 16.5, 6.0)	H-5, H-3	C-6, C-3, C-2
5	134.1 (CH)	5.86 (dt, 16.5, 6.5)	H-6, H-4	C-6, C-4, C-3
6	32.0(CH_2)	2.05 (m),	H-7, H-5	C-7, C-5, C-4
7	27.8 (CH_2)	1.39 (m)		C-8, C-6, C-5
8-10[‡]	28.0-29.0 (CH_2)	1.26-1.39		
11	28.9 (CH_2)	1.27 (m)	H-12, H-10	
12	29.0 (CH_2)	1.41 (m)	H-13, H-11	
13	28.0 (CH_2)	1.60 (q, 7.0)	H-14, H-12	C-15, C-14, C-12, C-11
14	19.2 (CH_2)	2.22 (td, 6.5, 2.0)	H-13	C-16, C-15, C-13, C-12
15	94.6 (C)			
16	79.2 (C)			
17	179.0 (CO)			
18	153.9 (CH)	7.10 (m)	H-19	C-20, C-19, C-17, C-16
19	132.4 (CH)	6.14 (m)	H-20, H-18	C-21, C-20, C-18, C-17
20	32.4 (CH_2)	2.28 (m)	H-21, H-19	C-22, C-21, C-19
21	29.0 (CH)	1.50 (m)	H-22, H-20	C-23, C-22, C-20, C-19
22	1.32 (CH_2)	1.32 (CH_2)		
23-25[‡]	28.0-29.0 (CH_2)	1.26-1.39 (m)		
26	28.9 (CH_2)	1.39 (m)	H-27, H-25	
27	30.0 (CH_2)	2.32 (q, 6.5)	H-28, H-26	C-29, C-28, C-26
28	146.1 (CH)	5.98 (dt, 10.5, 7.0)	H29, H-27	C-30, C-29, C-27
29	108.0 (CH)	5.43 (br d, 10.5)	H-31, H-28	C-30, C-28
30	80.1 (C)			
31	81.0 (CH)	3.07 (d, 2.0)	H-29	C-30, C-29

[†] Numbering defined as the primary alcohol in (**2.24**) at C-3 and the carbonyl carbon at C-17, while the terminal acetylenes are at C-1 and C-31. [§] ^{13}C NMR chemical shift values (δ ppm from $CDCl_3$ at 77.0) obtained on Unity 300 (75 MHz). [ζ] ^{1}H NMR spectrum recorded at 500 MHz in $CDCl_3$ (δ ppm from $CDCl_3$ at 7.25) followed by multiplicity and coupling constant(s) (*J*/Hz). [‡]Inconclusive chemical shift assignment and coupling constants ($J_{H\text{-}H}$), due to signals being overlapped.

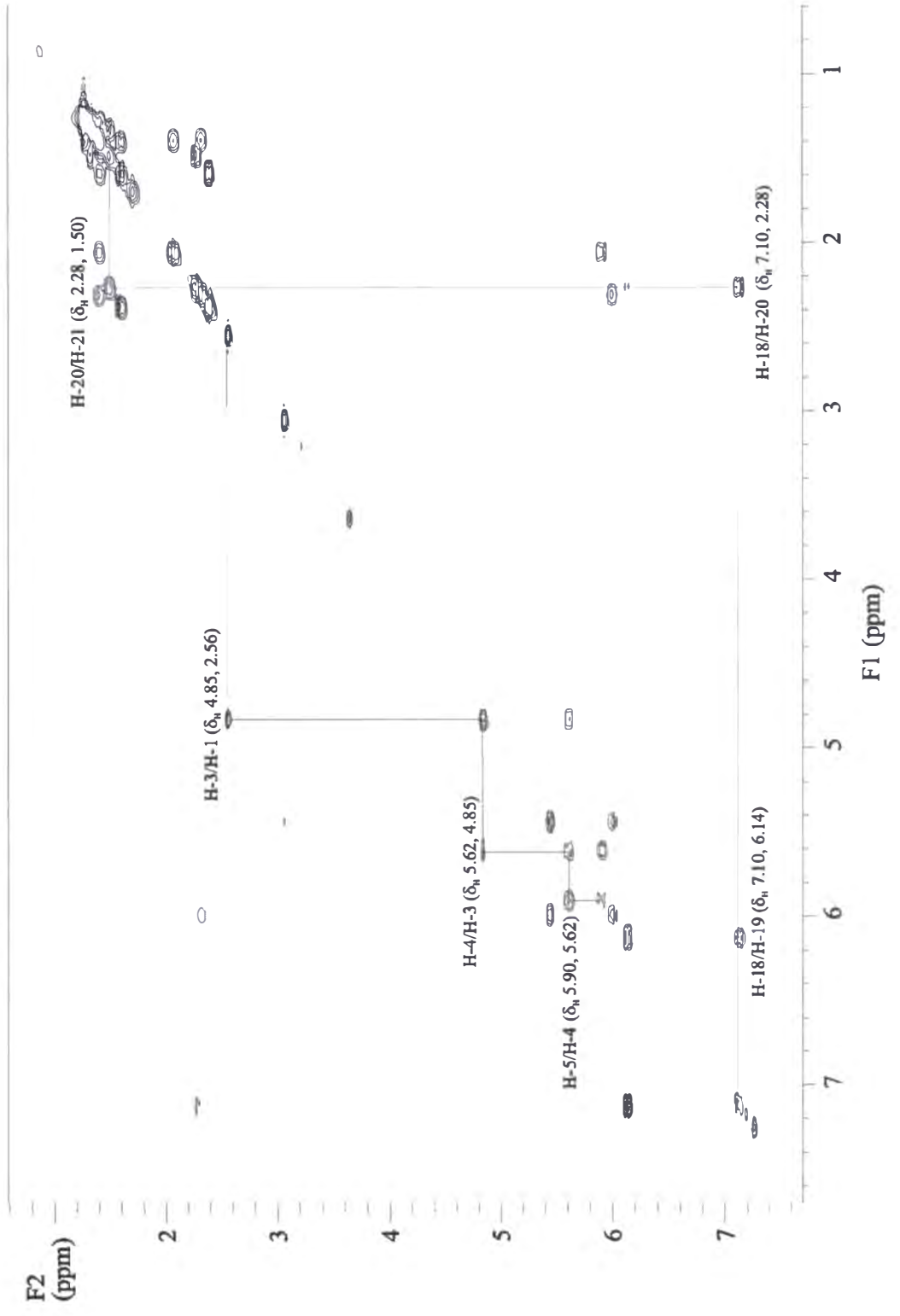

Figure 2.17: The COSY NMR spectrum of **2.24** indicating the correlations from the H-3 (δ_H 4.85) oxymethine proton (black), and the H-18 (δ_H 7.10) proton α to the C-17 carbonyl (blue).

2.5.3: Structural Elucidation of **2.25**

The third compound to elute was also isolated as a pale yellow oil (2.3 mg). HRESIMS identified a $[M+Cs]^+$ ion at *m/z* 583.2547 (calc. 583.2552) corresponding to a molecular formula of $C_{31}H_{46}O_2$. This compound was therefore isobaric with **2.23**. Both the ^1H (**Figure 2.18**) and COSY (**Figure 2.19**) NMR spectra had features in common with those observed for **2.23**. These included two acetylenic protons (δ_H 2.56, 3.07) and six olefinic protons (δ_H 5.45, 5.61 5.68, 5.91 6.00 and 6.03). However, an obvious difference was that although compound **2.25** contained two oxymethine protons, one had shifted upfield from δ_H 4.80 to 4.14 (δ_C 63.2 to 72.7, respectively) and was no longer a broad doublet, but a quartet (integrating for one proton), indicating that it was now located in a more electron rich environment.

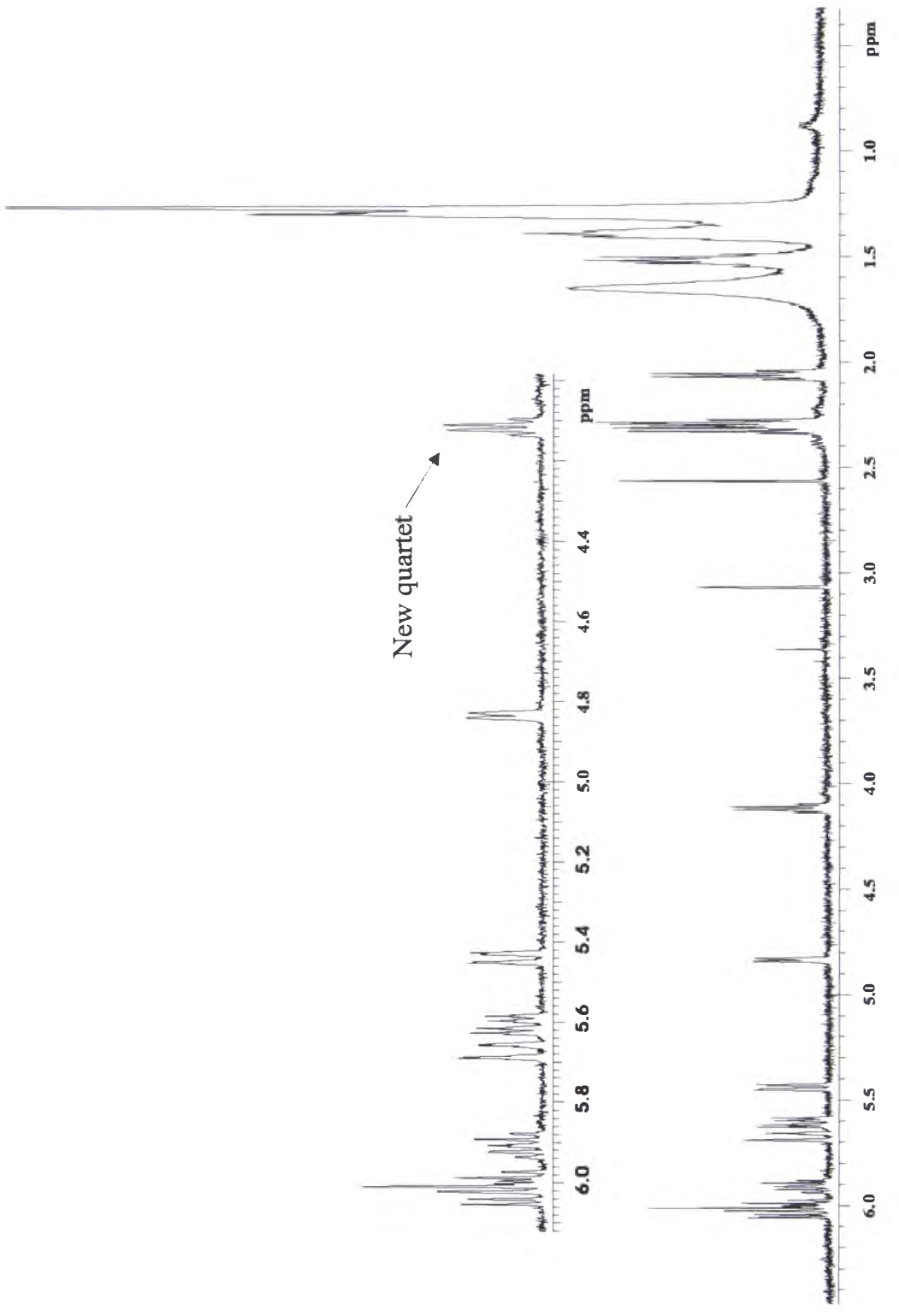

Figure 2.18: The ^{1}H NMR spectrum of **2.25** ($CDCl_3$), new quartet peak indicated.

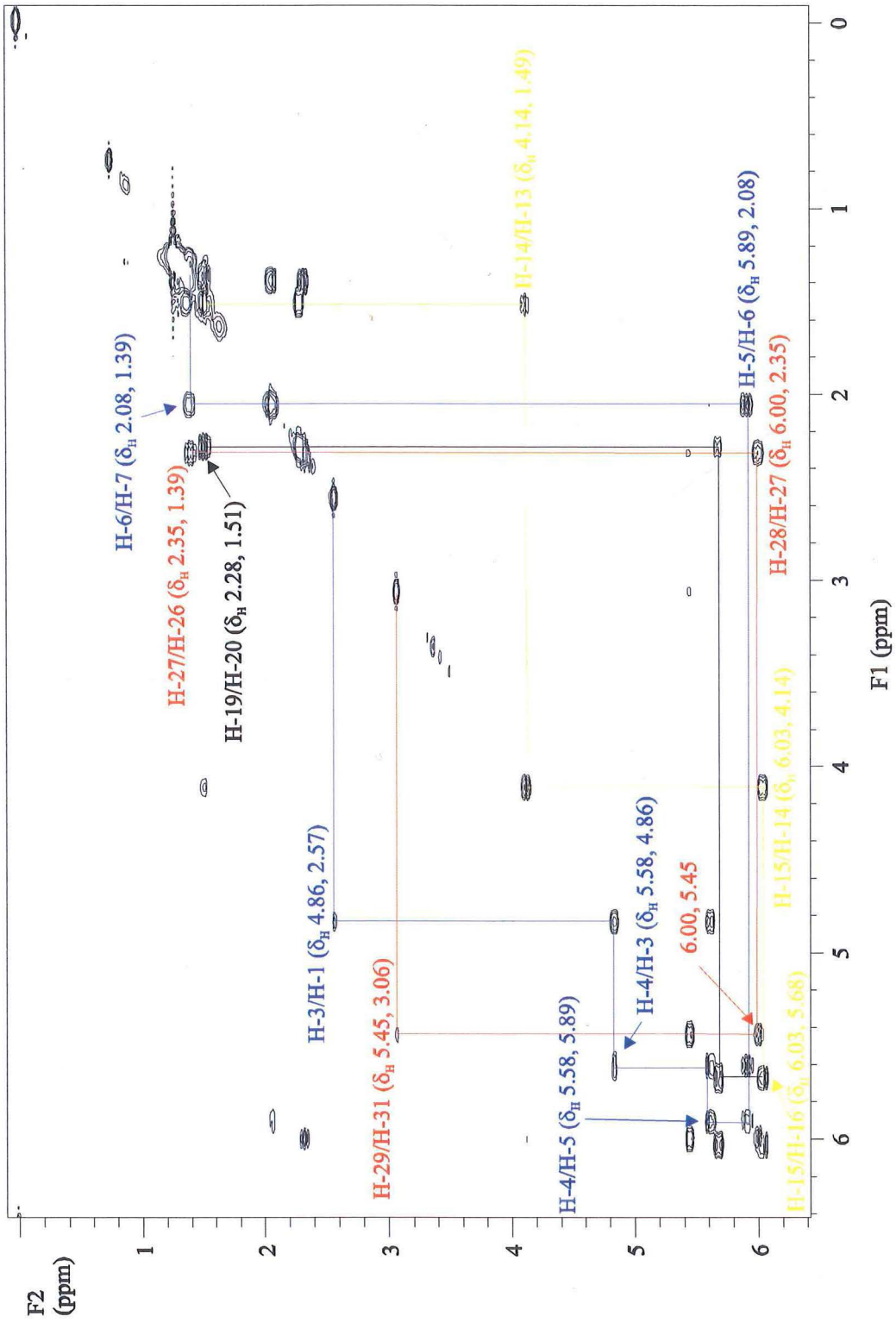

Figure 2.19: The COSY NMR spectrum of **2.25**, with key cross peak correlations from the H-1 and H-31 (δ_H 2.57 (blue) and 3.06 (red), respectively) terminal alkyne protons, the H-14 (δ_H 4.41, yellow) oxymethine proton and the H-16 (δ_H 5.68, black) olefinic proton ($CDCl_3$).

Due to the paucity of compound **2.25**, a minimal amount of carbon chemical shift data could be acquired and the little that was obtained was done so *via* the HSQC and CIGAR NMR experiments. Therefore it was necessary to elucidate the structure of **2.25** by careful comparison of the proton chemical shifts observed for the previously described compounds **2.23** and **2.24** (see **Sections 2.5.1** and **2.5.2**).

Partial structure **A** (**Figure 2.20**) was assembled by the sequential COSY cross peak correlations. The H-1 (δ_H 2.57) terminal acetylenic proton was coupled by long-range COSY correlations to the H-3 (δ_H 4.86) oxymethine proton. Consecutive correlations from the H-3 (δ_H 4.86) oxymethine proton to the H-4 and H-5 (δ_H 5.61 and 5.91, respectively) olefinic protons and the H-6 and H-7 (δ_H 2.08 and 1.39, respectively) methylene protons, terminated this section of the molecule and completed the assignment of carbons C-1 to C-7. Overlapping proton signals made the assignment of the protons on the long-alkyl chain past the C-7 (δ_H 1.39) position impossible. The configuration of the double bond at the C-4 and C-5 carbons was assigned as (*E*) based upon the coupling constants extracted from the ^{1}H NMR spectrum for the H-4 and H-5 (δ_H 5.61 and 5.91, respectively, $J_{4,5}$ = 16.5 Hz) protons.

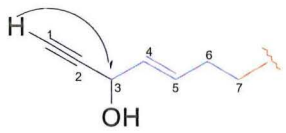

A

Figure 2.20: Key COSY correlations (blue) and the long-range correlation (black) observed in the elucidation of partial structure **A** for **2.25**.

Using the same methodology, substructure **B** (**Figure 2.21**) was constructed *via* correlations from the second terminal acetylenic proton at δ_H 3.06. Successive COSY cross peak correlations were observed from H-31 (δ_H 3.06) to the H-29, H-28, H-27 and H-26 (δ_H 5.45, 6.00, 2.35 and 1.43, respectively) protons. The poor resolution of the overlapping alkyl chain signals made any further assignment of the methylene groups beyond H-26 impossible, therefore substructure **B**, carbons C-31 to C-26, was assigned. The double bond geometry at the C-28 and C-29

carbons was defined as (*Z*) based on the proton coupling constants extracted from the ^{1}H NMR spectrum for the H-28 and H-29 (δ_H 6.00 and 5.45, respectively, $J_{28,29}$=10.5 Hz) protons, and the carbon chemical shifts observed in the CIGAR experiment for C-28 and C-29 (δ_C 146.5 and 108.2, respectively) as compared to compounds **2.23** and **2.24**.

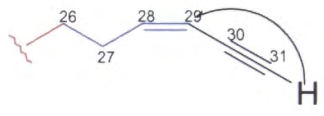

B

Figure 2.21: Observed COSY correlations (blue) for substructure **B**. Long-range correlation (black).

Substructure **E** (**Figure 2.22**) was elucidated using a combination of COSY and limited HSQC and CIGAR NMR correlations. The key COSY cross correlation was observed from the H-14 (δ_H 4.14) oxymethine proton to H-13 and H-15 (δ_H 1.49 and 6.03, respectively) protons. This indicated that the H-14 oxymethine proton was no longer α to an acetylenic carbon as in compound **2.24**. The location of the triple bond was determined by the observation of the CIGAR correlations from the H-16 (δ_H 5.68) olefinic proton to the C-17 and C-18 (δ_C 91.0 and 78.5, respectively) alkyne carbons. A long range COSY correlation was observed between the H-16 (δ_H 5.68) proton and the methylene protons at δ_H 2.28 which suggested that these alkyl protons were directly on the other side of the triple bond. This was confirmed by the CIGAR correlations from the H-19 (δ_H 2.28) methylene protons to both C-17 and C-18 (δ_C 91.0 and 78.5, respectively) alkyne carbons. Sequential COSY correlations from the H-19 (δ_H 2.28) protons to the H-20 and H-21 (δ_H 1.51 and 1.26-1.39, respectively) protons, established C-19 to C-21. The geometry of the C-15/C-16 double bond was assigned as (*E*) according to the coupling constant extracted from the ^{1}H NMR spectrum between the H-15 and H-16 (δ_H 6.03, 5.68, respectively, $J_{15,16}$ = 17.5 Hz) protons, combined with a ^{13}C NMR chemical shift comparison with similar compounds previously published.[122] This data confirmed connectivity from carbons C-13 to C-21 and allowed for the proposed partial structure **E** as shown in **Figure 2.22**.

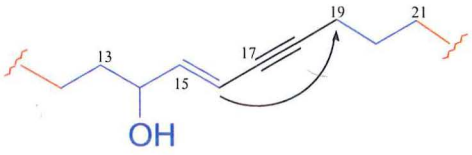

E

Figure 2.22: Partial structure **E** with key COSY (blue) and long-range COSY (black).

Connectivity between the confirmed fragments or orientation of the central partial structure **E** could not be achieved with the limited NMR experimental data. In order to satisfy the requirements of the mass spectrum, the alkyl chain fragment $C_{10}H_{20}$ (10 methylene units) required assignment. Due to the overlapped nature of the chemical shifts in this region of both the HSQC (δ_H 1.26-1.39) and ^{13}C (δ_C 28.0-29.0) NMR spectra, the exact number of carbons (X and Y) linking partial structures **A** to **E** and **E** to **B** could not be determined, however, X+Y has to equal 10. The overall structure for **2.25** is represented in **Figure 2.23** with the two possible orientations for partial structure **E**.

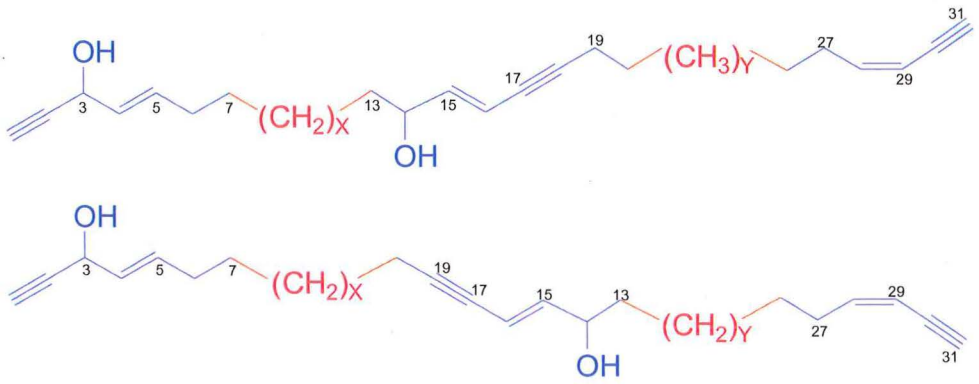

Figure 2.23: Proposed structure of compound **2.25**, where X+Y = 10.

As with the previously isolated compounds, degradation prevented any further structural information being gained; this included the stereochemistry at carbons

C-3 and C-14 and the unambiguous assignment of the central subunit by mass spectrometry or chemical modification.

Table 2.3: The ^{1}H, ^{13}C, COSY and CIGAR NMR data for **2.25** ($CDCl_3$).

Position[†]	$^{13}C\ \delta$ [§]	$^{1}H\ \delta$ [ξ]	COSY	CIGAR
1	74.2 (CH)	2.57 (d, 2.0)	H-3	
2	83.5 (C)			
3	63.0 (CH)	4.86 (br d, 5.5)	H-4, H-1	C-2
4	128.7 (CH)	5.61 (dd, 16.5, 6.0)	H-5, H-3	
5	134.8 (CH)	5.91 (dt, 16.5, 6.5)	H-6, H-4	C-6, C-3
6	32.0 (CH_2)	2.08 (m)	H-7, H-5	C-5, C-4
7	28.9 (CH_2)	1.39 (m)	H-8, H-6	
8-12[‡]	28.0-29.0 (CH_2)	1.26-1.39 (m)		
13	36.9 (CH_2)	1.49 (m)	H-12, H-14	
14	72.7(CH)	4.14 (q, 6.5)	H-15, H-13	
15	144.2 (CH)	6.03 (dd, 17.5, 6.5))	H-16, H-14	C-21, C-17
16	111.0 (CH)	5.68 (d, 17.5)	H-19, H-15	
17	91.0 (C)			
18	78.5 (C)			
19	19.5 (CH_2)	2.28 (m)	H-20, H-16	C-20, C-18, C-17
20	29.7 (CH_2)	1.51 (m)	H-21, H-19	C-21,
21-25[‡]	28.0-29.0 (CH_2)	1.26-1.39 (m)		
26	29.1 (CH_2)	1.43 (m)	H-27, H-25	
27	30.0 (CH_2)	2.35 (q, 6.5)	H-28, H-26	C-29, C-28, C-26
28	146.5 (CH)	6.00 (dt, 10.5, 7.0)	H29, H-27	C-29, C-27
29	108.2 (CH)	5.45 (br d, 10.5)	H-31, H-28	C-30, C-28
30	80.1 (C)			
31	81.1 (CH)	3.06 (d, 2.0)	H-29	

[†] Numbering defined as the two primary alcohols in (**2.25**) at C-3 and C-17 and the terminal acetylenes at C-1 and C-31. [§] ^{13}C NMR chemical shift values (δ ppm from $CDCl_3$ at 77.0) obtained from both HSQC and CIGAR experiments. [ξ] ^{1}H NMR spectrum recorded at 500 MHz in $CDCl_3$ (δ ppm from $CDCl_3$ at 7.25) followed by multiplicity and coupling constant(s) (J/Hz). [‡]Inconclusive chemical shift assignment and coupling constants ($J_{H\text{-}H}$), due to signals being overlapped.

2.5.4: Structural Elucidation of **2.26**

The final compound to elute was **2.26**; it was also isolated as a pale yellow oil (2.5 mg). HRESIMS identified a $[M+K]^+$ ion at *m/z* 503.3264 (calc. 503.3291) indicating a molecular formula of $C_{32}H_{48}O_2$, 14 mass units more than **2.25**, the previously described compound. Both the ^1H and COSY NMR spectra (**Figures 2.24** and **2.25**, respectively) were reminiscent of the compound **2.25** (**Figures 2.18** and **2.19** respectively); however two significant differences were observed. Firstly the appearance of a singlet proton signal at δ_H 3.26 (**Figure 2.24**), assigned as methyl ether protons on the basis of the HSQC correlation from δ_H 3.26 to a carbon at δ_C 56.7 (14-OCH_3), and secondly, the upfield shift of the H-14 (δ_H 4.14) quartet signal previously assigned as an oxymethine, to δ_H 3.51. The addition of a methyl ether at position C-14 would satisfy the additional mass requirement of 14 Da, and explain the chemical shift change observed for the H-14 oxymethine proton.

Due to the paucity of compound **2.26**, structural elucidation was performed by careful examination of the COSY (**Figure 2.25**) NMR data and limited HSQC and CIGAR NMR data. Partial structures **A** and **B** were easily deduced by direct comparison with data obtained from compounds **2.23** and **2.24** (**Tables 2.1** and **2.3**).

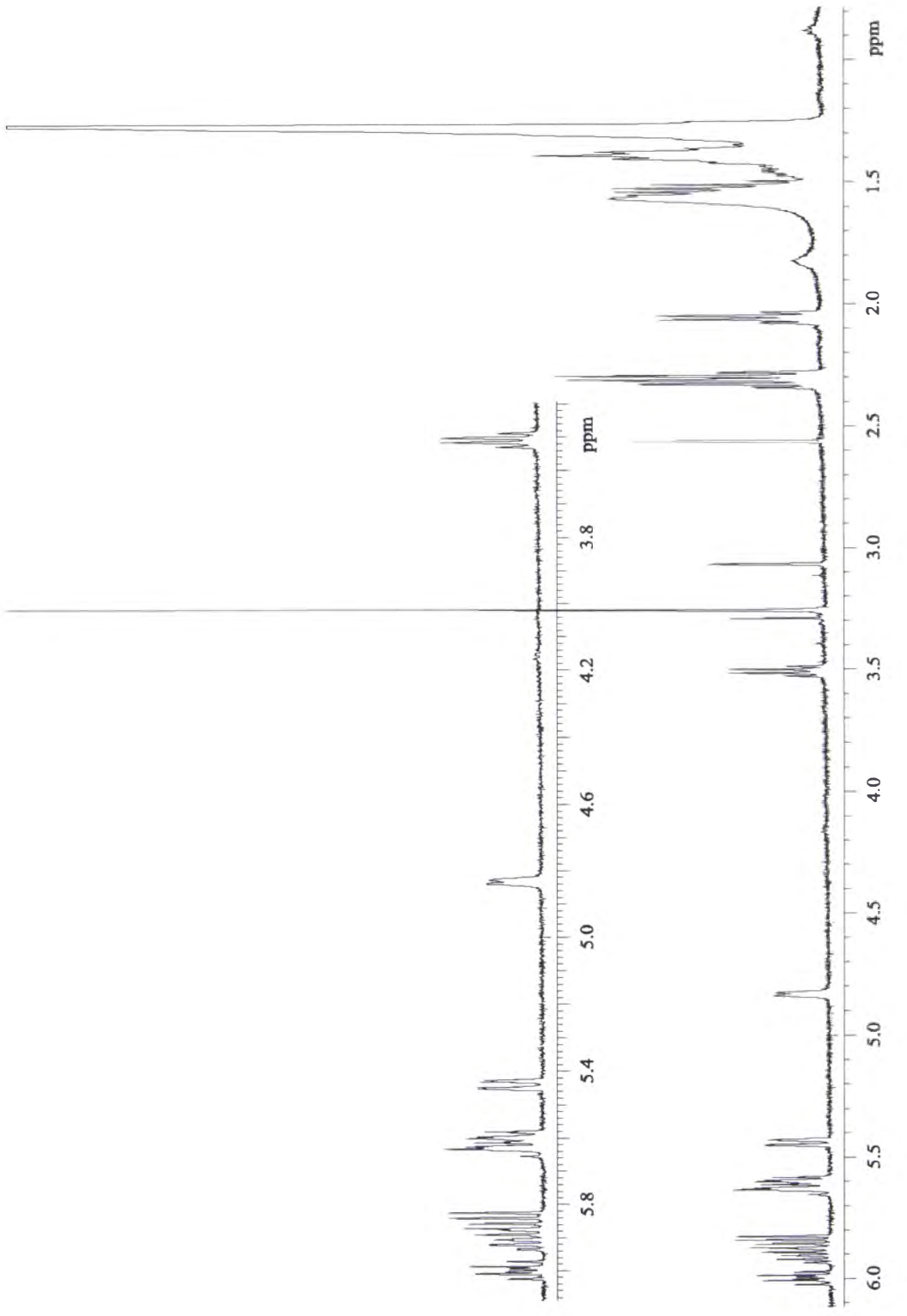

Figure 2.24: The ^{1}H NMR spectrum of **2.26** ($CDCl_3$).

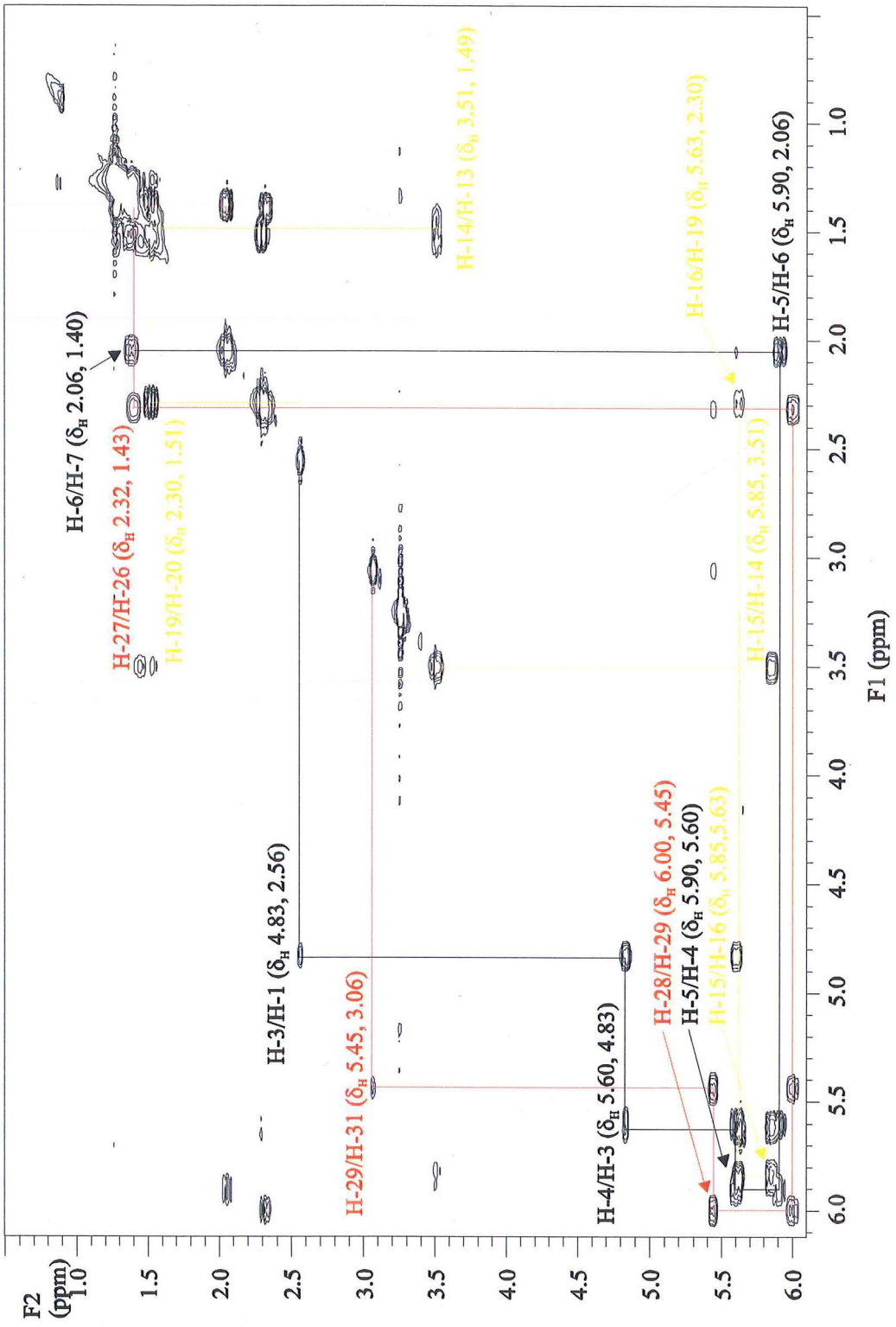

Figure 2.25: The COSY NMR spectrum of compound **2.26**, with key cross peak correlations from the H-1 and H-31 (black and red, respectively) terminal alkyne protons and the H-14 (yellow) oxymethine proton.

Partial structure **A** was assigned on the basis of COSY correlations from the H-1 (δ_H 2.56) terminal acetylenic proton to the H-3 (δ_H 4.83) oxymethine followed by sequential COSY correlations from the H-3 (δ_H 4.83) oxymethine proton to the H-4 and H-5 (δ_H 5.60 and 5.90, respectively) olefinic protons and from the H-6 (δ_H 2.06) methylene protons to both the H-5 (δ_H 5.90) olefinic proton and the H-7 (δ_H 1.40) methylene protons. This confirmed the connectivity from C-1 to C-7. As with the previous substructures, resonances for C-8 and H-8 and beyond were too heavily overlapped for individual chemical shift assignment. Therefore partial structure **A** is proposed in **Figure 2.26**.

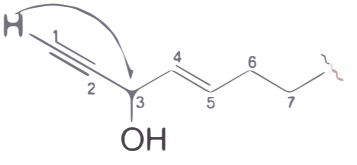

A

Figure 2.26: Key COSY (blue) and long-range COSY (black) correlations for the construction of partial structure **A**.

Partial structure **B** was elucidated using the cross peak correlation from H-31 (δ_H 3.06) the second terminal alkyl proton, to the H-29 (δ_H 5.45) olefinic proton, followed by the sequential correlations from H-29 (δ_H 5.45) to H-28 (δ_H 6.00) the second olefinic proton, and then from the H-27 (δ_H 2.32) methylene protons to both the methylene protons at 1.43 (H-26) and the olefinic proton at δ_H 6.00 (H-28). These correlations confirm the connectivity from C-26 to C-31. As before, the resonance H-25 (δ_H 1.26-1.39) was too overlapped for individual chemical shift assignment. Therefore, partial structure **B** proposed in **Figure 2.27**, was found to be identical to those elucidated for the previous compounds (see **Figures 2.9**, **2.15** and **2.21**).

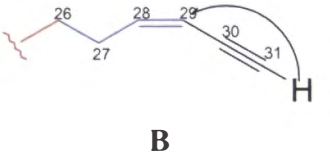

B

Figure 2.27: Key COSY (blue) and long-range COSY (black) correlations for partial structure **B**.

The geometry of the double bond for partial structure **A** (C-4/C-5) was determined as (*E*) on the basis of the direct comparison of the ^{13}C NMR chemical shift data obtained from the HSQC and CIGAR experiments, with those previously reported (**Tables 2.1**, **2.2** and **2.3**) and the coupling coupling constant extracted from the ^{1}H NMR spectrum ($J_{4,5}$ = 16.5 Hz). The double bond geometry assignment for partial structure **B** was determined as (*Z*) for the C-28 and C-29 carbons, and was achieved by direct comparison of the ^{13}C NMR chemical shift data obtained from the HSQC and CIGAR experiments with those previously reported (**Tables 2.1**, **2.2** and **2.3**), combined with the coupling constant extracted from the ^{1}H NMR spectrum between the H-28 and H-29 olefinic protons (δ_H 6.00 and 5.45, respectively, $J_{28,29}$=11.0 Hz).

Partial structure **F** (**Figure 2.28**) was elucidated using COSY (**Figure 2.25**) and limited HSQC and CIGAR NMR correlations. The key COSY cross peak correlations were observed from the H-14 (δ_H 3.51) oxymethine proton to both the H-13 alkyl and H-15 olefinic (δ_H 1.49 and 5.85, respectively) protons, confirming that this proton was in the same configuration as partial structure **E** for compound **2.25** (**Figure 2.22**). The location of the triple bond was determined by the observation of CIGAR correlations from the H-16 (δ_H 5.63) olefinic proton to the C-17 and C-18 (δ_C 91.6 and 78.6, respectively) carbons. A long range COSY correlation between the H-16 (δ_H 5.63) olefinic proton and the H-19 (δ_H 2.30) methylene protons placed the H-19 methylene proton directly on the other side of the triple bond, confirming that the ene-yne configuration as seen in **2.25** was still present. The geometry of the C-15/C-16 double bond was assigned as (*E*) due to the ^{13}C NMR chemical shifts comparison of C-16 and C-15 (CIGAR correlation from H-14 (δ_H 3.53) to carbons C-16 and C-15 (δ_C 111.0 and δ_C 144.2, respectively)) with those reported for **2.25**, combined with previously published data for similar compounds (see **Table 2.4**).

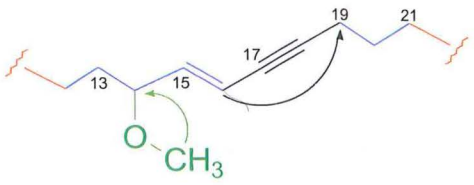

F

Figure 2.28: Key COSY (blue), long-range COSY (black) and CIGAR (green) NMR correlations used in determining partial structure **F**.

Connectivity between the confirmed fragments or orientation of the central partial structure **F** could not be achieved with the limited NMR experimental data. In order to satisfy the requirements of the mass spectrum, the alkyl chain fragment $C_{10}H_{20}$ (10 methylene units) required assignment. Due to the overlapped nature of the chemical shifts in this region of both the HSQC (δ_H 1.26-1.39) and CIGAR (δ_C 28.0-29.0) NMR spectra, the exact number of carbons (X and Y) linking partial structures **A** to **F** and **F** to **B** could not be determined, however, X+Y has to equal 10. The overall structure for **2.26** is represented in **Figure 2.29** with the two possible orientations for partial structure **F**.

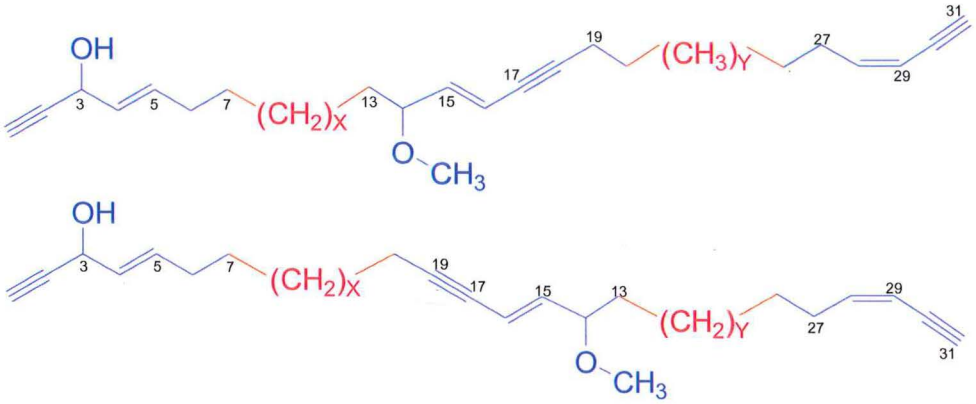

Figure 2.29: Overall proposed structure of **2.26**, where X+Y = 10.

As with the previously isolated compounds, degradation prevented the acquisition of any further structural information; this included the stereochemistry at carbons C-3 and C-14 and the unambiguous assignment of the central subunit by mass spectrometry or chemical modification.

The full NMR data for **2.26** is shown in **Table 2.4**.

Table 2.4: The ^{1}H, ^{13}C, COSY and CIGAR NMR data for **2.26** ($CDCl_3$).

Position†	^{13}C δ§	^{1}H δ ξ	COSY	CIGAR
1	74.2 (CH)	2.56 (d, 2.0)	H-3	
2	83.5 (C)			
3	63.0 (CH)	4.83 (br d, 5.5)	H-4, H-1	C-2
4	128.5 (CH)	5.60 (m)	H-5, H-3	
5	134.8 (CH)	5.90 (dt, 16.5, 6.0)	H-6, H-4	C-6, C-3
6	32.0 (CH_2)	2.06 (q, 7.5)	H-5, H-4	C-5, C-4
7	28.9 (CH_2)	1.40 (m)	H-8, H-6	
8-12‡	28.0-29.0 (CH_2)	1.26-1.39 (m)		
13	28.7 (CH_2)	1.49 (m)	H-12, H-14	
14	82.3 (CH)	3.51 (q, 6.5)	H-15, H-13	
14-OCH_3	56.7 (CH_3	3.26 (s)		C-14
15	144.2 (CH)	5.85 (m)	H-16, H-14	C-21, C-17
16	111.0 (CH)	5.63 (m)	H-19, H-15	
17	91.6 (C)			
18	78.6 (C)			
19	19.5 (CH_2)	2.30 (m)	H-20, H-16	C-18, C-17
20	29.7 (CH_2)	1.51 (m)	H-21, H-19	C-19
21-25‡	28.0-29.0 (CH_2)	1.26-1.39 (m)		
26	29.1 (CH_2)	1.43 (m)	H-27,H-25	
27	30.0 (CH_2)	2.32 (q, 6.5)	H-28, H-26	C-29, C-28, C-26
28	146.5 (CH)	6.00 (dt, 11.0, 7.5)	H29, H-27	C-29, C-27
29	108.0 (CH)	5.45 (brd, 11.0)	H-31, H-28	C-30, C-28
30	80.1 (C)			
31	81.1 (CH)	3.06 (d, 2.0)	H-29	

† Numbering defined as the primary alcohol in (**2.26**) at C-3 and the methyoxy at C-14 while the terminal acetylenes at C-1 and C-31. § ^{13}C NMR chemical shift values (δ ppm from $CDCl_3$ at 77.0) obtained from both HSQC and CIGAR experiments. ξ ^{1}H NMR spectrum recorded at 500 MHz in $CDCl_3$ (δ ppm from $CDCl_3$ at 7.25) followed by multiplicity and coupling constant (J/Hz). ‡Inconclusive chemical shift assignment and coupling constants ($J_{H\text{-}H}$), due to signals being overlapped

2.6: Biological Activity

Due to subsequent degradation, the purified compounds could not be individually tested for P388 activity. However, all of the purified compounds were isolated from fractions that displayed cytotoxic activity (IC_{50} < 975 ng/mL).

It has been recently reported that polyacetylenes possessing the 1-yn-3-ol terminal moiety (**2.27**) possess cytotoxic activity while those containing the alternate 1-yn-3-one moiety (**2.28**) display negligible activity when tested *in vitro* in the HCT-166 assay. Structure activity relationship measurements concluded that it is the 1-yn-3-ol terminal moiety that imparts activity to this class of compounds.[19,20,125] Therefore it would not be unreasonable to assume that compounds **2.23**, **2.24**, **2.25** and **2.26** would possess some degree of activity as they contain the 1-yn-3-ol functionality.

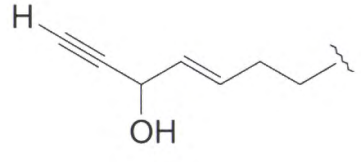

2.27

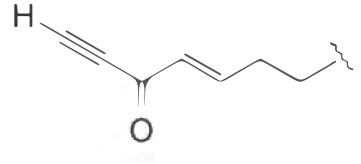

2.28

2.7: Concluding Remarks

The aim of this section of work was to isolate and identify the compounds responsible for the observed biological activity (P388) in the crude extract of the marine sponge *Rhabderemia stelletta* (01MNP0729).

Initial bioassay guided fractionation (HPLC microtitre plate collection) located the region of activity in the HPLC chromatogram which corresponded to several

non-polar compounds. With limited structural information (UV, retention time and inconclusive mass spectra), no positive identification for the compounds eluting in the region of activity could be made. Therefore further purification was deemed necessary. Several steps of chromatography, C_{18} and DIOL flash chromatography followed by semi-preparative reversed phase (C_{18}) HPLC chromatography yielded four novel, C_{31} long-chain unsaturated triacetylenes **2.23**, **2.24**, **2.25** and **2.26**. This work represents the first reported isolation of polyacetylenic compounds from the marine sponge *Rhabderemia stelletta* and also represents the first reported isolation of polyacetylenes from the marine sponge Order, Microcionina.

Subsequent biological activity assessment (P388 assay) on the purified compounds could not be achieved due to compound degradation. However, these four compounds were isolated from the region of activity as located by microtitre plate analysis of the crude extract and they contained the active 1-yne-3-ol moiety reported in the literature,[118,125,134] Therefore, on the basis of these two factors, all of these compounds should exhibit some degree of activity in the P388 assay.

Structural elucidation of these four compounds was achieved with the use of ^{1}H, ^{13}C, COSY, 1D-TOCSY, HSQC and CIGAR NMR spectroscopy, high resolution ESI mass spectrometry and subsequent comparisons of chemical shift data published for similar compounds.[122]

The absolute stereochemistry of all four compounds could not be determined using Mosher's or modified Mosher's method, as the compounds degraded before this analysis could be carried out. The most obvious pathway would be the light activated free radical polymerization as samples became more concentrated throughout the purification process, although samples were stored in the dark at 4 °C. The remaining frozen sponge material of *Rhabderemia stelletta* was extracted in an attempt to re-isolate **2.23**, **2.24**, **2.25** and **2.26** for further structural analysis, however after several steps of chromatography no significant biological activity was detected in any of the semi-purified fractions. Further work on these fractions was abandoned (see **Section 7.2.5**).

No optical rotation data was obtained nor was any IR or UV (except HPLC photo diode array (PDA)). Unambiguous positional assignment of the central substructure containing the double bond could not be achieved by EI or ESI (variable cone voltage) mass spectrometry at the University of Canterbury, although it is well reported that FAB-CID tandem mass spectrometry, is an effective tool for such an application.[119]

It is unlikely that long-chain polyacetylenic compounds will find clinical use as anticancer drugs due to their hydrophobic nature and tendency to degrade. However, derivatives that display a high degree of stability/solubility are more likely to succeed. One such compound (tazarotene **2.27**) containing an internal acetylene functionality is currently in phase I clinical trials for the treatment of basal cell carcinoma, the most common cancer in humans.[135]

Polyacetylenic compounds have a broad range of biological activities and their widespread occurrence and chemical simplicity warrant continued investigation into this class of compounds.

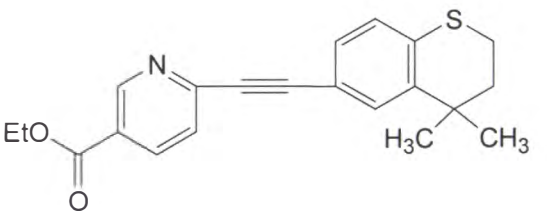

2.27

2.8: Summary of Isolation

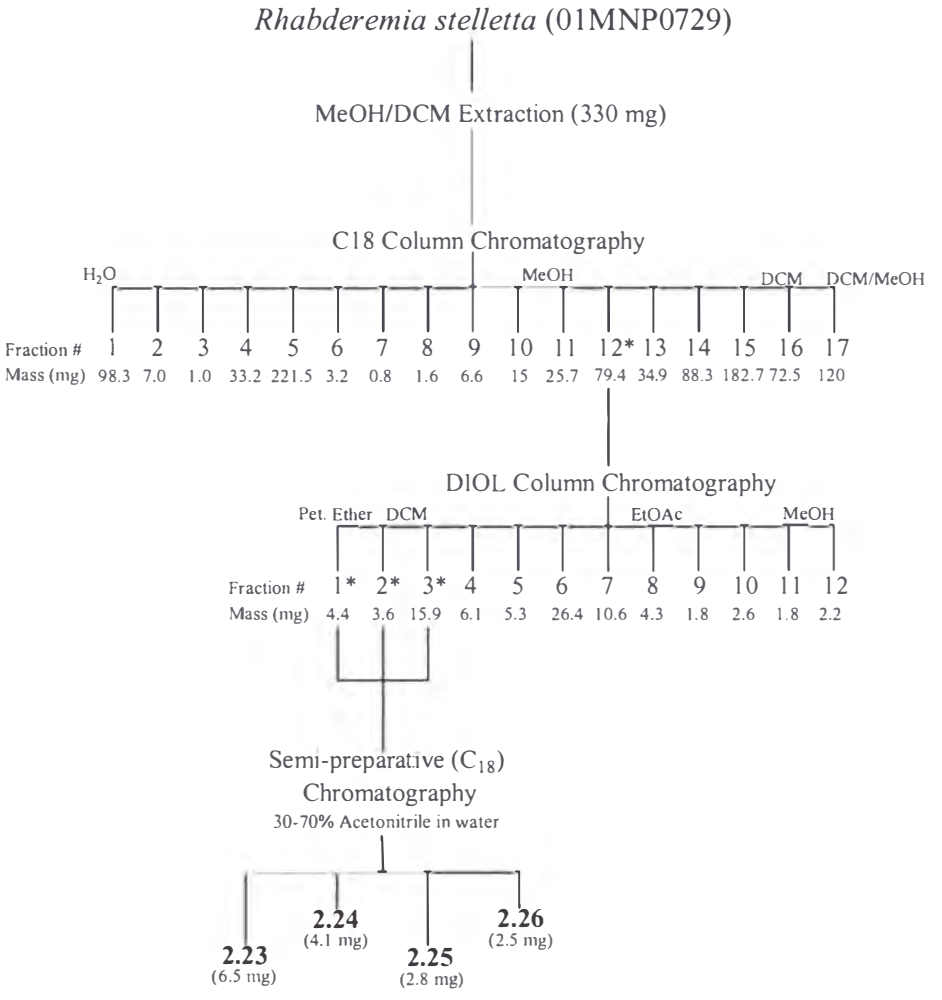

Scheme 2.1 : Chromatographic purification summary for the New Zealand marine sponge *Rhabderemia stelletta* (01MNP0729). *Fraction contains biologically active compound(s) of interest.

CHAPTER 3

ISOLATION OF COMPOUNDS FROM AN UNIDENTIFIED ANTARCTIC MARINE SPONGE (02WM01-33)

3.1: General Introduction

Pteridines are widely distributed throughout the animal kingdom, having been isolated from both terrestrial and marine organisms. They have long been known as yellow pigments from insects, serving as a growth factor in some cases, while their function in marine organisms is not entirely clear.[136] There seems little in the way of information relating to the biological activity of these compounds, and it can only be assumed that they provide some degree of chemical defense for the marine animal or in fact are representative of evolutionary convergence by unrelated species.[137]

In the marine environment, simple pteridines known from terrestrial sources have been isolated from sponges, ascidians, diatoms and copepods,[136,138] while

pteridines previously unknown from terrestrial sources have been isolated from the following marine organisms: dendrophylliid coral, sponges and a free polychaete.[136,139,140]

Leucettidine (**3.1**), was isolated as a minor metabolite from the calcareous sponge *Leucetta microraphis* in 1981 by Cardellina and Meinwald,[137] however, in 1984 Pfleiderer revised the structure of leucettidine (**3.1**) to that of 6-(1-hydroxypropyl)-1-methyllumazine (**3.2**) by direct comparison of the NMR data for the natural product with an authentic sample prepared by unambiguous synthesis.[140]

The structure of the lumazine **3.2** represented a departure from the usual substitution patterns of previously isolated pteridines, such as biopterin (**3.3**) from insects and 3-methylbiopterin (**3.4**) from the Mediterranean dendrophylliid coral *Astroides calycularis*, in that it did not possess an amino group at the C-2 position.[137] The lumazine **3.2**, along with the three 1'-keto analogues, 3-methyl-6-propionyllumazine (**3.5**), 1,3-dimethyl-6-propionyllumazine (**3.6**) and 6-propionyllumazine (**3.7**) isolated from the marine polychaete *Odontosyllis undecindonta* and isosepiapterin (**3.8**) and 6-(1-hydroxypropyl)-8-methylisoxanthopterin (**3.9**) isolated from the firefly *Photinus pyralis*, appear to be among the few naturally occurring pteridines that have a mono-oxygenated side chain.[136,137,139]

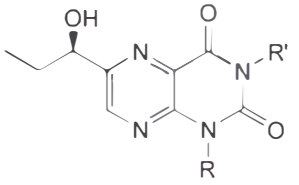

3.1 R=H, R'=CH_3
3.2 R=CH_3, R'=H

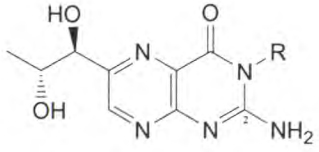

3.3 R=H
3.4 R=CH_3

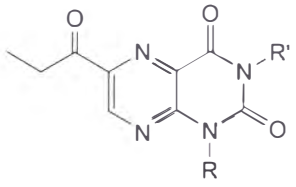

3.5 R=H, R'=CH_3
3.6 R=R'=CH_3
3.7 R=R'=H

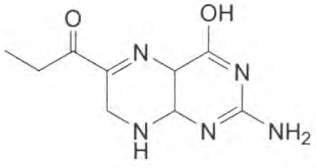

3.8

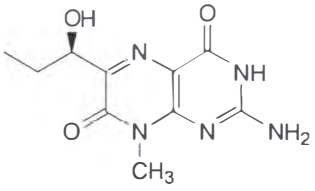

3.9

The pseudoanchynazines A-C (**3.10-3.12**)[141] isolated from the marine sponge *Clathria* sp. collected off the coast of Rio Negro, Argentina, represent a family of novel pteridines alkaloids. These compounds possess two pteridine moieties, a three carbon side chain, an unusual tryptophan unit that has its α-amino group blocked by a methyl carbamate and different pteridine substitution patterns. Pseudoanchynazine A (**3.10**) has pteridine substitution at C-2, pseudoanchynazine B (**3.11**) at N-1, and pseudoanchynazine C (**3.12**) at C-4 of the indole moiety. In all cases the tryptophan carboxyl forms an ester with the second pteridine unit.[141]

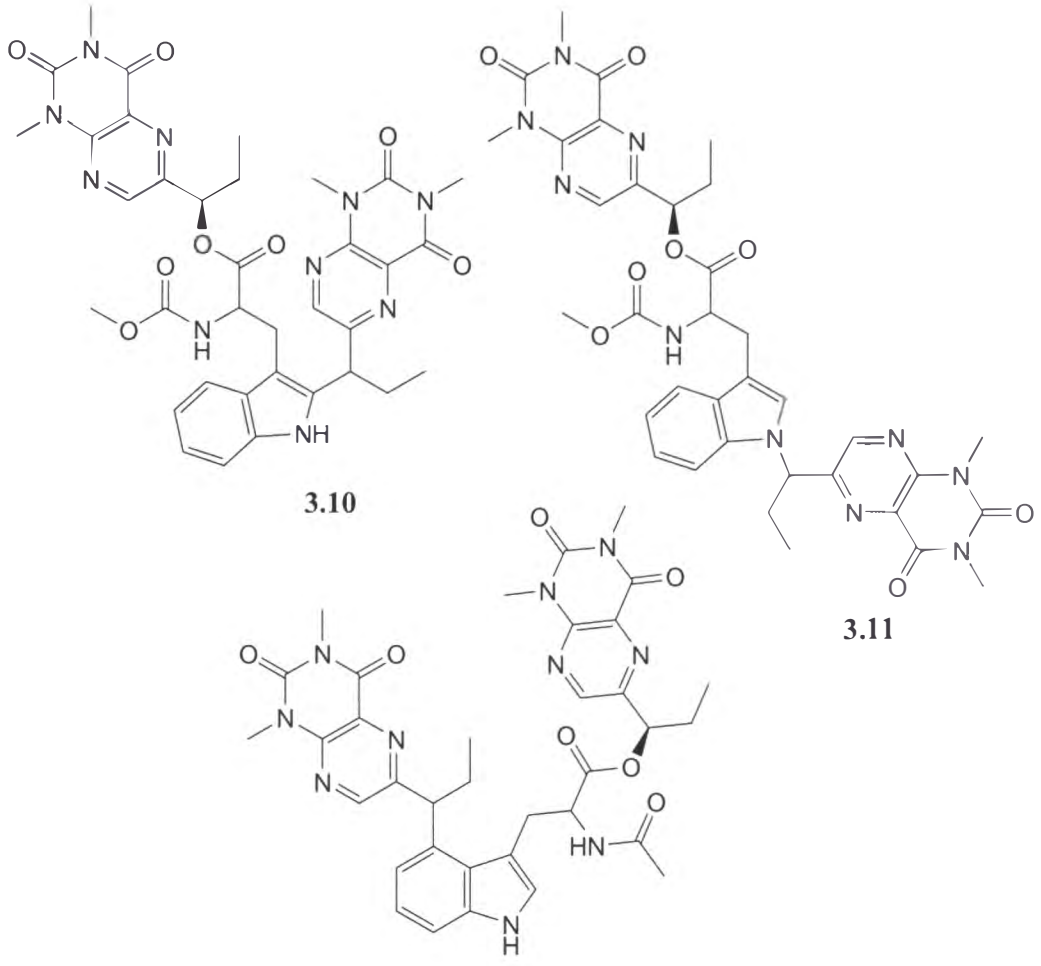

3.10

3.11

3.12

2-amino-O^4-benzylpteridine derivatives are known to be potent inactivators of the human DNA repair protein O^6-alkylguanine-DNA alkyltransferase. This repair protein is the primary source of resistance many tumour cells exhibit to chemotherapeutic agents that modify the O^6-position of guanine residues. Their *in vitro* activity has been shown to be as potent as the prototype alkyltransferase inactivator currently in clinical trials.[142]

Pteridines have been reported from several sources within the marine environment.[136] Since sponges are filter feeders they may obtain these compounds directly from their environment, by metabolizing substrates obtained in their diet or they may be synthesised *de novo* by the sponge as a secondary metabolite.

In this chapter, the isolation and structural elucidation of two previously undescribed pteridines, 6-hydroxymethyl-1*H*-pteridine-2,4-dione (**3.13**) and 6-hydroxymethyl-3-methyl-1*H*-pteridine-2,4-dione (**3.15**) (numbering assignment consistent with that proposed in the literature for similar compounds[136]), is described from the unidentified Antarctic marine sponge 02WM01-33.

3.2: Introduction

As part of our continuing effort to isolate novel biologically active compounds with pharmaceutical application, sponge specimens of various genera were collected at different sites in Antarctica for further chemical investigation. These samples were collected in collaboration with the Australian Institute of Marine Science (AIMS) as an ongoing investigation into the biological activity of benthic Antarctic organisms. In an effort to increase the probability of finding novel biologically active compounds, the collection team was instructed to collect samples they did not immediately recognize at a depth of 40 m, the limits of open circuit self contained underwater breathing apparatus (SCUBA). This depth is unprecedented at our collection sites. Due to the nature of the extreme conditions diving time at a depth of 40 m is very restricted (8 minutes); therefore only 58 samples were collected across multiple dives. Extracts from the collected samples were analyzed for *in vitro* anti-tumour activity (P388 assay), and of these, 02WM01-33 and 02WM01-46 were considered to have collected weight and activity sufficient for further investigation.

The first of the two active species of Antarctic sponges to be investigated was 02WM01-33 (Extraction of the active sponge specimen 02WM01-46 is discussed in Chapter 4). This unidentified sponge specimen was collected in October 2002 along the shoreline at Cape Armitage, Ross Island, Antarctica. The sample was immediately frozen and stored at -20 °C until it could be transported to the laboratory for biological activity assessment. The sponge was targeted for further analysis on the basis that the crude organic extract possessed activity in the in-house P388 assay (IC_{50} 11.8 μg/mL).

The exploitation of Antarctic sponges as a source of novel/biologically active compounds is discussed in detail in **Chapter 1, Section 1.9**.

3.3: Extraction of the Unidentified Antarctic Marine Sponge (02WM01-33)

The frozen specimen 02WM01-33 was thawed and extracted with combinations of MeOH and DCM (1:1, 500 mL). The extract was filtered through a bed of celite after homogenization; the solid material was re-suspended and extracted a further two more times with a mixture of MeOH and DCM. All filtrates were combined and the solvent was removed under vacuum. The organic extract was subjected to analysis *via* high performance liguid chromatography (HPLC) microtitre plate assay. Wells A4 to A9 were found to contain the biological activity (P388) observed in the crude organic extract. This region of activity corresponded to the compounds eluting between 2.8 and 4.2 minutes (**Figure 3.1**). These major peaks encompassed the bulk of the compounds observed in the entire extract as determined by Evaporative Light Scattering Detector (ELSD). UV spectra were obtained *via* HPLC PDA (CH_3CN/H_2O, 0.05 % TFA). The two major compounds eluting at 2.8 and 3.8 minutes displayed identical chromophores (λ_{max} 330 and 240 nm), suggesting the presence of a bicyclic heteroaromatic ring system. The component eluting at 4.2 minutes displayed a chromophore (λ_{max} 260, 210 nm) which suggested that an aromatic moiety was present in the molecule (**Figure 3.2**).[143] Liquid chromatography electrospray ionisation mass spectrometry (LCESIMS) was inconclusive as no direct correlations could be made relating the ions observed in the total ion current (TIC) trace and the compounds eluting in the chromatogram (PDA). With only UV and retention time data, it was unlikely that a search profile[130,131] based upon these two parameters would afford a positive identification of the compounds observed in the extract. It was on this basis that further purification was required.

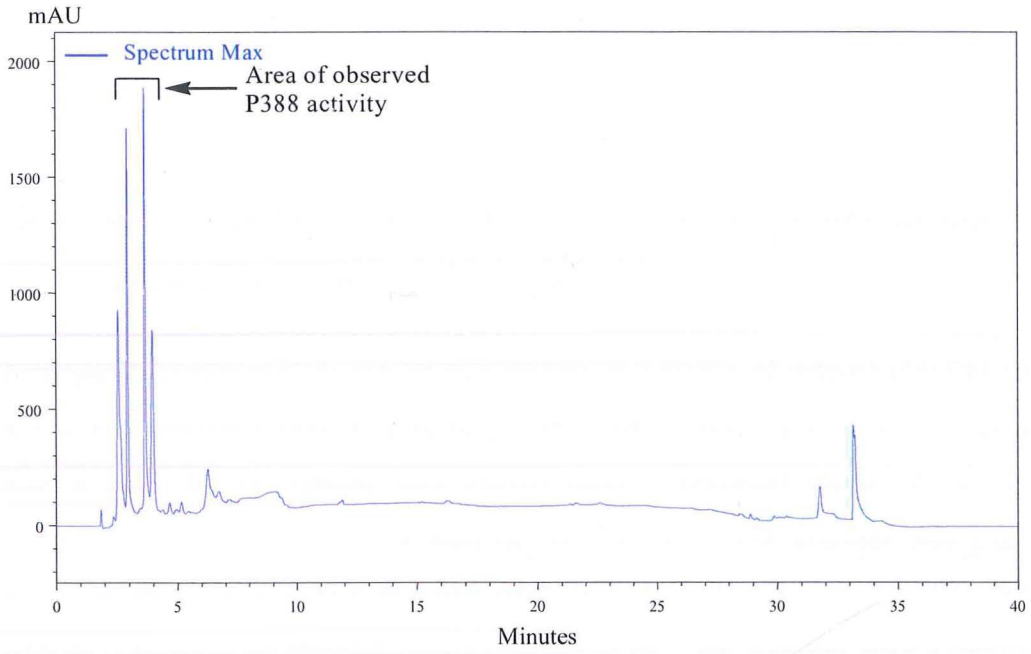

Figure 3.1: HPLC trace of DCM/MeOH crude extract (blue). Region of biological activity indicated between 2.8-4.2 minutes (black) as indicated by microtitre plate analysis.

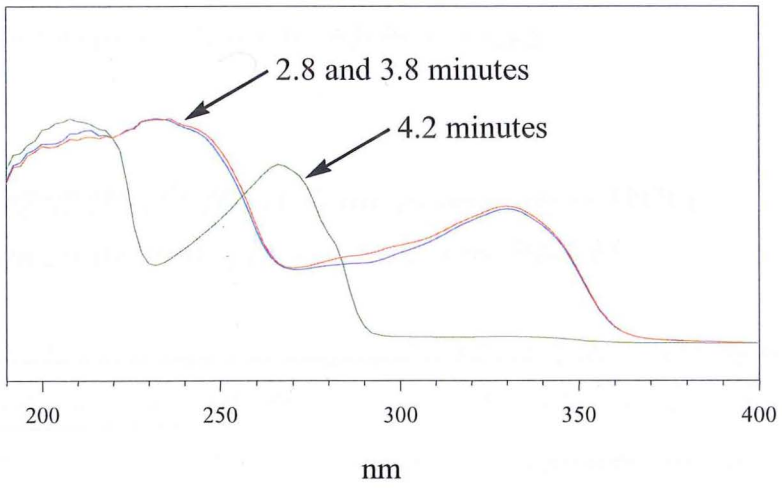

Figure 3.2: UV spectra (HPLC PDA) of the major compounds observed in the region of biological activity (2.8-4.2 minutes) as determined by the microtitre plate assay (P388). Compounds eluting at 2.8 and 3.8 minutes are identified as red and blue, respectively.

3.4: Chromatographic Isolation of Bioactives

3.4.1: Reversed Phase (C_{18}) Flash Chromatography of the Organic Extract of 02WM01-33

The organic extract was dissolved in a minimum volume of solvent (MeOH and DCM) and adsorbed onto C_{18} solid phase. The solvent was removed under vacuum, and the dry pellet was loaded onto a reversed phase (C_{18}) flash chromatography column, equilibrated to 100 % H_2O. The column was eluted using a steep solvent elution gradient from 100 % H_2O to 100 % MeOH. Any material remaining on the column was eluted as the final fraction with a mixture of MeOH and DCM (1:1). A total of 12 fractions were collected. Odd numbered fractions were analysed by reversed phase (C_{18}) analytical HPLC column to identify the fractions that contained the compounds responsible for the activity as located by microtitre plate analysis (**Figure 3.1**). Fraction wjm20-203 was determined to contain the compounds of interest and due to the complexity of the chromatogram further purification was deemed necessary.

3.4.2: Reversed Phase (C_{18}) Semi-preparative HPLC Chromatography of Fraction wjm20-203

Fraction wjm20-203 (41.2 mg) was subjected to further purification by reversed phase (C_{18}) semi-preparative HPLC chromatography using a gradient method developed on the analytical HPLC (C_{18}) column for maximum resolution. Four fractions were collected as peaks eluted, the purity of which were confirmed by re-injection on the analytical HPLC column (**Figure 3.3**). Fraction wjm20-203.3 was found to be contaminated with wjm20-203.2 and wjm20-203.3, and was deemed to contain too little mass for further purification *via* the same semi-preparative method. The ^1H NMR spectra of the three remaining fractions revealed that fraction wjm20-203.1 was not suitable for further structural analysis due to mass limitations, although it did display a similar UV chromophore to those observed for fractions wjm20-203.2 and wjm20-203.4. Therefore wjm20-

203.2 and 20-203.4 were subjected to the full range of 1D and 2D NMR spectroscopy experiments and high resolution ESI mass spectrometry. Structural elucidation of these pure compounds is discussed in **Sections 3.5.1** and **3.5.2** while the isolation procedure is summarized in **Scheme 3.1** (Page 104).

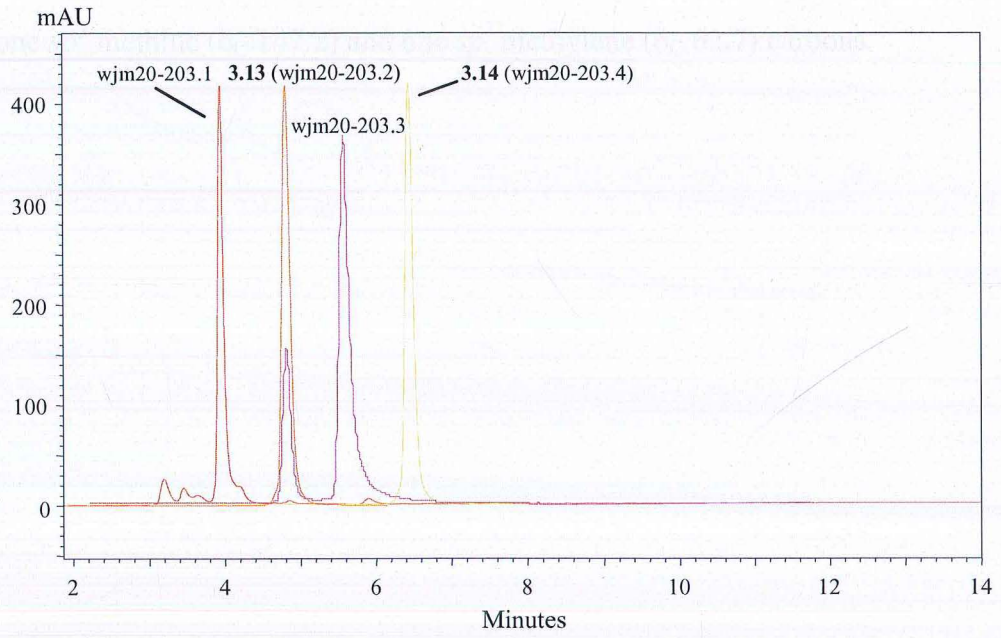

Figure 3.3: Overlaid HPLC chromatograms of isolated compounds from fraction wjm20-203. All traces are at spectrum max wavelength.

3.5: Structural Elucidation of Compounds Isolated from 02WM01-33

3.5.1: Structural Elucidation of 3.13

Compound **3.13** was isolated as a pale brown oil (14.0 mg). HRESI mass spectrometry identified a $[M+H]^+$ ion at *m/z* 193.0341 (calc 193.0362) which led to the molecular formula of $C_7H_6N_4O_3$ corresponding to 7 double bond equivalents (DBE). The ^1H NMR spectrum (**Figure 3.4**) was relatively simple, revealing the presence of only four well defined signals; these consisted of two broad, possibly exchangeable, N-H protons (δ_H 11.92 and 11.86), one proton

singlet at δ_H 8.69 indicative of a heteroaromatic proton, and finally a hydroxymethylene singlet at δ_H 4.66.

The ^{13}C NMR (**Figure 3.5**) and HSQC data disclosed the presence of two carbonyl (δ_C 161.6 and 150.4), three sp^2 quaternary (δ_C 152.5, 148.7 and 126.4), one sp^2 methine (δ_C 147.2) and one sp^3 methylene (δ_C 62.7) carbons.

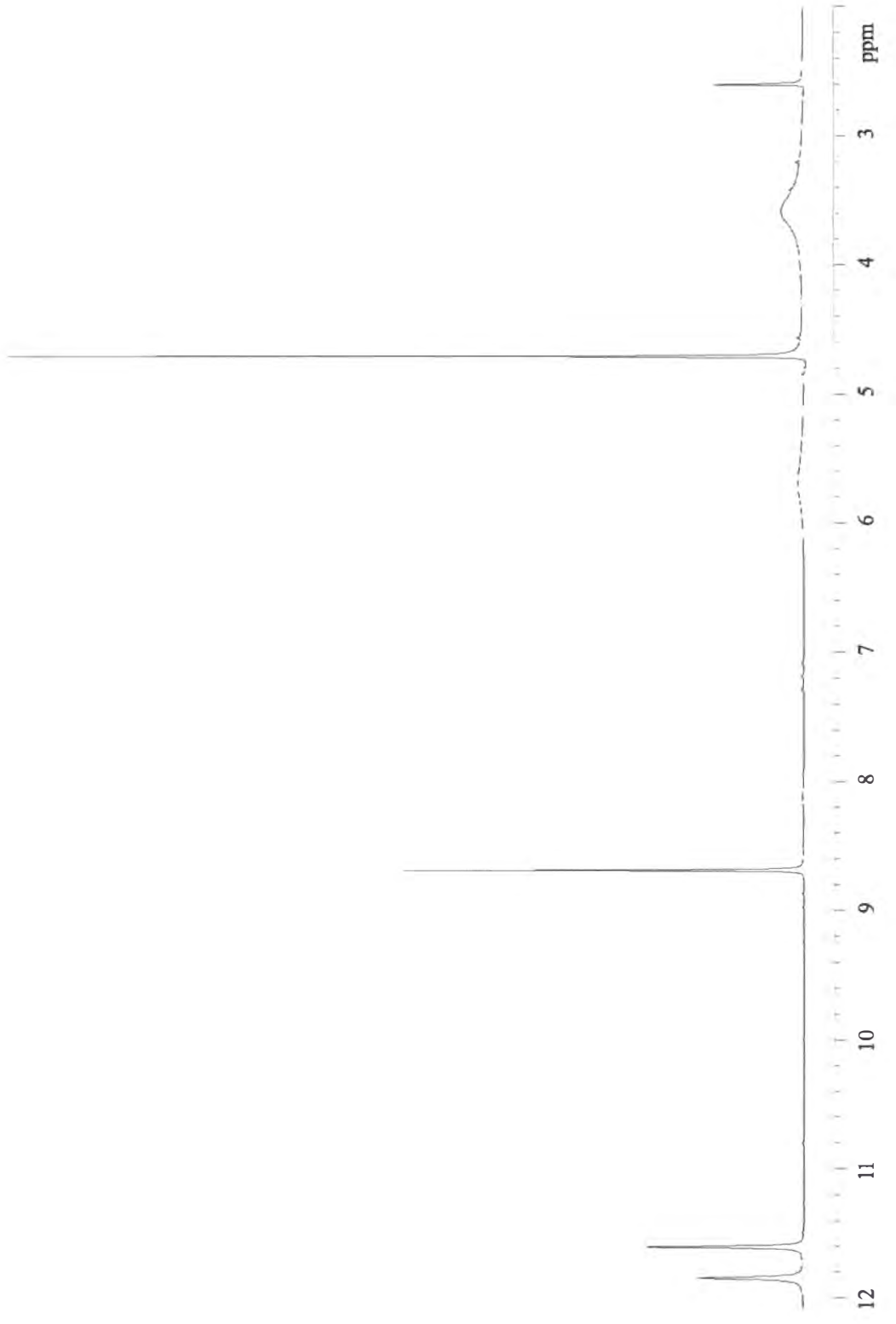

Figure 3.4: The ^{1}H NMR spectrum of **3.13** (DMSO-d_6).

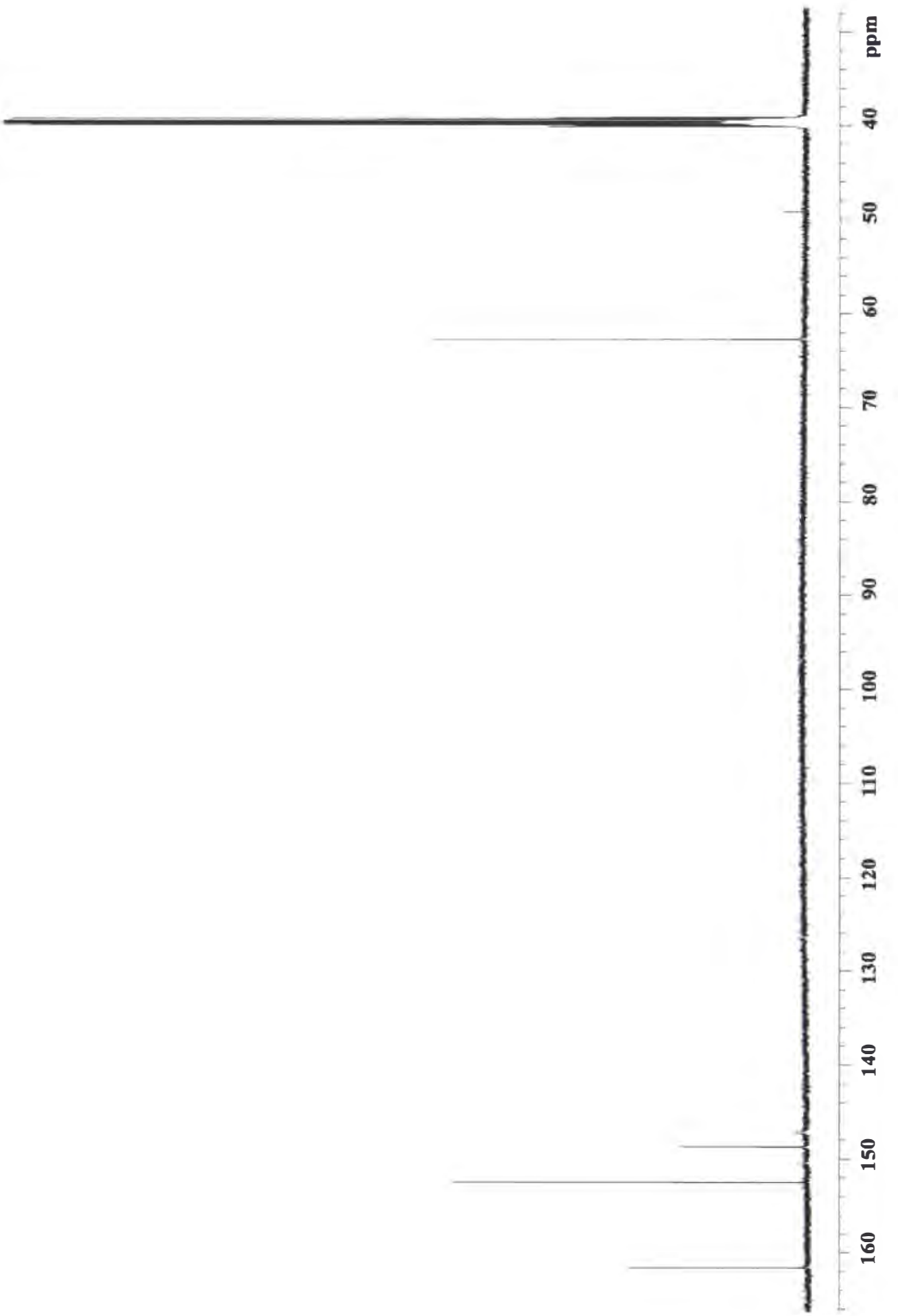

Figure 3.5: The ^{13}C NMR spectrum of **3.13** (DMSO-d_6).

The chemical shift of the hydroxymethylene proton δ_H 4.69 (δ_C 62.7) suggested that this moiety was most likely attached to the speculated aromatic nucleus. This was confirmed by the presence of CIGAR correlations from the H-7 (δ_H 4.69) methylene protons to the C-5 and C-6 (δ_C 152.5 and 147.2, respectively) aromatic carbons. No further $^3J_{CH}$ CIGAR correlations from the H-7 methylene protons were observed, suggesting that the proposed aromatic ring was substituted at the 4 position with a heteroatom. However, a very weak $^4J_{CH}$ coupling was observed from the H-7 (δ_H 4.69) protons to the C-3 (δ_C 126.4) carbon. The assignment of the heteroatom at the 4 position was validated by the presence of only two $^3J_{CH}$ CIGAR correlations from the H-6 (δ_H 8.69) aromatic proton to the C-7 and C-2 (δ_C 62.7 and 148.7, respectively) aromatic carbons. If position 4 was a carbon atom then a correlation would have been observed. The only $^2J_{CH}$ coupling observed from the H-6 (δ_H 8.69) proton was to the C-5 (δ_C 152.5) aromatic carbon, suggesting that a second heteroatom was located at the 1 position. The proposed heteroaromatic ring was tentatively assigned to be a pyrazine ring (i.e. positions 1 and 4 possessing tertiary nitrogen atoms and positions 2 and 3 quaternary carbons). The partial structure ring A is proposed as shown in **Figure 3.6** and accounts for 4 of the 7 required DBE's.

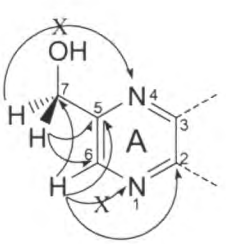

Figure 3.6: The key CIGAR correlations used to assign partial structure ring A. The absence of critical $^3J_{CH}$ and $^2J_{CH}$ coupling allowed for the assignment of the quaternary nitrogen atoms.

The two remaining carbonyls, positions C-4' and C-2', and the two NH's (NH-1' and NH-3') left to satisfy the molecular formula were assigned as a pyrimidine-2,4-dione ring system, ring B, entirely on the basis of the chemical shifts of carbons C-3 and C-2 as no CIGAR correlations were observed for either NH-1' or

NH-3', and comparison of ^{1}H and ^{13}C chemical shift data with published data[137] for compounds containing a similar pyrimidine-2,4-dione ring system. The two carbonyls combined with the formation of ring B, satisfied the remaining 3 DBE's.

The working structure for compound **3.13** (**Figure 3.7**) with arbitrary numbering assignment, was proposed.

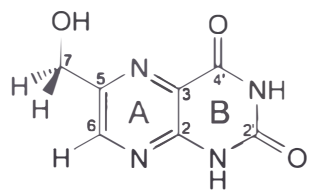

Figure 3.7: The proposed structure for **3.13** annotated with arbitrary numbering system used for structural elucidation and table of NMR data (**Table 3.1**).

After a literature search, this compound was deduced to be a novel pteridine with no structural matches identified. The compound **3.13** was tentatively named as the novel 5-hydroxymethyl-1*H*-pteridine-2',4'-dione (using the arbitrary numbering system assigned for structural elucidation). The 5-dehydroxymethyl-pteridine-2',4'-dione (lumazine (**3.14**)) and lumazine derivatives have been previously isolated from both terrestrial and marine animals.[140,144] The NMR data for **3.13** are displayed in **Table 3.1**.

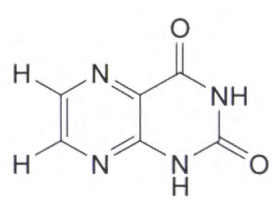

3.14

Table 3.1: The ^{1}H, ^{13}C, and CIGAR NMR data for compound **3.13** (DMSO-d_6).

Position	^{13}C δ §	^{1}H δ ξ	CIGAR
1‡	- (NH)	11.92 (1H, br s, NH)	
2'	150.4 (CO)		
3‡	- (NH)	11.68 (1H, br s, NH)	
4'	161.6 (CO)		
2	148.7 (CH)		
3	126.4 (C)		
5	152.5 (C)		
6	147.2 (CH)	8.69 (1H, s)	C-7, C-5, C-2
7	62.7 (CH_2)	4.69 (1H, s)	C-6, C-5, C-3

§ ^{13}C NMR spectra recorded at 125 MHz in DMSO-d_6. ^{13}C chemical shifts δ ppm from DMSO-d_6 (39.6). ξ ^{1}H NMR spectra recorded at 500 MHz. ^{1}H chemical shift values δ ppm from DMSO-d_6 (2.60) followed by number of protons and multiplicity. ‡Assigned on the basis of the chemical shifts assigned of **3.15** (**Section 3.5.2**).

*3.5.2: Structural Elucidation of **3.15***

The second compound, **3.15**, was isolated as a red oil (5.0 mg). High resolution ESI mass spectrometry identified a $[M+H]^+$ ion at *m/z* 207.0498 (calc. 207.0518), 14 mass units greater than **3.13**, which led to the molecular formula of $C_8H_8N_4O_3$. Both the ^{1}H and ^{13}C NMR spectra were representative of a compound structurally very similar to that of **3.13**, although the purity of this fraction was such that signals were observed for both the major compound **3.15** and **3.13** as a minor contaminant. The ^{1}H NMR spectrum (**Figure 3.8**) confirmed the presence of the following; a proton signal (δ_H 8.69) consistent with the heteroaromatic proton identified previously, a signal at δ_H 4.92 associated with the oxymethylene protons and a new signal at δ_H 3.23 integrating for three protons, suggesting the addition of a methyl group. However, one of the signals associated with the D_2O exchangeable protons at δ_H 11.68 (NH-1' or NH-3') was absent. The ^{13}C NMR (**Figure 3.9**) and HSQC data disclosed the presence of two carbonyls C-2' and C-2' (δ_C 161.6 and 150.4, respectively), three sp^2 quaternary carbons C-5, C-2 and C-3 (δ_C 152.5, 148.7 and 126.4, respectively), one sp^2 methine C-6 (δ_C 147.2), one sp^3 oxygenated methylene C-7 (δ_C 62.7) and the additional signal at δ_C 28.3 corresponding to an sp^3 methyl carbon.

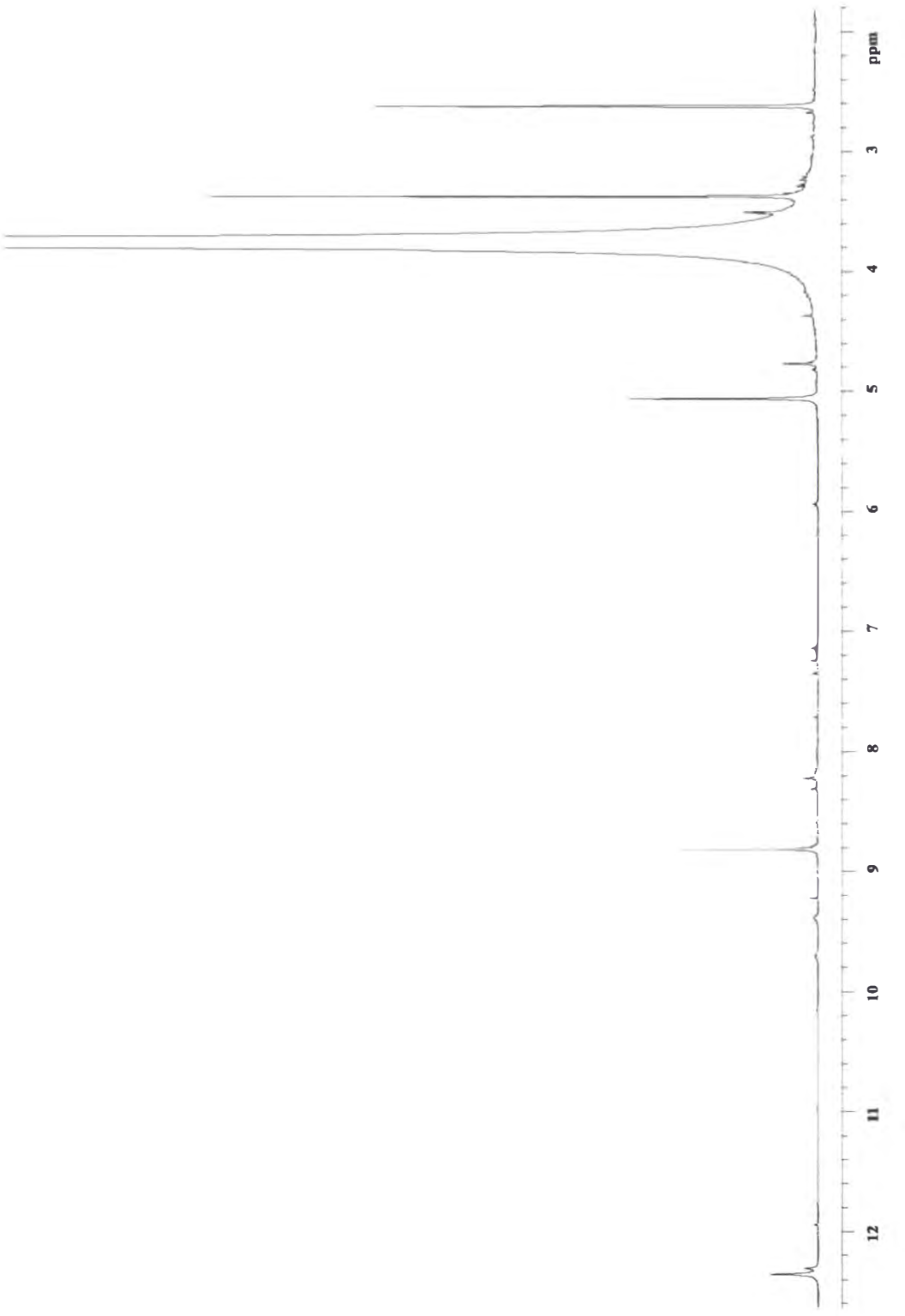

Figure 3.8: The ^{1}H NMR spectrum of **3.15** (DMSO-d_6).

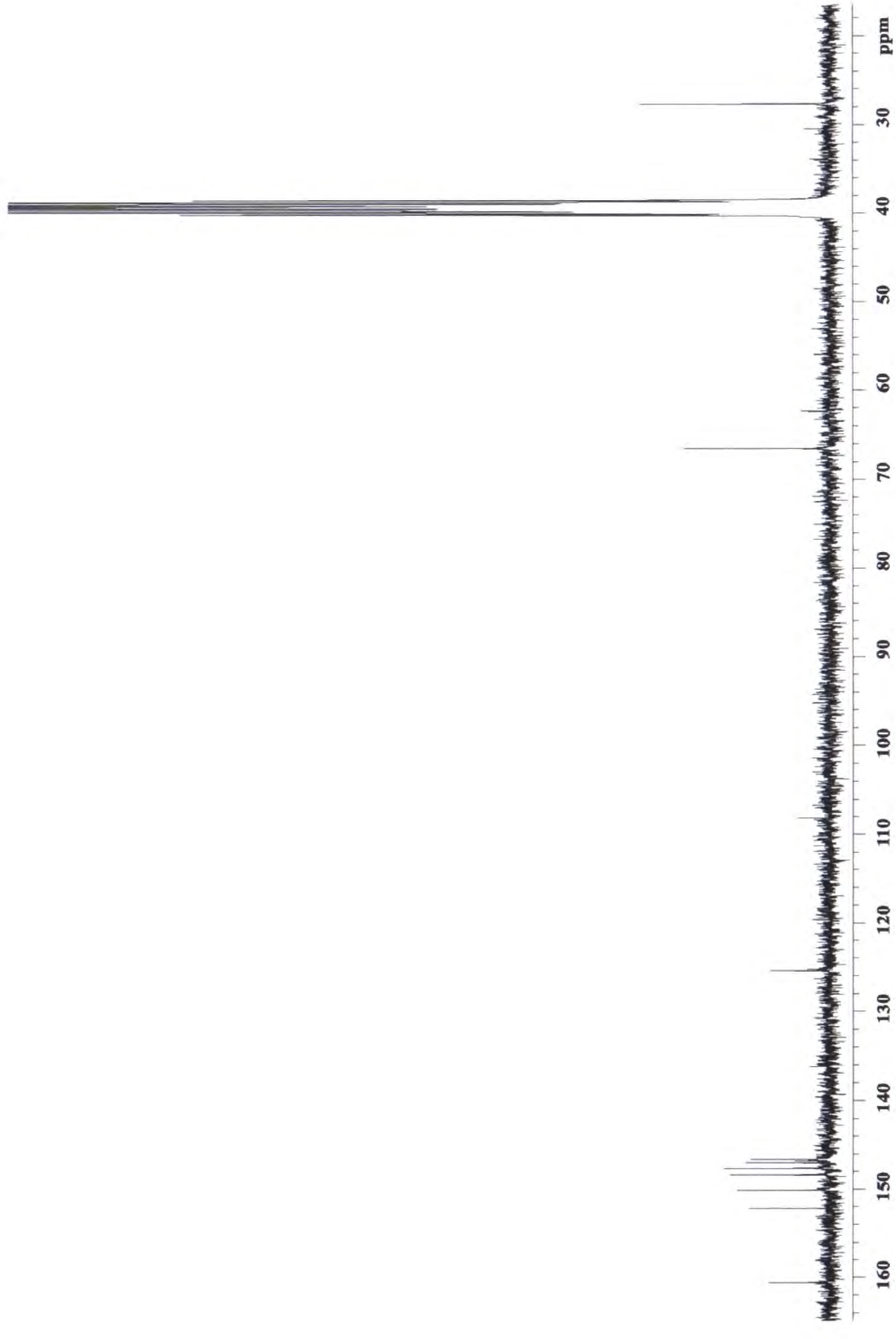

Figure 3.9: The ^{13}C NMR spectrum of **3.15** (DMSO-d_6).

CIGAR correlations from the H-6 (δ_H 8.69) aromatic proton to C-2, C-5 and C-7 (δ_C 148.7, 152.5 and 62.7, respectively) combined with the CIGAR correlations from the H-7 (δ_H 4.92) hydroxymethylene protons to the C-6 and C-5 (δ_C 147.2, 152.5) carbons confirmed the presence of the heteroaromatic pyrazine ring system identified in the previous structure **3.13** as ring A.(**Figure 3.10**).

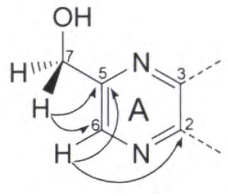

Figure 3.10: The key CIGAR (black) correlations for the assignment of ring A.

The remaining atoms were assigned by their ^{13}C NMR chemical shifts to be part of a pyrimidine-2,4-dione ring system (see **Section 3.5.1**, structural elucidation of **3.13**). The placement of the methyl group on the nitrogen at position 3' of the pyrimidine-2,4-dione ring system between the carbonyl groups, was based upon the CIGAR correlations observed from the H-5' (δ_H 3.23) methyl protons to both of the C-2' and C-4' (δ_C 150.4 and 161.6, respectively) carbonyl carbons completing ring B (**Figure 3.11**). This methylation at the N-3' position allows for the unambiguous assignment of the NH-1' and NH-3' (δ_H 11.92 and 11.68, respectively) protons in compound **3.15**.

A literature search[130,131,145] was performed resulting in no exact structural matches for the proposed structure **3.15**. Therefore, **3.15** the novel pteridine, was tentatively named 5-hydroxymethyl-3'-1*H*-pteridine-2',4'-dione (using arbitrary numbering assigned for structural elucidation), the $N^{3'}$-methyl derivative of **3.13**.

The working structure proposed for compound **3.15** is shown in **Figure 3.11**, with the arbitrary numbering system used for both structural elucidation and the NMR data in **Table 3.2**.

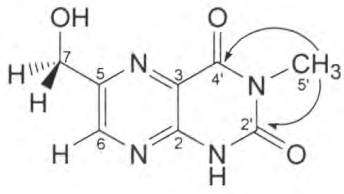

Figure 3.11: Proposed structure of **3.15** with key CIGAR correlations (black) and arbitrary numbering system used for structural elucidation and **Table 3.2**.

Table 3.2: The ^{1}H, ^{13}C and CIGAR NMR data for **3.15** (DMSO-d_6).

Position	^{13}C δ §	^{1}H δ ξ	CIGAR
1'	- (NH)	11.92 (1H, br s,NH)	
2'	150.4 (CO)		
4'	161.6 (CO)		
5'	28.3 (NCH_3)	3.23 (3H, s)	
2	148.7 (C)		
3	126.4 (C)		
5	152.5 (C)		
6	147.2 (CH)	8.69 (1H, s)	C-7, C-5, C-2
7	62.7 (CH_2)	4.92 (2H, s)	C-6, C-5, C-3

§ ^{13}C NMR spectra recorded at 125 MHz in DMSO-d_6. ^{13}C NMR chemical shifts δ ppm from DMSO-d_6 (39.6). ξ ^{1}H NMR spectra recorded at 500 MHz. ^{1}H chemical shift values δ ppm from DMSO-d_6 (2.60) followed by number of protons, multiplicity and coupling constant (*J*/Hz).

3.6: Biological Activity

All of the purified fractions were submitted for biological activity assessment. The compound **3.15** isolated as a major component of the organic extract was responsible for the biological activity (P388) observed in the crude organic extract of the unidentified Antarctic marine sponge 02WM01-46. The IC_{50} of the purified compound **3.15** was 9.6 μg/mL, and was consistent with the area of activity located by the initial microplate P388 assay analysis. It was interesting to note that the demethyl derivative of **3.15**, **3.13**, displayed no significant activity (IC_{50} >12.5 μg/mL).

3.7: Concluding Remarks

The aim of this project was to isolate and identify the compound(s) responsible for the biological activity (P388) observed in the crude extract of the unidentified sponge 02WM01-33.

Two novel pteridines, 5-hydroxymethyl-1*H*-pteridine-2,4-dione (**3.13**) and the *N*-methyl derivative 5-hydroxymethyl-3'-1*H*-pteridine-2',4'-dione (**3.15**) (numbering system used is consistent with that used for elucidation of structures) were isolated as the major components of the organic extract of the Antarctic marine sponge 02WM01-33.

These two compounds were initially identified by reversed phase (C_{18}) HPLC microtitre plate assay (P388). Compounds **3.13** and **3.15** were purified by successive chromatography consisting of reversed phase (C_{18}) flash column chromatography followed by semi-preparative reversed phase (C_{18}) HPLC. Biologically active 'peaks' of interest were located with the help of analytical reversed phase (C_{18}) HPLC analysis. Although four compounds were isolated only two contained enough material and were suitably pure enough for structural elucidation.

The purified compounds were evaluated for their cytotoxic activity in-house using the P388 (murine leukaemia) assay. The compound **3.15** was the only biologically active compound identified, with an IC_{50} of 9.6 μg/mL. The cytotoxic activity of **3.15** supported the initial data obtained by the microtitre plate (P388) assay performed on the organic extract, as **3.15** eluted within the located area of activity. Cytotoxicity against P388 cells from extracts containing pteridines has been reported in the literature previously (ID_{50} < 10 μg/mL).[144]

Structural elucidation of **3.13** and **3.15** was achieved with the use of ^{1}H, ^{13}C, HSQC and CIGAR NMR spectroscopy and high resolution mass spectrometry, assisted by the direct comparison of data obtained from NMR simulated predictions[146,191] and comparisons to the literature.[137] These compounds are

chemically interesting in that they possess a mono-oxygenated methyl side chain, which has not been previously reported among any naturally occurring pteridines.

Pteridines have found therapeutic use, with their derivatives currently undergoing clinical trials for the potent inhibition of the human-DNA repair proteins. This methodology is targeted at killing tumour cells by inactivating alkyl transferase in cells that over express folic acid receptors. They represent a promising new class of alkyl-transferase inhibitors with greater specificity and solubility than their predecessors.[142]

3.8: Summary of Isolation

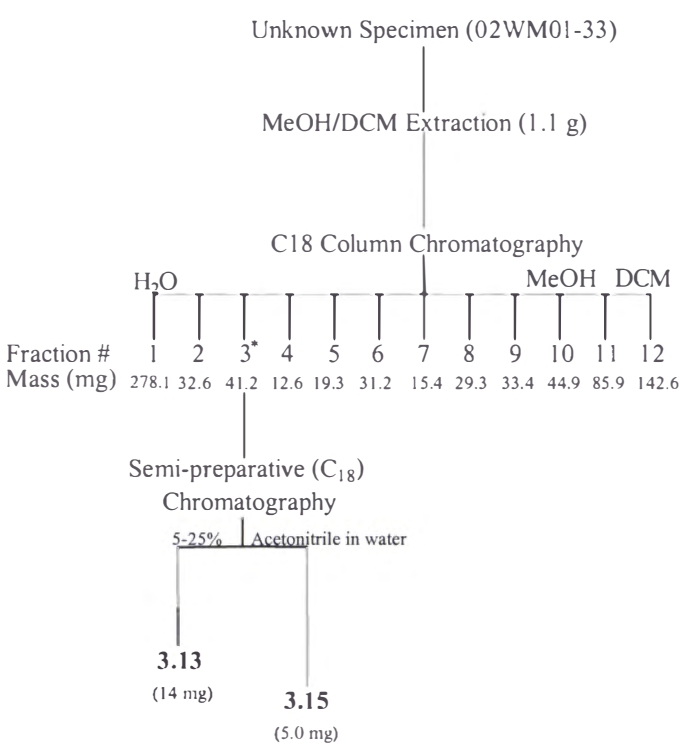

Scheme 3.1: Chromatographic purification summary for the Antarctic marine sponge 02WM01-33. *Fraction contains biologically active compound(s) of interest.

CHAPTER 4

ISOLATION OF COMPOUNDS FROM THE ANTARCTIC MARINE SPONGE *Suberites* sp. (02WM01-46)

4.1: General Introduction

There are approximately eighty described species of the genus *Suberites*. This genus is ubiquitous in distribution, but most commonly found in cold waters.[39] The *Suberites* spp appear to be specialized at producing a specific class of sesterterpenes (isoprenoid skeletal class), known as the suberitanes, which possess an unprecedented carbon skeleton. The absence or presence of these compounds could be used as taxonomic marker for Antarctic sponges of the genus *Suberites*.[65] To date four suberitenones, A (**4.1**), B (**4.2**), C (**4.3**) and D (**4.4**) along with caminatal (**4.5**) and two novel sesterterpenes (**4.6**) and (**4.7**), have been isolated from Antarctic *Suberites* species.[64,65,66,67] Bioactivity assessment of these compounds (**4.1**-**4.7**) revealed that they possess neither cytotoxicity, nor antiviral activity, but do contribute towards defense against a major Antarctic spongivore, the sea star *Perknaster fuscus*.[65] Suberitenone B (**4.2**) was shown to inhibit the cholesterol ester transferase protein (CETP), which mediates the transfer of

cholesterol ester and triglyceride between high-density lipoproteins (HDL) and low-density lipoproteins (LDL).[67] HDLs have been recognised as 'good cholesterol' as they transport surplus cholesterol back to the liver where it can be disposed of by bile acids. LDLs however, transport cholesterol to the peripheral tissues. Many studies have shown that there is an inverse correlation between levels of HDL and the incidence of atherosclerotic cardiovascular diseases.[67] Therefore, CETP has been recognised as a significant target protein, and these sesterterpene compounds may have potential as therapeutics in this area.

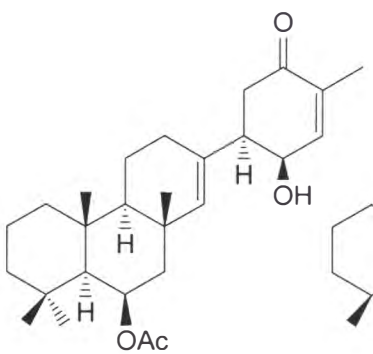

4.1

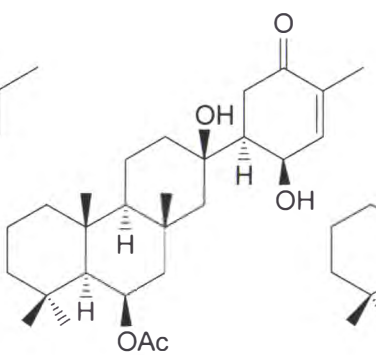

4.2

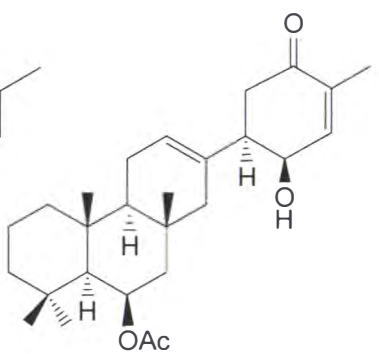

4.3

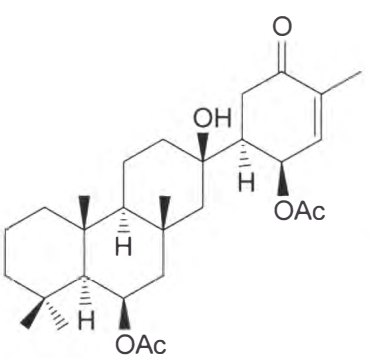

4.4

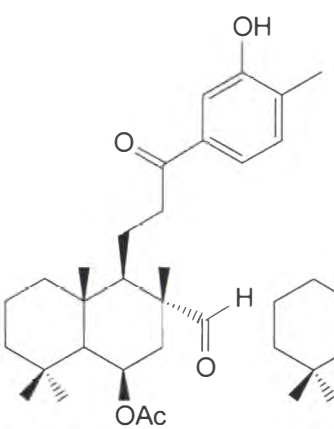

4.5

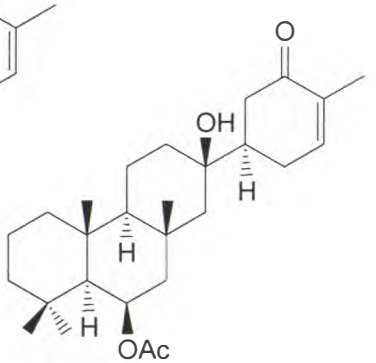

4.6

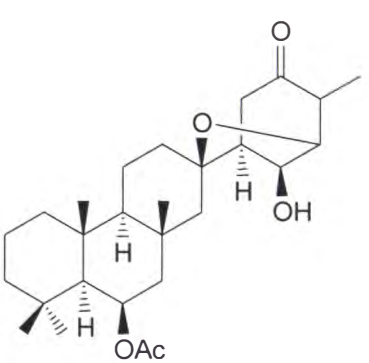

4.7

Work on this Antarctic marine sponge *Suberites* sp. to date has focused primarily on determining the bioactive compound(s) present in the extract. The suberitenones **4.1** and **4.2** were independently isolated, but shown to be inactive.[147] The bioactive compound was determined to be a previously undescribed C-5 substituted hydantoin alkaloid, (*Z*)-5-(3,4-dihydroxybenzylidene)-imidazolidine-2,4-dione (**4.8**).

4.2: Introduction

A specimen of a *Suberites* sp. (02WM01-46) was collected by SCUBA, at Scott Base, Ross Ice Shelf, Antarctica, at a depth of 40 m in October 2002. The specimen was stored frozen at -20 °C in the Scott Base laboratory until it could be transported to the University of Canterbury, New Zealand for chemical investigation. Taxonomy was performed on a voucher sample held at the Australian Institute of Marine Science (AIMS) by Professor Patricia Bergquist. Initial screening of the specimen in the University of Canterbury Chemistry Department in-house anti-tumour assay (P388) indicated that the organic extract possessed cytotoxic activity (IC_{50} 9.5 μg/mL). On the basis that this extract was active and the species was unidentified, it was deemed that further chemical investigation was required.

4.3: Extraction of the Antarctic Marine Sponge Suberites *sp. (02WM01-46)*

The frozen specimen, 02WM01-46 (62 g), was thawed, homogenised and successively extracted three times with combinations of MeOH and DCM. The solvent was removed under reduced pressure to yield a green extract (248 mg). An aliquot of the extract (250 μg) was subjected to reversed phase (C_{18}) analytical HPLC chromatographic microtitre plate analysis (see **Experimental, Section 7.1.6.2**) in an attempt to locate the compound associated with the observed

activity (P388). The biological assay results located the activity at 7.8 minutes, corresponding to a single peak, in the HPLC chromatogram (**Figure 4.1**)

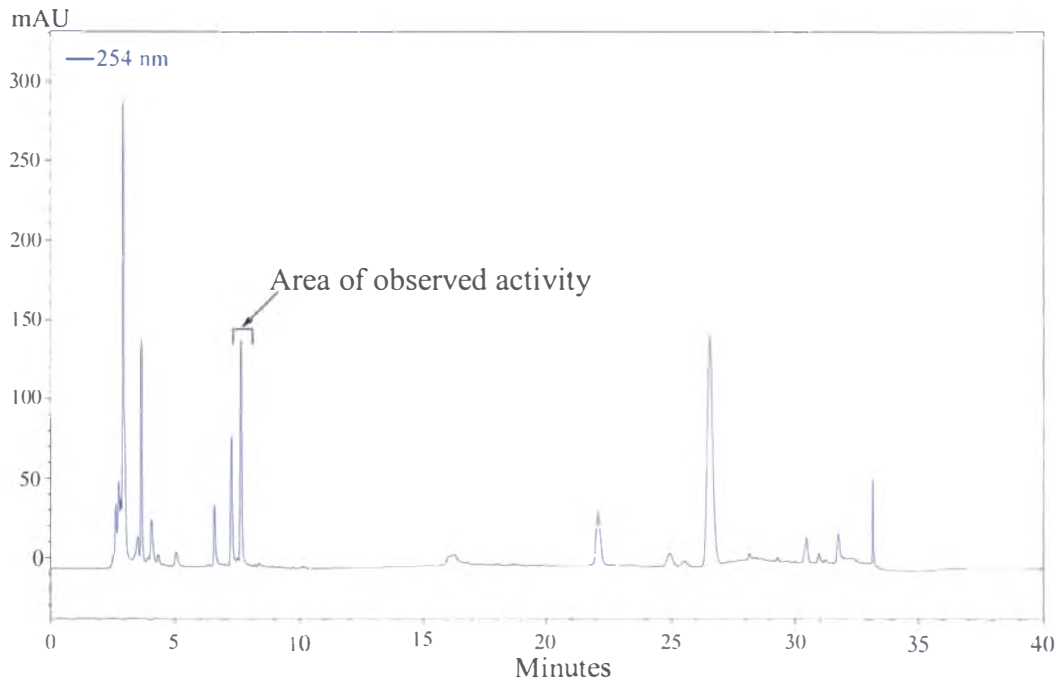

Figure 4.1: HPLC chromatogram of the organic extract of the marine sponge 02WM●1-46, indicating the region of activity as located by microtitre plate assay.

Analysis of the UV spectrum, (**Figure 4.2**, HPLC PDA, CH_3CN/H_2O 0.05 % TFA), revealed that this compound displayed a UV chromophore with a λ_{max} at 348 nm. The absorbance in the long wavelength region of the spectrum would suggest the presence of an aromatic ring with extended conjugation, or a bicyclic heteroaromatic ring. Low resolution ESI mass spectrometry of the active wells by direct injection was inconclusive. Although there were significant ion peaks observed in the spectrum, identification of the parent ion, or ion patterns for sodium/potassium adducts was difficult. It was at this point that further purification of the extract was deemed necessary as it was unlikely that a search profile based upon two parameters, UV (PDA) and retention time, would afford a positive identification of the active compound present in the extract.

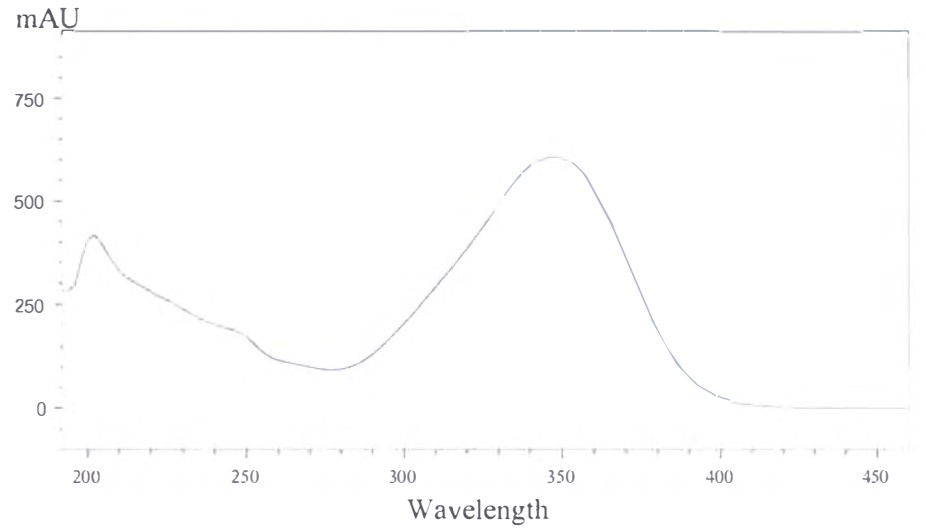

Figure 4.2: UV chromatogram of major compound located in region of activity (7.8 minutes) as identified by microtitre plate assay.

4.4: Chromatographic Isolation of Bioactives

4.4.1: Reversed Phase (C_{18}) Vacuum Chromatography of the Organic Extract of the Antarctic Marine Sponge Suberites *sp.*

The organic extract of 02WM01-46 was further purified by reversed phase (C_{18}) vacuum chromatography. The C_{18} vacuum chromatography column was equilibrated to H_2O and eluted with solvents ranging from H_2O through to MeOH. Any material remaining on the column was removed in the final fraction with DCM. Twelve fractions were collected, and odd numbered fractions were analysed by re-injection onto an analytical reversed phase (C_{18}) HPLC column to identify the fractions that contained the compound responsible for the observed P388 activity (as located by microtitre plate analysis, **Figure 4.1**). The compound of interest was concentrated into fractions wjm9-3204 to wjm9-3206. Therefore, these fractions were combined for further purification.

4.4.2: Reversed Phase (C_{18}) Semi-preparative HPLC Chromatography of Fractions wjm9-3204 to wjm9-3206

Due to the required resolution of separation (compounds eluting between 7 and 8 minutes), semi-preparative reversed phase (C_{18}) HPLC was chosen for the next stage of purification. After a suitable method had been developed on an analytical reversed phase (C_{18}) HPLC column, the fraction combination wjm9-3204 to wjm9-3206 was processed with consecutive injections. Four fractions were collected, and the purity of each fraction was confirmed by re-injection onto the reversed phase (C_{18}) analytical HPLC column. Fraction wjm9-3401.3 was selected for further analysis on the basis that it was the only fraction to contain the compound of interest. This compound now eluted at 11.3 minutes under the semi-preparative purification gradient conditions (previously 7.8 minutes by P388 microtitre plate analysis of the initial organic extract) as shown in **Figure 4.3**. This fraction was deemed to contain enough mass for 1D and 2D NMR experiments. Structural elucidation of the pure compound is discussed in **Section 4.5**.

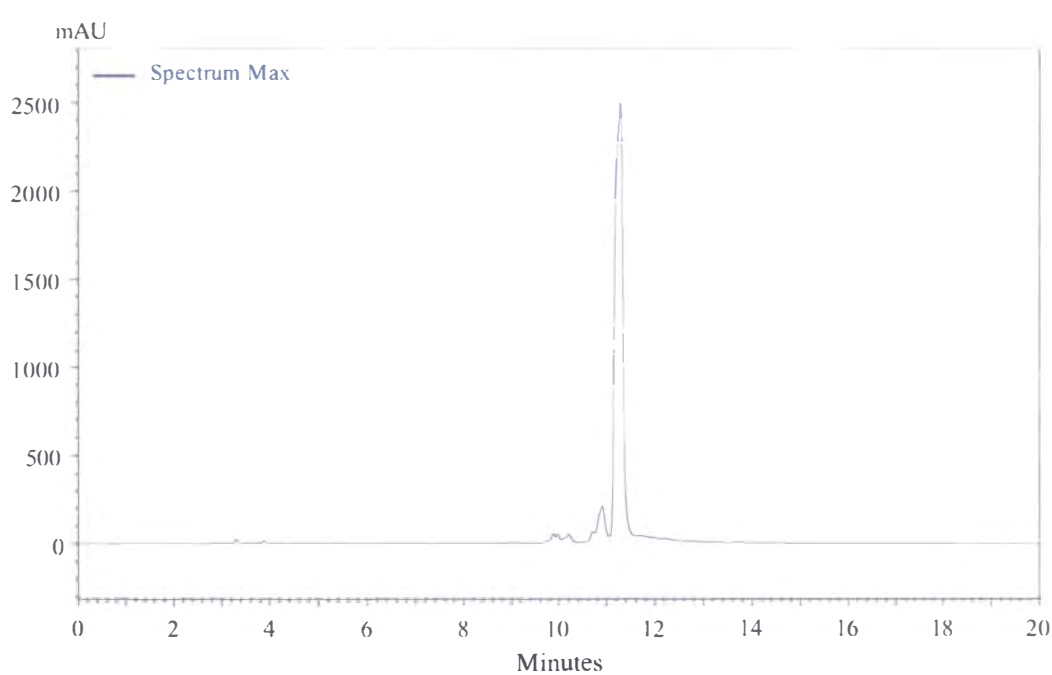

Figure 4.3: HPLC trace of purified compound **4.8** using semi-preparative gradient elution conditions (see **Experimental, Section 7.4.3**).

4.5: Structural Elucidation of **4.8**

Compound **4.8** was collected as a white powder (4.5 mg) from the third fraction eluting off the semi-preparative HPLC. HREI mass spectrometry indicated an ion at *m/z* 220.04691 (calc. 220.0484), which led to a molecular formula of $C_{10}H_8N_2O_4$, corresponding to 8 DBE. The ^{13}C NMR (**Figure 4.4**) and HSQC data confirmed the presence of 10 well defined signals, comprising two carbonyl (δ_C 165.8, 155.7), four sp^2 quaternary (δ_C 146.6, 145.5, 125.6 and 124.4) and four sp^2 methine (δ_C 121.5, 117.3, 115.5 and 109.9) carbons, which satisfied the requirements of the molecular formula. In the ^1H NMR spectrum (**Figure 4.5**), four olefinic protons (δ_H 7.07, 7.06, 6.86 and 6.36) and four exchangeable signals were observed. Two of these exchangeable signals were very broad at δ_H 9.55 and 9.10, possibly due to phenolic protons, while the remaining two broad signals at δ_H 11.19 and 10.36 were assigned as N-H protons.

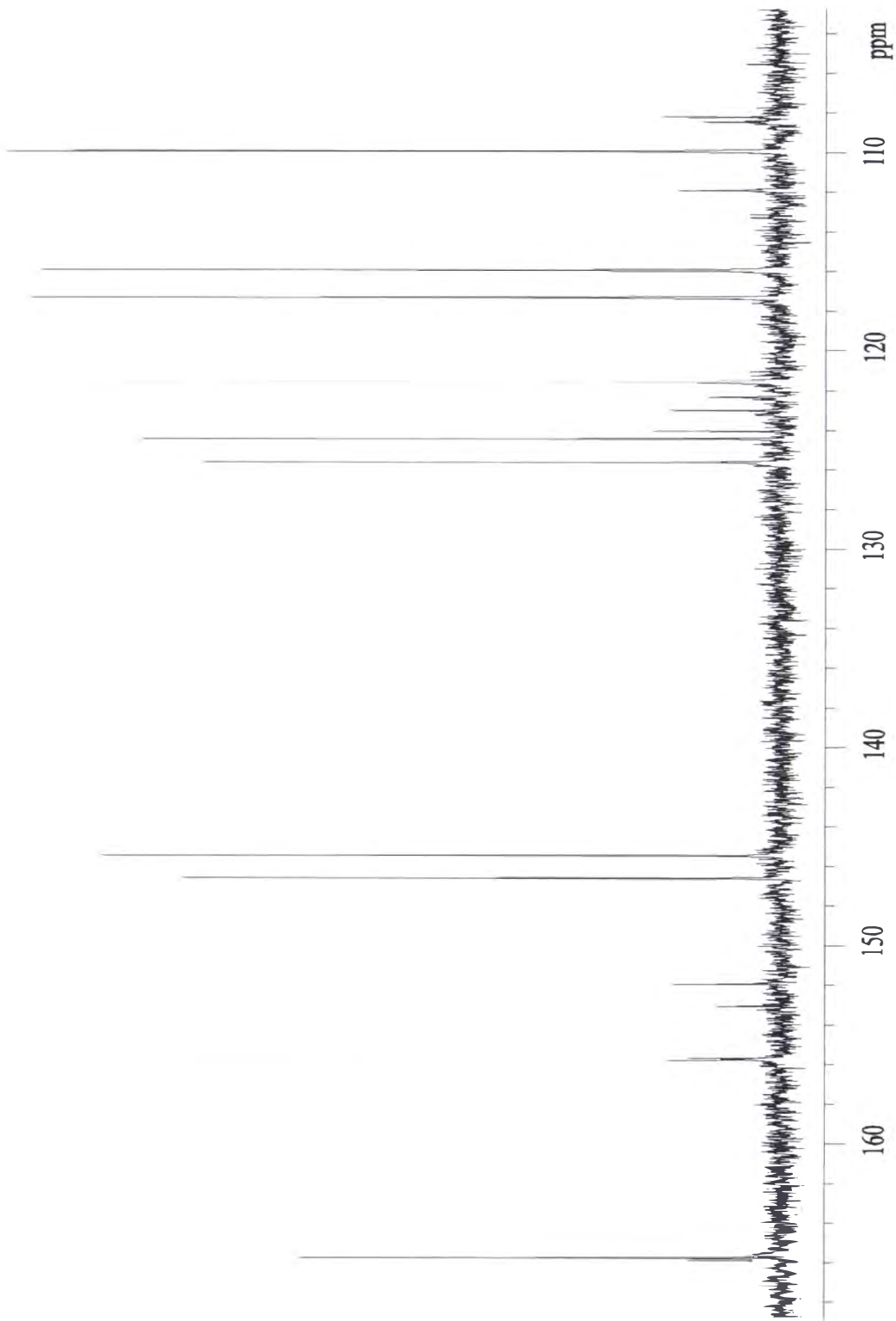

Figure 4.4: The ^{13}C NMR spectrum of **4.8** (DMSO-d_6).

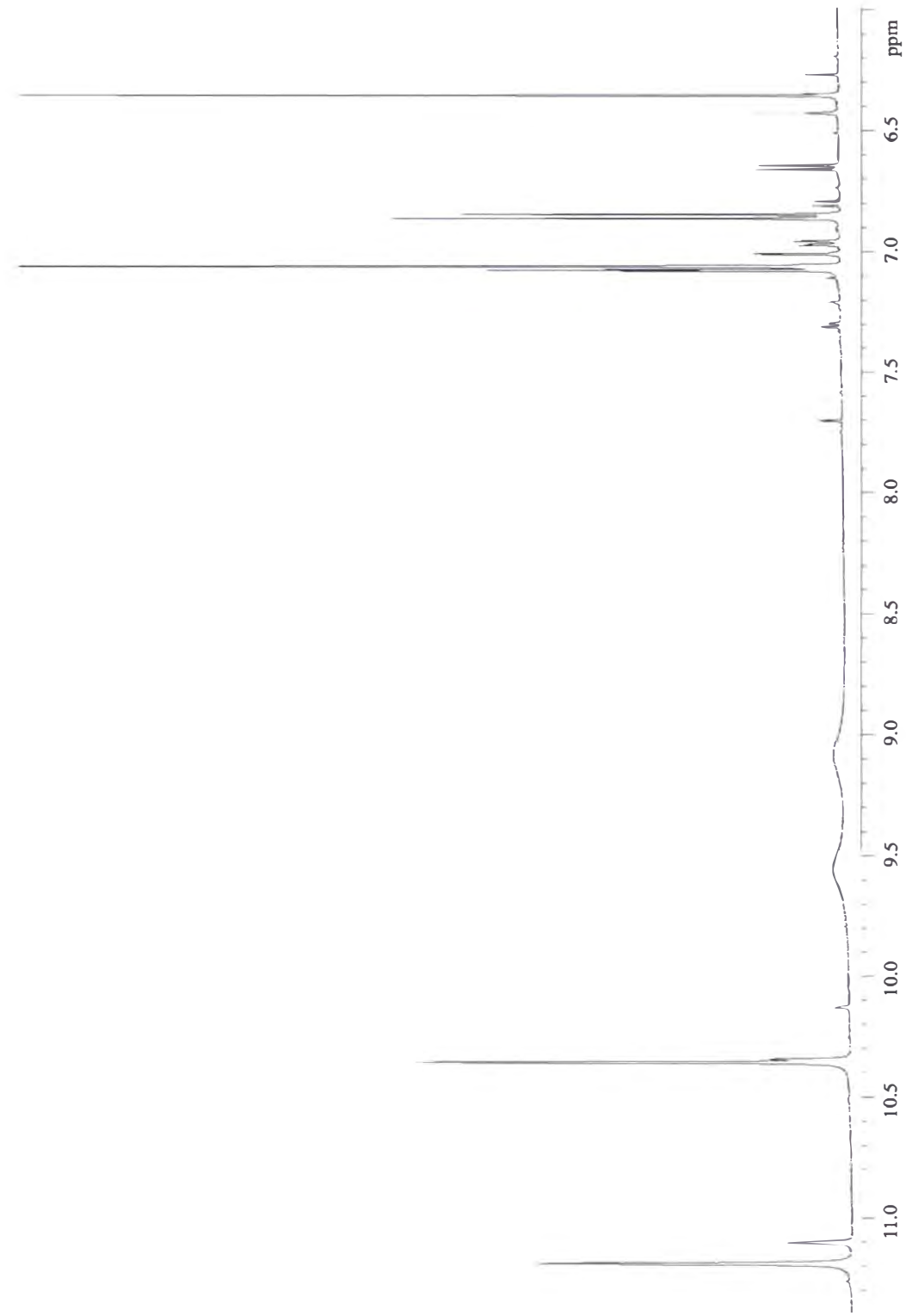

Figure 4.5: The ^{1}H NMR spectrum of **4.8** (DMSO-d_6).

COSY cross correlations (**Figure 4.6**) from the H-11 (δ_H 6.86) aromatic proton to the H-12 (δ_H 7.07) aromatic proton suggested that these two protons were adjacent to one another on an aromatic ring, while the long-range correlation from the H-8 (δ_H 7.06) proton to the H-12 (δ_H 7.07) aromatic proton implied that these protons were arranged on an aromatic ring (i.e. C-8, C-11 and C-12, respectively). However, H-6 (δ_H 6.36) was disqualified as being aromatic based on the observation there were no COSY correlations from either H-8 or H-11 (δ_H 7.06 and 6.86, respectively) to H-6 (δ_H 6.36). The H-6 location was confirmed by the long–range COSY correlations observed from the H-12 (δ_H 7.07) aromatic proton to the H-6 (δ_H 6.36) proton, placing H-6 α to the proposed aromatic ring on the sp^2 C-6 (δ_C 109.9) carbon. $^3J_{CH}$ CIGAR correlations from both H-8 and H-12 (δ_H 7.06 and 7.07, respectively) to C-6 (δ_C 109.9) validated the H-6 assignment.

The aromatic ring was constructed by $^3J_{CH}$ CIGAR correlations from the H-12 (δ_H 7.07) proton to both of the C-10 and C-8 (δ_C 146.6 and 121.5, respectively) carbons, the H-8 (δ_H 7.06) proton to both of the C-10 and C-12 (δ_C 146.6 and 117.3, respectively) and the H-11 (δ_H 6.86) proton to both of the C-7 and C-9 (δ_C 124.4 and 145.5, respectively) carbons. This data was combined with the $^2J_{CH}$ correlations from the H-8 (δ_H 7.06) proton to the C-6, C-10 and C-12 (δ_C 109.0, 146.6 and 117.3, respectively) carbons, from the H-11 (δ_H 6.86, δ_C 115.9) proton to the C-10, C-9 and C-7 (δ_C 146.6, 145.5 and 124.4, respectively) carbons, and finally fron the H-12 (δ_H 7.07) proton to both of the C-7 and C-9 (δ_C 124.4 and 145.5, respectively) carbons completed the assignment of the proposed aromatic ring. The chemical shifts for both the C-9 (δ_C 145.5) and C-10 (δ_C 146.6) carbons suggested that these sp^2 quaternary carbons were oxygenated (containing an hydroxy group). This observation was supported by the very broad signals observed in the ^{1}H NMR spectrum at δ_H 9.55 and 9.10. The remaining atoms consisted of two carbonyls, one sp^2 quaternary carbon and two exchangeable protons, which were assigned using CIGAR correlations. The proton NH-3 (δ_H 11.19) was placed between two carbonyl groups on the basis of the observed correlations to the C-4 and C-2 (δ_C 165.8 and 155.7, repectively) carbons, while the CIGAR correlation from the NH-1 (δ_H 10.36) proton to the C-2 (δ_C 155.7)

carbonyl carbon and the sp^2 C-5 (δ_C 125.6) carbon positioned NH-1 adjacent to C-2. Location of the NH-3 group between both of the carbonyls would account for the downfield shift difference between the NH-3 (δ_H 11.19) and NH-1 (δ_H 10.36) protons. Refer to **Figure 4.8**, the proposed structure for compound **4.8**.

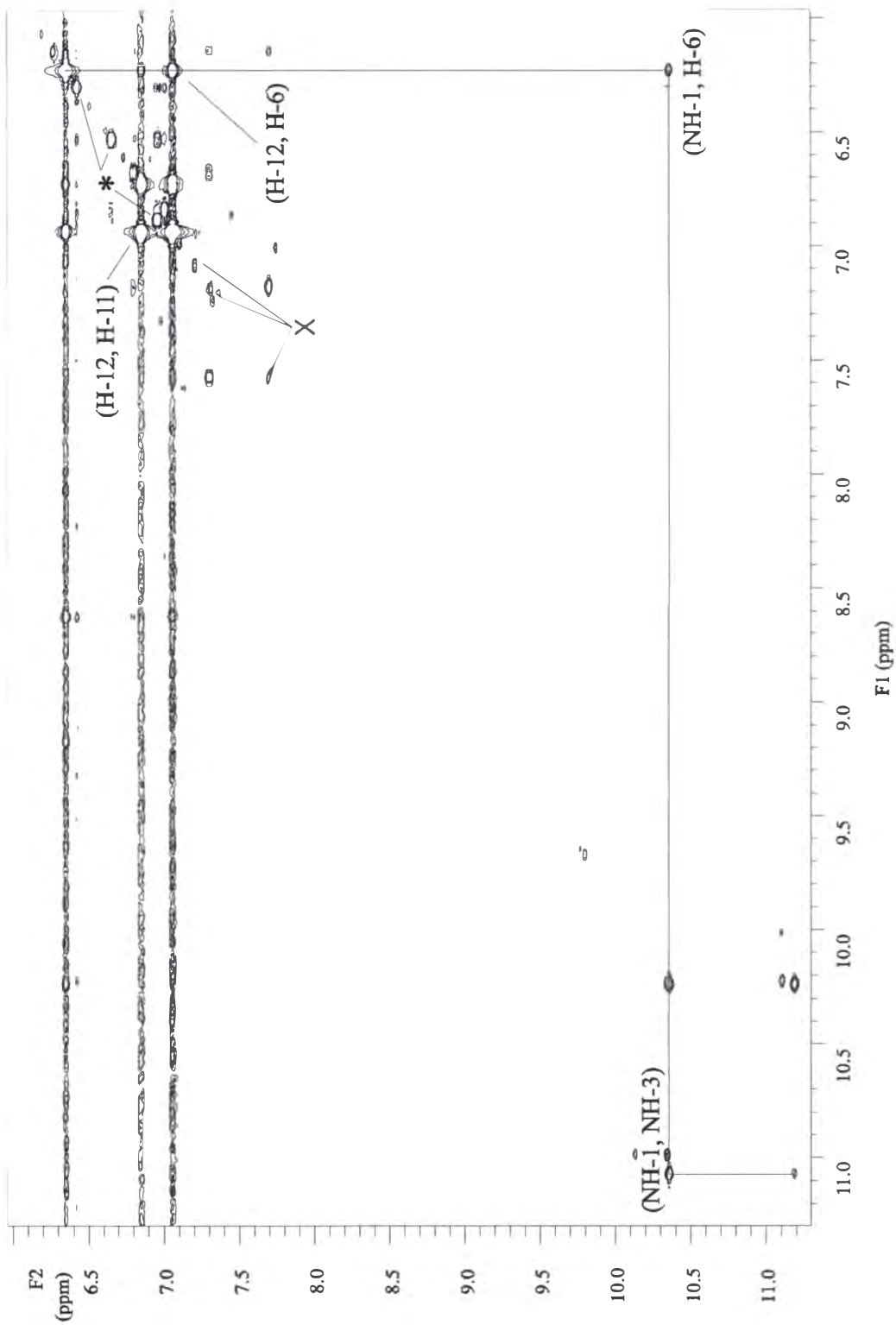

Figure 4.6: The long-range COSY correlations for **4.8**, with the minor isomer and impurities denoted by '*' and 'X', respectively (DMSO-d_6).

The presence of a hydantoin ring substituted at the C-5 (δ_C 125.6) carbon was confirmed by the critical CIGAR correlations from the exchangeable NH-3 (δ_H 11.19) proton to the C-5 (δ_C 125.6) carbon, combined with the correlation from the H-6 (δ_H 6.36) proton to the C-4 (δ_C 165.8) carbonyl carbon (**Figure 4.7**, red arrows).

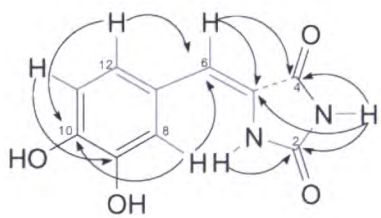

Figure 4.7: Proposed structure of compound **4.8** showing key COSY and long-range COSY correlations (blue) and key CIGAR correlations (black).

Experimental 1D and 2D NMR data for the proposed compound **4.8** are shown in **Table 4.1** while the arbitrary numbering system used for both the structural elucidation and **Table 4.1** is shown in **Figure 4.8**.

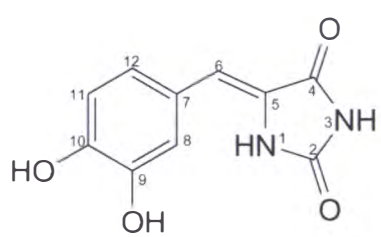

4.8

Figure 4.8: The proposed structure of **4.8** with arbitrary numbering assignment used for both structural elucidation and NMR data **Table 4.1**.

Table 4.1: The ^{1}H, ^{13}C, COSY and CIGAR NMR data obtained for **4.8** (DMSO-d_6).

Position	$^{13}C\ \delta$ §	$^{1}H\ \delta$ ξ	COSY	CIGAR
1	- (NH)	10.36 (1H, br s, NH)	H-6, NH-3	C-5, C-2
2	155.7 (CO)			
3	- (NH)	11.19 (1H, br s, NH)	NH-1	C-5, C-4, C-2
4	165.8 (CO)			
5	125.6 (C)			
6	109.9 (CH)	6.36 (1H, s)	H-12, NH-1	C-12, C-7, C-5, C-4
7	124.4 (C)			
8	121.5 (CH)	7.06 (1H, s)	H-12	C-12, C-10, C-9, C-6
9	145.5 (C)			
9-OH†	- (OH)	9.10 (1H,v br s)		
10	146.6 (C)			
10-OH†	- (OH)	9.55(1H, v br s)		
11	115.5 (CH)	6.86 (1H, d, 7.5)	H-12	C-12, C-10, C-9, C-7
12	117.3 (CH)	7.07 (1H, d, 7.5)	H-11, H-8, H-6	C-11, C-10, C-8, C-6

§ ^{13}C NMR spectra recorded at 125 MHz in DMSO-d_6. ^{13}C chemical shifts δ ppm from DMSO-d_6 (39.6). ξ ^{1}H NMR spectra recorded at 500 MHz. ^{1}H chemical shift values δ ppm from DMSO-d_6 (2.60) followed by number of protons, multiplicity and coupling constant (*J*/Hz). †Values may be interchanged within column.

4.5.1: Stereochemistry of **4.8**

Conformational isomerism of the C-5/C-6 double bond would imply that two possible stereoisomers exist for **4.8**. Careful analysis of the ^{1}H NMR spectrum (**Figure 4.5**) of the purified compound **4.8** revealed that the signals for the major compound were accompanied by weaker signals of the same multiplicity. This suggested that one major isomer is dominant in the isomeric mixture. It was noted that during the course of 2D-NMR structural elucidation experiments, the signals of the minor component were becoming more obvious. Compounds of this type (C-5 substituted hydantoins) that do not possess any substitution at the N-3 position are isolated in predominantly the (*Z*) configuration, but on irradiation with 350 nm light or under normal daylight conditions will slowly afford mixtures richer in the (*E*) isomer.[148] NMR samples were prepared under normal ambient laboratory conditions, and the observed increase in ^{1}H NMR spectrum peak intensity of the minor compound could therefore be explained by the reported phenomenon. In order to obtain NMR data for both isomers, the ^{1}H NMR spectra

were recorded after the addition of both two and four equivalents of pyridine-d_5, in an attempt to enrich the sample with the minor isomer. Comparison of the peak area ratios for the major and minor compounds in each ^{1}H NMR spectrum confirmed that the ratio of major (natural) to minor isomer had decreased from approximately 6:1 to 2:1 (major:minor) after the addition of four equivalents of base, as shown in **Figure 4.9**.

In addition, reports suggest that the carbonyl located at C-4 is responsible for the deshielding of the proton at C-8 (δ_H 7.06) while in the (*E*) configuration by up to as much as 1 ppm.[148] It is worth noting that the chemical shift of the aromatic proton H-8 (δ_H 7.06) in the major isomer is overlapped with that of H-12 (δ_H 7.07), while the H-8* (minor compound) proton in the initial ^{1}H NMR spectrum is clearly resolved. This initial data would suggest that the minor compound could be tentatively assigned as being in the (*E*) configuration based on the resolved chemical shift of the H-8* proton in the initial ^{1}H NMR spectrum.

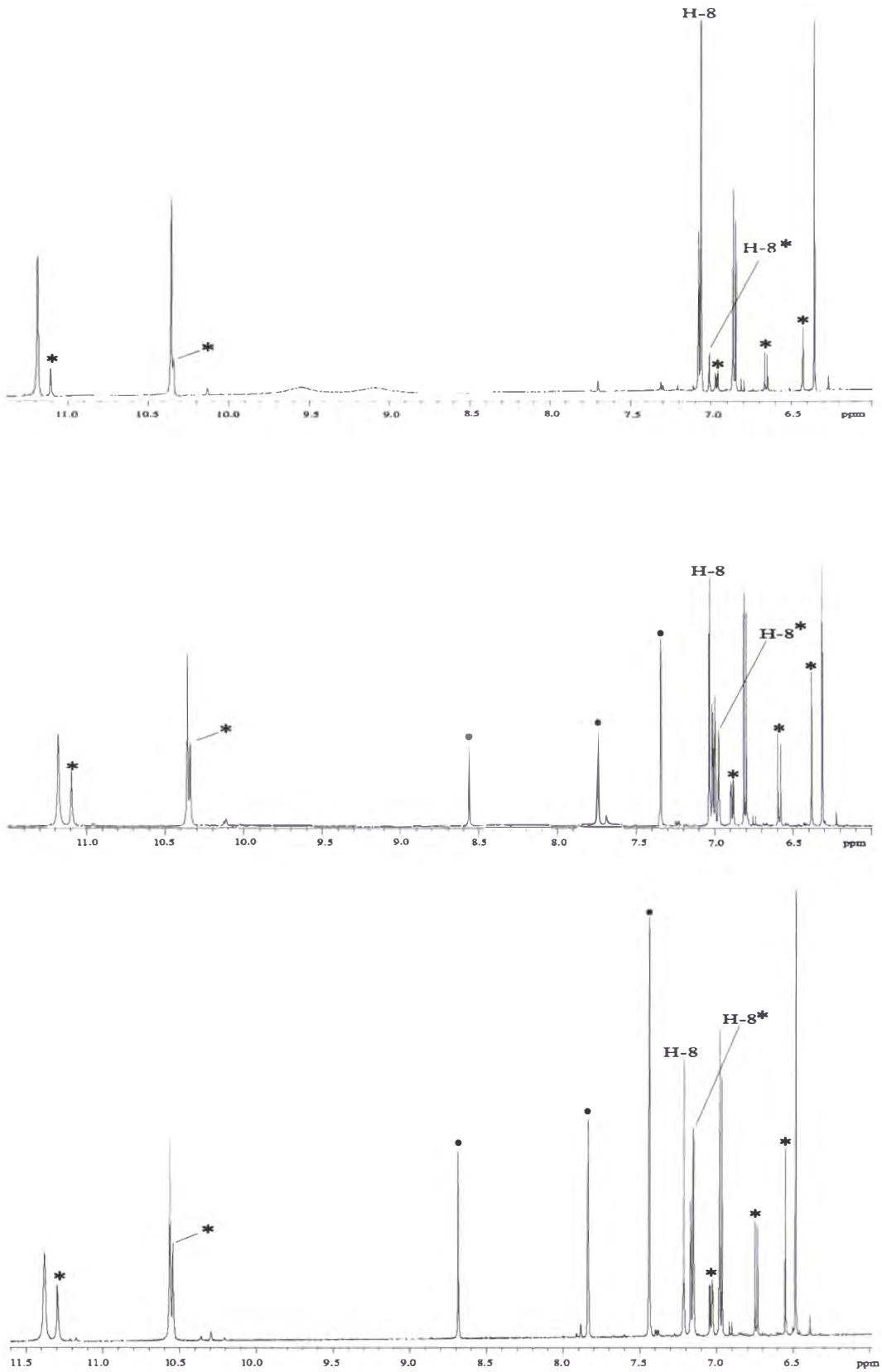

Figure 4.9: ^{1}H NMR spectra of **4.8**. Native isomer (top) after the addition of two (middle) and four (bottom) equivalents of pyridine-d_5. The minor isomer and solvent peaks (pyridine- d_5) are indicated with an '*' and '•' respectively. All spectra are referenced to DMSO-d_6 (δ_H 2.60).

In order to determine the unambiguous configuration of the natural isolated isomer, a 3D-structural analysis of **4.8** (MM2 minimized, Chem3D) was carried out (**Figure 4.10**) to determine the distance between the H-6 and NH-1 protons in the (*E*) and (*Z*) configurations. These data suggested that the structural geometry of $\Delta^{5,6}$ could be determined *via* NOE experiments, as the (*Z*) configuration affords a distance through space between H-6 and NH-1 that would result in no observable NOE enhancement (3.9 Å). Consequently, irradiation of the H-6 proton would result in correlations to both of the H-12 and H-8 aromatic protons, due to the C-6/C-7 carbon bond rotation if the natural isomer (major) is in the (*Z*) configuration. Equally, irradiation of the NH-1 proton would result in an NOE signal enhancement to both of the H-12 and H-8 protons.

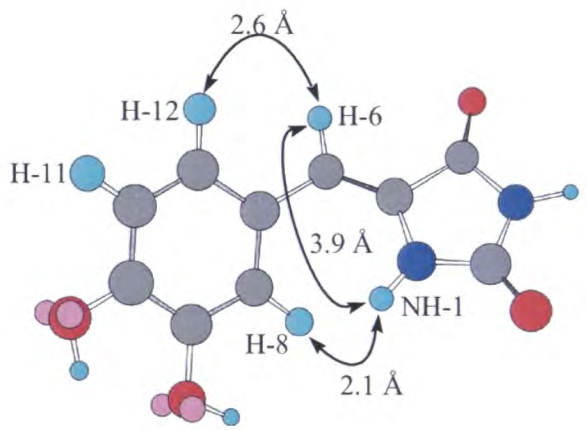

Z isomer

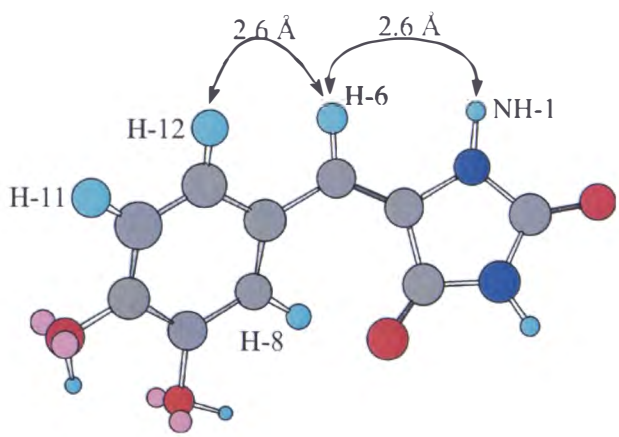

E isomer

Figure 4.10: Energy minimized Chem3D structures of the two possible isomers, (*Z*) and (*E*) respectively, for compound **4.8**.

On the basis of the 3D-structural analysis, the NOESY-1D experiment was used to determine the geometry of $\Delta^{5,6}$ by selective irradiation of both H-6 and NH-1. It is important to note that the chemical shifts displayed in the NOESY-1D NMR spectra (**Figure 4.11**, and the data reported in **Table 4.2**), have been affected by the addition of d_5-pyridine (four equivalents). These chemical shifts were obtained from the ^{1}H NMR spectrum (bottom spectrum of **Figure 4.9**, referenced to DMSO-d_6 (δ_H 2.60)).

Irradiation of the H-6 (now at δ_H 6.48) proton (**Figure 4.11**) resulted in the positive enhancement of both the H-8 (now at δ_H 7.21) and the H-12 (now at δ_H 7.17) protons, due to C-6/C-7 bond rotation. No enhancement of the NH-1 (δ_H 10.57) proton was observed. Alternatively, irradiation of the NH-1 (δ_H 10.57) proton resulted in the positive NOE enhancement of the H-8 and H-12 (δ_H 7.21 and 7.17, respectively) protons, while no enhancement of the H-6 (δ_H 6.48) proton was observed. These results strongly suggested that the major isomer was (*Z*), validating the initial speculation.

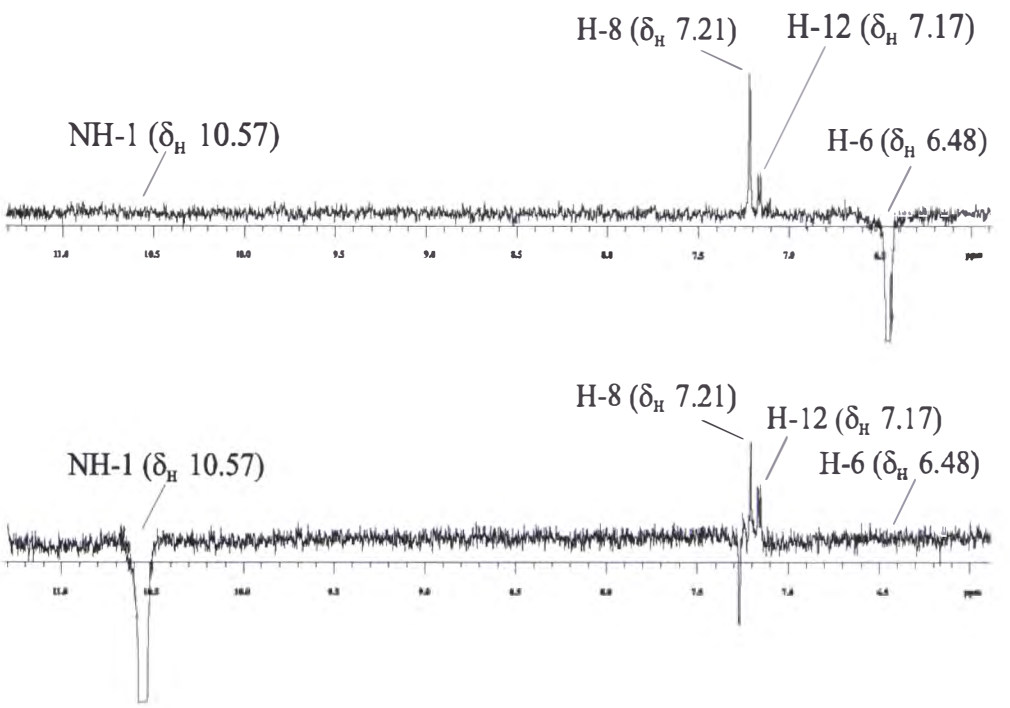

Figure 4.11: 1D-NOESY spectra from irradiation of the H-6 (δ_H 6.48, top) and NH-1 (δ_H 10.57, bottom) protons. Spectra are recorded in and referenced to DMSO-d_6 (δ_H 2.60) after the addition of four equivalents of pyridine-d_5.

The proton chemical shift data, referenced to DMSO-d_6, is shown in **Table 4.2** for the major isolated natural isomer of compound **4.8** before and after the addition of pyridine-d_5.

Table 4.2: ^{1}H NMR chemical shift comparison for the major isomer of **4.8** before and after the addition of four equivalents of pyridine-d_5 (in DMSO-d_6).

	4.8 (natural isomer)	**4.8** (four equivalents of pyridine-d_5)
Position	**^{1}H δ §**	**^{1}H δ §**
1	10.36 (1H, br s, NH)	10.57 (1H, br s, NH)
3	11.19 (1H, br s, NH)	11.38 (1H, br s, NH)
6	6.36 (1H, s)	6.48 (1H, s)
8	7.06 (1H, s)	7.21 (1H, s)
11	6.86 (1H, d, 7.5)	6.97 (1H, d, 7.5)
12	7.07 (1H, d, 7.5)	7.17 (1H, d, 7.5)

§ ^{1}H NMR spectra recorded at 500 MHz in DMSO-d_6. ^{1}H chemical shift values δ ppm from DMSO-d_6 (2.60) followed by number of protons, multiplicity and coupling constant (J/Hz).

The experimental ^{1}H NMR chemical shift data for both the major (Z) and minor (E) isomers of compound **4.8** isolated as natural products from the semi-preparative purification of the initial organic extract are shown in **Table 4.3**.

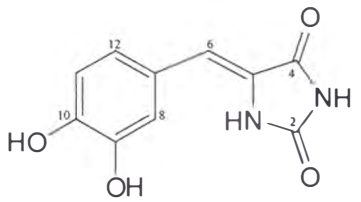

(Z) 5-(3,4-dihydroxybenzylidene)-imidazolidine-2,4-dione

(Z) **4.8**

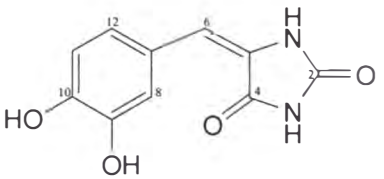

(E) 5-(3,4-dihydroxybenzylidene)-imidazolidine-2,4-dione

(E) **4.8**

Table 4.3: The ^{1}H NMR data obtained for the major (*Z*) and minor (*E*) isomers of compound **4.8** (DMSO-d_6) as determined from ^{1}H NMR spectrum (**Figure 4.5**).

	major (*Z*)	minor (*E*)
Position	**^{1}H δ** [§]	**^{1}H δ** [§]
1	10.36 (1H, br s, NH)	10.34 (1H, br s, NH)
3	11.19 (1H, br s, NH)	11.11 (1H, br s, NH)
6	6.36 (1H, s)	6.43 (1H, s)
8	7.07 (1H, s)	6.89 (1H, s)
9-OH[‡]	9.0 (1H, v br s)	9.0 (1H, v br s)
10-OH[‡]	9.5 (1H, v br s)	9.5 (1H, v br s)
11	6.86 (1H, d, 7.5)	6.65 (1H, d, 7.5)
12	7.07 (1H, d, 7.5)	6.97 (1H, d, 7.5)

[§]^{1}H NMR spectra recorded at 500 MHz in DMSO-d_6. ^{1}H chemical shift values δ ppm from DMSO-d_6 (2.60) followed by number of protons, multiplicity and coupling constant (*J*/Hz). [‡]Values may be interchanged within the column.

4.6: The Incidence and Biological Activity of Hydantoins

Hydantoins are a class of compounds containing an imidazolidine ring substituted at the C-5 position. The hydantoins are associated with a variety of biological properties. These include anticonvulsive,[149,150] antidepressant, antiviral,[151] antimicrobial and herbicidal[152] activity. They were introduced into medicine over 40 years ago as an alternative to barbiturates during chemical studies into the treatment of convulsive disorders such as epilepsy.[150] Diphenylhydantoin (phentoin, **4.9**) was synthesised by Wheeler and Hoffmann in 1911 *via* the condensation of benzaldehyde with the hydantoin moiety. Currently, phentoin (**4.9**) is still the drug of choice for the treatment of many seizure disorders, and possesses several attractive pharmacological features. There are, however, a number of side effects that limit the use of the drug.[149]

Many derivatives of hydantoin have been prepared in an effort to improve its pharmacokinetics by minimizing some of the less desirable side effects. The generation of hydantoin combinatorial libraries has emerged as a powerful tool for drug discovery, providing a wealth of spectroscopic and biological data.[153]

Naturally occurring hydantoins from terrestrial sources also possess biological activity. A novel hydantoin, hydantocidin (**4.10**) displays potent non-selective herbicidal activity, and was isolated from a fermentation broth of *Streptomyces hygroscopics* found in Annaka City, Japan.[154] This is a unique hydantoin compound, as it has a spiro-hydantoin ring fused at the anomeric position of β-D-ribofuranose. Herbicidal activity has been demonstrated by hydantocidin (**4.10**) at levels comparable to the commercially available glyphosate and bialaphos herbicides and it has been shown to be non-toxic to mammals (LD_{50} >1000 mg/kg).[152] Because of the potential commercial utility, hydantocidin (**4.10**) has become a synthetic target.

There are also a number of reports where hydantoins substituted at the C-5 carbon position have been isolated from the marine environment.

Aplysinopsin (**4.11**), an indole alkaloid, was first isolated from the sponge *Aplysinopsis reticulata* (Dictyoceratida) collected off the coast of Lizard Island, Great Barrier Reef, and was later reported from the taxonomically unrelated sponges *Verongia spengelii* from the Florida Keys, and *Dercitus* sp. from Belize.[148] Aplysinopsin has also been isolated from scleractinian corals of the family Dendrophylliidae, such as *Tubastraea aurea* from Japan and *Astroides calycularis* from the bay of Naples.[148]

Considerable interest in aplysinopsin (**4.11**) was provoked as it displayed specific cytotoxicity for cancer cells that was not surpassed by any synthetic analogue. The $N^{3'}$-methyl derivative (**4.12**), also isolated from *A. recticulata*, was most effective in affecting neurotransmission by directly inhibiting the biosynthesis of nitric oxide, an important secondary messenger that regulates neurotransmission among many other physiological processes.[148,155]

Aplysinopsin-type alkaloids can be classified into four structural types: aplysinposin (**4.11**), which was isolated from taxonomically unrelated sponges as well as from scleratinian corals; 3'-deimino-3'-oxoaplysinopsin (**4.13**) and 3'-deimino-2',4'-dedimethyl-3'-oxoaplysinopsin (**4.14**), which came from the dendrophylliid corals *Tubastraea* sp. and *Leptopsammia pruvoti*, respectively, and

finally 2'-demethylaplysinopsin (**4.15**) and the 6-bromo analogue (**4.16**), both isolated from the marine sponge *Dercitus* sp.[156] Although compounds **4.11** to **4.16** are structurally related, only 3'-deimino-3'-oxoaplysinopsin (**4.13**) and 3'-deimino-2',4'-dedimethyl-3'-oxoaplysinopsin (**4.14**) possess a hydantoin moiety.

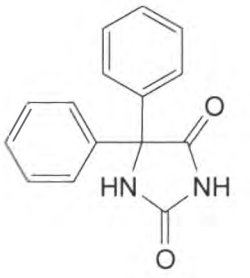

4.9

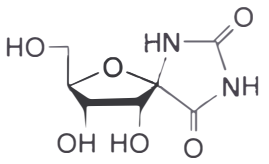

4.10

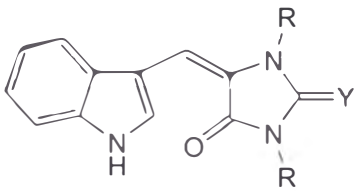

4.11 R=Me Y=NH
4.12 R=Me Y=NMe
4.13 R=Me Y=O
4.14 R=H Y=O

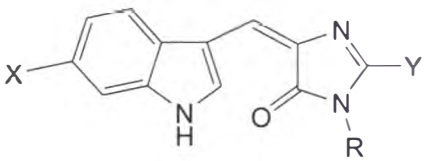

4.15 R=Me Y=NH_2 X=H
4.16 R=Me Y=NH_2 X=Br

In 1990, Pettit and co-workers[157] isolated (*E*)-axinohydantoin (**4.17**) from the sponge *Axinella* sp. The structure was determined by X-ray crystallography. Subsequently, the isolation of (*Z*)-axinohydantoin (**4.18**) and (*Z*)-debromoaxinohydantoin (**4.19**) from *Stylotella aurantium* and *Hymeniacidon* sp., respectively, has been reported by two groups.[158,159] Some of these tricyclic compounds have been shown to exhibit inhibitory activity against c-erbB-2 kinase and cyclin-dependent kinase 4, while others have shown no inhibitory activity against either kinase.[159]

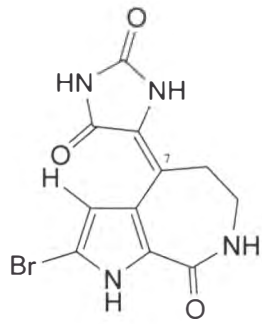

4.17 (*E*)-axinohydantoin

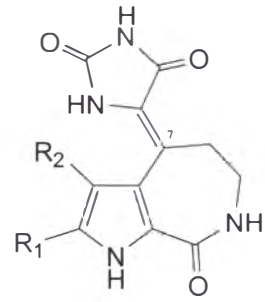

4.18 (*Z*)-axinohydantoin R_1=Br, R_2=H
4.19 (*Z*)-debromoaxinohydantoin R_1=R_2=H

The mukanadins A-C (**4.20**-**4.22**), isolated from the extracts of the Okinawan sponge *Agelas nakamurai* collected off Ie Island, also represent a series of bromopyrrole alkolids that possess unique biological activity.[160] However, only mukanadin B (**4.21**) contains a hydantoin moiety. The structurally related midpacamide (**4.23**) was isolated from a different species of *Agelas*, *A. mauritiana*.[161]

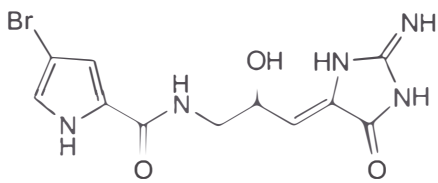

4.20

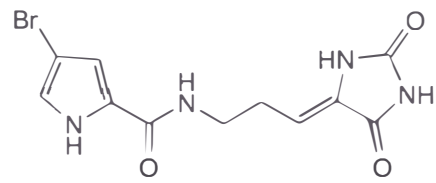

4.21

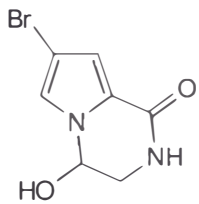

4.22

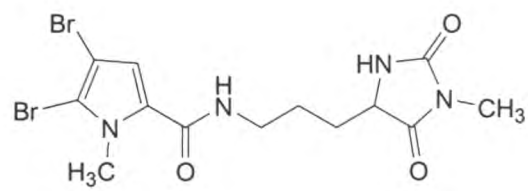

4.23

Ulosantoin (**4.24**), along with the structurally related compound dimethyl N^2-creatininylphosphate (**4.25**), were isolated from the sponge *Ulosa ruetzleri*. Although ulosantoin (**4.24**) is structurally extremely simple and represents the first report of a phosphorylated hydantoin, it exhibits potent insecticidal activity

against both the tobacco hornworm and the more persistent cockroach.[162] Feeding assays revealed that dimethyl N^2-creatininylphosphate (**4.25**) was void of activity, while ulosantoin (**4.24**) caused 100 % mortality within 24 hours at a dose of 200 ppm (in agar-based diet) against the tobacco hornworm. Topical applications of 0.2 and 2.0 μg, respectively, to the Mexican bean beetle and the southern armyworm were 100 % lethal.

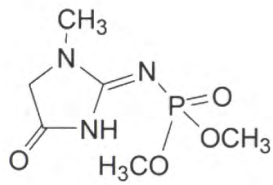

4.24

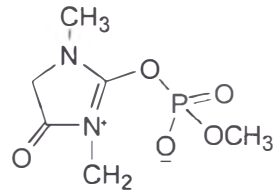

4.25

4.7: Concluding Remarks

The aim of this section of work was to isolate and identify the compound(s) responsible for the biological activity (P388) observed in the crude extract of the deep water Antarctic marine sponge *Suberites* sp. (02WM01-46).

Analytical reversed phase HPLC chromatography (in conjunction with a microtitre plate P388 assay) located the compound responsible for the observed activity in the crude extract, eluting at 7.8 minutes under standard 10 % CH_3CN/H_2O solvent gradient conditions. C_{18} flash column chromatography and reversed phase (C_{18}) semi-preparative HPLC yielded the purified novel C5-substituted hydantoin, (*Z*)-5-(3,4-dihydroxybenzylidene)-imidazolidine-2,4-dione (**4.8**).

Structural elucidation of **4.8** was achieved with the use of ^1H, ^{13}C, COSY (long-range), HSQC, CIGAR and NOESY NMR spectroscopy, accompanied by high resolution ESI mass spectrometry and comparison of ^{13}C NMR chemical shift data from previously reported synthetic analogues.[153]

The geometry of the C-5/C-6 double bond was determined using the 1D-NOESY NMR experiment after the addition of four equivalents of pyridine-d_5. The addition of base affected the chemical shifts of the protons observed in the ^{1}H NMR spectrum of the isolated compound. Irradiation of the olefinic proton H-6 (δ_H 6.48, initially at δ_H 6.36) resulted in an NOE enhancement of the aromatic protons positioned at H-8 and H-12 (δ_H 7.21 and 7.17, respectively, initially at δ_H 7.06 and 7.07, respectively) only, suggesting the (*Z*) configuration for the major natural product isolated, as no enhancement of the amide proton NH-1 (δ_H 10.24) was observed. The ratio of major to minor isomer was determined through direct comparison of the peak area integrals in the initial ^{1}H NMR spectrum of the purified compound **4.8** (*Z*/*E* 6:1). Reports indicate that if the N-2 position is methyl substituted, the (*E*) isomer is thermodynamically more stable, however if N-2 bears a proton or a lone pair in place of the methyl group, the (*Z*) isomer is thermodynamically more stable.[156] These reports also indicated that isomeric ratios for compounds of this type are photochemically and thermally enriched.[156] This phenomenon was observed in the current study, with increased exposure to ambient light conditions in the laboratory altering the signal ratios in the ^{1}H NMR spectra during structural elucidation. Isomeric ratios were also altered after the addition of base (pyridine-d_5), from 6:1 to 2:1 (*Z*/*E*). Therefore the equilibrium is dependant upon exposure to light and pH. The ratio was not restored upon the addition of a few drops of acid (TFA). Furthermore, thermal enhancement of isomer ratios was not observed in ^{1}H NMR experiments with a probe temperature increase from 23 °C to 43 °C. The photochemical equilibrium represents a useful means of obtaining the (*E*) isomer, provided that chromatographic methods are available to separate the stereoisomeric mixture.

This work represents the first isolation of (*Z*)-5-(3,4-dihydroxybenzylidene)-imidazolidine-2,4-dione (**4.8**) as a natural product from a marine sponge. The (*Z*)-5-(4-hydroxybenzylidene)-imidazolidine-2,4-dione (**4.9**) compound has been reported previously in the literature, but only as a synthetic product or as a derivative used in the synthesis of potential pharmaceuticals, pesticides and herbicides.[150,151,163]

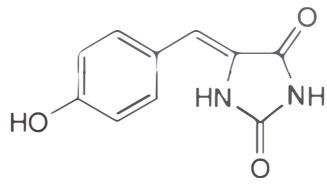

4.9

Evaluation of the cytotoxicity using the in-house anti-tumour assay system (P388) resulted in an IC_{50} of 4.5 μg/mL. Anti-tumour activity has been reported previously, however the 5-substituted hydantoins are more noted for their fungicidal and herbicidal activity.[148,150,151,163]

The ecological role of the novel hydantoin **4.8** can only be speculated on. Compounds of this class display a variety of biological activities, and as sponges are susceptible to overgrowth, predation and infection, such compounds may afford some level of chemical protection. It has also been suggested that the photoisomerisation of these compounds may be a non-destructive process for entrapping radiant energy, thus protecting the shallow water sponge from damaging UV rays.[148] However, it would seem unreasonable that a deep water Antarctic sponge, shielded from UV light by a thick layer of surface ice for a high percentage of the year, would require such an elaborate UV protection mechanism.

4.8: Summary of Isolation

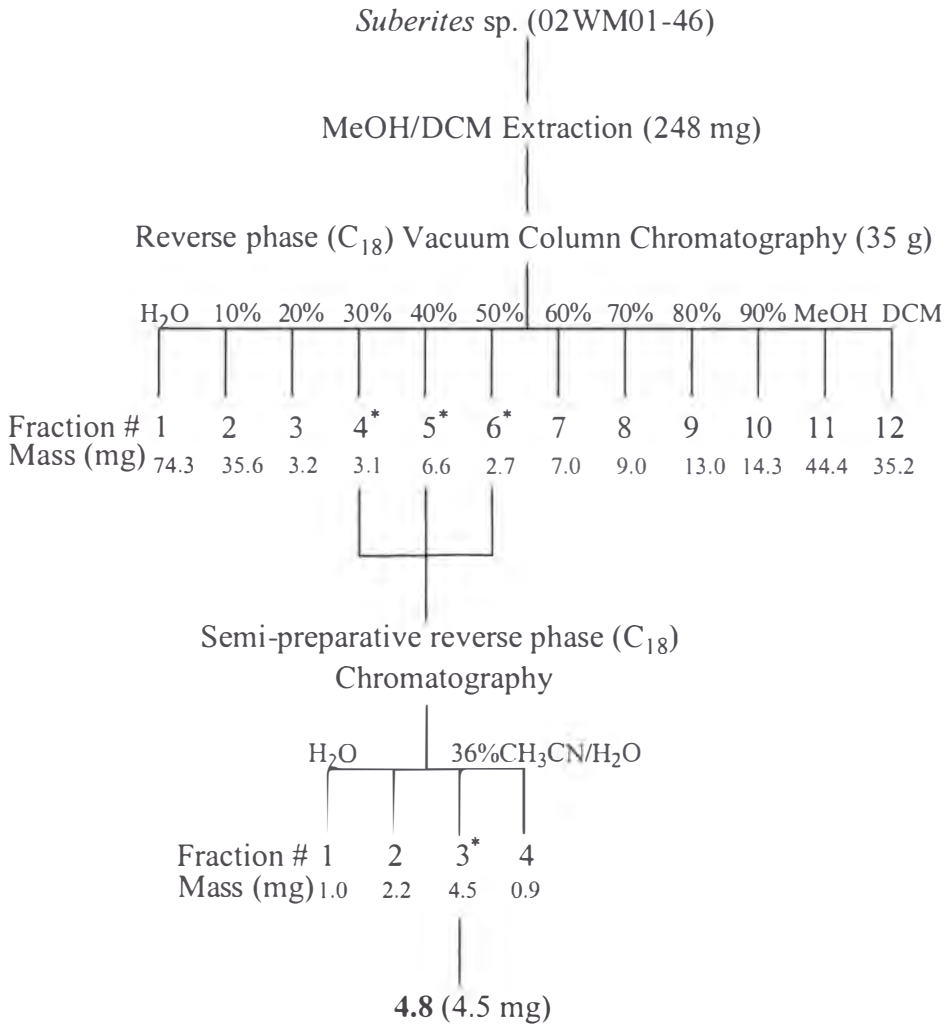

Scheme 4.1: Chromatographic purification summary for the Antarctic marine sponge *Suberites* sp. *Fraction contains biologically active compounds of interest.

CHAPTER 5

ISOLATION OF COMPOUNDS FROM THE ANTARCTIC MARINE SPONGE-DERIVED FUNGUS *Aspergillus* sp. (WS 76)

5.1: General Introduction

Aspergillus is one of the most commonly encountered and well recognised genera of terrestrial fungi.[164] They occupy a wide spectrum of habitats and rank among the most economically important fungi worldwide.[165] Although much of their impact is detrimental (food spoilage), they possess enormous economic utility in industrial applications. These include the production of synthetic chemicals, saccharification of rice starch for alcoholic liquors, the production of citric acid and other biosynthetic transformations.[166] *Aspergillus* enzymes are used extensively in the production/preservation of food stuffs, however, *Aspergilli* are frequently encountered in food products such as corn, rice and peanuts that are

stored incorrectly.[167] The most important consequence of their presence is mycotoxin contamination, which can cause serious toxic effects in humans and animals, including cancer (following ingestion) and acute/chronic respiratory disease (after inhalation).[168] The mycotoxins are secondary fungal metabolites produced by the fungi genera *Aspergillus*, *Penicillium* and *Fusarium*. Currently, more than 300 secondary metabolites from these filamentous fungi have been isolated and classified as mycotoxins.[169] Mycotoxins isolated from the genus *Aspergillus* include the aflatoxins (**5.1-5.5**) (*Aspergillus flavus* toxins). These five compounds are associated with the contamination of incorrectly stored grains and nuts.[170-174] The biosynthetic pathway leading to the aflatoxins is complex and involves many enzymes and genes. Simple anthraquinones are required early in the pathway where they are derivatised to xanthones, while the final stages consist of oxidative ring cleavage leading from xanthones to aflatoxins. Aflatoxin-producing species such as *A. flavus* only produce aflatoxins B_1 (**5.1**) and B_2 (**5.2**), while *A. parasiticus* and *A. nomius* are capable of further oxidative ring expansion to produce aflatoxins G1 (**5.3**) and G2 (**5.4**).[167,168,171,175] Aflatoxin B_1 (**5.1**), is generally the most common metabolite, and is considered the most toxic in terms of both acute and chronic toxicity. Despite there being only a small number of species of fungi producing aflatoxins, *A. flavus* and *A. parasiticus* are very widespread and are associated with a number of important food commodities consumed in all parts of the world.[168] While aflatoxin M_1 (**5.5**) is not as toxic or carcinogenic as aflatoxin B_1 (**5.1**),[173] it does, however, survive the pasteurization process and has even been reported in UHT milk.[174] The potential for widespread food contamination has prompted the world health organization to reclassify aflatoxins as Group I carcinogens and subsequently review the accepted concentration/kg in a range of foods destined for human consumption.[168]

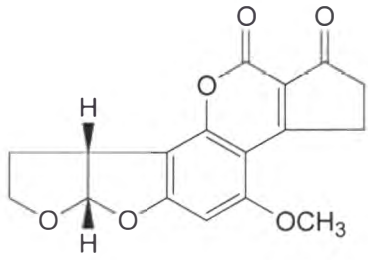

5.1

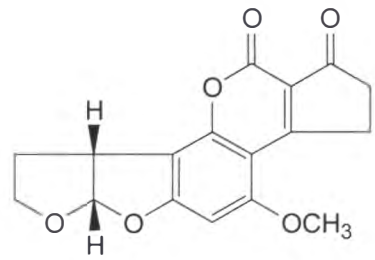

5.2

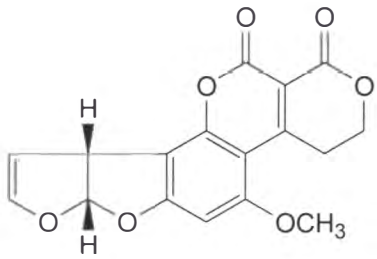

5.3

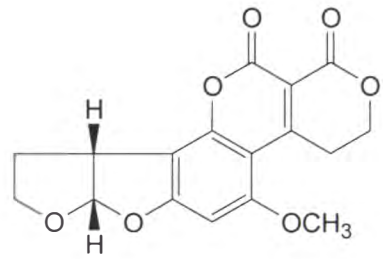

5.4

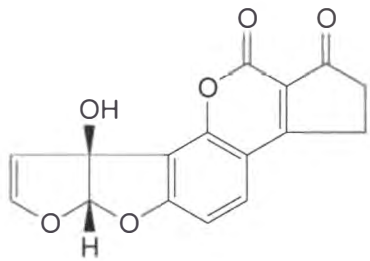

5.5

Native bioaerosols from compost facilities are a rich source of fungal secondary metabolites including mycotoxins.[176] The *Aspergillus* species *A. fumiagatus*, *A. versicolor* and *A. nidulans* are among the most frequently isolated species of fungi from the air space surrounding composting material.[169,176] Compounds frequently occurring in high concentrations from these species include gliotoxin (**5.6**), verruculogen (**5.7**), fumagillin (**5.8**) and sterigmatocystin (**5.9**). Exposure to these mycotoxins represents a genuine health hazard for workers at compost bio-waste handing facilities as they are attributable to both acute (toxic mould syndrome) and chronic (human lung cancer) health effects.[177] In order to establish the mechanism of toxicity of these compounds, gliotoxin (**5.6**), verruculogen (**5.7**), fumagillin (**5.8**) and sterigmatocystin (**5.9**) were tested *in vitro* against four established cell lines as a surrogate to tissues known or suspected to be targets of toxic effects of mycotoxins. These were the human lung cancer cell line (A-549), an epithelium-like cell line from human carcinoma (Hep-G2), murine fibroblasts from areolar and adipose connective tissue (L-929) and a neuronal cell line from

murine neuroblastoma (Neuro-2a). Of the four mycotoxins described, sterigmatocystin (**5.9**) possesses the highest toxicity. It was the most active against the A-549 cell line with an IC_{50} of 1.2 μg/ml.[169] No activity was observed for verruculogen (**5.7**) in any of the cell lines. The *in vivo* activity of sterigmatocystin (**5.9**) involves activation in the liver by enzymes where it binds covalently to DNA and induces various tumours. Non-cancer effects have also been observed following long term exposure to sterigmatocystin (**5.9**). Rats developed granulomatous lesions of the lung after two years of chronic airborne exposure to spores of *A. versicolor* containing sterigmatocystin (**5.9**).

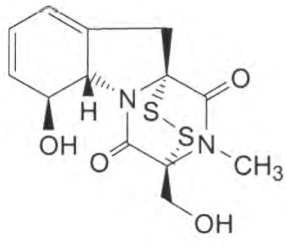

5.6

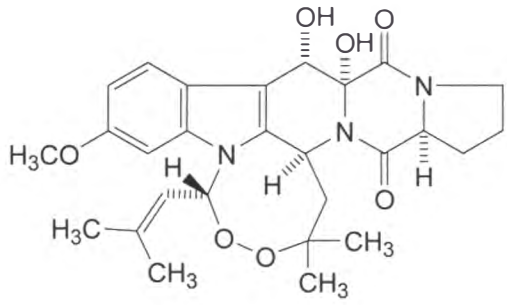

5.7

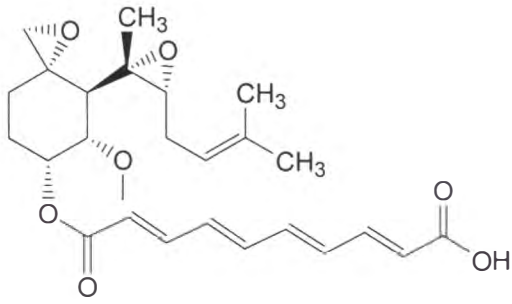

5.8

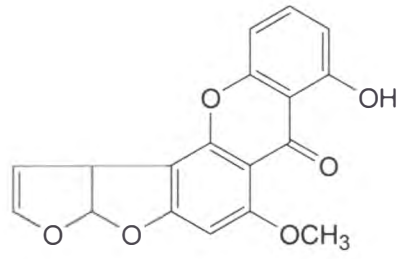

5.9

Another mycotoxin commonly isolated from airborne particulate associated with the processing of agricultural products infected with *Aspergillus ochraceus* is ochratoxin (**5.10**). This compound has been detected in settled and airborne dust at workplaces processing coffee, cocoa beans and spices. Elevated concentrations of ochratoxin (**5.10**) were detected in blood samples taken from exposed workers.[178] It has been shown to be potentially lethal when inhaled, and has been linked with renal failure.[179] As with the previously described mycotoxins, ochratoxin (**5.10**) possesses potent nephrotoxic and carcinogenic activity.

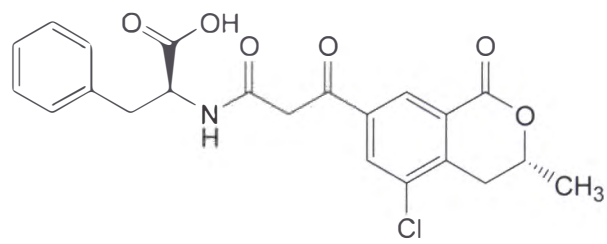

5.10

It has been known for many decades that marine-derived fungi are a rich source of diverse novel secondary metabolites.[11] Most commonly, the novel natural products are structural variations of compounds isolated from terrestrial fungi. Recently, many compounds have been reported from marine derived fungi of the genus *Aspergillus* isolated from sources that include red[180-182] and green[183] alga, sediment,[184] anenomes[185] and mussels.[186,187] Although reports in the literature for studies on the sponge-derived fungus *Aspergillus* are limited, those that have been published illustrate that sponge-derived fungi have enormous potential for the discovery of novel and/or biologically active natural products.

Sponges are filter feeders, and so accumulate a large variety of micro-organisms. Some of these are a direct representation of the microbes in the surrounding water column, while others are indicative of a specialized relationship. It is not clear, however, if the fungal cultures isolated from sponge tissue are from spores that have been accumulated from the feeding process, or whether they have been propagating within the host.[188]

A typical example of fungal biodiversity is shown with the isolation of five secondary metabolites from a seawater culture of a sponge-derived fungal isolate of *Aspergillus niger* by Crews *et al.* in 2000.[189] The saltwater culture of *A. niger* was obtained from the marine sponge *Hyrtios proteus* collected in the Dry Tortugas National Park in Florida. The organic extract afforded the novel compound asperic acid (**5.11**), along with the known compounds hexylitaconic acid (**5.12**), malformin C (**5.13**), pyrophen (**5.14**) and asperazine (**5.15**). Due to compound paucity, the absolute stereochemistry of asperic acid (**5.11**) was not

pursued. Structural assignment of the known compounds was achieved *via* direct comparison of experimental NMR data with that for the previously published structures. These compounds are representative of the ability of marine fungi to biosynthesize a variety of structural classes, including rearranged terpenes, polyketides, pyrones and unusual amino acids.

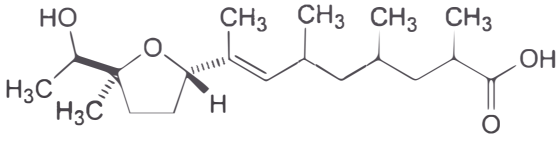

5.11

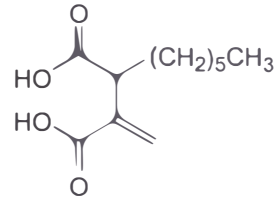

5.12

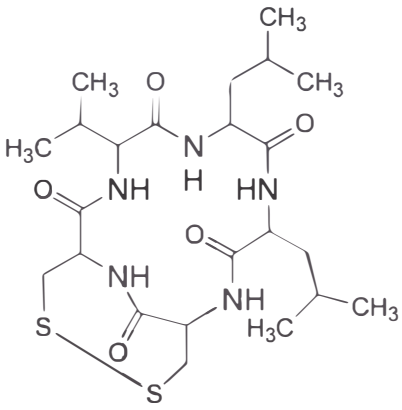

5.13

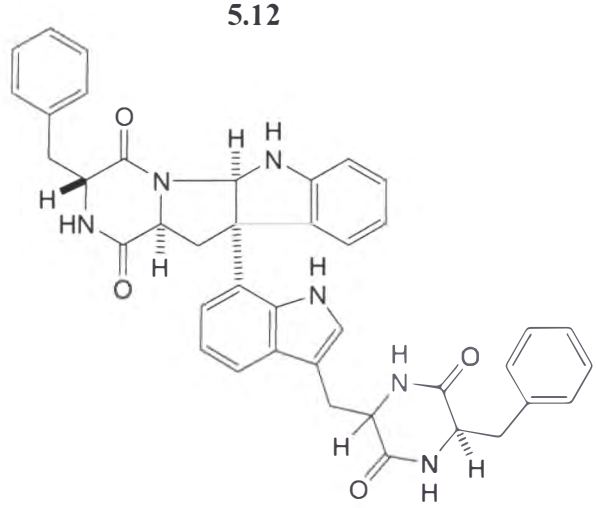

5.14

In 2003, seven new compounds were isolated from the fungus *Aspergillus versicolor*, derived from the marine sponge *Xestospongia exigua.* This sponge was collected by SCUBA diving at Mengangan Island, Bali, Indonesia, by Lin and co-workers.[190] The new compounds (**5.15-5.21**) represented previously undescribed angular chromones belonging to two structural classes. The compounds were subsequently named aspergillitine (**5.15**) and aspergione A-F (**5.16-5.21**). Aspergillitine (**5.15**) displayed only moderate antibacterial activity against *Bacillus subtilis*, while it was inactive against *Escherichia coli* and *Saccharomyces cerevisiae.* In the same assay system, aspergione C (**5.18**) and E (**5.20**) were inactive.

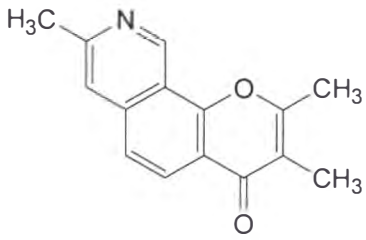

5.15

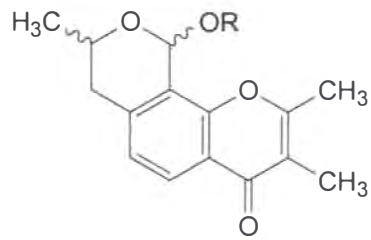

5.16 R = CH_3
5.17 R = H

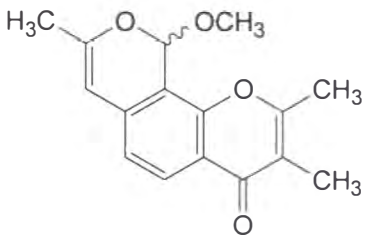

5.18

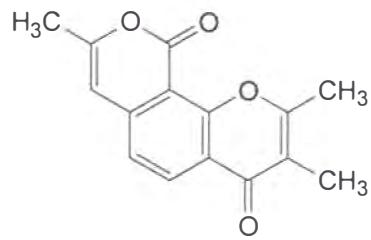

5.19

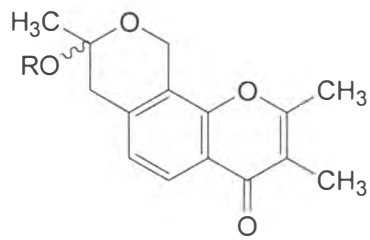

5.20 R = CH_3
5.21 R = H

More recently, eight metabolites, seven of which were novel, were isolated from the sponge-derived fungus *Aspergillus niger*, cultured from the marine sponge *Axinella damicornis* collected in the Mediterranean in 2004.[188] The compounds included the known fungal pigment cycloleucomelone (**5.22**), and the new compounds bicoumanigrin (**5.23**), the structurally unusual 4-benzyl-1*H*-pyridin-6-one derivatives aspernigrins A and B (**5.24** and **5.25**, respectively) and pyranonigrins A-D (**5.26-5.29**) which feature the novel pyrano[3,2-*b*]pyrrole skeleton previously undescribed in nature. All structures were elucidated using extensive 1D and 2D NMR techniques, and for the two chiral structures (**5.25** and **5.26**, respectively) absolute configurations were established by quantum chemical calculations of their circular dichroism spectra. Weak cytotoxicity *in vitro* against human cancer cell lines was reported for bicoumanigrin (**5.23**), while aspernigrin B (**5.25**) was found to display a strong neuroprotective effect against glutamic acid.

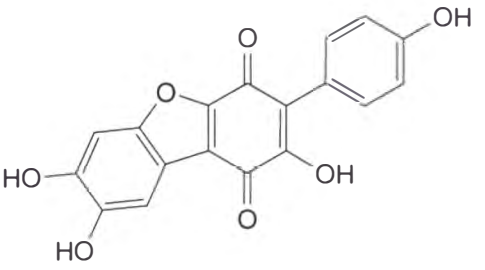

5.22

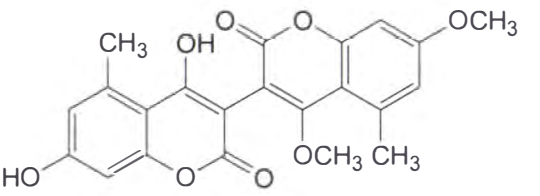

5.23

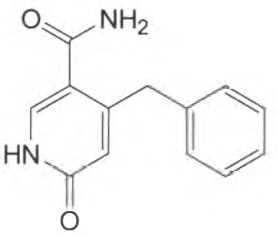

5.24

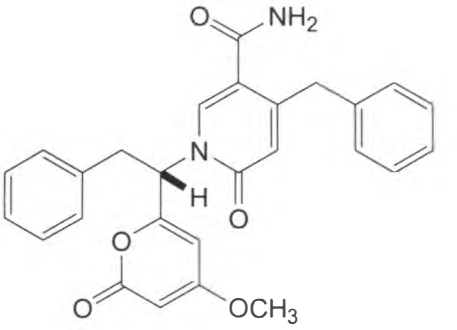

5.25

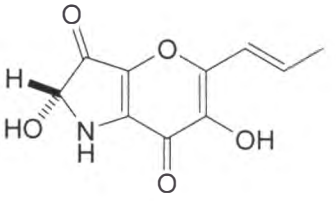

5.26

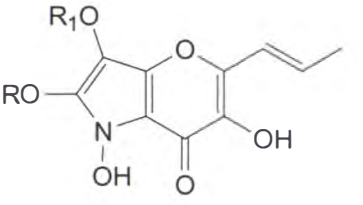

5.27 R = H $R_1 = CH_3$
5.28 R = CH_3 R_1 = H

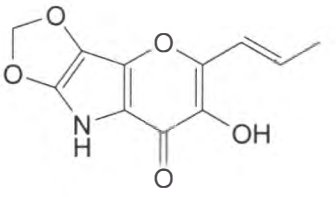

5.29

In this chapter, the previously undescribed anthraquinone compounds 6,8-*O*-dimethylbipolarin (**5.35**) and 5,6-dihydroxy-1,3-*O*-dimethoxy-2,3,4,5-tetrahydro-1-oxa-cyclohepta[*b*]anthracene (**5.41**) and the previously described 6,8-*O*-dimethylaverufin (**5.32**), 6,8-*O*-dimethylaverufanin (**5.34**), and 8-*O*-methylaverufin (**5.40**) were isolated from the organic extract of the Antarctic sponge-derived fungus *Aspergillus* sp. Structural elucidation was achieved using

1D and 2D NMR spectroscopy and mass spectrometry, and was aided by data comparisons with structural information reported in the literature. The biological activity of each compound was assessed in-house.

5.2: Introduction

The fungal culture (WS 132) was isolated from the Antarctic sponge *Kirkpatrickia varialosa* collected at Cape Armitage, Ross Island, Antarctica, at a depth of 25-30 m by SCUBA in Feburary 2002. The *K. varialosa* sponge tissue was sliced into 5 mm cubes, placed onto fungal-specific media and incubated at 26 °C until the cultures grew. To obtain enough material for structural elucidation, the isolate was re-cultured on rice (500 g) for 3-4 weeks at 26 °C, until all of the surface area of the solid rice media had been covered by the fungal growth.

5.3: Extraction of the Antarctic Marine Sponge-derived Fungus Aspergillus *sp. (WS 76)*

The entire fungal isolate WS 76 (500 mL) was extracted repeatedly with distilled EtOAc. The solvent was removed under vacuum, and the organic extract was further purified by partitioning between EtOAc/H_2O. The organic layer was collected, and the solvent removed under vacuum to yield an orange gum (229 mg). A small fraction (250 μg) of the extract was dissolved in MeOH, and subjected to reversed phase (C_{18}) analytical HPLC microtitre plate collection (see **Experimental, Section 7.1.6.2**). The dilution plates were analysed *via* the in-house P388 assay. Two areas of activity were identified. These were attributable to the compounds eluting between 12.5 to 16.5 and 25 to 30 minutes.

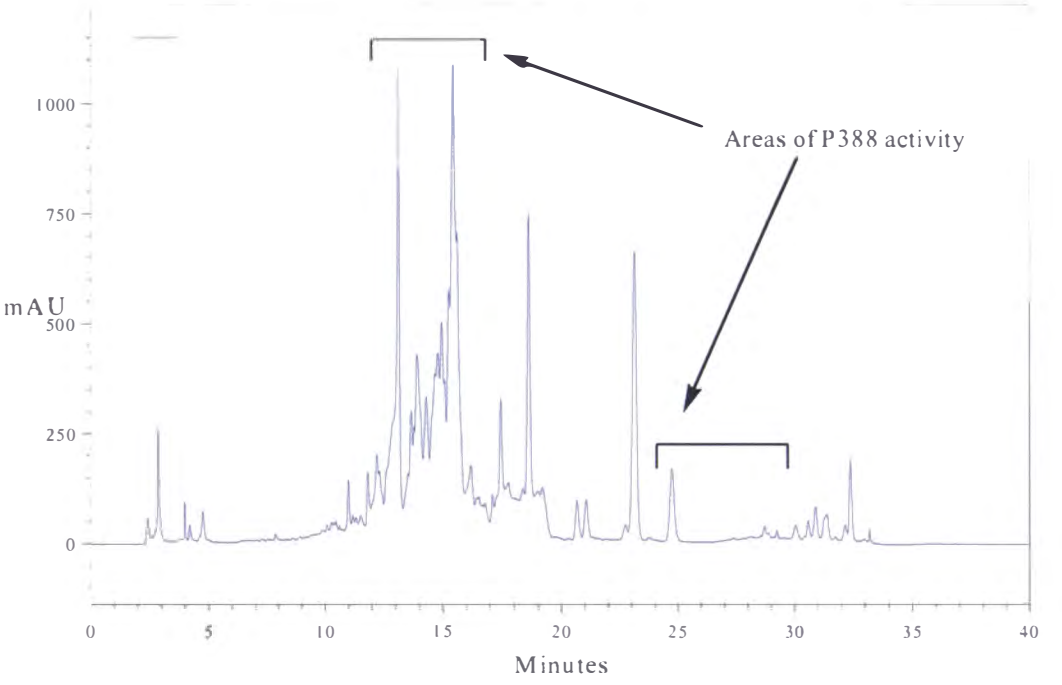

Figure 5.1: HPLC trace of EtOAc extract of WS 76, indicating the areas of activity determined by P388 assay.

Analysis of the UV chromophores (**Figure 5.2**) for the compounds associated with these areas of activity revealed that these compounds were all related, with λ_{max} at 225, 285 and 445 nm. However, it was also noted that the UV profiles of the major non-active compounds eluting at 18.6 and 23 minutes were also similar to those in the active region of the chromatograph. UV maxima (λ_{max}) at 225 and 285 nm are characteristic of a quinone moiety (**5.30**), however, the presence of the λ_{max} at 445nm (extended conjugation) suggested the presence of an anthraquinone chromophore (**5.31**).

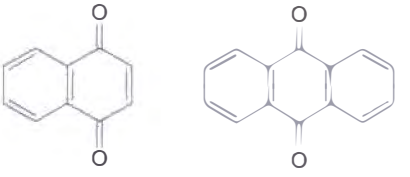

5.30 **5.31**

Positive LCESI mass spectrometry of the organic extract identified $[M+H]^+$ ions ranging from 369 to 399 Da for the compounds eluting in the region of observed

activity. A database search[130,145] based on mass and UV structural information resulted in 125 hits. The majority of these compounds possessed some level of biological activity. Due to the number of possible matches for the compounds present in the extract, further isolation was deemed necessary for an unambiguous identification of the compound(s) responsible for the observed activity.

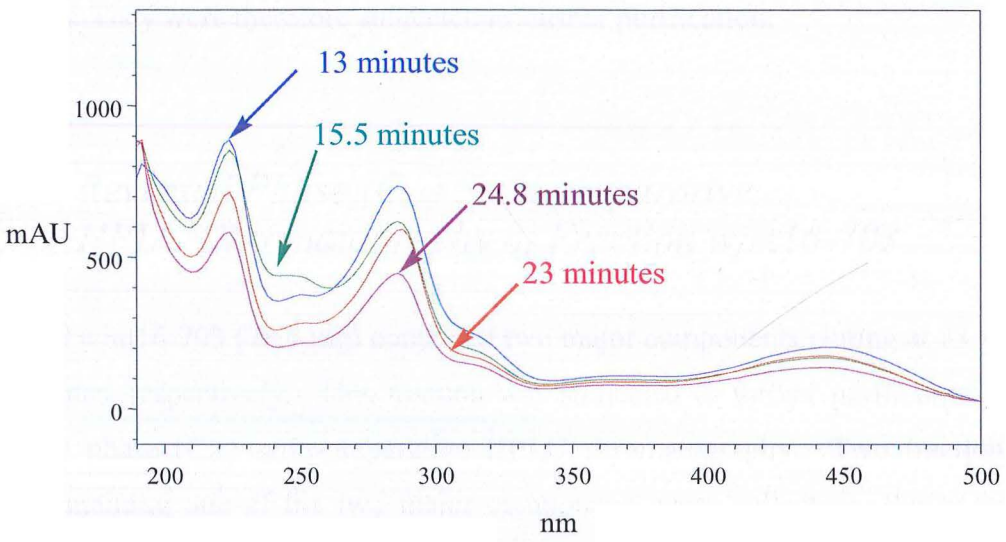

Figure 5.2: UV profile of peaks in areas of P388 activity as determined by microtitre plate assay. This includes the UV profile of the major (non-active) compound eluting at 23 minutes.

5.4: Chromatographic Isolation of Bioactives

5.4.1: Normal Phase (DIOL) Flash Chromatography of the Organic Extract of the Antarctic Marine Sponge-derived Fungus Aspergillus *sp (WS 76)*

The EtOAc-soluble fraction was subjected to further purification by normal phase (DIOL) flash chromatography. The column was eluted with a stepped solvent gradient from a pet. ether/DCM mixture to EtOAc. The remaining material was washed from the column with combinations of EtOAc and MeOH into the 17th fraction. All fractions were submitted for reversed phase C_{18} HPLC chromatographic analysis using the standard 10 % gradient (as described in

Experimental, Section 7.1.3.2). Fractions wjm16-703 (100 % DCM, 78.3 mg), wjm16-705 (4:1 DCM/EtOAc, 15.6 mg), wjm16-708 (1:1 DCM/EtOAc, 5.2 mg) and wjm16-710 (3:7 DCM/EtOAc, 5.4 mg) contained major components that exhibited the characteristic retention times and UV chromophores of the compounds responsible for the activity observed in the original organic extract of WS 76. None of these fractions were considered pure enough for spectroscopic analysis. They were therefore subjected to further purification.

5.4.2: Reversed Phase (C_{18}) Semi-preparative HPLC Chromatography of Fraction wjm16-703

Fraction wjm16-703 (78.6 mg) contained two major components eluting at 23 and 25 minutes, respectively. This fraction was subjected to further purification by reversed phase (C_{18}) semi-preparative HPLC chromatography. Two fractions, each containing one of the two major components were collected. Purity was confirmed by re-injection onto an analytical HPLC column. Both fractions were analysed by ^{1}H NMR, and were found to contain sufficient mass for COSY, HSQC and CIGAR 2D NMR spectroscopic experiments. Initial inspection of the NMR spectra confirmed that these compounds were related. Molecular mass was confirmed by HRESI mass spectrometry, which in combination with the NMR data led to the identification of the previously reported compounds 6,8-*O*-dimethylaverufin (**5.32**) and 6,8-*O*-dimethylaverufanin (**5.34**) (see **Sections 5.5.1** and **5.5.2**, respectively).

5.4.3: Reversed Phase (C_{18}) Semi-preparative HPLC Chromatography of Fraction wjm16-705

The compounds eluting in fraction wjm16-705 were not responsible for the observed biological activity, but did possess the characteristic UV profile of the compounds isolated in fraction wjm16-703. This fraction was further purified by semi-preparative reversed phase C_{18} chromatography. A separation gradient was developed on an analytical scale, and then scaled up by an appropriate factor to

make large scale injections possible. Fraction wjm16-705 was processed *via* consecutive injections onto the column, and fractions were collected as peaks eluted. The purity of the collected fractions was confirmed by re-injection onto the analytical HPLC column. One fraction contained sufficient mass and was sufficiently pure for structural elucidation by 1D and 2D NMR analysis. The previously unidentified compound 6,8-*O*-dimethylbipolarin (**5.35**) was subsequently identified (see **Sections 5.5.3**).

5.4.4: Reversed Phase (C_{18}) Semi-preparative HPLC Chromatography of Fraction wjm16-708

Analytical reversed phase HPLC analysis of fraction wjm16-708 established that this fraction was essentially pure, with only a minor contaminant eluting 1.5 minutes after the major component. Reversed phase (C_{18}) semi-preparative HPLC chromatography was used, and a gradient method was developed to facilitate further separation. One major fraction was collected and analysed using 1D and 2D NMR spectroscopy and mass spectrometry to identify the previously reported compound 8-*O*-methylaverufin (**5.40**) (see **Section 5.5.5**).

5.4.5: Reversed Phase (C_{18}) Semi-preparative HPLC Chromatography of Fraction wjm16-710

Fraction wjm16-710 was identified in earlier experiments, *via* microtitre plate analysis, to contain additional compounds responsible for the activity of the crude extract. This fraction, like fraction wjm16-708, was essentially one compound (C_{18}-HPLC), and was purified by the same reversed phase (C_{18}) semi-preparative HPLC chromatography. One major fraction was collected, and the purity was confirmed by re-injection onto the reversed phase (C_{18}) analytical HPLC column. Further examination of this fraction by 1D and 2D NMR spectroscopy and mass spectrometry resulted in the identification of the previously unreported cyclohepta[*b*]anthracene (**5.41**) (see **Section 5.5.6**).

5.5: Structural Elucidation of Compounds Isolated from the Antarctic Marine Sponge-derived Fungus Aspergillus *sp. (WS 76)*

5.5.1: Structural Elucidation of **5.32**

Compound **5.32** (4.4 mg) was isolated as a bright yellow powder from the first fraction of wjm16-703. The HRESI mass spectrum indentified a $[M+H]^+$ ion at *m/z* 397.1264 (calc. 397.1287), which led to the molecular formula of $C_{22}H_{20}O_7$ corresponding to 13 DBE. Analysis of the UV-VIS spectrum, combined with the fact that this compound was highly coloured, suggested that an extended conjugated aromatic system was present within the molecule, such as an anthraquinone ring system. The ^{1}H NMR spectrum (**Figure 5.3**) revealed the presence of 11 well-defined signals. These comprised a downfield phenolic proton (δ_H 13.45) hydrogen bonded to a carbonyl, three methine aromatic protons (δ_H 7.47, 7.22 and 6.79), a methine proton (δ_H 5.38), two methoxy signals (δ_H 4.04 and 3.99), six methylene signals (δ_H 2.06, 1.86, 1.66, 1.57, 2.02 and 1.86), and finally a methyl signal (δ_H 1.53). These proton signals satisfied the requirements of the molecular formula. The ^{13}C NMR chemical shift data was assigned from close examination of both the HSQC and CIGAR NMR spectra. Two carbonyl carbons (δ_C 205.4 and 183.1), nine sp^2 aromatic quaternary carbons (δ_C 165.2, 162.9, 159.8, 159.7, 137.5, 132.8, 117.2, 115.5 and 110.4), three protonated sp^2 aromatic carbons (δ_C 107.9, 105.1 and 104.5), one sp^3 carbon bearing oxygen (δ_C 67.1), three sp^3 methylene carbons (δ_C 27.3, 16.2 and 35.8), one sp^3 quaternary carbon bearing two oxygen atoms (δ_C 101.1), two sp^3 methyl carbons associated with two methoxy groups (δ_C 56.6 and 56.1) and one sp^3 methyl (δ_C 28.0) were detected.

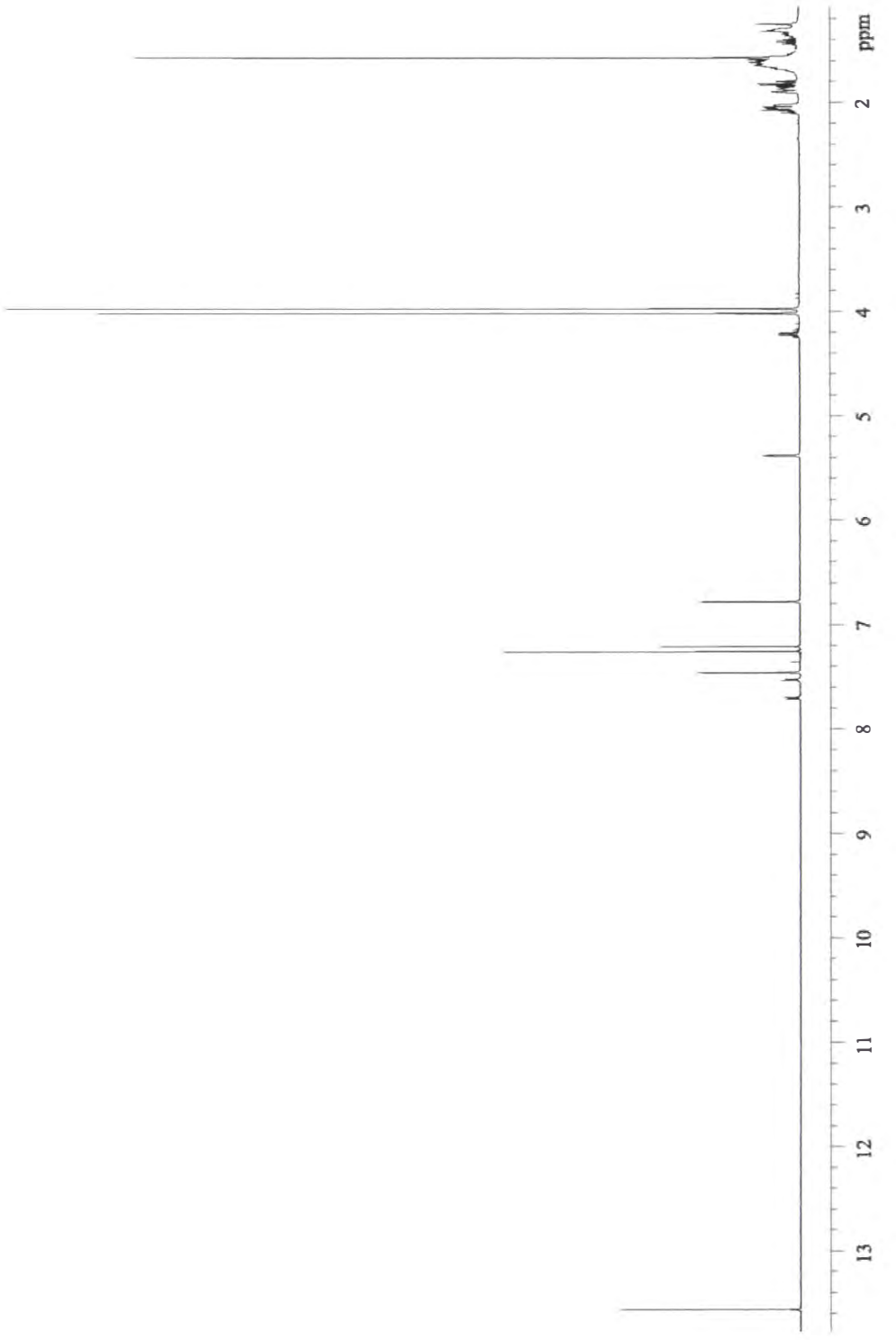

Figure 5.3: The ^{1}H NMR spectrum of **5.32** ($CDCl_3$).

Examination of the COSY spectrum established a partial structure *via* observations of the consecutive correlations from the H-11 (δ_H 5.38) oxygenated methine proton to the, H-8a,b (δ_H 2.02, 1.86), H-9a,b (δ_H 1.66, 1.57) and H-10a,b (δ_H 2.06, 1.86) methylene protons.

The CIGAR correlations from the H-16 (δ_H 1.53) methyl protons to the C-7 (δ_C 101.1) carbon confirmed the position of the methyl group at position C-7, while the additional CIGAR correlations to C-6a and C-8 (δ_C 159.8 and 35.8, respectively) carbons, combined with the correlations from the H-11 (δ_H 5.38) methine proton to the C-6a, C-7, and C-11a (δ_C 159.8, 101.1 and 117.2, respectively) carbons, established the connectivity of ring E through ring D to the aromatic core (**Figure 5.4**).

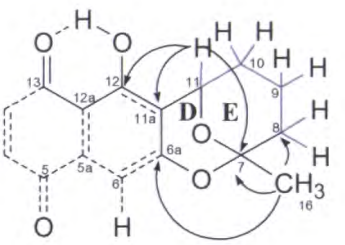

Figure 5.4: COSY (blue) and CIGAR (black arrows) correlations leading to the assignment of rings D and E, and establishing connectivity to the aromatic core.

The chemical shift of the C-12 (δ_C 159.7) aromatic carbon suggested phenolic substitution at this position. The phenolic proton observed in the ^{1}H NMR spectrum at δ_H 13.35 was hydrogen bonded to a carbonyl moiety forming a *pseudo* 6-membered ring, confirmed by the CIGAR correlation from OH-12 (δ_H 13.45) proton to the C-13 (δ_C 205.4) carbonyl carbon. This low field C-13 (δ_C 205.4) carbon established the presence of an aromatic ketone group, one of the two required for the anthraquinone moiety suggested by the UV data. The H-6 (δ_H 7.22) aromatic proton was correlated by the CIGAR experiment to the C-5, C-6a, C-11a and C-12a (δ_C 183.1, 159.8, 117.2 and 110.4, respectively) carbons, identifying the second downfield aromatic ketone positioned at carbon C-5. This satisfied the requirements of the partial anthraquinone core structure indicated by the initial UV spectral data, and confirmed ring C. However, no 2D NMR

correlations were observed for C-5a within ring C. A ^{13}C NMR spectrum simulation[191] estimated a chemical shift value of approximately δ_C 134. On this basis, the assignment of position C-5a (δ_C 132.8) *ortho* to the aromatic proton at H-6 (δ_H 7.22) was tentatively made (**Figure 5.5**).

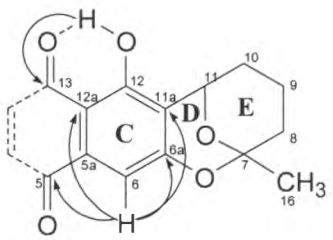

Figure 5.5: The key CIGAR (black arrows) correlations leading to the assignment of ring C and the partial structure of ring B, the central ring associated with the anthraquinone core structure.

The remaining connectivity was achieved utilising the signals of the remaining aromatic protons H-2 and H-4 (δ_H 6.79 and 7.47, respectively). The COSY cross peak correlation from H-2 (δ_H 6.79) to the H-4 (δ_H 7.47, $J_{2,4}$ = 2.5 Hz) proton, combined with the coupling constant extracted from the ^1H NMR spectrum, suggested that a *meta* relationship existed between these protons on the aromatic ring, establishing C-2 to C-4 connectivity. CIGAR correlations from the H-2 (δ_H 6.79) aromatic proton to the C-2, C-3, C-4a and C-5 (δ_C 105.1, 165.2, 137.5 and 183.1, respectively) carbons and correlations from the H-4 (δ_H 6.79) aromatic proton to the C-1, C-3, C-4 and C-13a (δ_C 162.9, 165.2, 104.5 and 115.5, respectively) carbons established ring A. This data also confirmed the previous assignment of C-5a (δ_C 132.8) to ring C as it had the most reasonable carbon chemical shift followed by the signal at δ_C 137.7. However C-3 (δ_H 137.7) was unambiguously assigned as being part of ring A. The two remaining methoxy methyl proton signals δ_H 3.99 and δ_H 4.04, were assigned as a result of the observed CIGAR correlations from the H-14 and H-15 (δ_H 4.04 and 3.99, respectively) methyl protons to the C-1 and C-3 (δ_C 162.9 and 165.2, respectively) aromatic carbons, therefore, the two methoxy groups H-14 and H-15 were positioned at C-1 and C-3, respectively (**Figure 5.6**).

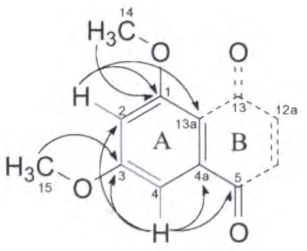

Figure 5.6: COSY (blue) and CIGAR (black arrows) correlations leading to the assignment of rings A and B of the anthraquinone core structure of **5.32**.

On the basis of these findings structure **5.32** was proposed, annotated with an arbitrary numbering system used for the structural elucidation process and also used in **Table 5.1**. This structure also satisfies the requirements of the DBE's.

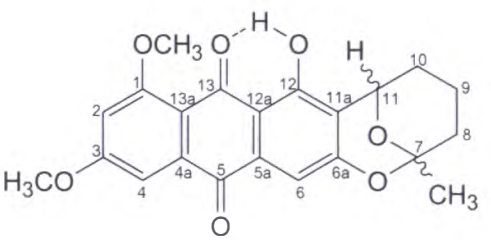

5.32

From a literature search,[130,145] this compound was identified as 6,8-*O*-dimethylaverufin (**5.32**), a 1-hydroxy-6,8-dimethoxy-anthraquinone that contains a 1,3-benzodioxan system. The numbering system used in the literature is shown in **Figure 5.7**.

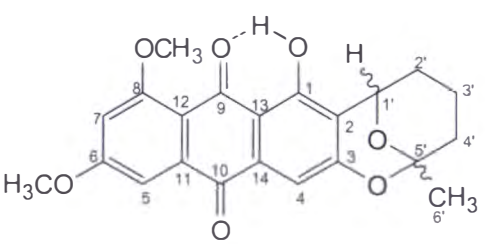

Figure 5.7: Numbering assignment for **5.32**, as reported in the literature.[192,193]

The demethyl compound averufin (**5.33**) was first isolated by Pusey *et al.* in 1963.[194] However, the structure was reported incorrectly, with the methyl group located at C-11. Three years later Holker *et al.*[193] isolated both 6,8-*O*-

dimethylaverufin (**5.32**) and averufin (**5.33**) as natural products, and suggested on the basis of ^{1}H NMR analysis that the methyl group should be positioned at C-7 not C-11 as originally reported.[194] The structure of averufin (**5.33**) was formally revised in a paper published by Roffey *et al.*,[195] where two benzo-1,3-dioxan ring moieties were synthesised with the methyl group positioned at C-11 in one compound and at the C-7 position in the other. Their NMR experiments confirmed that the methyl positioned at C-7 was consistent with Holker's hypothesis. In 1985, Maebayashi *et al.*[196] reported the isolation of 6,8-*O*-dimethylaverufin as a novel compound from a rice extract inoculated with *Emericella foeniculicola*. The first full NMR characterisation was published by Maebayashi,[196] and direct comparison of the current data (^{1}H, ^{13}C, MS, IR and optical rotation) with that of the known compound confirmed that the isolated metabolite was 6,8-*O*-dimethylaverufin (**5.32**) (**Table 5.1**).

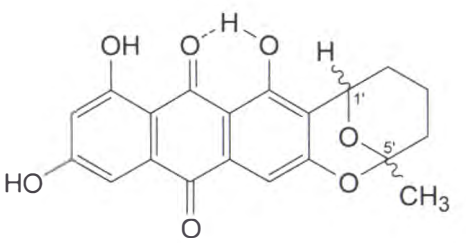

5.33

5.5.1.1: Stereochemistry of **5.32**

The optical rotation for 6,8-*O*-dimethylaverufin (**5.32**), $[\alpha]_D^{20}$ = -20° (c=0.22, $CHCl_3$)), was consistent, within experimental error, with the data reported[196] ($[\alpha]_D^{20}$ = -18° (c=0.22, $CHCl_3$)) suggesting the stereochemistry for **5.32**, was identical to that reported. However, no stereochemistry was indicated on the structure described in this paper. A later publication reported that atoms C-1' and C-5' of 6,8-*O*-dimethylaverufin (**5.32**) were assumed to have the *S*-configuration based upon direct comparisons of NMR data for structurally similar compounds produced by the same organism, although the published structure is graphically depicted as having incorrectly assigned stereochemistry at C-1' and C-5'.[197]

Based on the available NMR and optical rotation data no relative stereochemistry was assigned for **5.32**, as the *S*-isomer could not be unambiguously assigned over the *R*-isomer.

The full experimental NMR data for 6,8-*O*-dimethylaverufin (**5.32**) is shown in **Table 5.1**. Note that the arbitrary numbering system used for structural elucidation is also used in **Table 5.1** where 6,8-*O*-dimethylaverufin is equivalent to 1,3-*O*-dimethylaverufin.

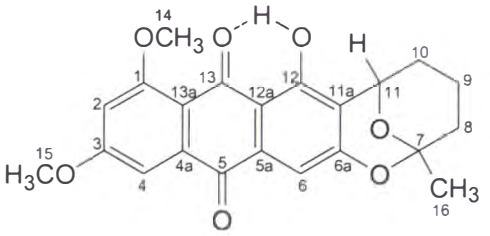

5.32

Table 5.1: The ^{1}H, COSY, HSQC and CIGAR NMR data for **5.32** ($CDCl_3$).

Position	^{13}C δ §	^{1}H δ ξ	COSY	CIGAR
1	162.9 (C)			
2	105.1 (CH)	6.79 (1 H, d, 2.5)	H-4	C-13a, C-4, C-3, C-1
3	165.2 (C)			
4	104.5 (CH)	7.47 (1 H, d, 2.5)	H-2	C-5, C-4a, C-3, C-2
4a	137.5 (C)			
5	183.1 (CO)			
5a	132.8 (C)			
6	107.9 (CH)	7.22 (1H, s)		C-12a, C-11a, C-6a, C-5
6a	159 8 (C)			
7	101.1 (C)			
8	35.8 (CH_2)	8a: 2.02 (1H, m)	H-9a, H-9b, H-8b,	
		8b: 1.86 (1 H, m)	H-9a, H-9b, H-8a,	
9	16.2 (CH_2)	9a: 1.66 (1 H, m)	H-10a, H-10b, H-9b, H-8a, H-8b	
		9b: 1.57 (1 H, m)	H-10a, H-10b, H-9a, H-8a, H-8b	C-11, C-8, C-7
10	27.3 (CH_2)	10a: 2.06 (1H, m)	H-11, H-10b, H-9a, H-9b, ,	C-11, C-8
		10b: 1.86 (1H, m)	H-11, H-10a, H-9a, H-9b,	C-11
11	67.1 (CH)	5.38 (1 H, dd, 2.5, 9)	H-10a, H-10b	C-12, C-11a, C-9, C-7, C-6a
11a	117.2 (C)			
12	159.7 (C)			
OH-12		13.45 (OH, s)		C-13
12a	110.4 (C)			
13	205.4 (CO)			
13a	115.5 (C)			
14	56.6 (OCH_3)	4.04 (3H, s)		C-1
15	56.1 (OCH_3)	3.99 (3H, s)		C-3
16	28.0 (CH_3)	1.53 (3H, s)		C-8, C-7

§ ^{13}C NMR chemical shift values (δ ppm from $CDCl_3$ at 77.0) obtained from both HSQC and CIGAR experiments. ξ ^{1}H NMR spectra recorded at 500 MHz in $CHCl_3$ (δ ppm from $CHCl_3$ at 7.25), followed by number of protons, multiplicity and coupling constants (*J*/Hz).

5.5.2: Structural Elucidation of **5.34**

Compound **5.34** (3.4 mg) was isolated as an orange powder, and was the second compound to elute from fraction 16-703. HRESIMS identified the $[M+H]^+$ ion at *m/z* 399.1450 (calc. 399.1444), which led to the molecular formula of $C_{22}H_{22}O_7$, which is 2 Da more than 6,8-*O*-dimethylaverufin (**5.32**) and equated to 12 DBE. Analysis of both the UV chromophore and the ^{1}H NMR spectrum (**Figure 5.8**) revealed that this compound was structurally related to 6,8-*O*-dimethylaverufin (**5.32**). However, several differences in the ^{1}H NMR spectrum were noted. These consisted of the addition of a second hydrogen bonded phenolic proton (δ_H 9.80), a variation in the splitting pattern for the oxymethine at δ_H 5.38 now at δ_H 5.16 (previously a doublet, but now a doublet of doublets, J = 2.5, 9.0 Hz), the appearance of a new signal at δ_H 3.72 (m) and the singlet methyl previously identified at δ_H 1.53 was now a doublet positioned upfield at δ_H 1.29 (J = 2.5 Hz). Overall, this suggested a change in the cyclic ketal functionality, ring D of 6,8-*O*-dimethylaverufin (**5.32**).

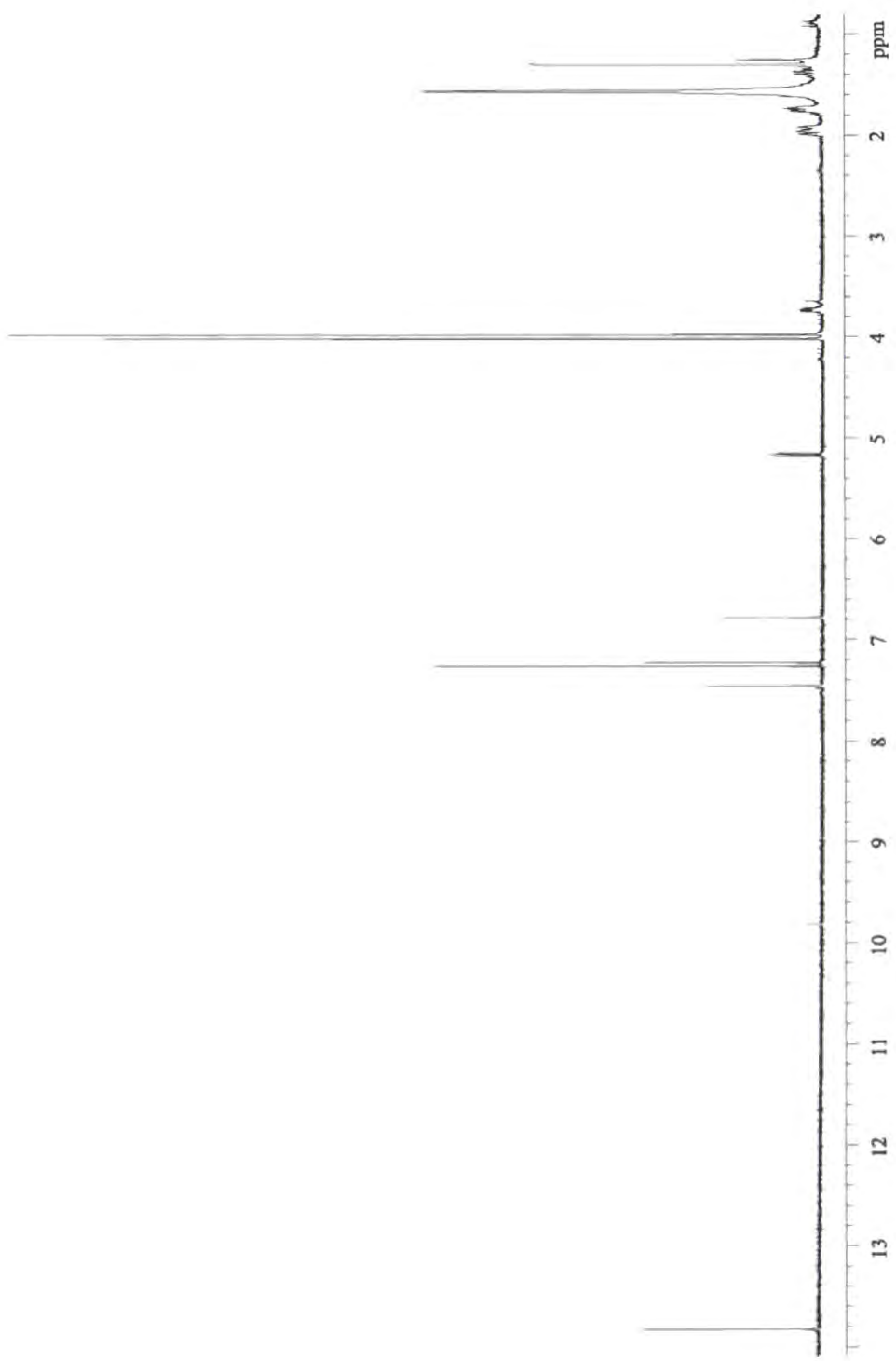

Figure 5.8: The ^{1}H NMR spectrum for **5.34** in $CDCl_3$.

The ^{13}C NMR data was obtained by careful examination of both the HSQC and the CIGAR spectra, due to the paucity of the compound. Comparison of the data with 6,8-*O*-dimethylaverufin (**5.32**) confirmed the presence of an anthraquinone core structure within compound **5.34**. The substitution pattern of the aromatic ring A was deduced by both the coupling constants for the H-4 and H-2 (δ_H 7.45 and 6.78, respectively, $J_{2,4}$ = 2.5 Hz) aromatic protons combined with the CIGAR correlations from the H-4 (δ_H 7.45) aromatic proton to the C-3, C-4a, C-5 and C-13a (δ_C 165.1, 137.6, 182.8 and 115.5, respectively) carbons and the correlations from H-2 (δ_H 6.78) the second aromatic proton to the C-1, C-3, C-4 and C-13a (δ_C 163.0, 165.1, 104.0 and 115.5, respectively) carbons. The two methyl signals associated with the methoxy groups were assigned *via* CIGAR correlations from the H-14 and H-15 (δ_H 4.01 and 3.99, respectively) methyl protons to the C-1 and C-4 (δ_C 163.0 and 104.0, respectively) carbons, respectively. CIGAR correlations from the H-6 (δ_H 7.23) aromatic proton to the C-5, C-6a, C-11a and C-12a (δ_C 182.8, 162.0, 120.2 and 110.6, respectively) carbons, confirmed the position of H-6 as *para* to the hydrogen bonded alcohol at position C-12 (δ_C 161.0). This data unambiguously assigned rings A, B and C (**Figure 5.9**).

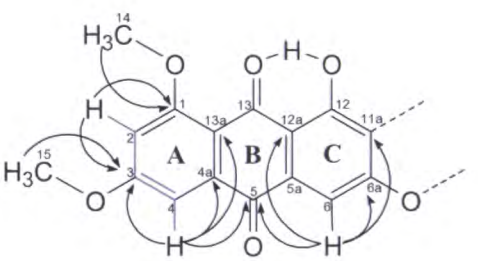

Figure 5.9: COSY (blue) and CIGAR (black arrows) correlations leading to the assignment of rings A, B and C (the anthraquinone core structure).

The partial structure C-11 to C-9 was constructed *via* COSY correlations from the H-10a,b (δ_H 1.96 and 1.56, respectively) methylene protons to both the H-11 (δ_H 5.16) oxymethine proton and the H-9 (δ_H 1.91) methylene protons. The partial structure C-9 to C-16 was established *via* COSY correlations. The COSY correlations from the H-8a,b (δ_H 1.75 and 1.37) methylene protons to the H-9 (δ_H 1.91) methylenes, combined with the COSY correlations from the H-7 (δ_H 3.72) oxymethine proton to both the H-8a,b (δ_H 1.75, 1.37) and H-16 (δ_H 1.29) protons

completed C-9 to C-11. The pyran ring D was established on the basis of the mass and DBE requirements. One ring assignment remained, as eleven of the twelve DBE had already been accounted for. Therefore, positions C-11 and C-7 were proposed to be sharing the oxygen atom. However, no CIGAR correlations were observed from the H-7 (δ_H 3.72) methine proton to the C-11 (δ_C 76.6) carbon or from the H-11 (δ_H 5.16) oxymethine proton to the C-7 (δ_C 75.9) carbon. Connectivity of the pyran ring, ring D, was achieved *via* the observed CIGAR correlations from both the H-10ab and H-11 (δ_H 1.56, 1.96 and 5.16,respecively) protons to the C-11 and C-6a (δ_C 76.6 and 162.0, respectively) aromatic carbons respectively. The remaining proton at δ_H 9.80 was assigned to the oxygen at C-6a (δ_C 162.0) on the basis of the observed hydrogen bond formation between the phenolic proton and the oxygen of the pyran ring, to give a *pseudo* 6-membered ring. On the basis of these findings, the structure of **5.34** was proposed (**Figure 5.10**).

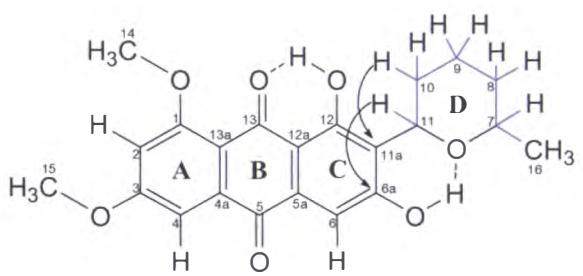

Figure 5.10: The COSY (blue) and CIGAR (black arrows) correlations observed leading to the assignment and connectivity to the aromatic core structure of the pyran ring, ring D of **5.34**.

From a literature search,[130,145] the proposed compound was identified as 6,8-*O*-dimethylaverufanin (1,3-dihydroxy-6,8-dimethoxy-2-(6'-methyl-tetrahydropyran) anthraquinone (**5.34**), **Figure 5.11**), which was first reported by Holker *et al.* from the culture broth of a mutant *Aspergillus versicolor*[193] and was later characterised by Aucamp and Holzapfel.[198] The structure was confirmed *via* direct comparison with the reported NMR data. The numbering system reported in the literature for the structure of **5.34** is shown in **Figure 5.11**.[198]

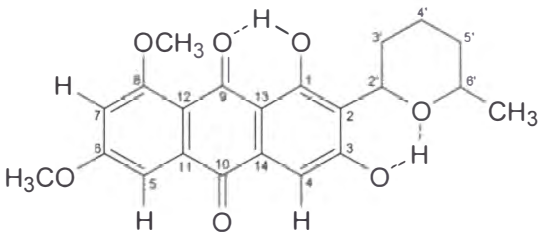

Figure 5.11: The numbering assignment reported in the literature for 6,8-*O*-dimethylaverufanin (**5.34**).

5.5.2.1: Stereochemistry of **5.34**

The stereochemistry was determined *via* NOESY experiments (**Figure 5.12**). It was assumed, not unreasonably, that the pyran ring was in the chair conformation,[199,200] with the C-11/C-11a bond in the equatorial position. This positioned the H-11 proton axial on the pyran ring. In contrast, the 16-CH_3 group could be located in either an axial or equatorial orientation. Irradiation of the H-11 (δ_H 5.16) methine proton resulted in the NOESY enhanced signal of the H-7 (δ_H 3.72) methine proton which indicated that the H-7 proton was in the axial position. Additional correlations were also observed to both of the H-10a,b and H-9 (δ_H 1.96a, 1 56b and 1.91, respectively) protons. The converse NOESY correlation was observed when the H-7 (δ_H 3.72) proton was irradiated, enhancing the H-11 (δ_H 5.16) proton signal, additional enhancements of both the H-16 (δ_H 1.29) methyl and the adjacent H-8a,b (δ_H 1.75 and 1.37, respectively) methylene protons were also observed. This data validated the initial hypothesis that the H-11 (δ_H 5.16) proton was in the axial position, as no cross ring correlations would be observed if either proton were in the equatorial position. In order to establish the axial protons at C-8 and C-10, the methylene protons H-10a and H-8a (δ_H 1.96 and 1.75, respectively) were sequentially irradiated. No NOESY correlation was observed between these protons. No signal enhancement in this case implies that both of these protons are in the equatorial position, and that both H-10b and H-8b (δ_H 1.56 and 1.37, respectively) are in the axial orientation. This was confirmed by the sequential irradiation of both of the H-10b and H-8b (δ_H 1.56 and 1.37,

respectively) protons, which resulted in the NOESY signal enhancements of the H-8b and H-10b (δ_H 1.37 and 1.56, respectively) protons respectively. Therefore, the relative stereochemistry for **5.34** was proposed as 11*S*, 7*S*. Due to the lack of signal resolution, the H-9 axial and equatorial protons could not be assigned.

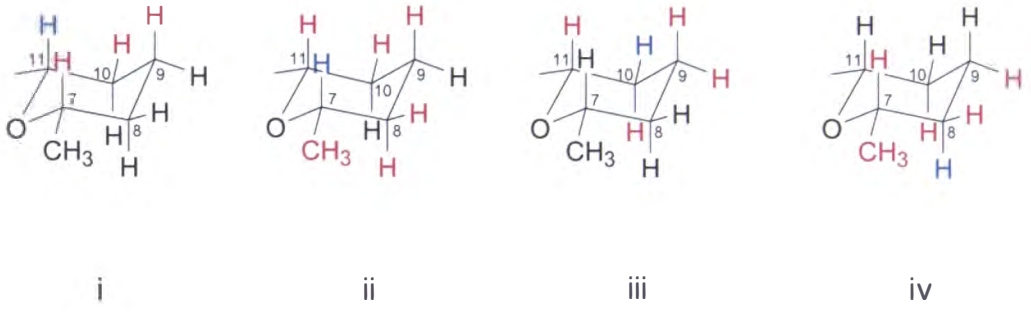

i ii iii iv

Figure 5.12: Observed NOESY correlations (red) for irradiated proton (blue). i) irradiation of H-11, ii) irradiation of H-7, iii) irradiation of H-10a and iv) irradiation of H-8b, for the pyran ring of **5.34**.

The experimental NMR data for 6,8-*O*-dimethylaverufanin (**5.34**) is displayed in **Table 5.2**. The arbitrary numbering assignment, shown in **Figure 5.13**, is consistent with that used in the structural elucidation and in **Table 5.2**.

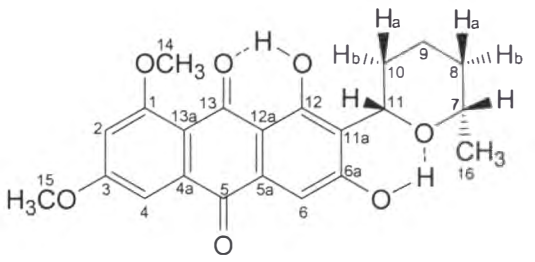

5.34

Figure 5.13: The arbitrary numbering system of **5.34**, used for in both structural elucidation and **Table 5.2**.

Table 5.2: The ^{1}H, COSY and CIGAR NMR data for **5.34** ($CDCl_3$).

Position	$^{13}C\ \delta$ §	$^{1}H\ \delta$ ξ	COSY	CIGAR
1	163.0 (C)			
2	105.1 (CH)	6.78 (1H, d, 2.5)	H-4	C-13a, C-4, C-3, C-1
3	165.1 (C)			
4	104.0 (CH)	7.45 (1H, d, 2.5)	H-2	C-5, C-4a, C-3, C-2
4a	137.6 (C)			
5	182.8 (CO)			
5a	132.0 (C)			
6	109.2 (CH)	7.23 (1H, s)		C-12a, C-11a, C-6a, C-5
6a	162.0 (C)			
OH-6a		9.80 (OH, s)		
7	75.9 (CH)	3.72 (1H, m)	H-16, H-8a, H-8b	C-16, C-9
8	33.0 (CH_2)	8a: 1.75 (1H, m)	H-9, H-8b, H-7	C-10, C-7
		8b: 1.37 (1H, m)	H-9, H-8a, H-7	C-10, C-9, C-7
9	23.3 (CH_2)	1.91 (1H, m)	H-10a, H-10b, H-8a, H-8b,	C-11, C-7
10	30.1 (CH_2)	10a: 1.96 (1H, m)	H-11, H-10b, H-9	C-11, C-11a, C-8
		10b: 1.56 (1H, m)	H-11, H-10a, H-9	C-11
11	76.6 (CH)	5.16 (1H, dd, 2.5, 9.0)	H-10a, H-10b	C-11a, C-10, C-9, C-6a,
11a	120.2 (C)			
12	161.0			
12a	110.6 (C)			
OH-12		13.48 (OH, s)		
13	†			
13a	115.5 (C)			
14	56.8 (OMe)	4.01 (3H, s)		C-1
15	56.2 (OMe)	3.97 (3H, s)		C-3
16	22.3 (CH_3)	1.29 (3H. d, 2.5)	H-7	C-8, C-7

§ ^{13}C NMR chemical shift values (δ ppm from $CDCl_3$ at 77.0) obtained from both HSQC and CIGAR experiments. ξ ^{1}H NMR spectra recorded at 500 MHz in $CDCl_3$ (δ ppm from $CHCl_3$ at 7.25) followed by number of protons, multiplicity and coupling constants (*J*/Hz). † No ^{13}C NMR chemical shift data obtained for this carbon.

5.5.3: Structural Elucidation of **5.35**

The third purified compound **5.35** (3.1 mg), was again isolated as an orange powder from fraction 16-705. HRESIMS identified a $[M+H]^+$ ion at *m/z* 371.1137 (calc. 371.1131), 28 Da less than that of the previous compound 6,8-*O*-dimethylaverufanin (**5.34**), which led to the molecular formula $C_{20}H_{18}O_7$, corresponding to 12 DBE. Analysis of the UV data confirmed that this compound was related to the previous compounds and possessed the anthraquinone core structure. Examination of the combined ^{1}H NMR and CIGAR data established that the substitution patterns of rings A, B and C were identical to that of 6,8-*O*-dimethylaverufin (**5.32**) and 6,8-*O*-dimethylaverufanin (**5.34**). However, on closer inspection of the ^{1}H NMR spectrum (**Figure 5.14**), several differences were identified. These comprised an additional multiplet at δ_H 4.17 and 2.69, each signal integrating for one proton, the downfield shift of the oxymethine proton from δ_H 3.72 to 3.97 as well as the absence of a doublet methyl signal at δ_H 1.23. This NMR data suggested the structural differences were again located in ring D.

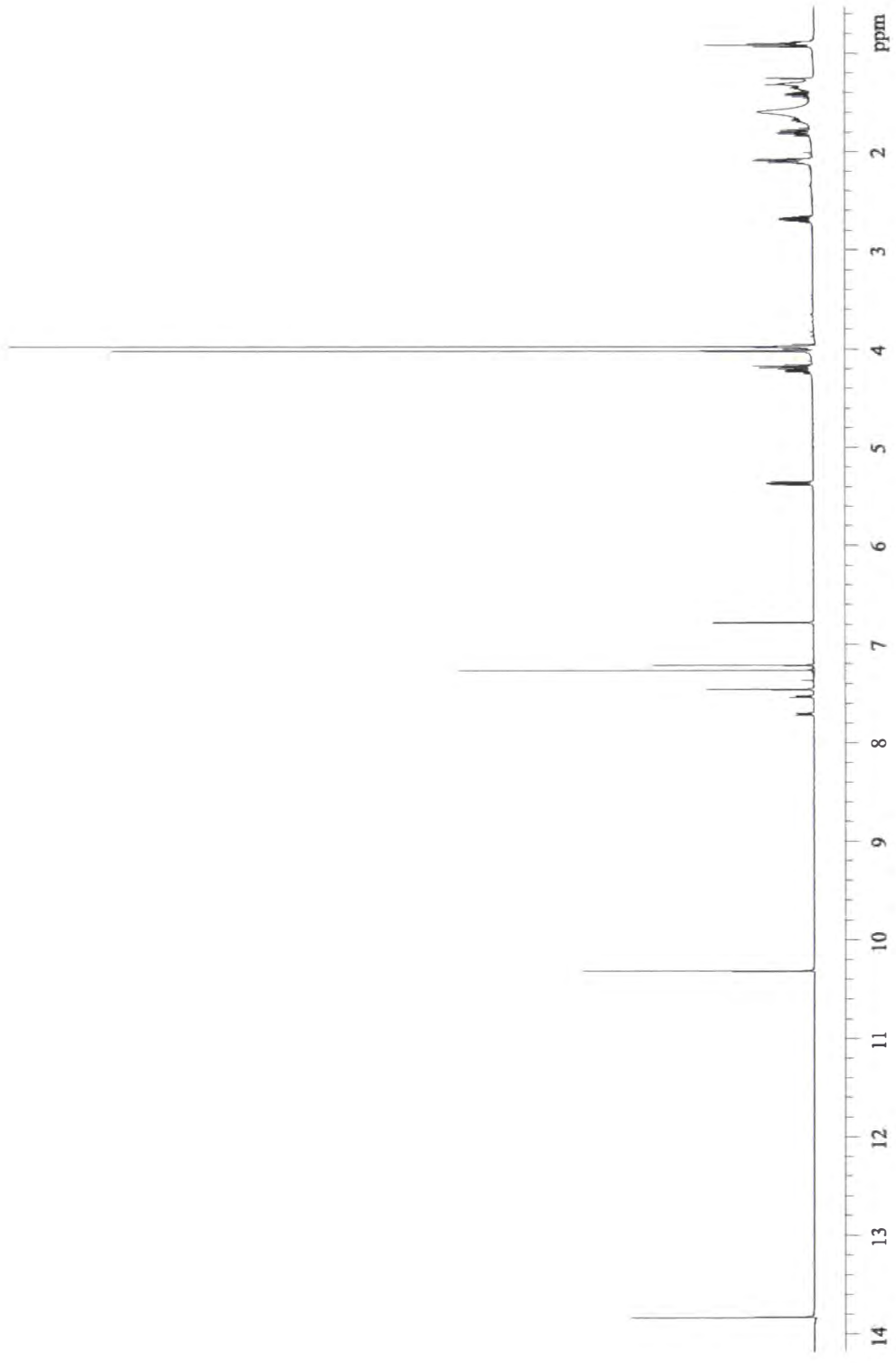

Figure 5.14: The ^{1}H NMR spectrum of **5.35** ($CDCl_3$).

The partial structure C-11 to C-8 was constructed by careful examination of the COSY and HSQC correlations. The H-10 (δ_H 5.38) oxymethine proton displayed cross peak COSY correlations to the H-9a,b (δ_H 2.69 and 1.81) methylene protons, while the H-8 (δ_H 2.08) methylene protons were coupled to both the H-9a,b (δ_H 2.69 and 1.81) methylene and H-7a,b (δ_H 3.97 and 4.17) oxymethylene protons. A furan ring (ring D) was defined through the CIGAR correlation from the H-7a (δ_H 3.97) methylene proton to the C-10 (δ_C 79.3) carbon, which satisfied the loss of 28 mass units (CH_3-CH) observed in the mass spectrum. Connectivity of the furan ring to the anthraquinone core structure at C-11 was established with the CIGAR correlations from the H-10 (δ_H 5.38) oxymethine proton to the C-6a and C-11 (δ_C 161.9 and 118.0, respectively) aromatic carbons of ring-C (**Figure 5.15**).

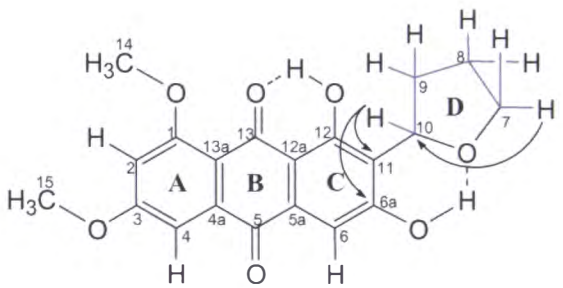

Figure 5.15: The observed COSY (blue) and CIGAR (black arrows) correlations leading to the assignment of the furan ring, ring D, and its connectivity to the aromatic core for compound **5.35**.

From this data, structure **5.35** was proposed. From a literature search,[130,145] no direct matches were found. Repeating the literature search by replacing the 6,8-OCH_3 groups for 6,8-OH groups, identified a structural match for the compound bipolarin (**5.36**). Therefore, **5.35** was identified as being novel, and tentatively named 6,8-*O*-dimethylbipolarin (**5.35**) (using the numbering assigned in the literature, **Figure 5.16**).

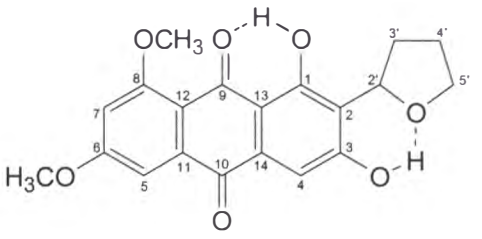

Figure 5.16: The numbering assignment for **5.35**, which is consistent with that used in the literature for bipolarin (**5.36**).

Bipolarin (**5.36**) was isolated by Aucamp and Holzapfel from the maize cultures of *Bipolaris sorokiniana*.[198] In 1977, the total synthesis of (±)-bipolarin was achieved by Castonguay and Brassard,[200] however an authentic sample of bipolarin (**5.36**) was unavailable for the direct comparison of the structural data, although the physical and spectral properties were in excellent agreement with those reported for the natural product by Aucamp and Holzapfel. [198,200] Mayes and Steyn, in a later report,[201] suggested that the structure proposed for bipolarin (**5.36**) by Aucamp and Holzapfel[198] was not consistent with the accepted biosynthetic pathway leading to sterigmatocystin (**5.8**), a higher metabolite. To unambiguiously assign the structure of bipolarin (**5.36**), Mayes and Steyn[201] re-examined the maize cultures of *B. sorokiniana*. After several steps of chromatography only the compound versiconol (**5.37**) was identified. No other compound resembling bipolarin (**5.36**) was isolated. Their interpretation of the mass spectral data reported by Aucamp and Holzapfel[198] for bipolarin (**5.36**), compared to that obtained experimentally for versiconol (**5.37**), led them to the reassignment of bipolarin (**5.36**) to versiconol (**5.37**).[201]

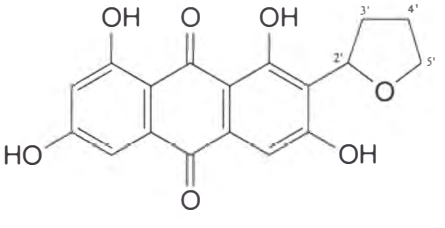

5.36

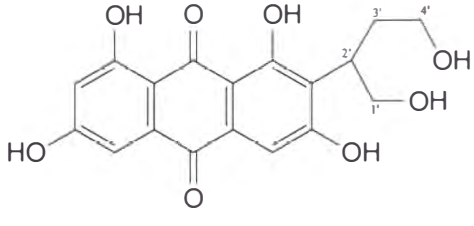

5.37

Differentiation between these two compounds could be easily achieved by close inspection of the ^{1}H NMR spectra. The splitting pattern of the H-2' proton would

be diagnostic for the differentiation of these two structures. The signal for H-2' in bipolarin would be inherently less complex. Unfortunately, the resolution of the reported ^{1}H NMR data in bipolarin (**5.36**) was not sufficient enough to confirm that this oxymethine signal is a doublet of doublets, rather than a multiplet. However, the chemical shift of H-2' (δ_H 5.17-5.41) in bipolarin (**5.36**) is consistent with an oxymethine rather than an alkyl methine, as required in versiconol (**5.37**).

In a further complication, an alternate isomeric structure for 6,8-*O*-dimethylbipolarin (**5.35**) was proposed in the AntiBase database.[145] This compound, **5.38**, was structurally different, having the oxygen located between positions C-3' and C-5' of the furan ring (**Figure 5.17**). If this is the correct assignment, then the H-2' methine proton would be coupled to two sets of methylene protons and would no longer appear as a doublet of doublets. Secondly, no hydrogen bond could exist between the phenolic proton of the anthraquinone core structure and the oxygen of the furan ring. The ^{1}H NMR spectrum was obtained from the author of AntiBase following electronic communication, and, after careful comparison of the spectral data, the proposed structure for 6,8-*O*-dimethylbipolarin (**5.35**) (**Figure 5.16**) was unambiguously assigned to be identical to the ^{1}H data obtained, supporting the hypothesis that the oxygen is incorrectly positioned in the database structure. A translational error may have occurred during the creation of the chemical structure for entry into the database. However, the most recent database update for this compound displays yet another isomeric structure (**5.39**) (**Figure 5.17**). The oxygen is still incorrectly located between positions C-3' and C-5' within the furan ring, however the C-8 methoxy is now positioned at C-1. No stereochemistry has been indicated for either compound **5.38** or **5.39**.

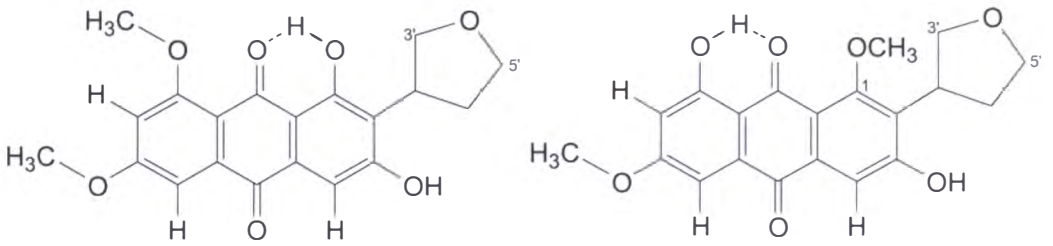

5.38 **5.39**

Figure 5.17: Two structures **5.38** and **5.39** proposed for 6,8-O-dimethylbipolarin (**5.35**) as indicated by the AntiBase[145] database using reported numbering annotation.

5.5.3.1: Stereochemistry of **5.35**

No stereochemistry has been reported for any of the bipolarin isomers isolated in the literature (**5.35-5.39**). NOESY experiments were used to determine the relative stereochemistry of the furan ring system (**Figure 5.18**). The numbering system used in the NOESY experiments is identical to that used during structural elucidation. Irradiation of the H-10 (δ_H 5.38) methine proton resulted in NOESY signal enhancement of the H-9a,b (δ_H 2.69, 1.81), H-8 and H-7a (δ_H 2.08 and 3.97, respectively) methylene protons, and irradiation of the H-9a (δ_H 2.69) methylene proton NOESY enhanced both the H-10 and H-7a (δ_H 5.38 and 3.97, respectively) proton signals. Irradiation of the H-7a (δ_H 3.97) proton NOSEY enhanced both H-8 and H-9a (δ_H 2.08 and 2.69, respectively) proton signals. This data suggested that H-7a, H-9a and H-10 protons must be on the same side of the ring in order to correlate. Due to the complexity of the methylene protons at H-8 the orientation could not be resolved.

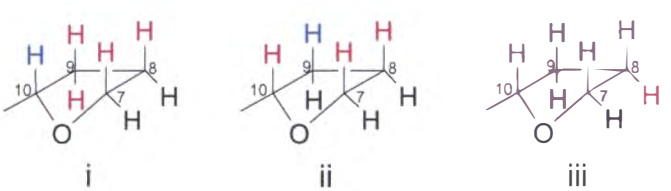

i ii iii

Figure 5.18: NOESY correlations (red) for the irradiated proton (blue) observed for the furan ring of **5.35**, i) irradiation of H-10, ii) irradiation of H-9a and iii) irradiation of H-7a The numbering system used in identical to that used in structural elucidation.

The experimental NMR data for the isolated compound **5.35** is displayed in **Table 5.4**. The numbering system assigned for **5.35** is identical to that used during compound elucidation and used in **Table 5.4** (**Figure 5.19**).

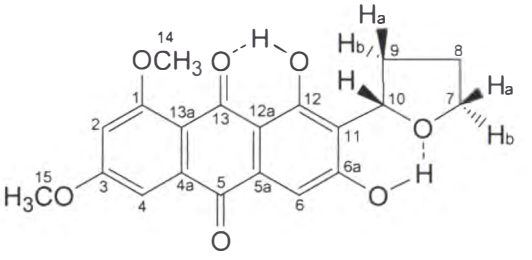

5.35

Figure 5.19: The structure of **5.35** with the proposed relative stereochemistry assigned. Structural numbering system is consistent with that used for structural elucidation and **Table 5.3**.

Table 5.3: The ^{1}H, COSY, HSQC and CIGAR NMR data for **5.35** ($CDCl_3$).

Position	^{13}C δ §	^{1}H δ ξ	COSY	CIGAR
1	163.0 (C)			
2	105.1 (CH)	6.80 (1H, d, 2.5)	H-4	C-13a, C-4, C-3, C-1
3	165.2 (C)			
4	104.0 (CH)	7.47 (1H, d, 2.5)	H-2	C-5, C-4a, C-3, C-2
4a	137.0 (C)			
5	183.0 (CO)			
5a	132.9 (C)			
6	109.0 (C)	7.23 (1H, s)		C-12a, C-6a, C-5, C-5a
6a	161.9 (C)			
OH-6a		9.80 (OH, s)		
7	68.8 (CH_2)	7a: 3.97 (1H, m)	H-8, H-7b	C-9, C-8
		7b: 4.17 (1H, m)	H-8	C-9, C-8
8	25.7 (CH_2)	2.08 (2H, m)	H-9a, H-9b, H-7a, H-7b	C-9, C-7
9	33.0 (CH_2)	9a: 2.69 (1H, m)	H-10, H-9b, H-8	C-11, C-8, C-7
		9b: 1.81 (1H, m)	H-10, H-9a, H-8	C-11, C-8, C-7
10	79.3 (CH)	5.38 (1H, dd, 2.5,9.0)	H-9a, H-9b	C-12, C-11, C-6a
11	118.0 (C)			
12	161.8 (C)			
OH-12		13.80 (OH, s)		
12a	110.0 (C)			
13	† (CO)			
13a	115.4 (C)			
14	56.8 (OCH_3)	4.01 (3H, s)		C-1
15	56.2 (OCH_3)	3.97 (3H, s)		C-3

§ ^{13}C NMR chemical shift values (δ ppm from $CDCl_3$ at 77.0) obtained from both HSQC and CIGAR experiments. ξ ^{1}H NMR spectra recorded at 500 MHz in $CDCl_3$ (δ ppm from $CHCl_3$ at 7.25), followed by number of protons, multiplicity and coupling constants (*J*/Hz). † No ^{13}C NMR chemical shift data obtained for this carbon.

5.5.4: Structural Elucidation of **5.40**

The fourth compound isolated, again as an orange powder from fraction 16-708, was **5.40** (3.3 mg). HREIMS identified the $[M]^+$ ion at *m/z* 382.1037 (calc. 382.1053) which led to the molecular formula $C_{21}H_{18}O_7$, 14 Da less than 6,8-*O*-dimethylaverufin (**5.32**) corresponding to 13 DBE. Close examination of the ^1H NMR spectrum (**Figure 5.20**) revealed that this compound had very similar spectroscopic characteristics to 6,8-*O*-dimethylaverufin (**5.32**). However, only one methyoxy signal was present (δ_H 3.94). The substitution of an hydroxy for a methyoxy group would satisfy the requirements of the mass spectrum. The structures of rings C, D and E were unambiguously assigned using HSQC, CIGAR and COSY NMR experimental correlations (**Figure 5.21**), and by direct comparison to data obtained for 6,8-*O*-dimethylaverufin (**5.32**) (see **Table 5.1**).

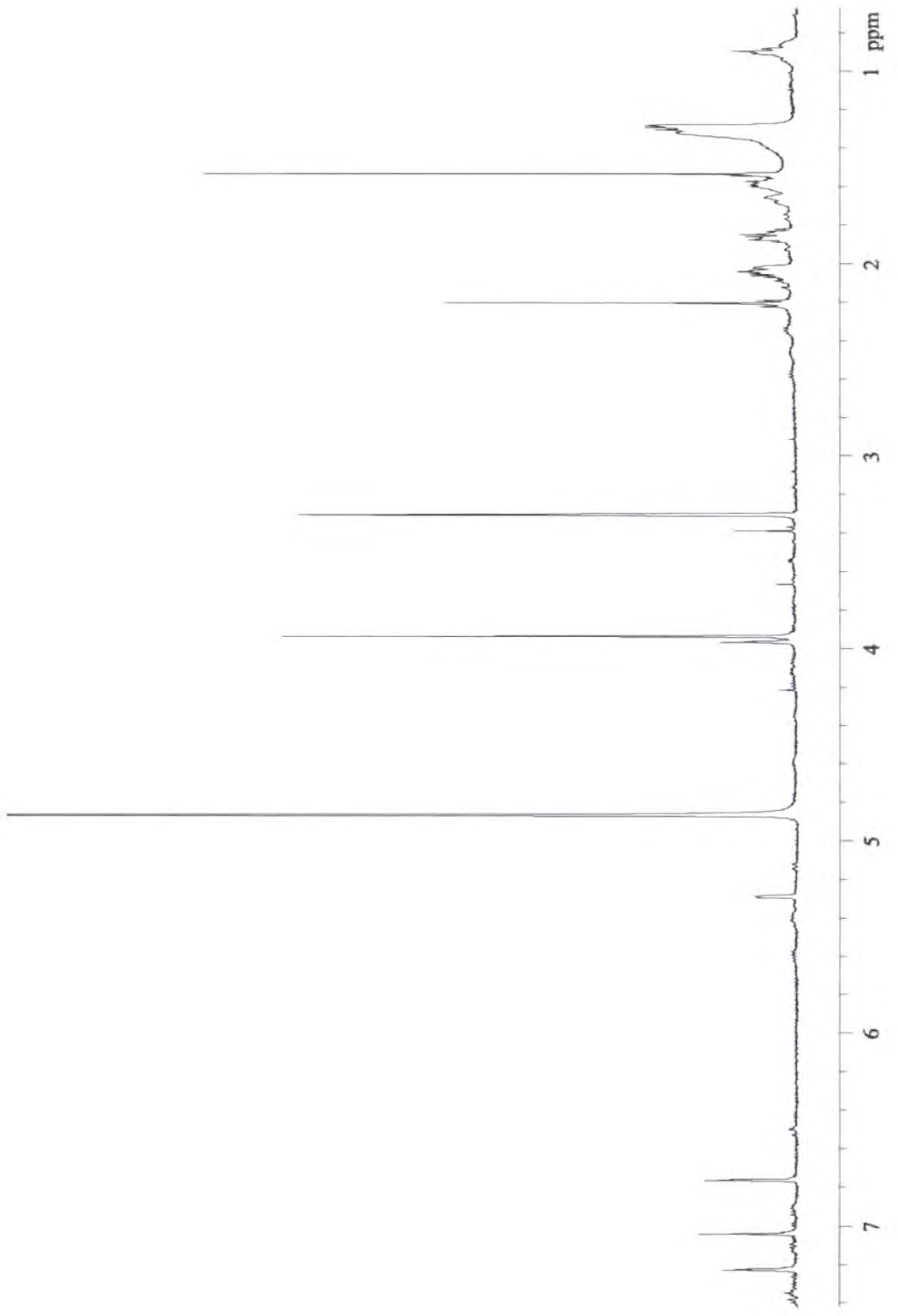

Figure 5.20: The ^{1}H NMR spectrum of **5.40** (CD_3OD).

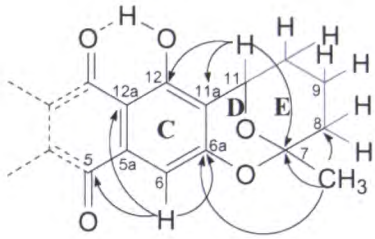

Figure 5.21: The key COSY (blue) and CIGAR (black arrows) correlations observed for the complete assignment of rings C, D and E of **5.40**.

Therefore, the structural difference between 6,8-*O*-dimethylaverufin (**5.32**) and **5.40** had been narrowed down to being on either ring A or B. The coupling constant for the H-4 and H-2 (δ_H 7.24 and 6.78, respectively, $J_{2,4}$ = 2.5 Hz) aromatic protons extracted from the ^{1}H NMR spectrum, suggested that the *meta* substitution pattern previously observed, was still present. The CIGAR correlations from the H-4 (δ_H 7.24) aromatic proton to the C-2 and C-5 (δ_C 104.5 and 182.7, respectively) carbons, and the H-2 (δ_H 6.78) aromatic proton to the C-1, C-3, C-4 and C-13a (δ_C 163.8, 165.6, 107.8 and 112.7, respectively) carbons established the presence of ring B and the substitution pattern of ring A (**Figure 5.22**).

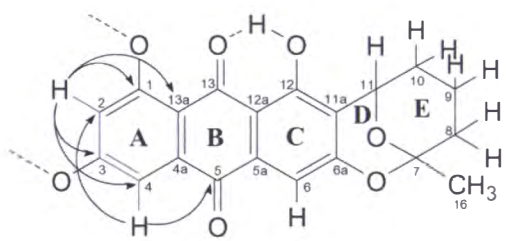

Figure 5.22: The key COSY (blue) and CIGAR (black arrows) correlations contributing to the assignment of rings A and B of the anthraquinone core.

However, because the H-2 (δ_H 6.78) proton was correlated to both the C-1 and C-3 (δ_C 163.8 and 165.6, respectively) carbons, and no CIGAR correlation was observed from the H-4 (δ_H 7.24) proton to the C-3 (δ_C 165.6) carbon, location of the remaining methyoxy group was impossible with the available NMR data. Unambiguous assignment of the methyl group's location was achieved using the ROESY experiment. Irradiation of the δ_H 3.94 methyoxy protons resulted in a positive ROESY correlation (**Figure 5.23**) to the H-2 (δ_H 6.78) aromatic proton,

while irradiation of the H-2 (δ_H 6.78) aromatic proton gave the reciprocal correlation to the methyoxy protons at δ_H 3.94. No ROESY correlations were observed when the H-4 (δ_H 7.24) proton was irradiated (**Figure 5.23**).

Therefore, the methyl group was positioned on the oxygen at C-1. This data also confirmed the presence of only one hydroxyl group attached to ring A, and validated the initial speculation that a methyoxy group had been substituted by an hydroxy group.

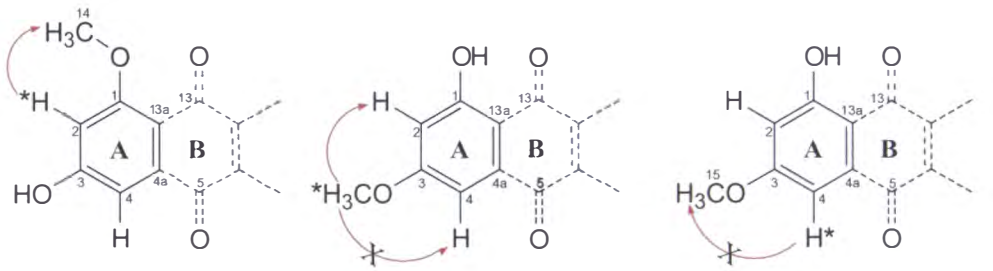

Figure 5.23: ROESY correlations (red) for irradiated protons (*). Correlations not observed are denoted with an 'X'.

A literature search[130,145] was performed on the structure proposed for **5.40**. The structure was an exact match for the compound 8-*O*-methylaverufin isolated by Maskey *et al.* in 2003 from the ethyl acetate extract of a *Penicillium chrysogenum*[197] (**Figure 5.24**, with numbering assignment as reported in the literature). The structure was confirmed by direct comparison of the ^{1}H and ^{13}C NMR data reported for 8-*O*-methylaverufin (**5.40**).

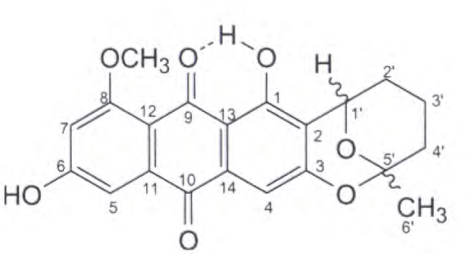

Figure 5.24: Numbering assignment for **5.40**, as reported in the literature.[197]

5.5.4.1: Stereochemistry of ***5.40***

No experimental optical rotation data was reported for **5.40**.[197] The experimental optical rotation data ($[\alpha]_D^{20}$ = -17° (c 0.20, $CHCl_3$)) obtained was within experimental error of that reported in the literature for 6,8-*O*-dimethylaverufin (**5.32**) ($[\alpha]_D$ = -18° (c 0.22, $CHCl_3$).[196] This would suggest that the stereochemistry at C-11 and C-7 of **5.40** (using the numbering system in **Figure 5.25**) is in the same configuration as that for **5.32**. The full NMR data for the strucuture of **5.40** is shown in **Table 5.4**.

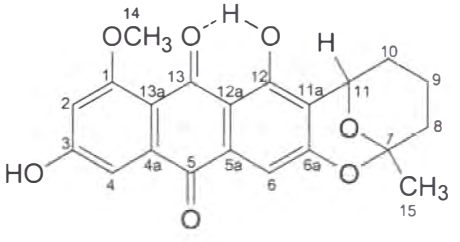

Figure 5.25: The proposed structure for **5.40** annotated with the same numbering used during structural elucidation and in **Table 5.4**.

Table 5.4: The ^{1}H, ^{13}C, COSY, ROESY and CIGAR NMR data for **5.40** (CD_3OD).

Position	^{13}C δ§	^{1}H δ ‡	COSY (ROESY)	CIGAR
1	163.8 (C)			
2	104.5 (CH)	6.78 (1H, d, 2.5)	H-4	C-13a, C-4, C-3, C-1
3	165.6 (C)			
4	107.8 (CH)	7.24 (1H, d, 2.5)	H-2 (H-14)	C-5, C-2
4a	† (C)			
5	182.7 (CO)			
5a	132.8 (C)			
6	107.9 (CH)	7.05 (1H, s)		C-12a, C-11a, C-6a, C-5
6a	159.4 (C)			
7	101.1 (C)			
8	35.4 (CH_2)	8a: 2.02 (1H, m)	H-9a, H-9b, H-8b	C-15, C-10, C-9, C-7
		8b: 1.86 (1H, m)	H-9a, H-9b, H-8a	C-15, C-10, C-9, C-7
9	16.2 (CH_2)	9a: 1.66 (1 H, m)	H-10a, H-10b, H-9b, H-8a, H-8b	C-11, C-8, C-7
		9b: 1.57 (1 H, m)	H-10a, H-10b, H-9a, H-8a, H-8b	C-11, C-8, C-7
10	27.3 (CH_2)	10a: 2.06 (1H, m)	H-11, H-10b, H-9a, H-9b	C-11, C-8
		10b: 1.86 (1H, m)	H-11, H-10a, H-9a, H-9b, ,	C-11
11	67.1 (CH)	5.38 (1H, d, 2.5, 9.0)	H-10a, H-10b	C-12, C-11a, C-9
11a	116.5 (C)			
12	159.7 (C)			
OH-12		14.12 (OH, s)		C-13
12a	110.1 (C)			
13	† (CO)			
13a	112.7 (C)			
14	55.5 (OCH_3)	3.94 (3H, s)	(H-2)	C-1
15	26.9 (CH_3)	1.53 (3H, s)		C-8, C-7

§ ^{13}C NMR chemical shift values (δ ppm from CD_3OD at 49.3) obtained from both HSQC and CIGAR experiments. ‡ ^{1}H NMR spectra recorded at 500 MHz in CD_3OD (δ ppm from CD_3OD at 3.3) followed by number of protons, multiplicity and coupling constants (*J*/Hz). † No ^{13}C NMR chemical shift data obtained for these carbons.

5.5.5: Structural Elucidation of ***5.41***

Compound **5.41** (2.5 mg), again a bright orange powder, was isolated from fraction 16-710. HRESIMS established the $[M+H]^+$ ion at *m/z* 370.1061 (calc. 370.1053) which led to the molecular formula $C_{20}H_{18}O_7$, corresponding to 12 DBE. UV data confirmed the presence of the anthraquinone core structure, while the ^1H NMR spectrum (**Figure 5.26**) suggested that **5.41** was structurally related to the previously isolated compounds. However, a minor difference was observed. This was the convergence of the two O-CH_3 groups to a chemical shift of δ_H 3.97.

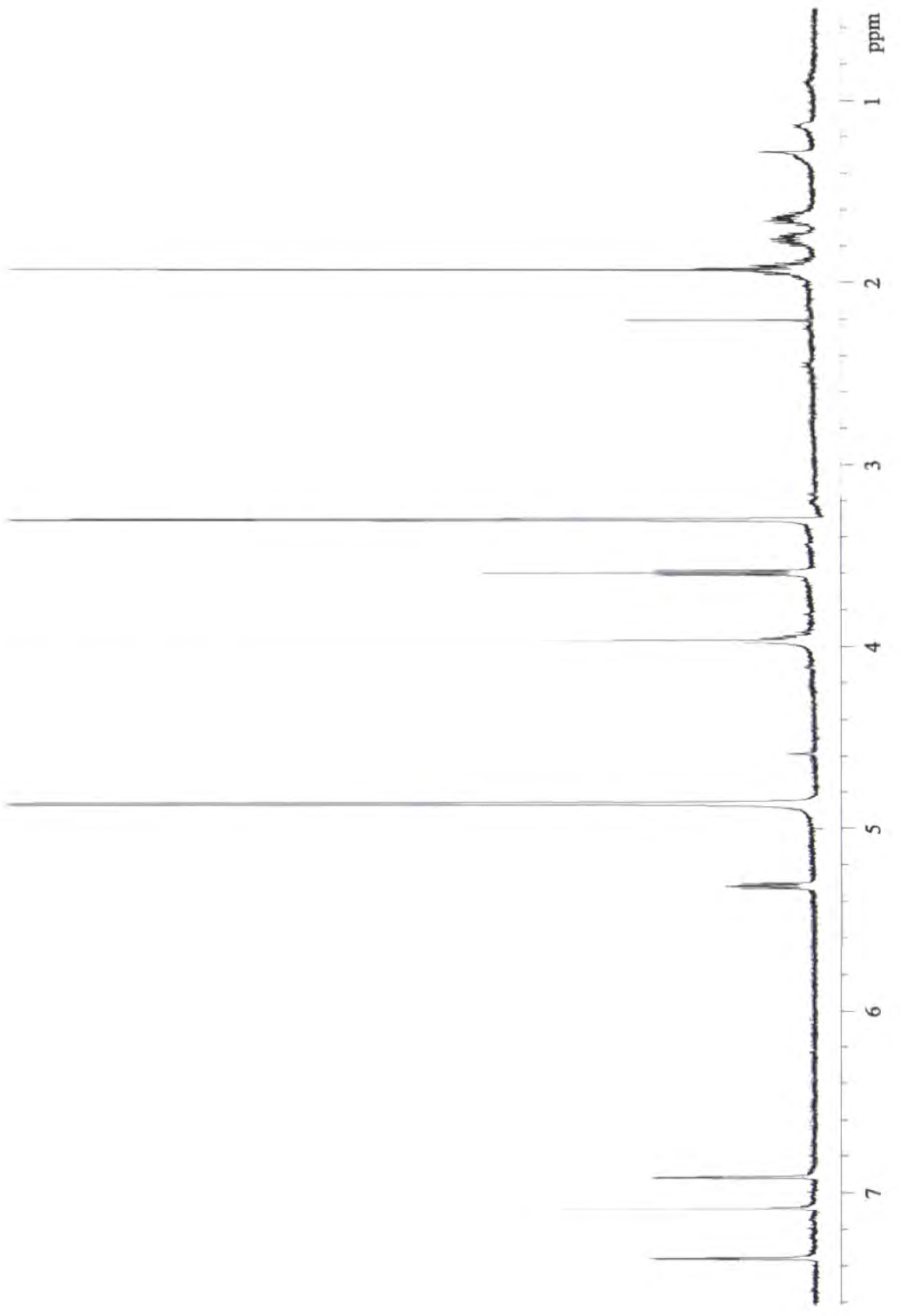

Figure 5.26: The ^{1}H NMR spectrum of **5.41** (CD_3OD).

Ring A was easily deduced by comparison of ^{1}H NMR chemical shift data, COSY and CIGAR correlations. The H-2 and H-4 (δ_H 6.92 and 7.36, respectively) were still COSY correlated and the coupling constant ($J_{2,4}$ = 2.5 Hz) extracted from the ^{1}H NMR spectrum, suggested that these protons were still *meta* related. Carbons C-1 and C-3 were located via the observed CIGAR correlations from the H-2 (δ_H 6.92) proton to the C-1 and C-2 (δ_C 162.9 and 104.8, respectively) carbons. The 14-OCH_3 and 15-OCH_3 groups were located at C-1 and C-3, respectively based on the observed CIGAR correlations from H-14 and H-15 (δ_H 3.97 and 3.97) to the C-1 and C-3 (δ_C 162.9 and 165.6, respectively) carbons, respectively. The CIGAR correlations from the H-4 (δ_H 7.36) proton (δ_H 7.36) to the C-3, C-5 and C-13a (δ_C 165.6, 182.3, 163.9) carbons led to the assignment of partial structure ring A (**Figure 5.27**). The chemical shift of C-4a was not able to be assigned with the available NMR data.

Rings B and C were elucidated *via* CIGAR correlations from the H-6 (δ_H 7.09) proton to the C-5, C-11 and C-12a (δ_C 182.3, 121.9 and 110.1, respectively) carbons. An hydroxyl group was tentatively positioned at C-12, due to the presence of a hydrogen bonded phenolic proton signal at δ_H 14.12, and because of the chemical shift of C-12 (δ_C 162.8). At this point of the structural assignment, 11 of the required 12 DBE had been accounted for (**Figure 5.27**).

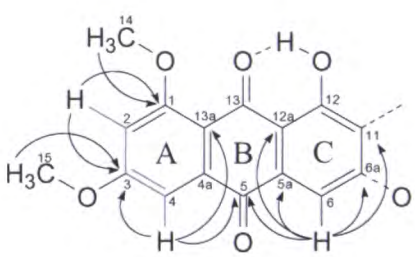

Figure 5.27: Key CIGAR (black arrows) and COSY (blue lines) correlations leading to the assignment of rings A, B and C.

A partial structure C-11 to C-7 (**Figure 5.28**) was constructed from the COSY, 1D and 2D TOCSY experiments. COSY cross peak correlations were observed from the oxymethine proton H-10 (δ_H 5.32) to the H-9 (δ_H 1.92) protons, while the H-

8a,b (δ_H 1.76 and 1.65) methylene protons were in turn COSY correlated to both the H-7 and H-9 (δ_H 3.60, 1.92) methylene protons.

The position of the H-10 oxymethine proton was determined by the observed CIGAR correlations from the H-10 (δ_H 5.32) oxymethine proton to the C-6a, C-11, and C-12 (δ_C 161.6, 121.9 and 162.8, respectively) carbons, which connected this fragment to the anthraquinone core structure. The C-10 to C-7 partial structure terminates with a methylene unit (C-7) not a methyl, therefore, in order to satisfy the one remaining DBE requirement, as determined by the molecular formula, it was proposed that C-7 must connect back into the anthraquinone core forming a fourth ring. This seven-membered ring, ring D, was therefore connected through the oxygen located at the C-6a position into the anthraquinone core structure, as shown in **Figure 5.28**. The chemical shift of C-7 (δ_C 61.6) also validates this hypothesis.

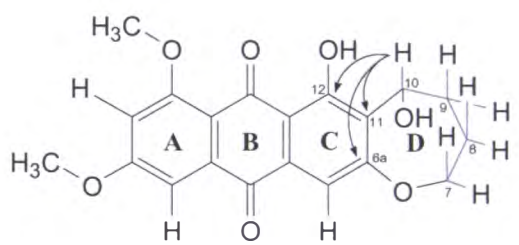

Figure 5.28: Connectivity of partial structure C-11 to C-7, ring-D, with key COSY (blue) and CIGAR (black arrows) correlations.

A series of 1D TOCSY experiments (**Figures 5.29** and **5.30**) were utilized to confirm the linear sequence from H-10 to H-7. The H-10 (δ_H 5.32) oxymethine proton was irradiated and consecutive correlations were observed as the mixing time was increased from 0.005 ms to 0.08 ms. The first correlation observed at T1 (0.005 ms) consisted of a correlation from the H-10 (δ_H 5.32) oxymethine proton to the H-9 (δ_H 1.92) methylene protons, followed by the H-8a,b (δ_H 1.76, 1.65) methylene protons. At T2 (0.08), the final correlation corresponding to the H-7 (δ_H 3.60) methylene protons was observed (**Figure 5.29**).

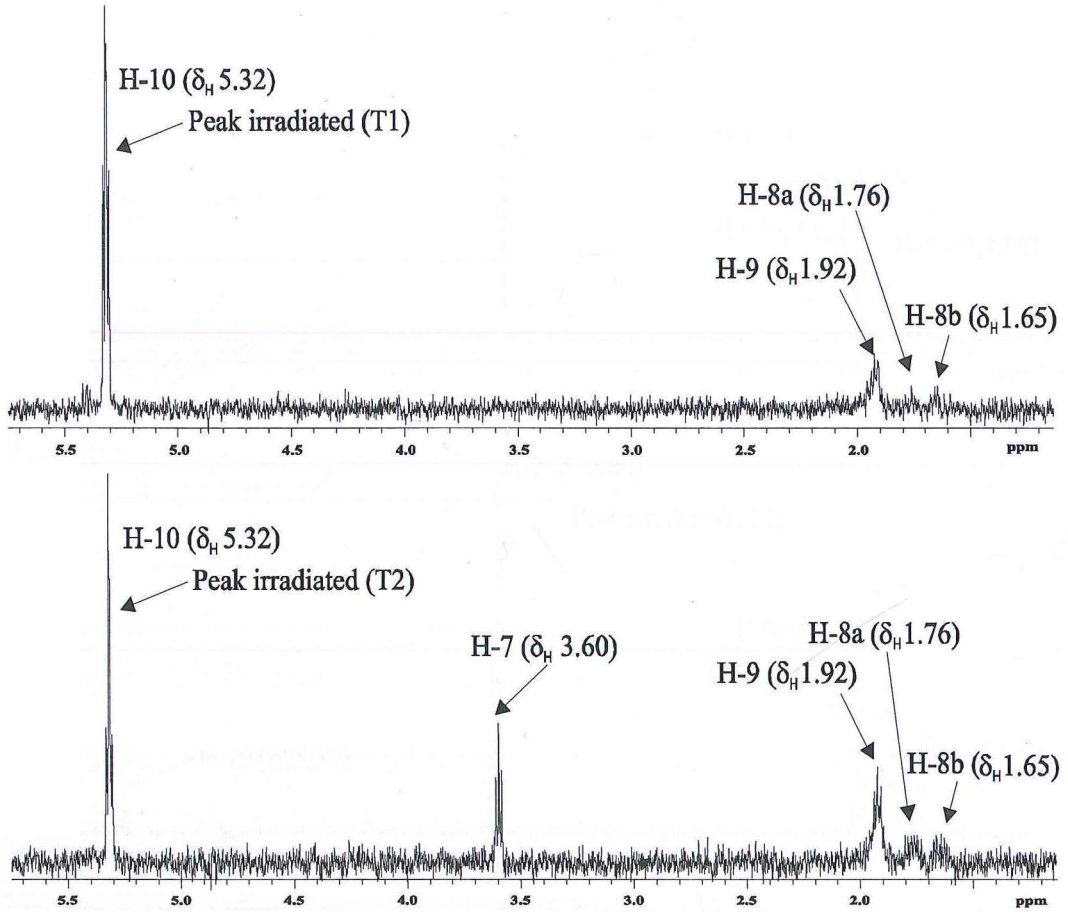

Figure 5.29: TOCSY correlations for irradiated proton H-10 (δ_H 5.32) at mixing times T1 (0.005 ms) and T2 (0.08 ms).

The H-10 to H-7 sequence was further confirmed by irradiation of the H-7 (δ_H 3.60) methylene protons (**Figure 5.30**) with the same mixing times used in the previous TOCSY experiment. Correlations were observed at T1 (0.005 ms) from the H-7 (δ_H 3.60) methylene protons to both H-8a,b (δ_H 1.76, 1.65) and H-9 (δ_H 1.92). At mixing time T2 (0.08 ms) the final correlation to the oxymethine at H-10 (δ_H 5.32) was observed.

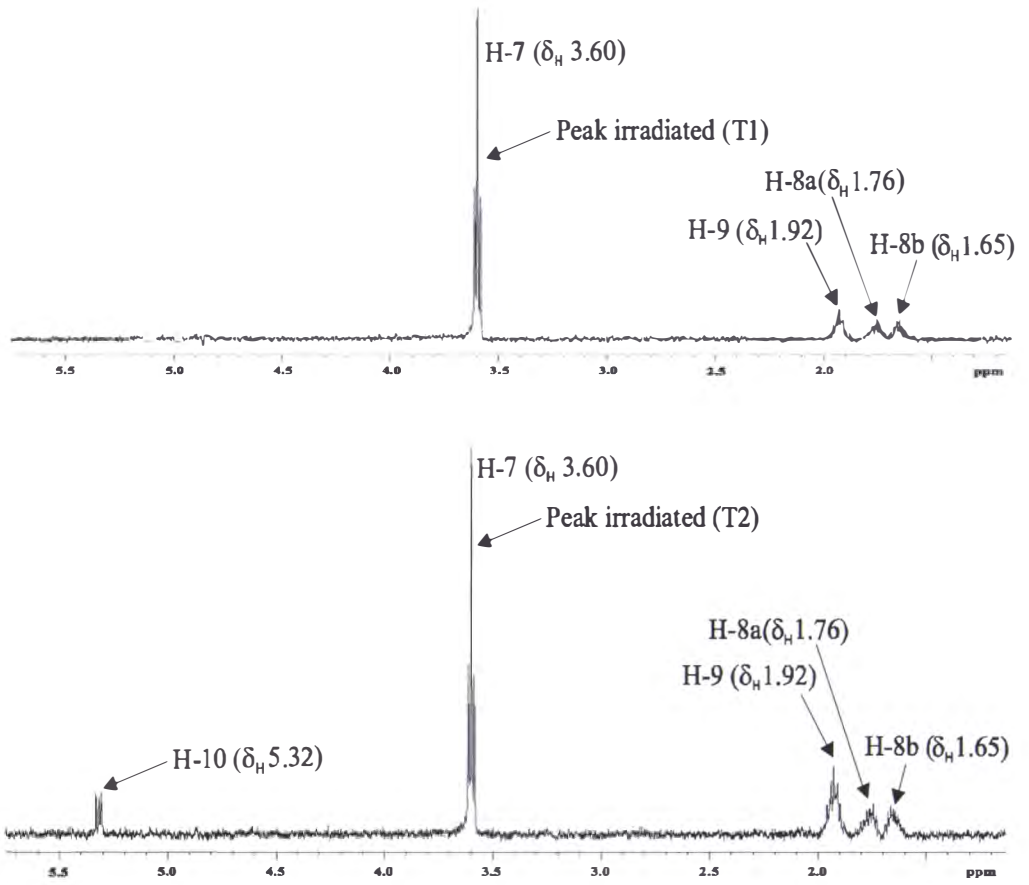

Figure 5.30: TOCSY correlations for irradiated proton H-7 (δ_H 3.60) at mixing times T1 (0.005 ms) and T2 (0.08 ms).

A structure for compound **5.41** was proposed. A literature search[130,145] for **5.41** returned no exact matches. The novel compound was tentatively named 5,6-dihydroxy-1,3-*O*-dimethoxy-2,3,4,5-tetrahydro-1-oxa-cyclohepta[*b*]-anthracene (**5.41**), using the numbering system assigned for structural elucidation.

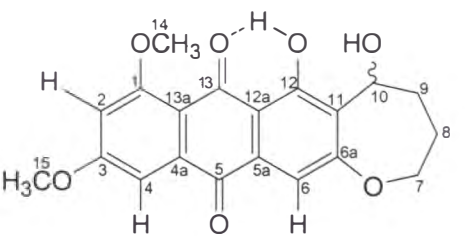

5.41

5.5.5.1: Stereochemistry of ***5.41***

Optical rotation measurements indicated that a racemic mixture was present ($[\alpha]_D^{25} = 0.00°$ (c 0.05 $CHCl_3$)).

Compound **5.41** was subjected to a NOESY 1D experiment in order to confirm that a racemic mixture was present. It was anticipated that irradiation of the H-10 (δ_H 5.32) proton would enhance both of the H-8a,b (δ_H 1.76, 1.65) methylene protons, indicating that C-10 (δ_C 68.3) exists in both the (*R*) and (*S*) configurations. During the NOESY experimental setup procedure it was observed that the ^{1}H NMR spectrum recorded for **5.41** was different to that obtained during the initial structural elucidation process. This degradation compound (**5.42**) on closer inspection revealed a second phenolic proton signal at δ_H 10.25 (**Figure 5.31**), similar to that observed for both 6,8-*O*-dimethylaverufanin (**5.34**) and 6,8-*O*-dimethylbipolarin (**5.35**). The ^{1}H NMR spectrum of **5.42** was obtained in $CDCl_3$ as it was no longer soluble in CD_3OD, the solvent the original data was recorded from.

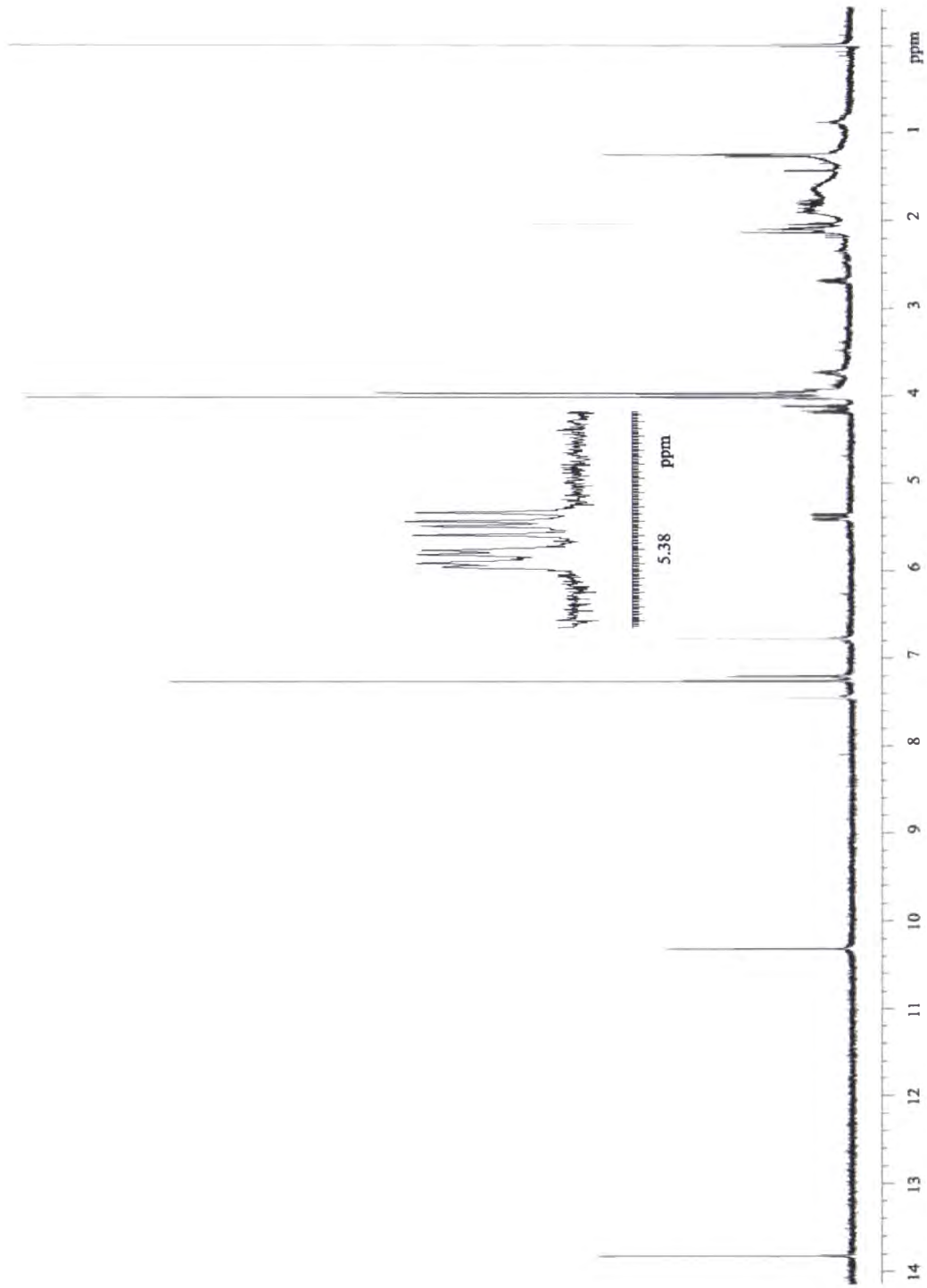

Figure 5.31: The ^{1}H NMR spectrum of **5.42** ($CDCl_3$).

The appearance of the new proton signal suggested that a structural rearrangement had occurred. Compound **5.42** was not fully characterised by NMR analysis. One possible mechanism for the conversion of **5.41** to **5.42** which accounts for the observed additional signal involves the opening of the seven-membered ring, followed by cyclisation to form a more thermodynamically stable five-membered ring (**Figure 5.32**).

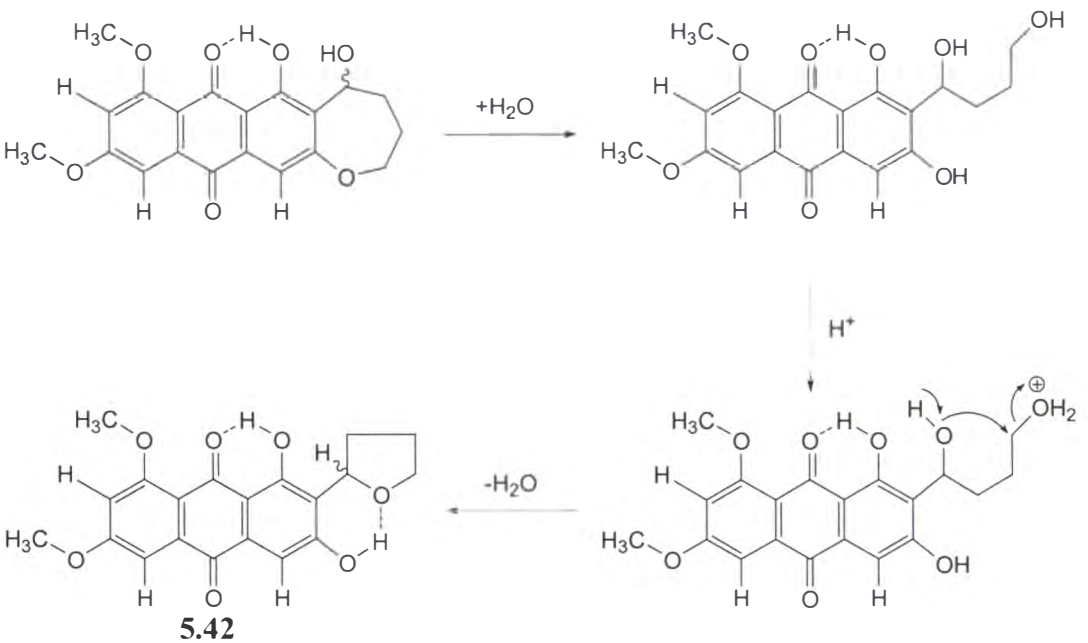

Figure 5.32: The formation of the degraded compound **5.42**, containing a more thermodynamically stable five-membered ring, *via* hydrolysis of **5.41** followed by the intramolecular loss of H_2O.

Closer inspection of the ^1H NMR signals at δ_H 5.34 to 5.44 revealed a pair of doublet of doublets, this suggested that each signal was associated with the H-10 proton in either the (*R*) or (S) configuration. This would validate the optical rotation data indicating that **5.41** was racemic. As before the NOESY experiment was used to irradiate the H-10 (δ_H 5.34 and 5.44) protons in an attempt to observe the NOESY enhanced correlations for the H-8 protons (δ_H 1.76 and 1.65), however no NOESY correlations were observed.

The full experimental NMR data for **5.41** is displayed in **Table 5.5**. The structure is annotated with the arbitrary numbering system used for the structural elucidation (**Figure 5.33**).

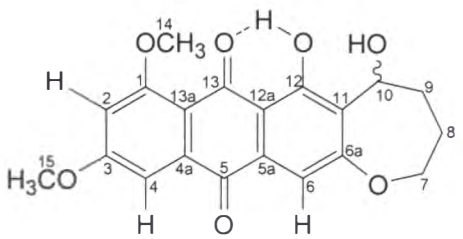

Figure 5.33: The proposed structure of **5.41** with arbitrary numbering system used for structural elucidation and **Table 5.5**.

Table 5.5: The ^{1}H, ^{13}C, COSY and CIGAR NMR data for **5.41** (CD_3OD).

Position	^{13}C δ §	^{1}H δ ξ	COSY	CIGAR
1	162.9 (C)			
2	104.8 (CH)	6.92 (1H, d, 2.5)	H-4	C-13a, C-4, C-3, C-1
3	165.6 (C)			
4	104.8 (CH)	7.36 (1H, d, 2.5)	H-2	C-13a, C-5, C-3, C-2
4a	†			
5	182.3 (CO)			
5a	133.0 (C)			
6	107.7 (CH)	7.09 (1H, s)		C-12a, C-11, C-6a, C-5, C-5a
6a	161.6 (C)			
7	61.6 (CH_2)	3.60 (1H, m)	H-8a, H-8b	C-9, C-8
8	28.9 (CH_2)	8a: 1.76 (1H, m)	H-9, H-8b, H-7	C-9, C-7
		8b: 1.65 (1H, m)	H-9, H-8a, H-7	C-9, C-7
9	32.5 (CH_2)	1.92 (2H, m)	H-10, H-8a, H-8b,	C-10, C-8, C-7
10	68.3 (CH)	5.32 (1H, dd, 2.5, 5)	H-9	C-12, C-11, C-9
11	121.9 (C)			
12	162.8 (C)			
12a	110.1 (C)			
OH-12		14.12 (OH, s)		
13	163.9 (C)			
13a	114.4 (C)			
14	55.7 (OCH_3)	3.97 (3H, s)		C-1
15	55.7 (OCH_3)	3.97 (3H, s)		C-3

§ ^{13}C NMR chemical shift values (δ ppm from CD_3OD at 49.3) obtained from both HSQC and CIGAR experiments. ξ ^{1}H NMR spectra recorded at 500 MHz in CD_3OD (δ ppm from CD_3OD at 3.30) followed by number of protons, multiplicity and coupling constants (*J*/Hz). † No ^{13}C NMR chemical shift data obtained for this carbon.

5.6: Biological Activity

All of the purified compounds were submitted for biological activity assessment in the P388 (murine leukaemia) assay the results of which are shown in **Table 5.6**.

Table 5.6: P388 Activity for the compounds isolated from the organic extract of the fungal isolate *Aspergillus* sp.

COMPOUND	ACTIVITY (IC_{50} µg/mL)
5.32	7.5
5.34	4.6
5.35	3.2
5.40	6.7
5.41	> 12.5

No biological data was obtained for the degraded compound **5.42**. As expected, compounds located in the area of activity determined by the initial microtitre plate assay (P388) of the crude extract were biologically active, however **5.32**, eluting at 23 minutes, was not within this region but displayed significant activity when submitted as a pure compound. The novel compound **5.41** did not display any significant P388 activity.

5.7: Concluding Remarks

The aim of this section of work was to isolate and identify the compound(s) responsible for the observed biological activity (P388) associated with the crude extract of the marine fungi *Aspergillus* sp. isolated from the tissue of the Antarctic marine sponge *Kirkpatrickia varialosa* (WS 76).

Initial bioassay guided fractionation (HPLC microtitre plate collection) located regions of activity in the HPLC chromatogram corresponding to compounds displaying a variety of polarities. UV data revealed that the compounds were related, and displayed a chromophore consistent with that of an anthraquinone core. Mass and UV data did not narrow the database search profile sufficiently, as

more than 100 possible compounds were identified. Therefore, further purification was deemed necessary to unambiguously characterise the compounds responsible for the observed activity.

Several steps of chromatography, including DIOL flash chromatography followed by semi-preparative reversed phase (C_{18}) HPLC chromatography, yielded six compounds. Structural elucidation of these six compounds was achieved with the use of ^{1}H, ^{13}C, COSY, 1D-TOCSY, NOESY, ROESY, HSQC and CIGAR NMR spectroscopy, high resolution ESI mass spectrometry, and subsequent comparisons with chemical shift data published for similar compounds.

The two novel compounds 6-8-*O*-dimethylbipolarin (**5.35**) and 5,6-dihydroxy-1,3-*O*-dimethoxy-2,3,4,5-tetrahydro-1-oxa-cyclohepta[*b*]anthracene (**5.41**) were isolated, along with the known compounds 6,8-*O*-dimethylaverufin (**5.32**), 6,8-O-dimethylaverufanin (**5.34**) and 8-*O*-methylaverufin (**5.40**).

This series of work revealed several areas in the literature that require revising.

1) The compound 6,8-*O*-dimethylaverufin (**5.32**) was reported as a new metabolite isolated from the fungus *Emericella foeniculicola* by Maebayashi *et al.*[196] in 1985, however this compound was reported earlier by Holker *et al.*[193] in 1966 after having been isolated from a UV mutated fungus *Aspergillus versicolor*.

2) The compound 8-*O*-methylaverufin (**5.40**) reported by Maskey *et al.*[197] as a new metabolite from the ethyl acetate extract of the fungus *Penicillium chrysogenum* in 2003 had also been previously isolated by Holker *et al.*[193] from an *A. versicolor* mutant in 1966.

3) The structure of bipolarin (**5.36**), suggested by Aucamp and Holzapfel[198] in 1970 was incorrectly reassigned by Mayes *et al.*[201] in 1984. The reassignment was made on the basis that the structure of bipolarin (**5.36**) was not consistent with the currently accepted biosynthetic pathway to higher metabolites. Therefore, Mayes *et al.*[201] concluded that the pigment called bipolarin (**5.36**) was identical with the subsequently discovered compound versiconol (**5.37**) although the NMR

data strongly indicates that these are two distinct compounds. Bipolarin (**5.36**) was prepared synthetically in 1977 by Castonguay and Brassard.[200] Although an authentic sample of bipolarin (**5.36**) was not available, they report that physical and spectral properties of the synthetic compound were in excellent agreement with those reported by Aucamp and Holzapfel[198] for the original natural product.

4) Alternative isomeric structures have been reported in the AntiBase database for 6,8-*O*-dimethylbipolarin (**5.35**), where the oxygen is located between the C-3' and C-5' of the furan ring (**5.38**) (using the reported structural numbering assignment). Analysis of the original ^{1}H NMR spectrum of 6,8-*O*-dimethylbipolarin (**5.35**), supplied by the author, supported the hypothesis that the oxygen is incorrectly positioned in the database structure. Nevertheless, the most up to date database still has the oxygen positioned between C-3' and C-5' within the furan ring, although the methoxy previously postioned at C-8 is positioned at C-1 (**5.39**). No stereochemistry was reported for either compound **5.38** or **5.39**.

Partial stereochemical assignments were determined for 6,8-*O*-dimethylaverufanin (**5.34**) and 6,8-*O*-dimethylbipolarin (**5.35**) *via* comparison of optical rotations with reported data along with 1D NOESY experiments.

All purified compounds were assessed in-house for cytotoxic activity in the P388 assay. The compound **5.41** did not display any biological activity (IC_{50} > 12.5 μg/mL). This result was expected as this compound was identified as being outside the area of activity indicated by the initial microtitre plate assay (P388). Suprisingly, **5.32**, was cytotoxic (IC_{50} 7.5 μg/mL) when submitted for assay despite being located outside the areas of activity on the microtitre plate assay.

Anthraquinones represent an important group of anti-cancer drugs that display a wide spectrum of activity and have great potential in the field of cancer chemotherapy.[202] These compounds undergo addition and substitution reactions, with direct activity on cellular nucleophiles such as thiols. Their primary mode of action is the damage of cellular DNA. Many of these compounds, such as doxorubicin (**1.16**), exert their activities through a number of mechanism such as redox cycling (resulting in generation of reactive oxygen species), direct

intercalation into DNA and inhibition of the enzyme topoisomerase II.[202] Doxorubicin (**1.16**) has shown a wide range of activity in solid human tumours, such as the breast, lung, ovary, head and bladder, and is currently the most effective single agent against soft-tissue sarcomas in adults.[202] This preclinical position is likely to be challenged, however, when the first marine anti-cancer drug ecteinascidin 743 (Yondelis™ **1.67**), developed by PharmaMar, is licensed, most likely in 2006. Yondelis™ (**1.67**) is also very effective against soft-tissue scarcomas. Clearly anthraquinones represent an important class of therapeutic agents and warrant further investigation.

5.8: Summary of Isolation

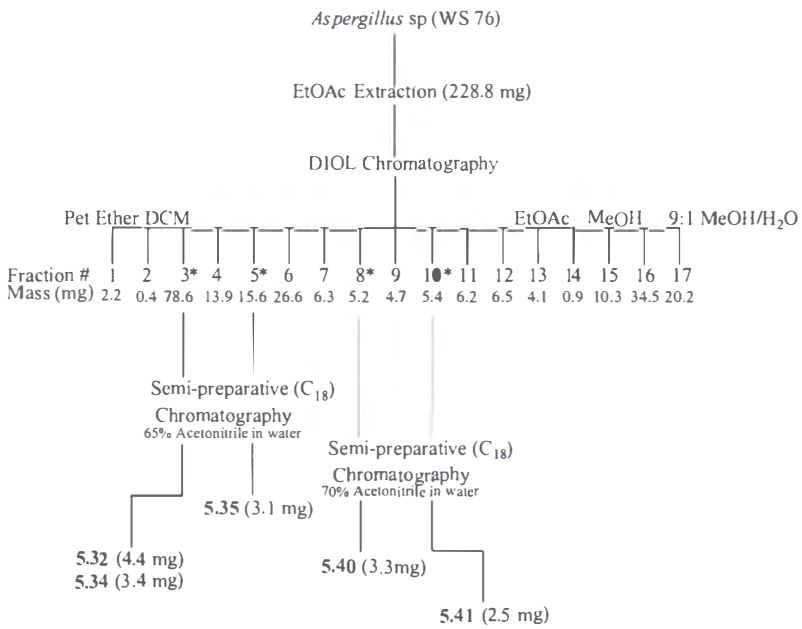

Scheme 5.1: Chromatographic purification summary for the Antarctic marine sponge-derived (*Kirkpatrickia varialosa*) fungus *Aspergillus* sp. *Fraction contains biologically active compounds of interest.

CHAPTER 6

ISOLATION OF COMPOUNDS FROM THE ANTARCTIC MARINE SPONGE-DERIVED FUNGUS *Ulocladium* sp. *(WS 132)*

6.1: General Introduction

The fungal genus *Ulocladium* is widely distributed throughout nature, most commonly being isolated from soil and decaying herbaceous material. *Ulocladium* has at least seven species described, two of which are associated with causing disease in both healthy and immunocompromised patients.[203] The most common clinical manifestations associated with *Ulocladium* sp. are subcutaneous infection and respiratory disease. [203,204]

Literature relating to biologically active compounds isolated from *Ulocladium* spp. is limited, with only a handful of biologically active compounds having been reported to date.

The tyrosine kinase (TK, $p56^{lck}$) inhibitor ulocladol (**6.1**), along with the related compound botrallin (**6.2**), were isolated from the fungus *Ulocladium botrytis* derived from the marine sponge *Callyspongia vaginalis* collected in the Caribbean, by Höller *et al.*[205] Since $p56^{lck}$ is necessary for T-cell activation, inhibition by compounds like ulocladol (**6.1**) could prove useful for treating autoimmune diseases.[10] Botrallin (**6.2**), has also been reported previously from the fungus *Botrytis allii* by Kameda *et al.*[206] However, it was only tentatively identified from the extracts of *Ulocladium botrytis* by ^{1}H NMR spectroscopy and ESI mass spectrometry as the amount of material obtained could not afford unequivocal characterization.

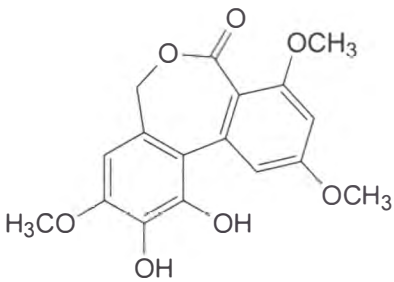

6.1

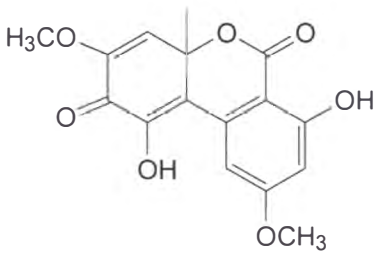

6.2

Ulocladol A (**6.3**) and ulocladol B (**6.4**), novel terpenoid compounds, were isolated from the culture filtrate of *Ulocladium chartarum*.[207] Both of these compounds are structurally related to the host-specific phytotoxins of *Alternaria citri*, a morphologically related genus.

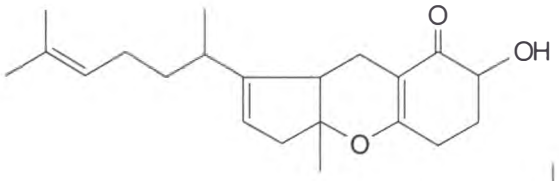

6.3

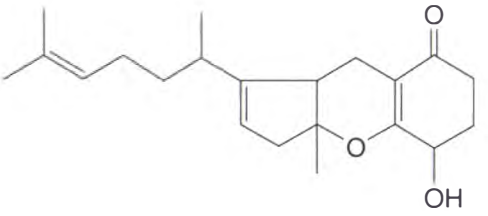

6.4

Alternaria infectoria, a filamentous fungal isolate, was chemically investigated by Larsen *et al.* as this species was recognised as the most common fungus infecting barley.[208] Infection of cereals and feedstuffs is of increasing concern as these fungal species are capable of producing a broad range of secondary metabolites that have an impact on human health. The compound infectopyrone (**6.5**) was isolated and characterised from the isolate of *Alternaria infectoria*. During this investigation, HPLC screening of *Ulocladium* isolates showed that *Ulocladium consortiale* could also produce infectopyrone (**6.5**).[208] However, no cytotoxic activity was reported for infectopyrone (**6.5**).

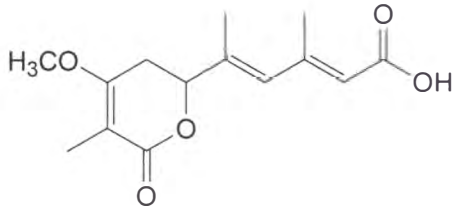

6.5

The *Ulocladium* sp. specimen (WS 132) isolated from an Antarctic marine sponge was targeted for further investigation due to the lack of literature relating to biologically active compounds isolated from the *Ulocladium* genus. This hinted strongly at the possibility of discovering new chemistry.

Work in this chapter focused on the isolation and structural elucidation of the biologically active compounds present in the extract. As a result, six compounds were isolated *via* bioassay guided fractionation (HPLC microtitre plate P388 assay) of the crude extract. These were comprised of three previously reported

compounds trypacidin (**6.6**),[209,210] sulochrin-2'-*O*-methyl ether (**6.7**)[218] and pseurotin A (**6.16**),[211-216] along with three previously unreported compounds: asterric acid-3'-*O*-methyl ether (**6.9**), methyl asterrate-3'-*O*-methyl ether (**6.13**); and the methyl asterrate-4-*O*-acetyl-3'-*O*-methyl ether (**6.15**).

6.2: Introduction

The fungus *Ulocladium* sp. (WS 132) was derived from the Antarctic marine sponge *Mycale acerata*, collected at McMurdo Sound, Ross Island, Antarctica, at a depth of 25-30 m by SCUBA. The sponge tissue was sliced into cubes (5 mm), and placed onto fungal-specific media and incubated at 26 °C until cultures appeared. The EtOAc extract of the small-scale culture displayed anti-tumour activity (IC_{50} 6 μg/mL). The isolate was re-cultured on brown rice (500 g) to obtain enough material for extraction and structural elucidation of the compound(s) responsible for the observed activity.

6.3: Extraction of the Antarctic Marine Sponge-derived Fungus Ulocladium *sp. (WS 132)*

The solid culture rice medium (500 g) of WS 132 was extracted with various combinations of the solvents EtOAc, DCM and MeOH. The extract was filtered through a bed of celite after homogenization. The solid material was then re-suspended and extracted a further two times with the same solvent combinations. The solvent was removed under vacuum to yield a deep green extract (1.54 g). The organic extract was subjected to further analysis *via* HPLC microtitre plate assay (P388). The region of activity corresponded to the compounds eluting between 11.5 and 14.8 minutes (**Figure 6.1**). Four major compounds were contained within this region of activity, consisting of approximately half of the mass detected in the entire organic extract of WS 132 (Evaporative Light Scattering Detection (ELSD)). UV spectra (**Figure 6.2**) were obtained for compounds within the region of activity *via* HPLC PDA (CH_3CN/H_2O, 0.05 TFA).

The chromophores of the major components eluting between 14 and 15 minutes were similar, with λ_{max} at both 215 and 285 nm, while the compound at 14.76 minutes displayed an extended chromophore with an additional maximum at 432 nm. This data suggested that these compounds were structurally related and possessed aromaticity. The compound eluting at 12.96 minutes seemed unrelated, with a λ_{max} at 205. Analysis of these compounds by LCMS of the crude extract resulted in ion mass peaks ranging from 320 to 450 mass units. Over 11,000 compound matches were found in the AntiMarin database, searching on the mass parameters. Addition of the UV data narrowed the list of possible structures to 67, which still encompased a wide variety of structural classes. At this point of the isolation, no further structural information was available to supplement the search parameters and restrict the number of possible compound candidates. It was unlikely that an unambiguous identification of these compounds could be achieved, therefore it was determined that further purification of the compounds was necessary.

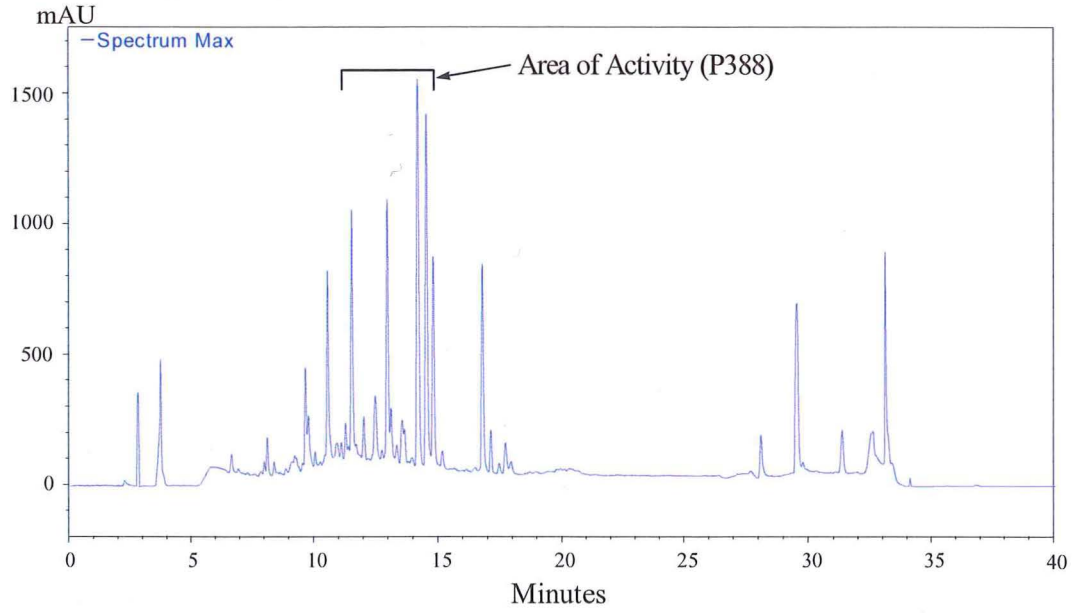

Figure 6.1: HPLC trace of crude organic extract of WS 132 (blue). The region of biological activity indicated between 11.5 and 14.8 minutes (black) as determined by microtitre plate analysis (P388).

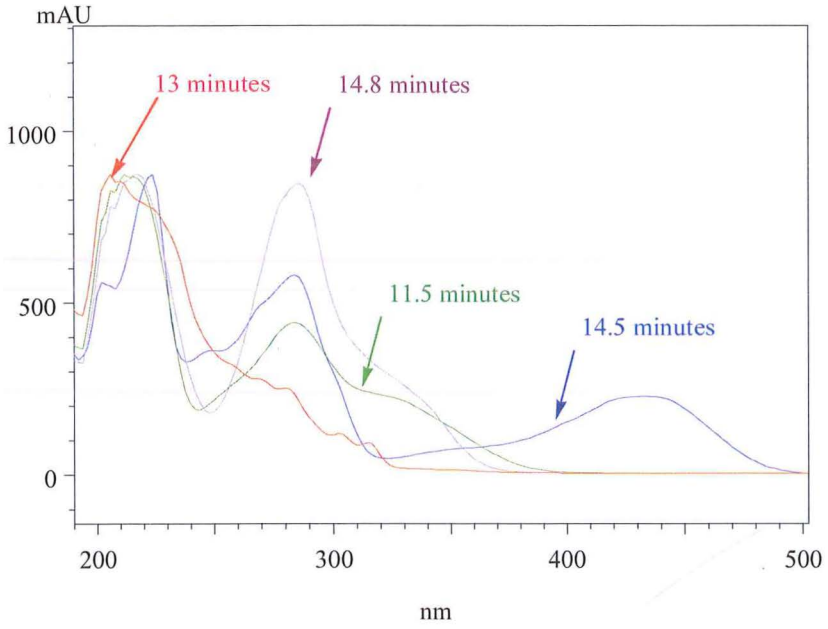

Figure 6.2: UV profiles of the major compounds observed in the region of biological activity (11.5 to 14.8 minutes), as determined by microtitre plate analysis (P388).

6.4: Chromatographic Isolation of Bioactives

6.4.1: Reversed Phase (C_{18}) Flash Chromatography of the Organic Extract of the Antarctic Marine Sponge-derived Fungus Aspergillus *sp. (WS 132)*

The organic extract (1.54 g) was dissolved in a minimum volume of solvent and loaded onto a reversed phase (C_{18}) flash chromatography column. The column was equilibrated to 90 % H_2O/10 % MeOH, and eluted using a steep stepped solvent gradient consisting of varying mixtures of H_2O, MeOH and DCM. The column was washed clean of any remaining material with MeOH and DCM (0.1 % TFA). All twelve fractions collected were analysed on a reversed phase (C_{18}) HPLC column to locate the fractions that contained the peaks responsible for the observed activity, as identified by the initial microtitre plate assay analysis. Fractions wjm23-1007 and wjm23-1008 were recognised to contain the

compounds of biological interest. Due to their complexity, these two fractions required further chromatographic purification.

6.4.2: Reversed Phase (C_{18}) Semi-preparative HPLC Chromatography of Fractions wjm23-1007 and wjm23-1008

Fractions wjm23-1007 and wjm23-1008 were combined (wjm23-1007-8), based upon the HPLC analysis, and dissolved in a minimum volume of MeOH. During storage at 4 °C, crystalline material formed in the methanolic solution. This fraction was filtered, and the crystals (wjm23-1007-8.xtl) were collected and analysed by ^{1}H, ^{13}C and 2D NMR spectroscopy and mass spectrometry. Structural elucidation of the purified compound (**6.6**) (corresponding to peak number 2) is described in **Section 6.5.1**.

Fraction wjm23-1007-8, the supernatant, was further purified by reversed phase (C_{18}) semi-preparative HPLC chromatography using a gradient solvent system ranging from 30 % CH_3CN/H_2O to 55 % CH_3CN/H_2O (0.05 % TFA) over 25 minutes. The gradient solvent system had been developed on the analytical HPLC for maximum resolution of the eluting compounds. Seven fractions were collected as peaks eluted (**Figure 6.3**), however, both peaks one and seven were outside the region of activity as determined by HPLC microtitre plate analysis. The purity of the collected compounds was confirmed by re-injection onto the reversed phase (C_{18}) analytical HPLC column.

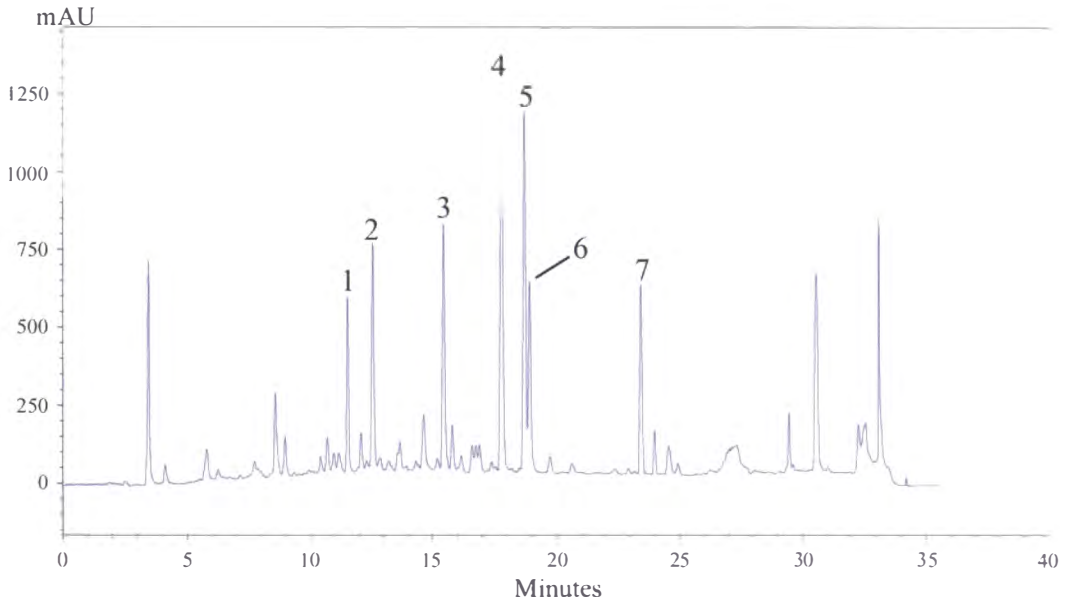

Figure 6.3: HPLC trace of combined fractions wjm23-1007 and wjm23-1008 after elution gradient development. The seven fractions of interest are indicated.

Insufficient material from the first fraction was collected to allow for structural elucidation. Only peaks numbered two to seven were subsequently examined by ^{1}H, ^{13}C and 2D NMR spectroscopy and ESI mass spectrometry. Structural elucidation of these purified compounds is discussed in **Section 6.5**.

6.5: Structural Elucidation of Compounds Isolated from the Antarctic Marine Sponge-derived Fungus Ulocladium *sp. (WS 132)*

6.5.1: Structural Elucidation of **6.6**

The first compound, (**6.6**), which had crystallised from MeOH (corresponding to peak number two), was separated from the filtrate of the combination of fractions wjm23-1007 and wjm23-1008 as white needles (6.0 mg). HRESI mass spectrometry identified a $[M+H]^+$ ion at *m/z* 345.0987 (calc. 345.0974) which led to the molecular formula $C_{18}H_{17}O_7$, possessing 11 DBEs. The ^{13}C NMR (**Figure 6.4**) combined with the HSQC identified 18 well defined carbon signals corresponding to three carbonyl carbons (δ_C 190.5, 185.7 and 169.5), one sp^3

quaternary carbon (δ_C 84.0), six sp^2 quaternary carbons (δ_C 174.2, 163.4, 158.2, 152.2, 138.0 and 108.0), four sp^2 methine carbons (δ_C 137.2, 105.5, 105.3 and 103.9), three methoxy carbons (δ_C 56.6, 55.9 and 52.7) and one methyl carbon (δ_C 23.3), satisfying the carbon requirements of the molecular formula. The presence of three methoxy groups (δ_H 3.94, 3.68 and 3.66) and one methyl (δ_H 2.44) group was confirmed by the presence of four singlet signals visible in the ^{1}H NMR spectrum (**Figure 6.5**). The remaining proton signals were located in the olefinic/aromatic region (δ_H 7.01, 6.55, 6.37 and 5.77). These 16 protons satisfied the proton requirements of the molecular formula, leaving just one oxygen atom to assign.

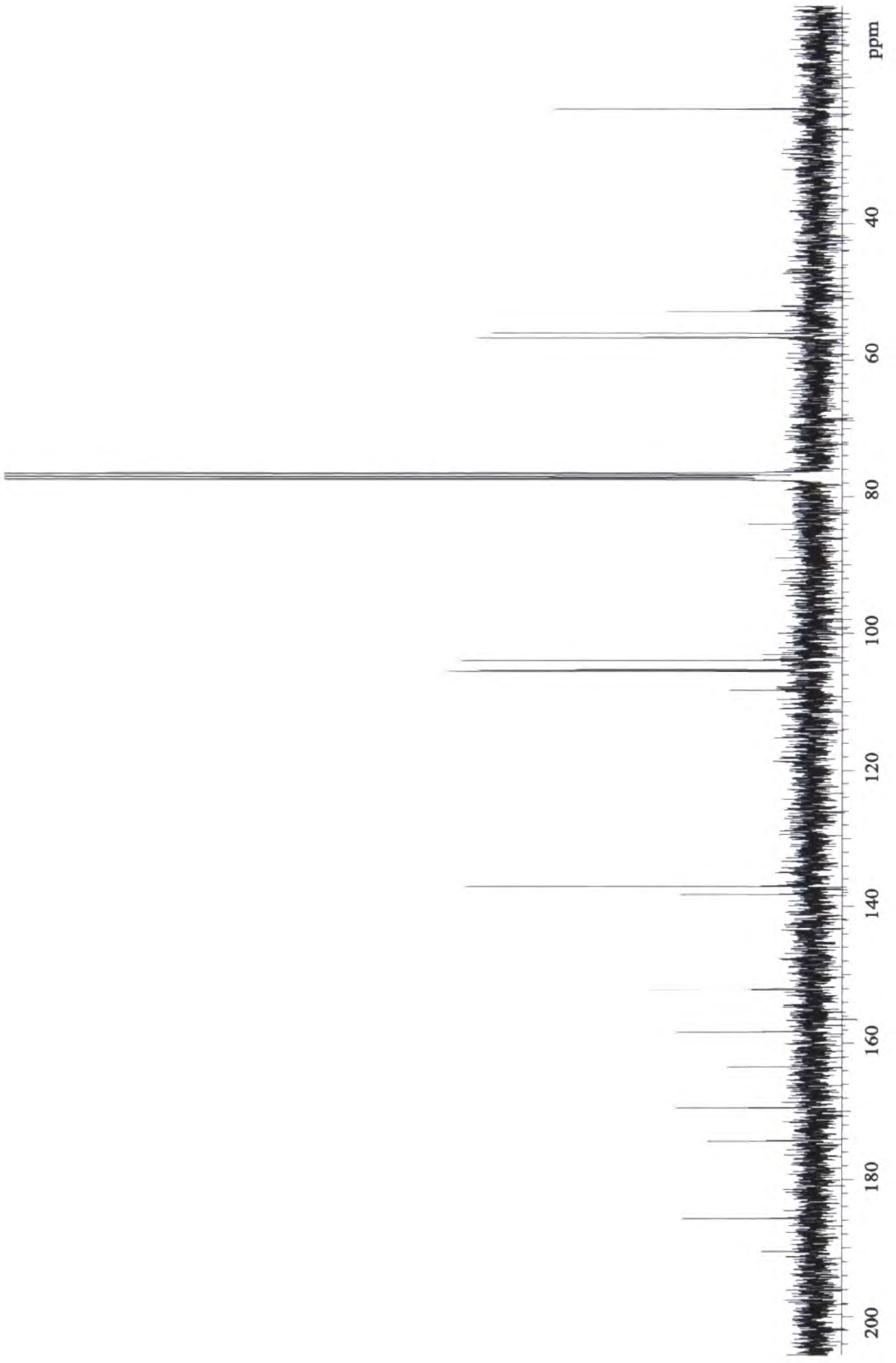

Figure 6.4: The ^{13}C NMR spectrum of compound **6.6** ($CDCl_3$).

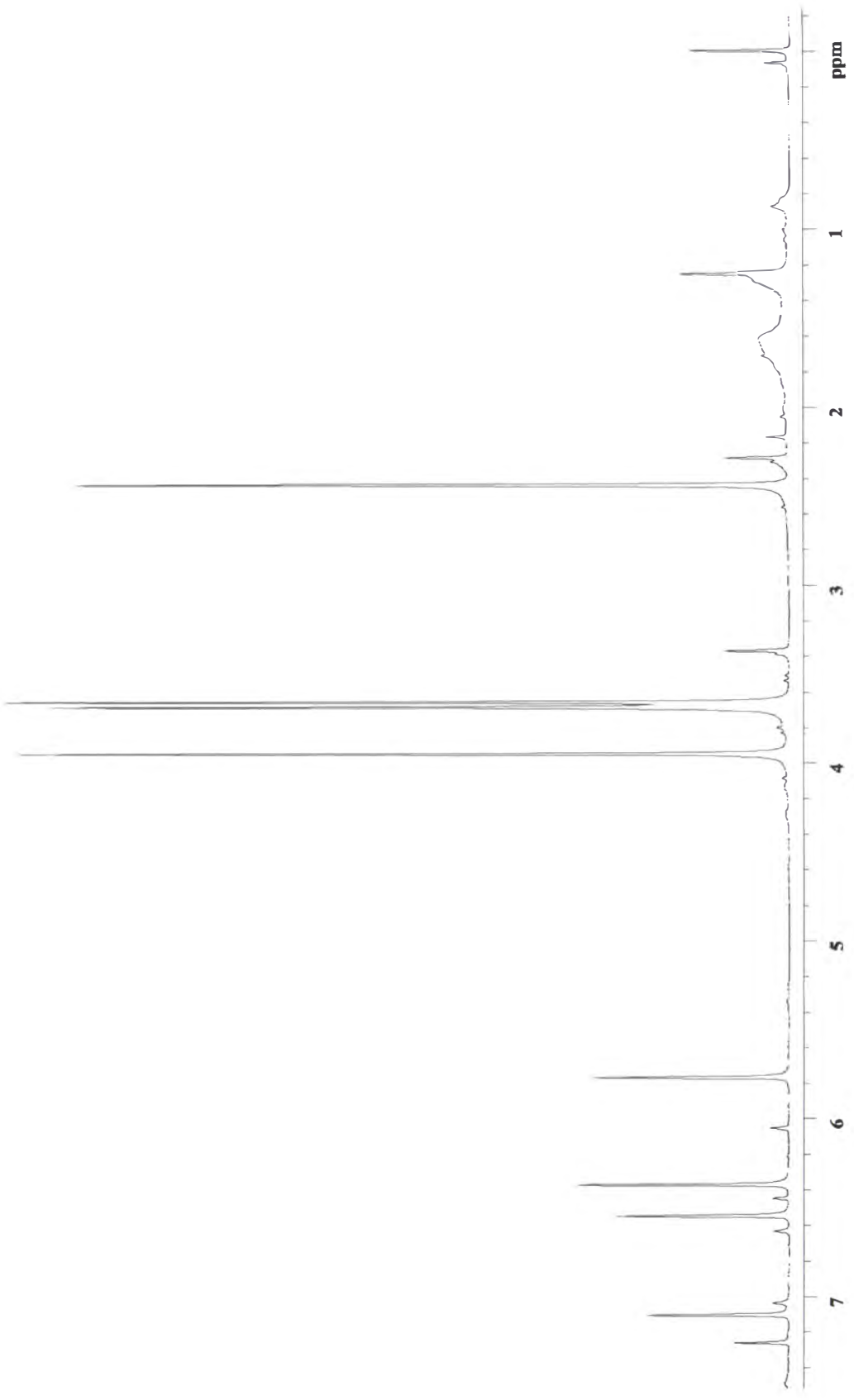

Figure 6.5: The ^{1}H NMR spectrum of compound **6.6** ($CDCl_3$).

Connectivity of the carbons from C-3 to C-5 was achieved by close inspection of both the ^{1}H NMR and COSY spectra. A COSY cross peak correlation was observed from the H-3 (δ_H 7.01) proton to the H-5 (δ_H 5.77) proton, combined with the small coupling constant extracted from the ^{1}H NMR spectrum ($J_{3,5}$ = 1.5 Hz), initially suggested that these protons (H-3 and H-5) might be *meta* to one another on an aromatic ring system. However CIGAR correlations from both of the H-3 and H-5 (δ_H 7.01 and 5.77, respectively) protons to the C-4 (δ_C 185.7) carbonyl carbon indicated that the suspected ring system was not aromatic. The chemical shift of C-4 (δ_C 185.7) suggested the presence of a ketone functionality at this position. Therefore H-3 and H-5 were assigned as olefinic not aromatic, α to the ketone moiety at C-4. The methoxy group (δ_H 3.68) was assigned at position C-2 on the basis of the observed CIGAR correlations from both the H-3 (δ_H 7.01) olefinic proton and the H-9 (δ_H 3.68) methyl protons to the C-2 (δ_C 163.4) carbon, and also confirmed by the observed NOE signal enhancement of the H-9 (δ_H 3.68) methyl protons following irradiation of the H-3 (δ_H 7.01) olefinic proton. The partial structure for **6.6**, ring A was proposed on the basis of this NMR data (**Figure 6.6**).

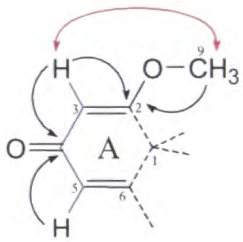

Figure 6.6: Partial structure of **6.6**, ring A, showing key COSY (blue), CIGAR (black) and NOESY (red) experimental correlations.

The remaining atoms of ring A were assigned utilising the CIGAR experiment. Carbons C-1, C-6 and C-7 were assigned by the observed CIGAR correlations from the H-5 (δ_H 5.77) methine proton to the C-7 carbonyl and C-1 quaternary carbons (δ_C 169.5 and 84.0, respectively), together with a weak correlation to the C-6 (δ_C 138.0) carbon. The methyl ester consisting of the C-7 carbonyl and C-8 methyl carbons (δ_C 169.5 and 56.6, respectively) was positioned on the C-6 carbon, based on a NOESY correlation between the H-8 (δ_H 3.66) methyl protons

and the H-5 (δ_H 5.77) olefinic proton, combined with the CIGAR correlations from the H-8 methyl protons (δ_H 3.66) to the C-7 (δ_C 169.5) carbonyl carbon. The C-1 carbon position was confirmed *via* the CIGAR correlation from the H-3 (δ_H 7.01) protons to the C-1 (δ_C 84.0) carbon. The HSQC spectrum confirmed that the C-1 carbon was quaternary, while the ^{13}C chemical shift suggested that this carbon was a spiro centre.[191] The completed ring, A, was therefore proposed for **6.6** (**Figure 6.7**).

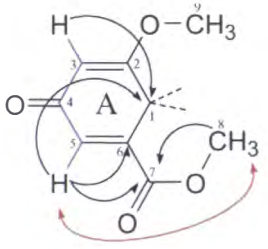

Figure 6.7: Ring A proposed for **6.6**, with key COSY (blue), CIGAR (black) and NOESY (red) experimental correlations.

The assignment of ring C was achieved by careful examination of the NOESY and CIGAR spectra. Carbons C-1' and C-5' were assigned using the observed CIGAR correlations from the H-3' (δ_H 6.37) proton to the C-1' and C-5' carbons (δ_C 108.0 and δ_C 105.5, respectively), while the CIGAR correlation from the H-5' (δ_H 6.55) proton to the C-1' and C-3' (δ_C 108.0 and 105.3 respectively) carbons confirmed the assignment of the C-1' and C-3' positions. Irradiation of the H-3' (δ_H 6.37) aromatic proton resulted in two NOESY enhanced signals corresponding to both of the H-7' and H-8' (δ_H 3.94 and 2.44, respectively) methyl protons, placing the H-3' proton between these two functionalities, while the H-8' methyl group was positioned between both H-3' and H-5' based upon the NOESY enhanced signals observed after irradiation of the H-8' (δ_H 2.44) protons, which resulted in the signal enhancement of both the H-3' and H-5' (δ_H 6.37 and 6.55, respectively) aromatic protons. The H-8' (δ_H 2.44) aromatic methyl protons were tentatively positioned at C-4' (δ_C 152.2), based upon the CIGAR correlation from the H-8' (δ_H 2.44) methyl protons to the C-4' (δ_C 152.2) aromatic carbon. The H-7' (δ_H 3.94) methyoxy group was positioned at C-2' (δ_C 158.2) based upon the previously observed NOESY correlation from the H-7' (δ_H 3.94) protons to the H-

3' (δ_H 6.37) proton combined with the additional CIGAR correlation from the H-7' (δ_H 3.94) proton to the C-2' (δ_C 158.2) aromatic carbon. The remaining aromatic carbon (δ_C 174.2) was determined by a $^2J_{CH}$ CIGAR correlation from the H-5' (δ_H 6.55) proton to the C-6' (δ_C 174.2) sp^2 carbon. From this data the substitution pattern for the aromatic ring, ring C was proposed for **6.6** (**Figure 6.8**).

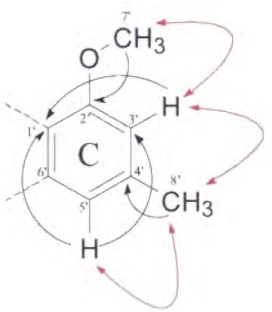

Figure 6.8: Proposed partial structure, ring C of **6.6**, with key CIGAR (black) and NOESY (red) experimental correlations.

However, because ring C does not possess any symmetry (i.e. the functional groups on C-1' and C-6' are not equivalent, by the requirements of the molecular formula and the carbon chemical shifts), there are two possible aromatic ring substitution patterns (**Figure 6.9**).

The experimental CIGAR data confirmed that both the H-5' and H-3' (δ_H 6.55 and 6.37, respectively) aromatic protons are $^3J_{CH}$ correlated to the C-1' (δ_C 108.0) carbon, while the H-5' (δ_H 6.55) proton is $^2J_{CH}$ correlated to the C-6' (δ_C 174.2) carbon. The proposed substitution pattern for ring C was therefore validated as shown in **Figure 6.9**.

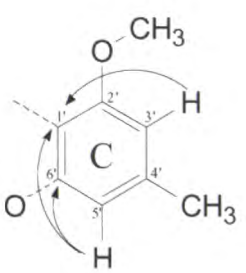

Figure 6.9: The partial structure, ring C of **6.6**, with key CIGAR correlations in black used to assign the substitution pattern.

The atoms left to assign, as determined by the molecular formula, consisted of one oxygen and one carbon (δ_C 190.5) atom. The ^{13}C chemical shift of this carbon suggested that it was part of a carbonyl group. Its assignment was achieved through the very weak CIGAR correlation observed from the H-3' (δ_H 6.37) aromatic methine proton to the C-10 (δ_C 190.5) carbonyl carbon (**Figure 6.10**).

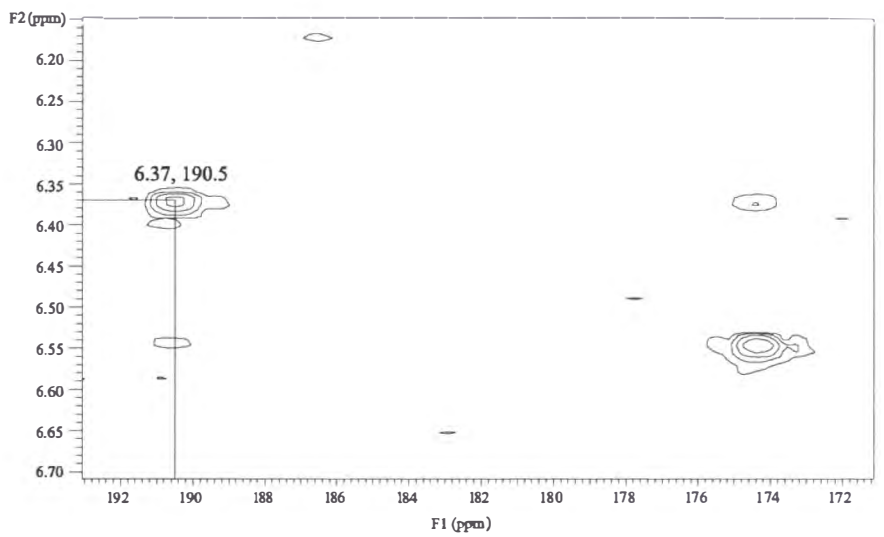

Figure 6.10: The $^4J_{CH}$ CIGAR correlation observed from aromatic proton H-3' (δ_H 6.37) to the C-10 (δ_C 190.5) carbonyl carbon ($CDCl_3$).

As no further atoms were left to assign (as determined by the HRESI derived molecular formula), ring B was tentatively assigned as a furanone. The proposed connectivity of the spiro center at C-1 (δ_C 84.0) to ring A was through both the C-6' oxygen and the C-10 (δ_C 190.5) carbonyl carbon to the C-1 (δ_C 84.0) quaternary carbon. The structure as shown in **Figure 6.11**, was proposed for compound **6.6** which also satisfied the remaining DBE requirement.

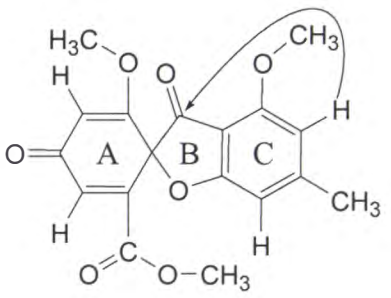

Figure 6.11: The very weak CIGAR correlation observed from the H-3' (6.37) aromatic proton to the C-10 (δ_C 190.5) carbonyl carbon, completing the assignment of the proposed structure for **6.6**.

A literature search[130,145] on the proposed structure for compound **6.6** revealed that a compound with an identical structure, trypacidin, had been isolated as a new antibiotic from the fungal culture of an *Aspergillus fumigatus* collected from a sample of Chinese soil in 1963.[210] Trypacidin (**6.6**) had been identified by the use of various physical and spectroscopic experiments including melting point, UV and IR spectroscopy, elemental analysis and mass spectrometry combined with salting-out paper chromatographic techniques. The ^{1}H NMR data of trypacidin (**6.6**) was presented several years later by Balan *et al.*,[209] where their NMR assignments were supported by previous studies of similar compounds, griseofulvin derivatives.[217]

The literature numbering system for trypacidin (**6.6**) used in the structural elucidation, is shown in **Figure 6.12**, while the experimental ^{1}H, ^{13}C, COSY, NOESY and CIGAR NMR data are shown in **Table 6.1**.

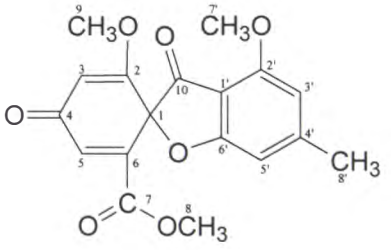

Figure 6.12: Numbering system of trypacidin (**6.6**) used in **Table 6.1**.

Table 6.1: The ^{1}H, ^{13}C, COSY, NOESY and CIGAR NMR data for compound trypacidin (**6.6**) ($CDCl_3$).

Position	$^{13}C\ \delta^{\S}$	$^{1}H\ \delta^{\zeta}$	COSY (NOESY)	CIGAR
1	84.0 (C)			
2	163.4 (C)			
3	137.2 (CH)	7.01 (1H, d, 1.5)	H-5 (H-9)	C-5, C-4, C-2, C-1
4	185.7 (CO)			
5	103.9 (CH)	5.77 (1H, d, 1.5)	H-3 (H-8)	C-7, C-6 (w), C-4, C-3, C-1
6	138.0 (C)			
7	169.5 (CO)			
8	56.6 (OCH_3)	3.66 (3H, s)	(H-5)	C-7
9	52.7 (OCH_3)	3.68 (3H, s)	(H-3)	C-2
10	190.5 (CO)			
1'	108.0 (C)			
2'	158.2 (C)			
3'	105.3 (CH)	6.37 (1H, s)	(H-8', H-7')	C-10(vw), C-8', C-5', C-2', C-1'
4'	152.2 (C)			
5'	105.5 (CH)	6.55 (1H, s)	(H-8')	C-8', C-6', C-3', C-1'
6'	174.2(C)			
7'	55.9 (OCH_3)	3.94 (3H, s)	(H-3')	C-2'
8'	23.2 (CH_3)	2.44 (3H, s)	(H-5', H-3')	C-5', C-4', C-3'

§ ^{13}C NMR spectra recorded at 125 MHz in $CDCl_3$. ^{13}C NMR chemical shifts δ ppm from **C**DCl_3 (77.0). ζ ^{1}H NMR spectra recorded at 500 MHz. ^{1}H chemical shift values δ ppm from C**H**Cl_3 (7.25) followed by number of protons, multiplicity and coupling constant (*J*/Hz).

6.5.2: Structural elucidation of **6.7**

The second compound (**6.7**) was isolated as a pale yellow powder (5.4 mg). HRESI mass spectrometry identified a $[M+H]^+$ ion at *m/z* 347.1013 (calc. 347.1131), which led to the molecular formula $C_{18}H_{18}O_7$, and corresponded to 10 DBE, 2 Da greater than that for trypacidin (**6.6**). Both the ^{1}H and ^{13}C NMR spectra were also reminiscent of trypacidin (**6.6**), suggesting that these compounds might be structurally related. The ^{1}H NMR spectrum (**Figure 6.13**) revealed the presence of one methyl group associated with an aromatic ring (δ_H 2.42) and three methoxy groups (δ_H 3.64, 3.61 and 3.33), however the most significant difference was the downfield shift of the H-5 (δ_H 5.77) methine proton in trypacidin (**6.6**) to δ_H 6.95 in compound **6.7**. The ^{13}C NMR spectrum (**Figure 6.14**) confirmed the presence of three methoxy groups (δ_C 56.0, 55.6 and 52.1), two carbonyl carbons (δ_C 199.9 and 166.7), four sp^2 methines (δ_C 110.3, 107.8, 103.3 and 103.1) and

eight sp^2 quaternary carbons (δ_C 163.7, 161.0, 157.6, 156.9, 148.0, 128.2, 126.8 and 110.7). However, the absence of the sp^3 C-1 (δ_C 84.0) spiro carbon and the conjugated C-4 (δ_C 185.7) dienone carbonyl carbon strongly suggested that this cyclic system was aromatic.

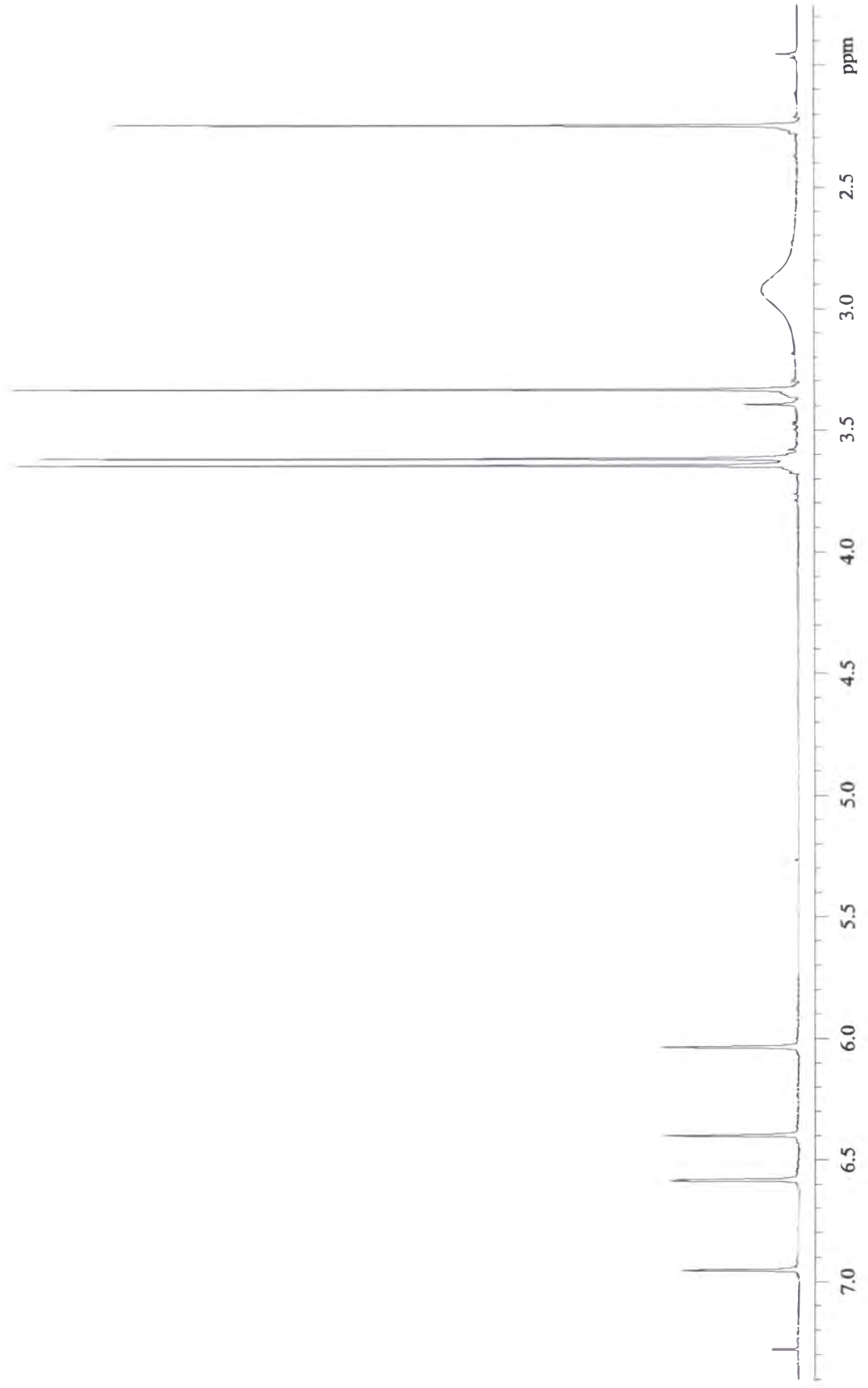

Figure 6.13: The ^{1}H NMR spectrum of compound **6.7** ($CDCl_3$).

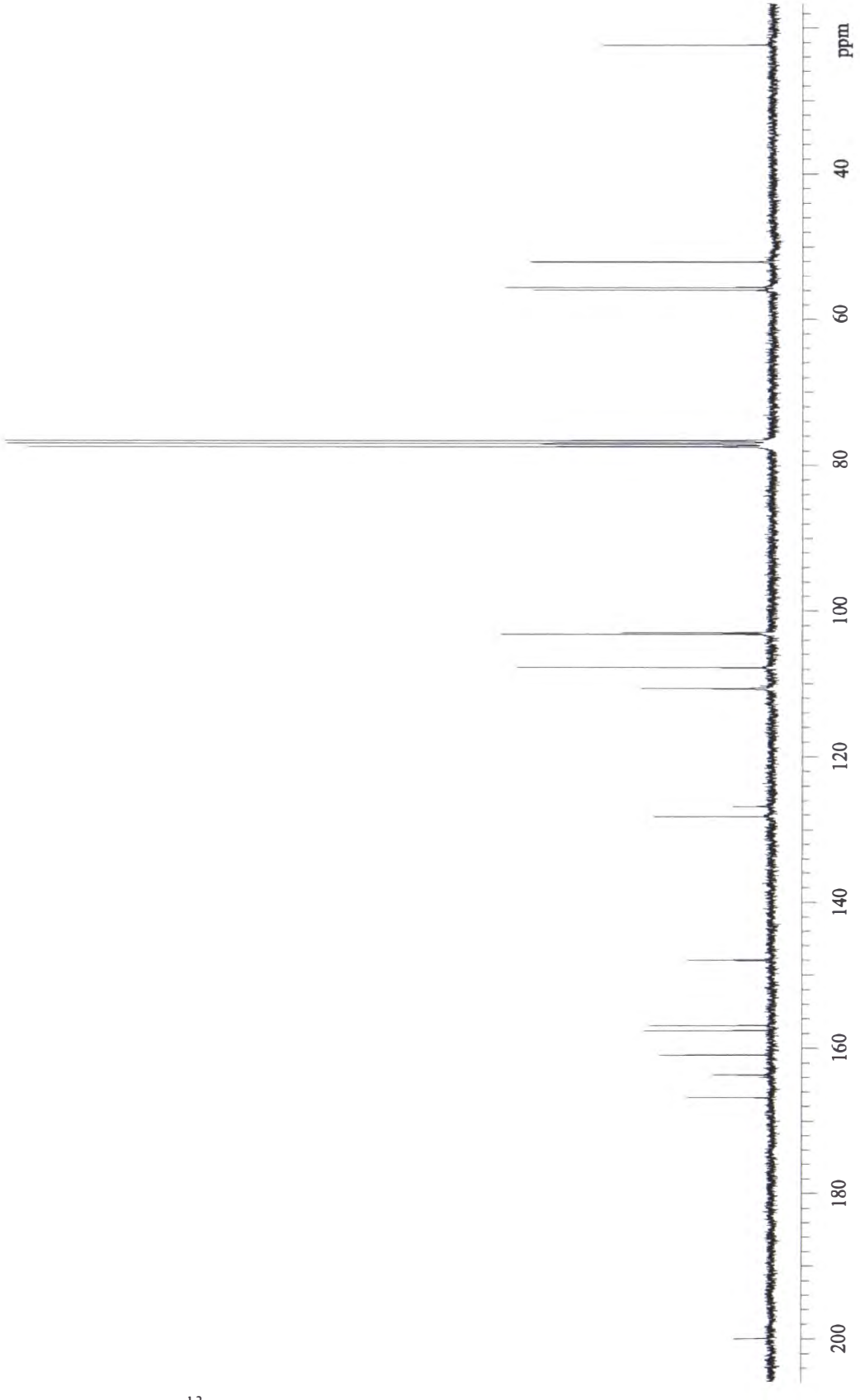

Figure 6.14: The ^{13}C NMR spectrum of compound **6.7** ($CDCl_3$).

Ring A was constructed by careful comparison of the NMR spectra (^{1}H, ^{13}C and CIGAR) for **6.7** with that obtained for trypacidin (**6.6**). Connectivity from C-3 to C-5 was established *via* the coupling constant extracted from the ^{1}H NMR spectrum between the H-3 and H-5 (δ_H 6.58 and 6.95, respectively, $J_{3,5}$= 1.5 Hz) aromatic protons, suggesting a *meta* configuration, while CIGAR correlations from the H-3 and H-5 (δ_H 6.58 and 6.95, respectively) aromatic protons to the C-4 (δ_C 157.6) carbon implied that carbon C-4 was between both of these protons. The ^{13}C chemical shift of C-4 also suggested that this carbon was no longer part of a carbonyl but was still substituted with an oxygen (hydroxyl group). As before, the methoxycarbonyl group was positioned at C-6 (δ_C 128.2) on the basis of the $^{3}J_{CH}$ CIGAR correlations from both the H-5 methine and H-8 methoxy protons (δ_H 6.95 and 3.61, respectively) to the C-7 (δ_C 166.7) carbonyl carbon. The H-9 (δ_H 3.64) methyl protons associated with the methoxy group were positioned at C-2 (δ_C 156.9) on the basis of the CIGAR correlations from both the H-3 (δ_H 6.58) aromatic proton and the H-9 (δ_H 3.64) methoxy protons to the C-2 (δ_C 156.9) aromatic carbon. NOESY correlations were used to confirm the proposed substitution pattern for ring A. Irradiation of the H-3 (δ_H 6.58) aromatic proton enhanced the H-9 (δ_H 3.64) methyl proton signal, while the irradiation of the H-5 (δ_H 6.95) aromatic proton enhanced the H-8 (δ_H 3.61) methyl proton signal. Carbon C-1 was assigned by CIGAR correlations from the H-3 and H-5 (δ_H 6.58 and 6.95, respectively) aromatic protons to the C-1 (δ_C 126.8) carbon. The proposed partial structure for **6.6**, ring A, is shown in **Figure 6.15**.

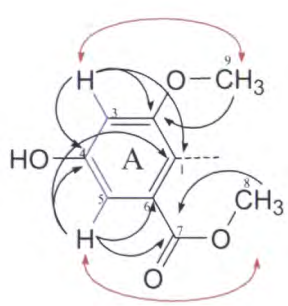

Figure 6.15: Proposed structure for ring A of **6.7**, indicating key CIGAR (black), COSY (blue) and NOESY (red) correlations.

The remaining portion of the structure (**Figure 6.16**) was constructed using the ^{1}H and ^{13}C NMR chemical shift data comparison with trypacidin (**6.6**), combined

with experimental NOESY data. The substitution pattern of the suspected aromatic ring for carbons C-2' to C-5' was determined by irradiation of the H-3' (δ_H 6.03) methine proton to give NOE enhanced signals for both the H-7' and H-8' (δ_H 3.94 and 2.42, respectively) methyl protons, confirming H-3' was still located between these two methyl groups. Irradiation of the H-5' (δ_H 6.39) aromatic proton resulted in only one NOE enhanced signal, that of the H-8' (δ_H 2.42) methyl protons, placing the H-5' proton adjacent to the H-8' methyl group as indicated by red arrows in **Figure 6.16**.

The CIGAR correlation from the H-7' (δ_H 3.94) methyoxy protons to the C-2' (δ_C 161.0) carbon located the 7'-methoxy group on position C-2', and the correlation from the H-8' (δ_H 2.42) methyl protons to the C-4' (δ_C 148.0) carbon, located the methyl group on C-4', while the $^3J_{CH}$ correlations to the C-3' and C-5' (δ_C 103.1 and 110.3) carbons confirmed that the 8'-methyl group was between H-3' and H-5', as previously determined by the NOESY data. The $^3J_{CH}$ correlations from both H-3' and H-5' (δ_H 6.03 and 6.39, respectively) protons to the C-1' (δ_C 110.7) carbon, combined with the $^2J_{CH}$ CIGAR correlation from the H-5' (δ_H 6.39) proton to the C-6' (δ_C 163.7) carbon completed the assignment and substitution pattern of the proposed partial structure ring C, for **6.7** (**Figure 6.16**). The ^{13}C chemical shift of C-6' (163.7) suggested that this position was substituted with an oxygen (hydroxyl group), similar to that of the previously isolated compound trypacidin (**6.6**).

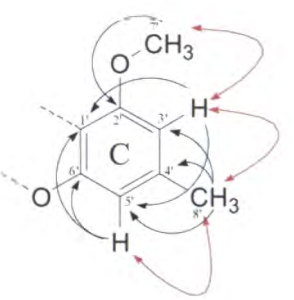

Figure 6.16: Proposed structure ring C, for **6.7** with key CIGAR (black) and NOESY (red) correlations.

One carbonyl carbon and one proton were left to assign, as required by the ^{13}C and ^{1}H NMR spectra, and one DBE by the molecular formula. Careful examination of the CIGAR spectrum revealed a very weak correlation from the H-3' (δ_H 6.03) aromatic proton to the C-10 (δ_C 199.9) carbonyl carbon. The chemical shift comparison of the C-1 and C-1' carbons assigned for both trypacidin (**6.6**) and **6.7** confirmed that a carbonyl was bridging rings C and A at these positions; this assignment accounted for the remaining DBE. The remaining proton was assigned on the oxygen at the C-6' position. A working structure for compound **6.7** was therefore proposed (**Figure 6.17**).

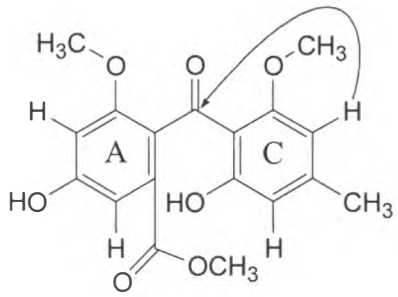

Figure 6.17: Final structure proposed for **6.7,** showing the very weak CIGAR (black) correlation from the H-3' (δ_H 6.03) proton, to the C-10 (δ_C 199.9) carbonyl carbon, connecting ring A to ring C.

A literature search[130,145] was performed on the proposed structure for **6.7**. The isolated compound (**6.7**) was found to be sulochrin-2'-*O*-methyl ether, previously isolated from the fungal culture of *Aspergillus terreus var. aureus* by Inamori *et al.*[218] The experimental NMR data was also compared to that reported in the literature for sulochrin (**6.8**), the 2'-*O*-demethyl metabolite, as no NMR data was reported with **6.8**.[219,220] The chemical shift data was found to match closely with those reported for **6.8**, excluding the C-2' position.

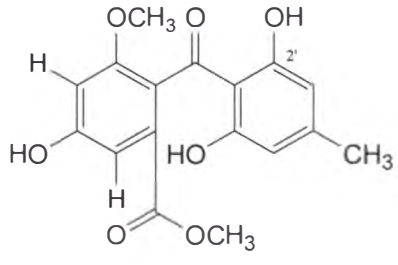

6.8

The arbitrarily assigned numbering for sulochrin-2'-*O*-methyl ether (**6.7**) is shown in **Figure 6.18** while the full experimental ^{1}H, ^{13}C, COSY, NOESY and CIGAR NMR data for sulochrin-2'-*O*-methyl ether (**6.7**) are shown in **Table 6.2.**

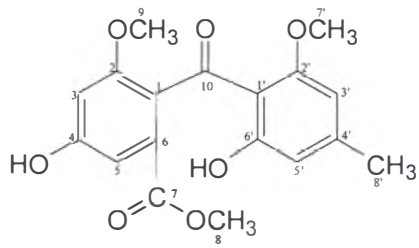

Figure 6.18: Numbering system assigned for sulochrin-2'-*O*-methyl ether (**6.7**). as used in **Table 6.2**.

Table 6.2: The ^{1}H, ^{13}C, COSY, NOESY and CIGAR NMR data for sulochrin-2'-*O*-methyl ether (**6.7**) ($CDCl_3$).

Position.	^{13}C δ §	^{1}H δ ξ	COSY (NOESY)	CIGAR
1	126.8 (C)			
2	156.9 (C)			
3	103.3 (CH)	6.58 (1H, d, 1.5)	H-5 (H-9)	C-5, C-4, C-2, C-1
4	157.6 (C)			
5	107.8 (CH)	6.95 (1H, d, 1.5)	H-3 (H-8)	C-7, C-6, C-4, C-3, C-1
6	128.2 (C)			
7	166.7 (CO)			
8	52.1 (OCH_3)	3.61 (3H, s)	(H-5)	C-8', C-2'
9	56.0 (OCH_3)	3.64 (3H, s)	(H-3)	C-2
10	199.9 (CO)			
1'	110.7 (C)			
2'	161.0 (C)			
3'	103.1 (CH)	6.03 (1H, s)	(H-8', H-7')	C-10(vw), C-8', C-5', C-4', C-2', C-1'
4'	148.0 (C)			
5'	110.3 (CH)	6.39 (1H, s)	(H-8')	C-8',C-6', C-4', C-3', C-1'
6'	163.7(C)			
7'	55.6 (OCH_3)	3.94 (3H, s)	(H-3')	C-2'
8'	22.3 (CH_3)	2.42 (3H, s)	(H-5', H-3')	C-5', C-4', C-3'

§ ^{13}C NMR spectra recorded at 125 MHz in $CDCl_3$. ^{13}C chemical shifts δ ppm from $CDCl_3$ (77.0).
ξ ^{1}H NMR spectra recorded at 500 MHz. ^{1}H chemical shift values δ ppm from $CHCl_3$ (7.25) followed by number of protons, multiplicity and coupling constant (*J*/Hz).

6.5.3: Structural elucidation of **6.9**

The third compound (**6.9**) was also isolated as a pale yellow powder (6.7 mg). The HRESI mass spectrometry identified the $[M+Na]^+$ ion at *m/z* 385.0879 (calc 385.0899), 16 Da greater than that of sulochrin-2'-*O*-methyl ether (**6.7**), which led to a molecular formula of $C_{18}H_{18}O_8$, corresponding to 10 DBE. Both the ^1H and ^{13}C NMR spectra were reminiscent of the data obtained for sulochrin-2'-*O*-methyl ether (**6.7**), suggesting that these compounds were structurally related. The ^1H NMR spectrum (**Figure 6.19**) revealed the presence of one methyl group associated with an aromatic ring (δ_H 2.20), three methoxy groups (δ_H 3.86, 3.76 and 3.73) and four aromatic methine protons (δ_H 6.86, 6.78, 6.53 and 5.89). Although the signals observed in the ^{13}C NMR spectrum (**Figure 6.20**) were weak, two carbonyl carbons were tentatively assigned at δ_C 166.4 and 168.3, while the absence of a third carbonyl in the δ_C 200 region suggested that this compound was no longer a diphenylketone.

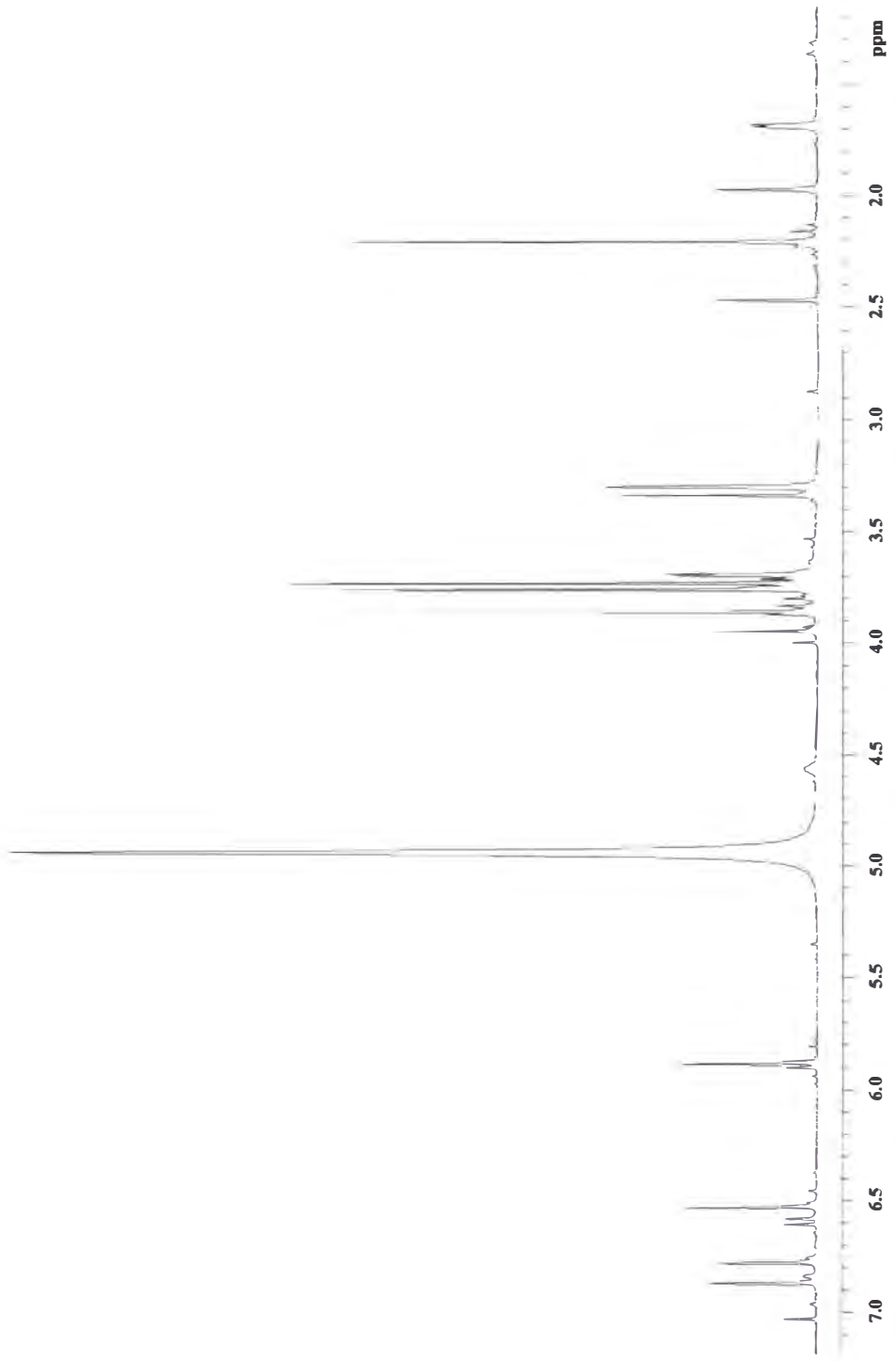

Figure 6.19: The ^{1}H NMR spectrum of compound **6.9** (CD_3OD).

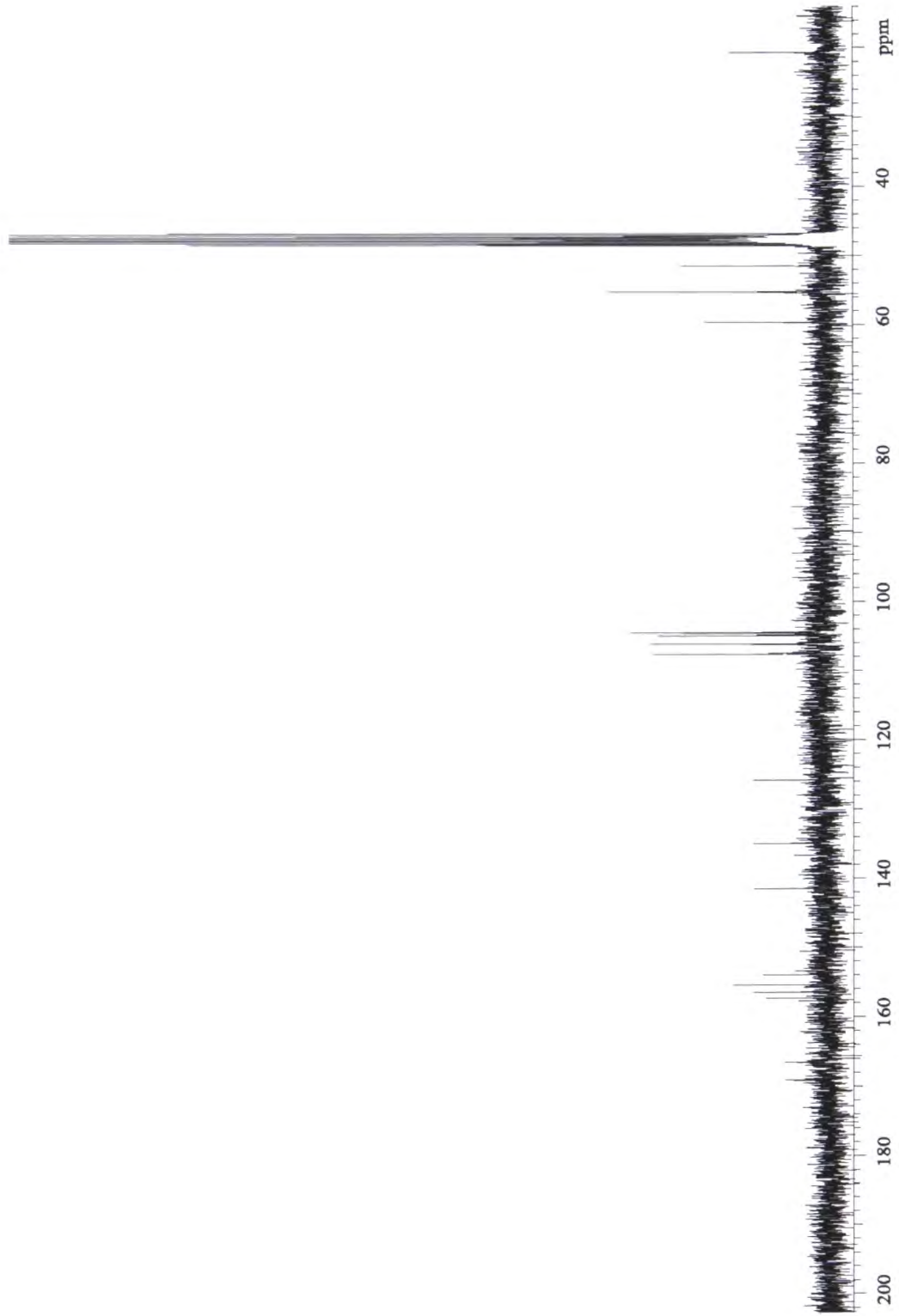

Figure 6.20: The ^{13}C NMR spectrum of compound **6.9** (CD_3OD).

As before, ring A was readily deduced by direct comparison of the NMR data (HSQC, CIGAR) with that obtained for the two previously isolated compounds **6.6** and **6.7**. The H-3 and H-5 (δ_H 6.86 and 6.78, respectively, $J_{3,5}$ = 1.5 Hz) aromatic protons were still COSY correlated, confirming the connectivity from the C-3 to C-5 carbons. Carbon C-4 was determined by the CIGAR correlations from both the H-3 and H-5 (δ_H 6.86 and 6.78, respectively) aromatic protons to the C-4 (δ_C 155.4) aromatic carbon. The ^{13}C chemical shift of C-4 suggested that this position was again phenolic. The carboxylic acid ester group was located at the C-6 (δ_C 125.6) carbon (CIGAR correlations from both the H-5 and H-8 (δ_H 6.78 and 3.73, respectively) protons to the C-7 (δ_C 166.4) carbonyl carbon). The location of the 9-methoxy group at C-2 (δ_C 154.0) was confirmed *via* the CIGAR correlations from both the H-3 (δ_H 6.86) aromatic proton and the H-9 (δ_H 3.76) methyl protons to the C-2 (δ_C 154.0) aromatic carbon. Carbon C-1 was located by $^3J_{CH}$ CIGAR coupling from both of the H-3 and H-5 (δ_H 6.86 and 6.78, respectively) aromatic protons to the C-1 (δ_C 134.7) quaternary carbon. This data established that ring A (**Figure 6.21**) was identical to that of sulochrin-2'-*O*-methyl ether (**6.7**), previously isolated and identified in **Section 6.5.2**. This data inferred that the difference in the structure was associated with the arrangement of the remaining atoms.

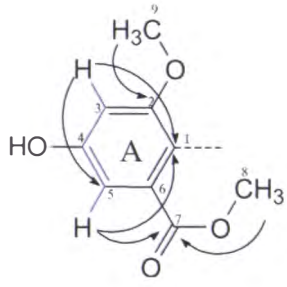

Figure 6.21: The key COSY (blue) and CIGAR (black) correlations for the proposed partial structure, ring A of **6.9**.

Ring C was also constructed by careful interpretation of the ^1H and CIGAR NMR data. The CIGAR correlations from the H-9' (δ_H 2.20) methyl protons to the C-4', C-5' and C-6' (δ_C 104.5, 141.4 and 106.1, respectively) aromatic carbons confirmed that the H-9' methyl group was still located between both methine

protons at the C-5' (δ_C 141.4) position. This was further established *via* NOESY correlations from the irradiated H-9' (δ_H 2.20) methyl protons to the signals corresponding to the H-4' and H-6' (δ_H 6.53 and 5.89, respectively) aromatic protons. The orientation of H-4' and H-6' was determined *via* sequential irradiation of protons utilising the NOESY experiment. Irradiation of the H-8' (δ_H 3.86) methoxy protons resulted in the single NOE enhancement corresponding to the H-4' (δ_H 6.53) aromatic proton signal, positioning the H-8' methoxy group adjacent to H-4' (δ_H 6.53) on the C-3' (δ_C 157.3) carbon. This was confirmed by the CIGAR correlation observed from the H-8' (δ_H 3.86) methyl protons to the C-3' (δ_C 157.3) carbon. Irradiation of the H-4' (δ_H 6.53) proton in a NOESY experiment enhanced both the H-8' and H-9' (δ_H 3.86 and 2.20, respectively) methyl protons positioning the 9'-methyl group on C-5' (δ_C 141.4). Finally, the H-9' (δ_H 2.20) methyl protons were irradiated, giving NOE enhancement of both the H-4' and H-6' (δ_H 6.53 and 5.89, respectively) aromatic protons, positioning H-6' adjacent to the 9'-methyl group. The C-4' and C-6' carbon assignments were confirmed by the CIGAR correlations observed from the H-9' (δ_H 2.20) methyl protons to C-4' and C-6' (δ_C 104.5 and 106.1, respectively) carbons. The C-2' position was located by the observed $^3J_{CH}$ CIGAR correlations from both the H-4' and H-6' (δ_H 6.53 and 5.89, respectively) aromatic protons to the C-2' (δ_C 110.0) carbon. Carbon C-1' was assigned using the $^2J_{CH}$ CIGAR correlations from the H-6' (δ_H 5.89) proton to the C-1' (156.3) carbon. The partial structure, ring C, for **6.9** was proposed as shown in **Figure 6.22**.

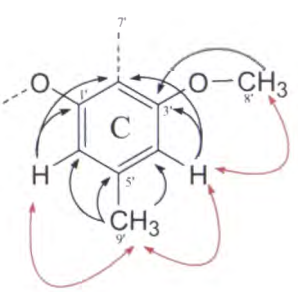

Figure 6.22: The key CIGAR (black) and NOESY (red) correlations for the proposed structure, ring C, of **6.9**.

An ether bridge connecting ring A to C was inferred from the ^{13}C chemical shift data for both carbons C-1 and C-1' (δ_C 134.7 and 156.3 respectively) in **6.9**. If a

carbonyl was involved in bridging the two rings then the chemical shift for both C-1 and C-1' carbons would be closer to those observed for sulochrin-2'-*O*-methyl ether (**6.7**) (δ_C 126.8 and 110.7, respectively). Additionally, no ketone carbonyl resonance was observed in the δ_C 180-200 region of the ^{13}C NMR spectrum.

In order to complete the structure, it was necessary to ascertain the substituent at C-2'. There were very weak CIGAR correlations from both the H-4' and H-6' (δ_H 6.53 and 5.89, respectively) aromatic protons to the C-7' (δ_C 168.3) carbonyl carbon, possibly associated with a carboxylic acid group. This was in keeping with the remaining atoms left to assign from the molecular formula. The working structure proposed for **6.9** is shown in **Figure 6.23**. The arbitrary numbering system shown is subsequently used for the NMR data shown in **Table 6.3**.

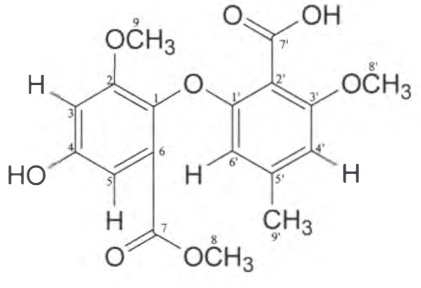

Figure 6.23: Proposed structure of **6.9**, with arbitrary numbering system as used for NMR data displayed in **Table 6.3**.

Table 6.3: The ^{1}H, ^{13}C, COSY, NOESY and CIGAR NMR data for asterric acid-3'-*O*-methyl ether (**6.9**) (CD_3OD).

Position.	^{13}C δ §	^{1}H δ ξ	COSY (NOESY)	CIGAR
1	134.7 (C)			
2	154.0 (C)			
3	104.5 (CH)	6.86 (1H, d, 1.5)	H-5	C-7, C-6, C-4, C-3, C-1
4	155.4 (C)			
5	107.6 (CH)	6.78 (1H, d, 1.5)	H-3	C-7, C-6, C-4, C-3, C-1
6	125.6 (C)			
7	166.4 (CO)			
8	51.3 (OCH_3)	3.73 (3H, s)		C-7
9	55.1 (OCH_3)	3.76 (3H, s)		C-2
1'	156.3 (C)			
2'	110.0 (C)			
3'	157.3 (C)			
4'	104.5 (CH)	6.53 (1H, s)	(H-9', H-8')	C-9', C-7'(vw), C-6', C-3', C-2'
5'	141.4 (C)			
6'	106.1 (CH)	5.89 (1H, s)	(H-9')	C-9', C-7'(vw), C-2', C-1'
7'	168.3 (CO)			
8'	55.0 (OCH_3)	3.86 (3H, s)	(H-4')	C-3'
9'	20.6 (CH_3)	2.20 (3H, s)	(H-6', H-4')	C-6', C-5', C-4'

§ ^{13}C NMR spectra recorded at 125 MHz in CD_3OD, chemical shift values δ ppm from $\mathbf{C}D_3OD$ at 49.3. ξ ^{1}H NMR spectra recorded at 500 MHz in CD_3OD (δ ppm from $C\mathbf{D}_3OD$ at 3.3) followed by number of protons, multiplicity and coupling constant (*J*/Hz).

A literature search[130,145] on the proposed structure for **6.9** returned no exact structural matches. A wider search profile was performed by replacing the 3'-*O*-methoxy group with 3'-OH, resulting in the identification of asterric acid (**6.10**).

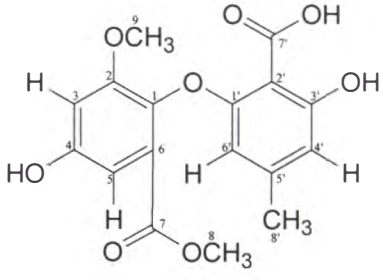

6.10

Asterric acid (**6.10**) was isolated from the culture medium of a new strain of fungus, *Aspergillus terrus* Thom., by Hassell *et al.*[221] Structural elucidation of this compound was achieved *via* chemical degradation experiments, where the evidence led to a likely structure based on their extensive knowledge of related compounds. No NMR data was reported in this paper. Asterric acid (**6.10**) was

later isolated by Hargreaves *et al.*,[219] from the mycelium extract of the fungus *Aspergillus* sp. recovered from leaf litter collected from Perth, Western Australia. The NMR data for **6.9** was compared to that reported in this subsequent isolation of asterric acid (**6.10**). The ^{13}C and ^{1}H NMR chemical shifts for the mutual atoms (excluding C-3') were in good agreement. Compound **6.9** was therefore tentatively assigned as the novel 3'-*O*-methyl ether derivative of asterric acid (**6.9**). It is interesting to note that although the NMR chemical shift assignments have been reported correctly, the structure of asterric acid (**6.10**) has been incorrectly drawn in the literature by both Hargreaves[219] (**6.11**) and Adeboya[222] (**6.12**). Hargraves was mistaken as to which carboxylic acid had been methylated, as no carbon data is reported for C-9', while Adeboya inexplicably drew the dimethyl ester.

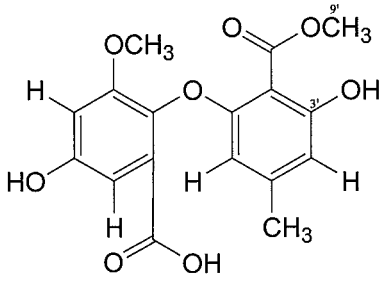

6.11

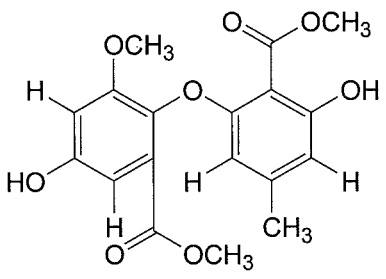

6.12

6.5.4: Structural elucidation of ***6.13***

The compound (**6.13**) was also isolated as a pale yellow powder (4.9 mg). HRESI mass spectrometry identified a $[M+Na]^+$ ion at *m/z* 399.1027 (calc. 399.1057) which led to the molecular formula $C_{19}H_{20}O_8$, corresponding to 10 DBE. Analysis of the ^{1}H NMR spectrum (**Figure 6.24**) revealed that this compound was structurally related to the previously isolated compound asterric acid-3'-*O*-methyl ether (**6.9**). Initial interpretation of the NMR data (**Figure 6.24** and **Figure 6.25**) identified the presence of four aromatic proton signals at δ_H 6.84, 6.77 6.52 and 5.88 (δ_C 107.5, δ_C 104.4, 104.8 and 106.2, respectively), one aromatic methyl

group at δ_H 2.22 (δ_C 20.4), and four methoxy groups at δ_H 3.88, 3.84, 3.76 and 3.72 (δ_C 51.3, 55.2, 55.3 and 51.4, respectively). The data differed from that observed for asterric acid-3'-*O*-methyl ether (**6.9**) by the addition of a methoxy signal at δ_H 3.72 (δ_C 51.4).

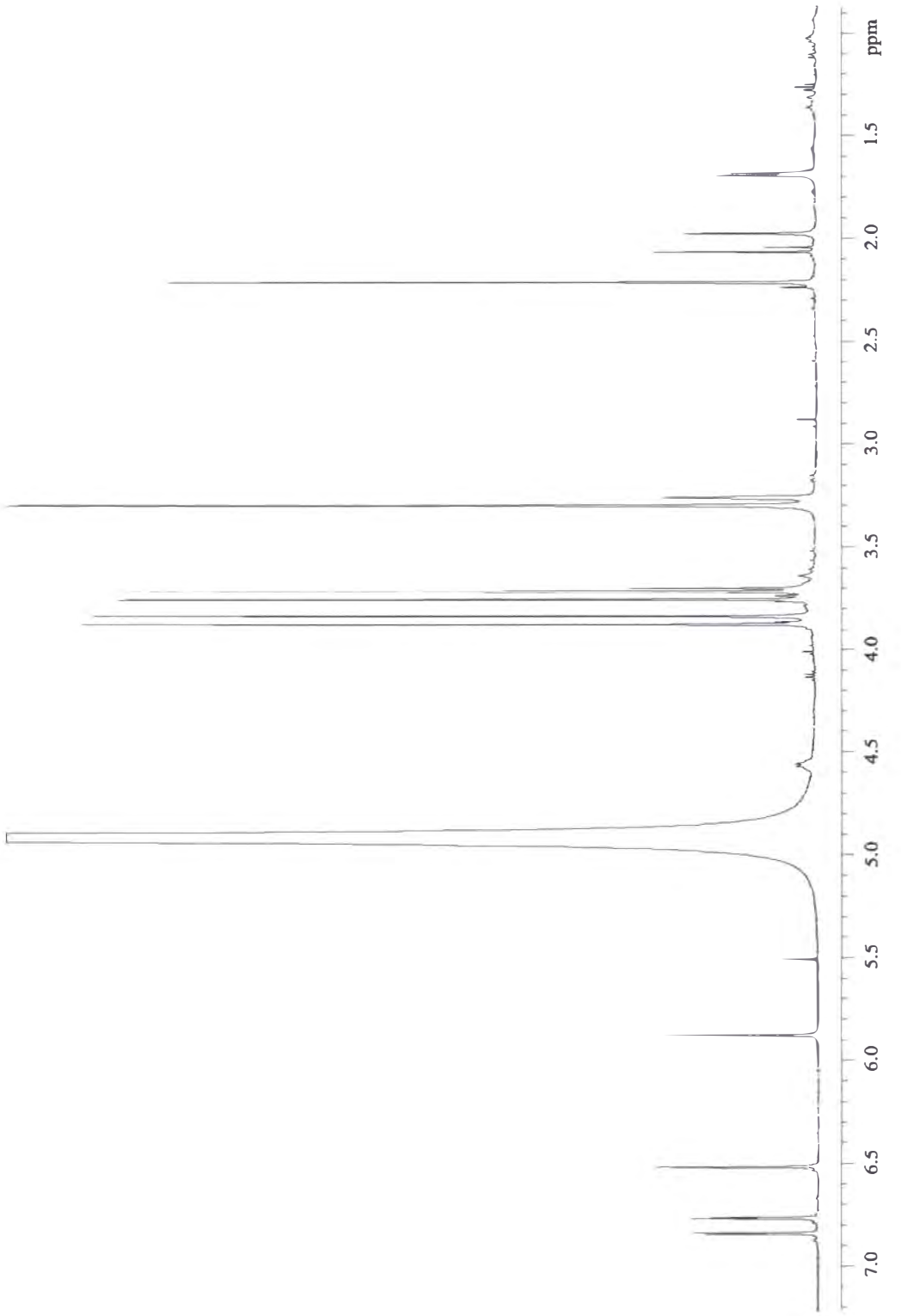

Figure 6.24: The ^{1}H NMR spectrum of compound **6.13** (CD_3OD).

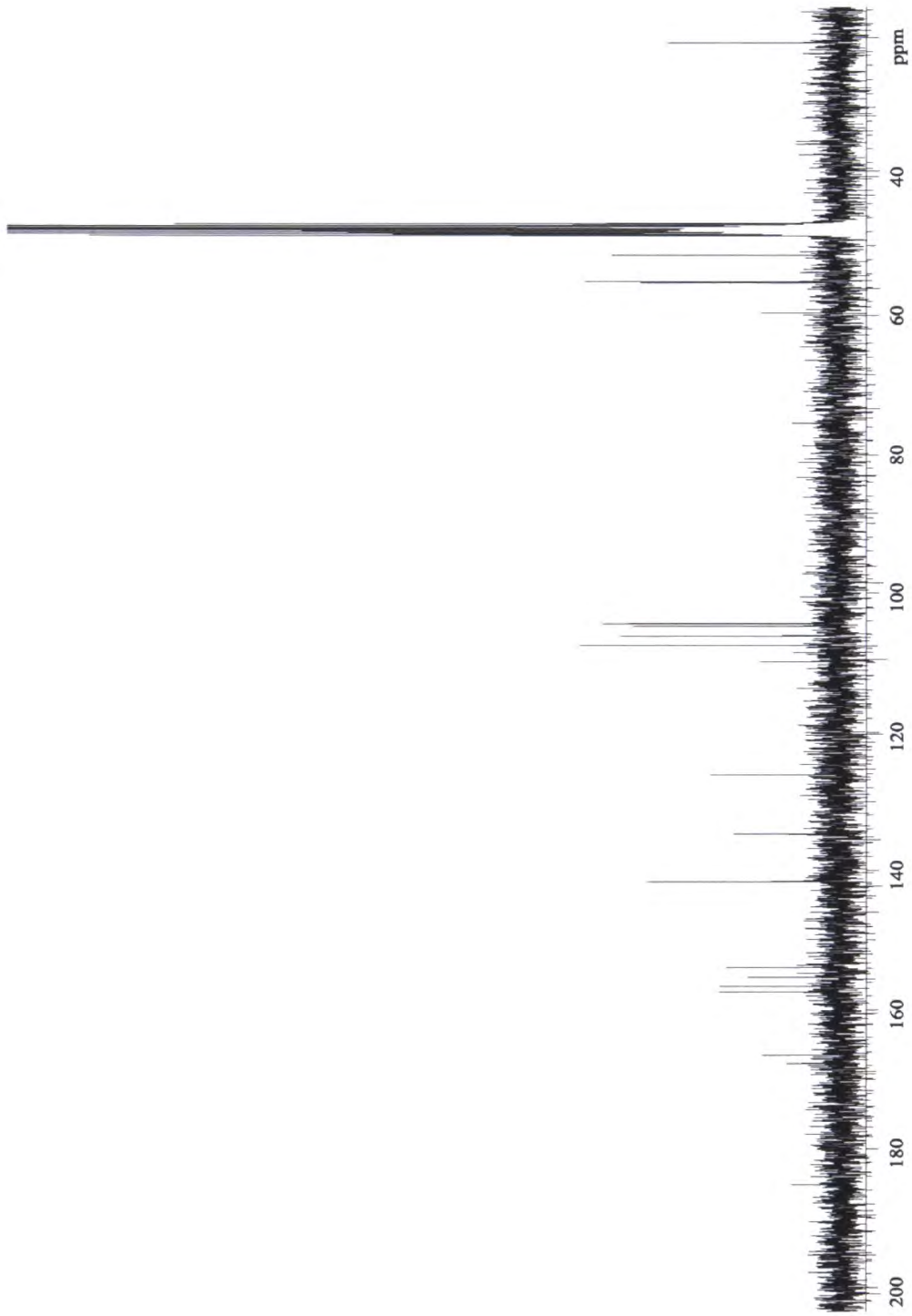

Figure 6.25: The ^{13}C NMR spectrum of compound **6.13** (CD_3OD).

As before, ring A was readily deduced by CIGAR correlations and chemical shift comparison with asterric acid-3'-*O*-methyl ether (**6.9**). The H-3 (δ_H 6.77) aromatic proton displayed COSY cross peak correlations to the H-5 (δ_H 6.84) proton, and CIGAR correlations to the C-1, C-2 and C-4 (δ_C 134.7, 153.9 and 155.3, respectively) carbons. The H-5 (δ_H 6.84) proton was CIGAR correlated to the C-1, C-4, C-6 and C-7 (δ_C 134.7, 155.3, 126.1 and 167.6, respectively) carbons. This combined data completed the connectivity from C-1 to C-7. Carbon C-4 was assigned as being substituted with an hydroxyl group, based on the chemical shift comparison with the C-4 (δ_C 155.4) carbon of asterric acid-3'-*O*-methyl ether (**6.9**). The first of the four methoxy groups was located at C-7, based on the CIGAR correlations observed from both of the H-5 aromatic and H-8 methyl (δ_H 6.84 and 3.76, respectively) protons to the C-7 (δ_C 167.6) carbonyl carbon. The second methoxy group was positioned at C-2 on the basis of the CIGAR correlations observed from both the H-3 aromatic and H-9 methyl (δ_H 6.77 and 3.72, respectively) protons to the C-2 (δ_C 153.9) aromatic carbon. The proposed partial structure, ring A, for **6.13**, is shown in **Figure 6.26**. This data suggested that the structural differences between **6.13** and asterric acid-3'-*O*-methyl-ether (**6.9**) were associated with the remaining atoms.

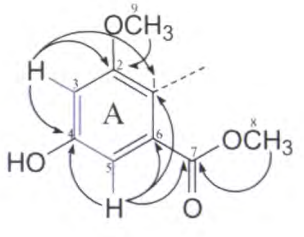

Figure 6.26: The key COSY (blue) and CIGAR (black) correlations used to construct the partial structure, ring A, of **6.13**.

Ring C was also assembled by careful comparison of both the ^{1}H NMR and CIGAR data. The connectivity of carbons C-1' to C-6' was established with CIGAR correlations from the H-4' (δ_H 6.52) aromatic proton to the C-2', C-3', C-5' and C-6' (δ_C 109.9, 156.6, 141.5 and 106.2 respectively) carbons, combined with the CIGAR correlations from the H-6' (δ_H 5.88) proton to the C-1', C-2', C-4' and C-5' (δ_C 157.4, 109.9, 104.8 and 141.5, respectively) carbons. The aromatic

methyl group was still positioned at C-5', based on the CIGAR correlation from the H-9' (δ_H 2.22) methyl protons to the C-5' (δ_C 141.5) carbon. The H-9' (δ_H 2.22) methyl protons were NOE enhanced when the H-4' and H-6' (δ_H 6.52 and 5.88, respectively) protons were sequentially irradiated suggesting that the H-9' methyl group was positioned between the H-4' and H-6' protons on C-5'. This was validated by the CIGAR correlations observed from the H-9' (δ_H 2.22) protons to both the C-4' and C-6' (δ_C 104.8 and 106.2, respectively) carbons. An additional NOESY enhanced signal corresponding to the resonance at δ_H 3.84 was observed when H-4' (δ_H 6.52) was irradiated, this combined with the CIGAR correlation from the H-8 (δ_H 3.84) methyl protons to the C-3' (δ_C 156.6) carbon, confirmed that a methoxy group (8'-methoxy) was still located at the C-3' carbon. However, irradiation of the H-8' (δ_H 3.84) methoxy protons, resulted in NOE enhanced signals associated with both the H-4' (δ_H 6.52) aromatic proton and the remaining unassigned methoxy protons (H-10', δ_H 3.88). The observed CIGAR correlation from the H-10' (δ_H 3.88) methoxy protons to the C-7' (δ_C 166.5) carbonyl carbon suggested that the acid group previously positioned at C-2' in asterric acid-3'-*O*-methyl ether (**6.9**), was now methylated. The ^{13}C chemical shift data for C-2' in both asterric acid-3'-*O*-methyl ether (**6.9**) and **6.13** were within 0.1 ppm of each other, validating the C-2' assignment. Therefore, the partial structure ring C, was proposed for **6.13** (**Figure 6.27**).

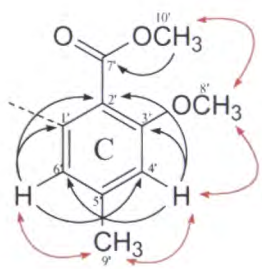

Figure 6.27: The partial structure, ring C, of **6.13**, with key CIGAR (black) and NOESY (red) correlations.

In order to complete the structure, it was necessary to ascertain the substituent at both C-1 and C-1'. One oxygen atom was left to assign as determined by the molecular formula. By direct comparison of the ^{13}C chemical shift data for both of the C-1 and C-1' carbons with those of asterric acid-3'-*O*-methyl ether (**6.9**), the

oxygen was assigned as an ether bridge linking ring A to C. This also satisfied the requirements of the DBE. The completed working structure for **6.13** is proposed in **Figure 6.28**.

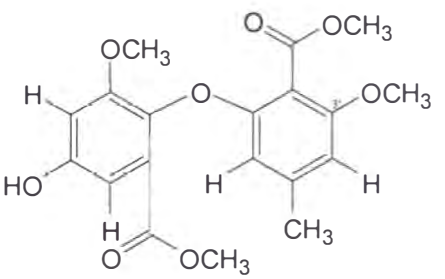

Figure 6.28: Proposed structure for isolated compound **6.13**.

A literature search[130,145] on the proposed structure for **6.13** gave no exact structural matches. A wider search profile was again performed by replacing the 3'-methoxy group with 3'-OH. This resulted in the identification of methyl asterrate (**6.14**), a compound previously reported from the fungus *Oospora sulphure ochrace* by Natori *et al.*[223] Methyl asterrate (**6.14**) was subsequently isolated by Hargreaves *et al.* from the EtOAc extract of an *Aspergillus* sp. fungus.[219] As the spectral data previously reported by Natori did not unambiguously define the substitution pattern of the phenyl rings, Hargreaves undertook single-crystal X-ray diffraction studies to confirm the structure.[219]

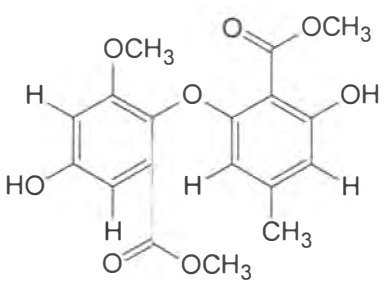

6.14

The isolated compound **6.13** was tentatively named methyl asterrate-3'-*O*-methyl ether. The arbitrary numbering system used for the NMR data (**Table 6.5**) is shown in **Figure 6.29**.

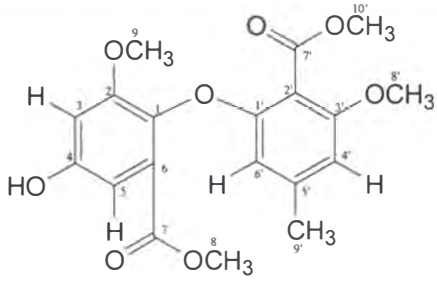

Figure 6.29: Numbering system assigned to methyl asterrate-3'-*O*-methyl ether (**6.13**) used in **Table 6.4**.

Table 6.4: The ^{1}H, ^{13}C, COSY, NOESY and CIGAR NMR data for methyl asterrate-3'-*O*-methyl ether (**6.13**) (CD_3OD).

Position	$^{13}C\ \delta$ §	$^{1}H\ \delta$ ξ	COSY (NOESY)	CIGAR
1	134.7 (C)			
2	153.9 (C)			
3	104.4 (CH)	6.77 (1H, d, 1.5)	H-5	C-5, C-4, C-2, C-1
4	155.3 (C)			
5	107.5 (CH)	6.84 (1H, d, 1.5)	H-3	C-7, C-6, C-4, C-3, C-1
6	126.1 (C)			
7	167.6 (CO)			
8	55.3 (OCH_3)	3.76 (3H, s)		C-7
9	51.4 (OCH_3)	3.72 (3H, s)		C-2
1'	157.4 (C)			
2'	109.9 (C)			
3'	156.6 (C)			
4'	104.8 (CH)	6.52 (1H, s)	(H-9', H-8')	C-9', C-6', C-5', C-3' C-2'
5'	141.5 (C)			
6'	106.2 (CH)	5.88 (1H, s)	(H-9')	C-9', C-5', C-4' C-2', C-1'
7'	166.5 (CO)			
8'	55.2 (CH_3)	3.84 (3H, s)	(H-10', H-4')	C-3'
9'	20.7 (CH_3)	2.22 (3H, s)	(H-6', H-4')	C-6', C-5', C-4'
10'	51.3 (OCH_3)	3.88 (3H, s)	(H-8')	C-7'

§ ^{13}C NMR spectra recorded at 125 MHz in CD_3OD, chemical shift values δ ppm from CD_3OD at 49.3. ξ ^{1}H NMR spectra recorded at 500 MHz in CD_3OD (δ ppm from CD_3OD at 3.3) followed by number of protons, multiplicity and coupling constant (*J*/Hz).

6.5.5: Structural elucidation of ***6.15***

The compound (**6.15**) was isolated as a pale yellow oil (3.7 mg). HRESI mass spectrometry identified a $[M+Na]^+$ ion at *m/z* 441.1164 (calc. 441.1162) which led to the molecular formula $C_{21}H_{22}O_9$, corresponding to 11 DBE and 42 Da more than methyl asterrate-3'-*O*-methyl ether (**6.13**). The ^{1}H NMR spectrum (**Figure 6.30**) revealed that this compound was again structurally related to the previously isolated compounds. Initial interpretation of the ^{1}H NMR data identified the presence of an additional singlet signal at δ_H 2.35 that integrated for three protons. This was paired with a carbon signal at δ_C 22.0 in the HSQC spectrum, allowing for the tentative assignment of an acetyl group. The remaining spectral features were identical with those reported for methyl asterrate-3'-*O*-methyl ether (**6.13**) (see **Table 6.6**).

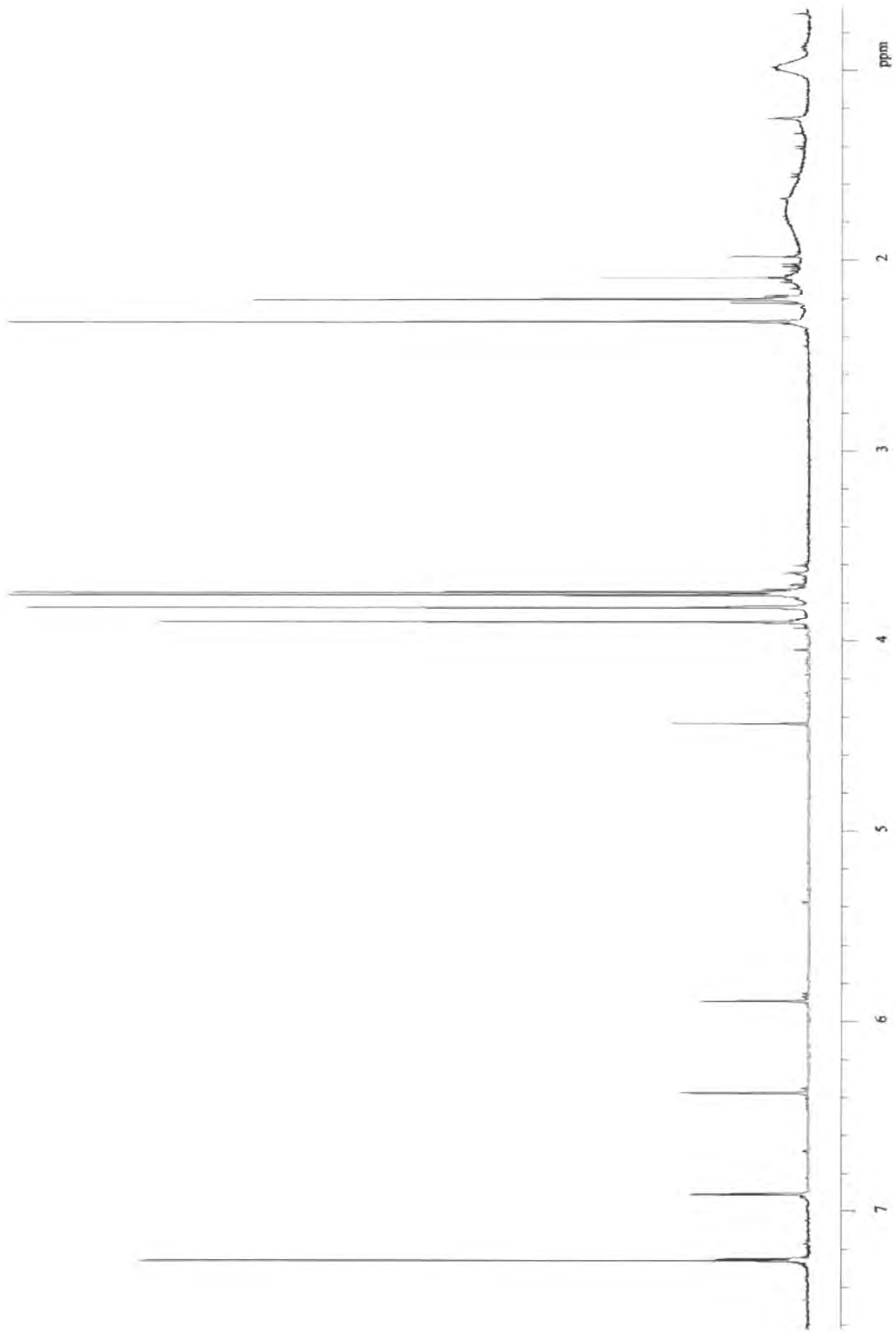

Figure 6.30: The ^{1}H NMR spectrum of compound **6.15** ($CDCl_3$).

As with the previously isolated compounds, ring C was easily deduced by CIGAR correlations and chemical shift comparisons with methyl asterrate-3'-*O*-methyl ether (**6.13**). The substitution pattern of the aromatic ring was confirmed with NOESY experiments. These consisted of irradiation of the H-9' (δ_C 2.22) methyl protons which NOE enhanced the signals corresponding to both the H-4' and H-6' (δ_H 5.94 and 6.42, respectively) aromatic protons, while irradiation of the H-8' (δ_H 3.86) methoxy methyl protons resulted in the NOESY enhancement of both the H-4' and H-10' (δ_H 5.95 and 3.94) protons. This NMR data suggested that ring C was identical to that of methyl asterrate-3'-*O*-methyl ether (**6.13**) and this partial structure for **6.15** is proposed in **Figure 6.31**.

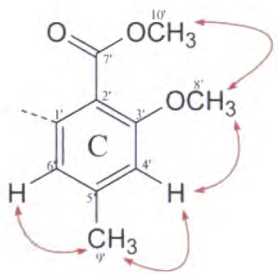

Figure 6.31: The proposed partial structure, ring C, for **6.15** with important NOESY (red) correlations.

The data suggested that the additional signal observed in the NMR data must be associated with ring A. The H-3 (δ_H 7.24) aromatic proton displayed COSY cross peak correlations to H-5 (δ_H 6.94, $J_{3,5}$ = 1.5 Hz) and CIGAR correlations to the C-1, C-2 and C-4 (δ_C 140.7, 154.0 and 147.8, respectively) carbons, confirming connectivity from C-1 to C-5.

The C-2 carbon methoxy substitution was confirmed by CIGAR correlations from both the H-3 (δ_H 7.24) aromatic and H-9 (δ_H 3.80) methoxy protons to the C-2 (δ_C 154.0) carbon, while the C-6 substitution was confirmed with the $^3J_{CH}$ CIGAR correlations observed from both the H-5 and H-8 (δ_H 6.94 and 3.76, respectively) protons to the C-7 carbonyl carbon at δ_C 165.2.

In order to complete the structure, the substituents at C-1, C-1' and C-4 had to be ascertained. Direct comparison of the ^{13}C NMR chemical shift data with methyl asterrate-3'-*O*-methyl ether (**6.13**) suggested that the ether linkage connecting

rings A and C through C-1 to C-1' was still present. This left assignment of the substituent at C-4. There was a upfield chemical shift associated with C-4 (δ_C 147.8) in **6.15** compared to that for methyl asterrate-3'-*O*-methyl ether (**6.13**) C-4 (δ_C 155.3) carbon. This suggested that the acetyl group associated with the H-10 (δ_H 2.35) methyl signal was attached at the C-4 position. This was confirmed by the CIGAR experiment as a correlation from the H-10 (δ_H 2.35) methyl protons to the C-11 (δ_C 169.2) carbonyl carbon was observed. Therefore the structure for the isolated compound **6.15** was proposed as the acetyl derivative of **6.13** (**Figure 6.32**).

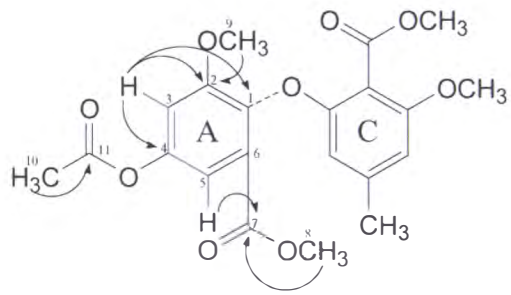

Figure 6.32: The proposed structure of **6.15**, with key COSY (blue lines) and CIGAR (black arrows) correlations.

A literature search,[130,145] was performed on the proposed structure for the isolated compound **6.15** which resulted in no exact matches. Therefore, this compound was tentatively named as the novel 4-*O*-acetyl-3'-*O*-methyl ether derivative of methyl asterrate (**6.15**).

The arbitrary numbering assignment for **6.15** used in **Table 6.5** is shown in **Figure 6.33**.

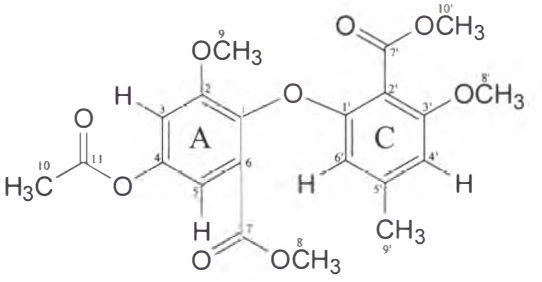

Figure 6.33: Numbering system assigned for methyl asterrate-4-*O*-acetyl-3'-*O*-methyl ether (**6.15**) as used in **Table 6.5**.

Table 6.5: The NMR data for methyl asterrate-4-*O*-acetyl-3'-*O*-methyl ether (**6.15**) ($CDCl_3$).

Position	^{13}C δ §	^{1}H δ ξ	COSY (NOESY)	CIGAR
1	140.7 (C)			
2	154.0 (C)			
3	115.6 (CH)	7.24 (1H, d, 1.5)	H-5	C-5, C-4, C-2, C-1
4	147.8 (C)			
5	110.8 (CH)	6.94 (1H, d, 1.5)	H-3	C-7, C-6, C-4, C-3, C-1
6	*			
7	165.2 (CO)			
8	52.4 (OCH_3)	3.76 (3H, s)		C-7
9	56.5 (OCH_3)	3.80 (3H, s)		C-2
10	22.0 (CH_3)	2.35 (3H, s)		C-11
11	169.2 (CO)			
1'	157.5 (C)			
2'	110.8 (C)			
3'	157.3 (C)			
4'	106.5 (CH)	5.94 (1H, s)	(H-9', H-8')	C-9', C-6', C-5', C-3', C-2'
5'	141.5 (C)			
6'	105.4 (CH)	6.42 (1H, s)	(H-9')	C-9', C-5', C-4', C-2', C1'
7'	166.9 (CO)			
8'	55.9 (CH_3)	3.86 (3H, s)	(H-10', H-4')	C-3'
9'	22.0 (CH_3)	2.22 (3H, s)	(H-6', H-4')	C-6', C-5', C-4'
10'	52.3 (OCH_3)	3.94 (3H, s)		C-7'

§ ^{13}C NMR spectra recorded at 125 MHz in $CDCl_3$. ^{13}C chemical shifts δ ppm from $CDCl_3$ (77.0). ξ ^{1}H NMR spectra recorded at 500 MHz. ^{1}H chemical shift values δ ppm from $CHCl_3$ (7.25) followed by number of protons, multiplicity and coupling constant (*J*/Hz). * No ^{13}C NMR chemical shift data recorded for this carbon.

6.5.6: Structural elucidation of **6.16**

The final compound **6.16** was isolated as a white powder (2.9 mg). HRESI mass spectrometry identified a $[M+Na]^+$ ion at *m/z* 454.1476 (calc. 454.1478) which led to the molecular formula $C_{22}H_{25}NO_8$, corresponding to 11 DBE. The ^1H NMR spectrum (**Figure 6.34**) revealed that this compound was structurally unrelated to the previously isolated compounds. Initial interpretation of the ^1H and HSQC NMR data revealed the presence of proton signals associated with an aromatic ring δ_H 8.38, 7.68 and 7.54 (δ_C 131.7, 134.8 and 129.5, respectively). These signals were a doublet, a triplet and a triplet, respectively, representing a pattern consistent with a mono-substituted aromatic ring system, two olefinic methine protons at δ_H 5.65 and 5.51 (δ_C 137.3 and 128.7, respectively), three methyl signals, one of which was a triplet at δ_H 1.01 (δ_C 14.5), the second, a vinyl at δ_H 1.79 (δ_C 5.8), and the third, a singlet methoxy group at δ_H 3.37 (δ_C 52.5); three oxymethines at δ_H 4.71, 4.58 and 4.53 (δ_C 69.6, 76.2 and 72.9, respectively) and a multiplet methylene signal at δ_H 2.13-2.24 (δ_C 22.2). The ^{13}C NMR data (**Figure 6.35**) confirmed the presence of additional functionalities. These consisted of three carbonyl carbons (two at δ_C 199.3 and 197.0, and a third was reminiscent of an amide carbonyl carbon at δ_C 169.1), two sp^2 quaternary carbons at δ_C 188.8 and 135.2, and two sp^3 quaternary carbons at δ_H 93.9 and 93.6.

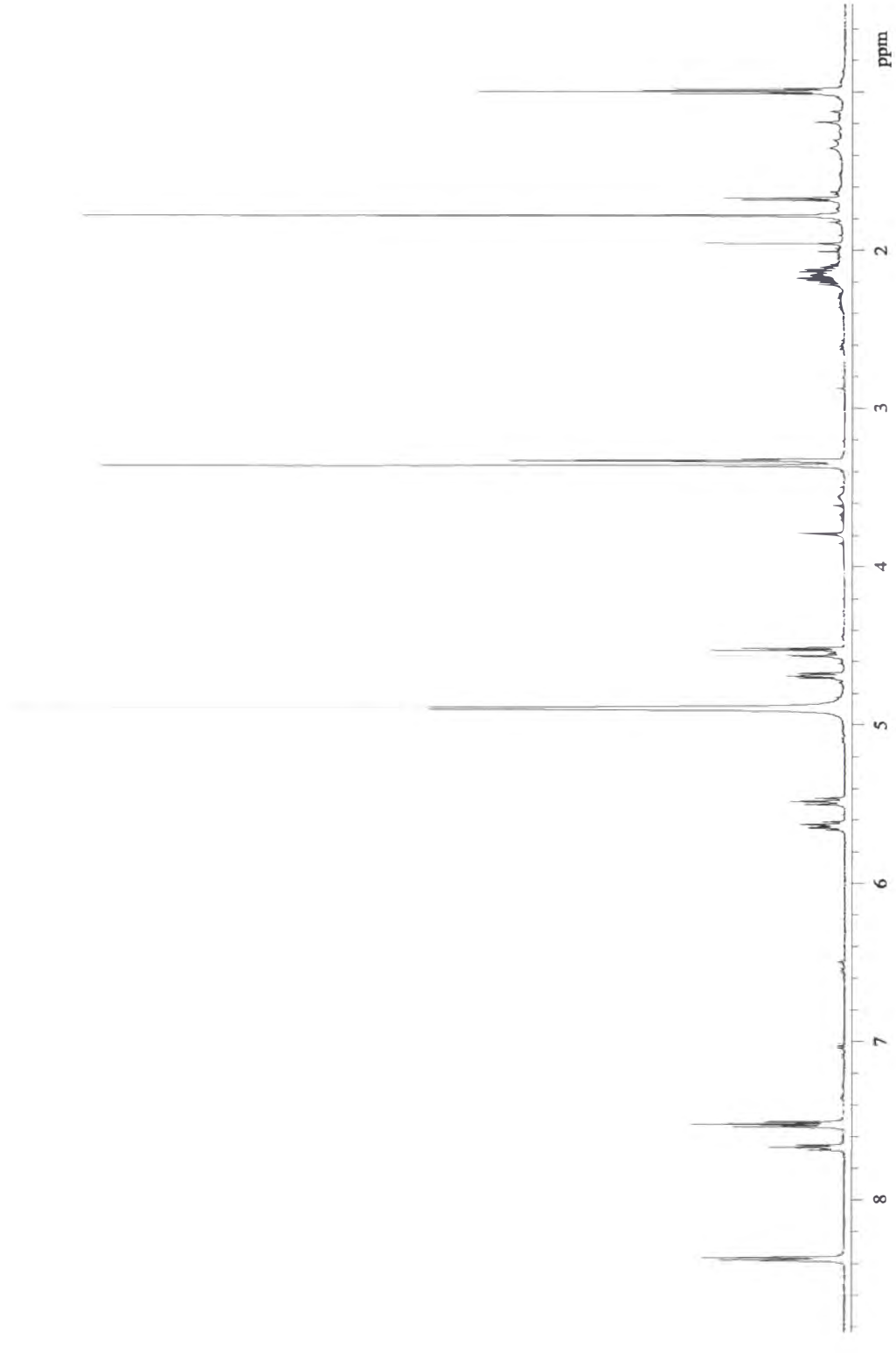

Figure 6.34: The ^{1}H NMR spectrum of compound **6.16** (CD_3OD).

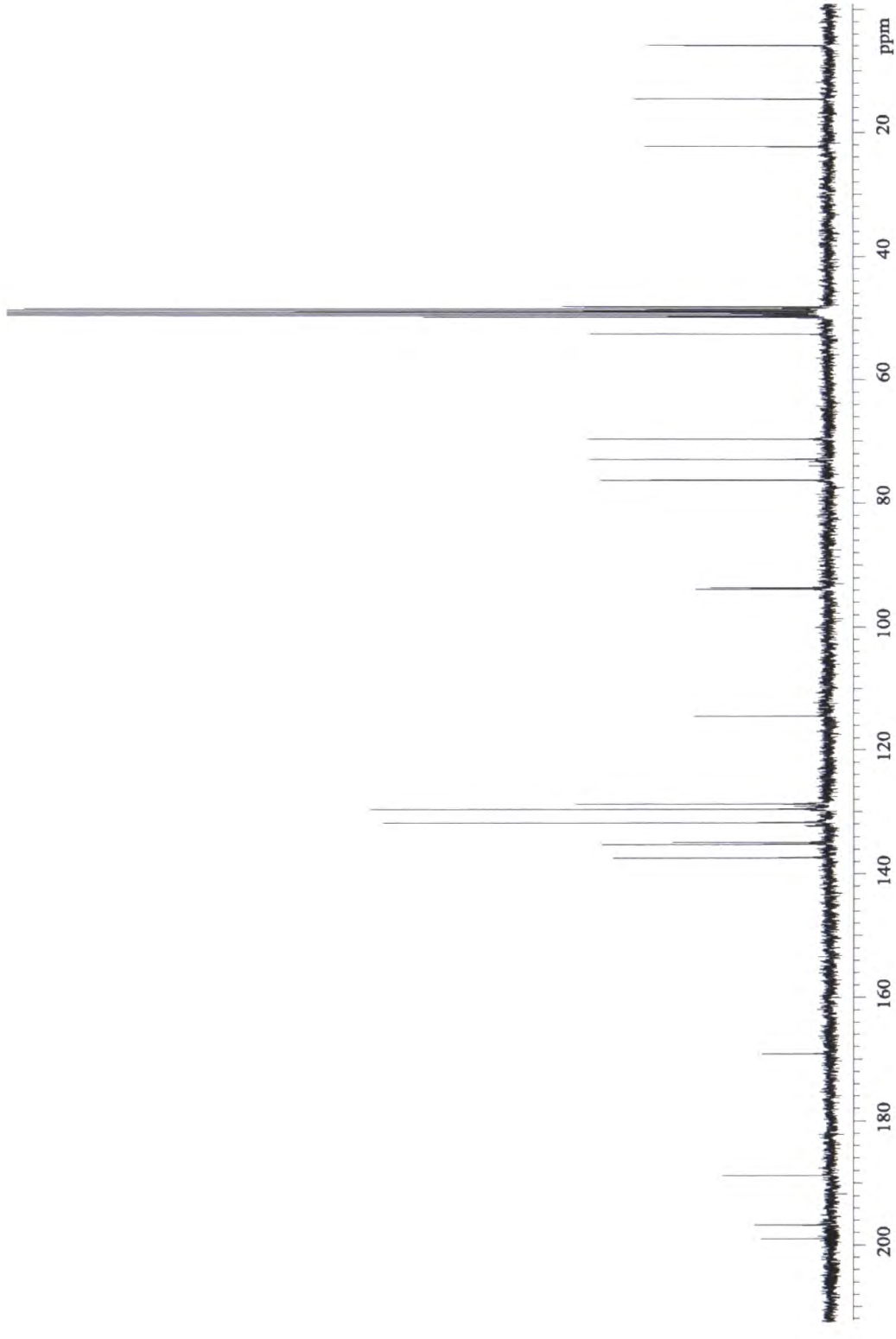

Figure 6.35: The ^{13}C NMR spectrum of compound **6.16** (CD_3OD).

The COSY, HSQC and CIGAR NMR experimental data were employed to assign connectivity and deduce the structure of **6.16**.

The starting point was the methylene protons at δ_H 2.13-2.24 (H-2), which displayed COSY cross correlations to both the H-1 (δ_H 1.01) methyl and the H-3 (δ_H 5.65) olefinic protons. This was reinforced by the observed CIGAR correlations from the H-1 (δ_H 1.01) methyl protons to both C-2 and C-3 (δ_C 22.2 and 137.3, respectively). CIGAR correlations from the H-4 (δ_H 5.51) olefinic proton to C-3, C-5 and C-6 (δc 137.3, 69.6 and 72.9, respectively), established the sequence C-3 to C-6, which was confirmed with the sequential COSY correlations from H-3 (δ_H 5.65) to H-4, H-5 and H-6 (δ_H 5.51, 4.71 and 4.53, respectively) (**Figure 6.36**).

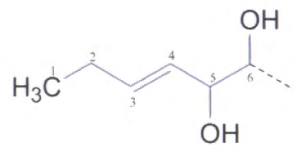

Figure 6.36: The partial structure, C-1 to C-6 of **6.16**, with key COSY correlations shown in blue.

The strong CIGAR correlation observed from the H-5 (δ_H 4.71) oxymethine proton to a quaternary carbon at δ_C 188.8 positioned this carbon adjacent to C-6 (C-7), but the chemical shift of this carbon was at first puzzling. The dilemma was solved with the assignment of C-8 and C-9. These were deduced *via* CIGAR correlations from the H-6 (δ_H 4.53) oxymethine proton to the clearly olefinic C-8 (δ_C 114.4) carbon, while the δ_H 1.79 protons from a methyl group located at the C-8 position (by CIGAR correlations from the C-20 methyl protons at δ_H 1.79 to the C-8 (δ_C 114.4) carbon) were correlated to both C-7 and C-9 (δ_C 188.8 and 199.3, respectively). The very low field carbon C-7 (δ_H 188.8) was considered in keeping with an oxygenated sp^2 carbon at the β position of an α,β-unsaturated carbonyl system (**Figure 6.37**).

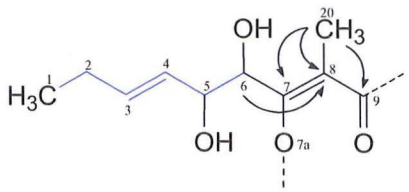

Figure 6.37: The assignment of C-1 to C-9, including the methyl group at C-20, with key CIGAR correlations (black).

The sequence of carbons C-9 to C-13 and C-22 was defined *via* CIGAR correlations from the H-11 (δ_H 4.58) oxymethine proton (see **Figure 6.38**). This included correlations to three carbonyl carbons, two at δ_C 199.3 and 197.0 (C-9 and C-13, respectively) while the third, consistent with that of an amide carbonyl, was at δ_C 169.1 (C-22), as well as to two sp^3 quaternary carbons at δ_C 93.6 and 93.9 (C-10 and C-12, respectively). The methyl protons associated with a methoxy group at δ_H 3.37 were positioned at C-12 by the CIGAR correlation from the H-21 (δ_H 3.37) methyl protons to the C-12 (δ_C 93.9) carbon (**Figure 6.38**).

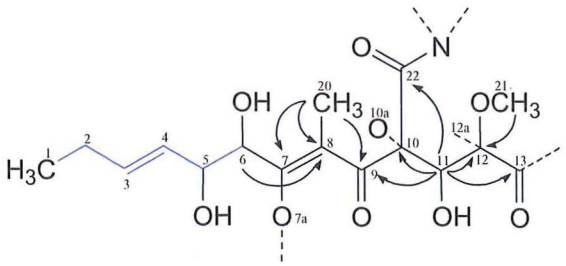

Figure **6.38**: The assignment of partial structure C-1 to C-13 of **6.16**, including the C-21 methoxy and C-22 amide carbonyl groups. The key CIGAR correlations are shown in black.

The aromatic ring, incorporating carbons C-14 to C-19, was established *via* observed CIGAR and COSY correlations, and also from coupling constants extracted from ^{1}H NMR data. This unit was then joined to the sequence as the $^3J_{CH}$ CIGAR correlations were observed from both the H-19 and H-15 (δ_H 8.38) aromatic protons to the C-13 (δ_C 197.0) carbonyl carbon. The aromatic carbon C-14 was located by the CIGAR correlation from both aromatic protons H-16 and

H-18 (δ_H 7.54) to the C-14 (δ_C 135.2) carbon. The partial structure for **6.16** was proposed as shown in **Figure 6.39**.

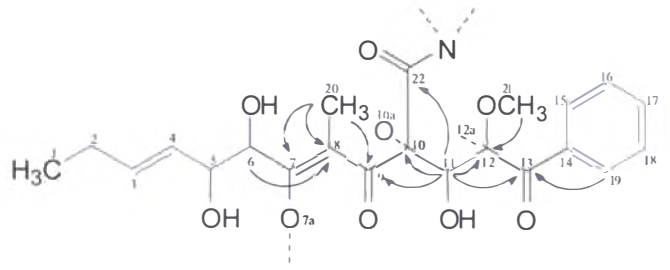

Figure 6.39: The proposed partial structure for **6.16**, with key COSY (blue) and CIGAR (back) correlations. An arbitrary numbering system has been assigned to the structure to aid structural elucidation.

This left positions 7a, 10a and 12a to assign. The partial structure requires nine degrees of unsaturation, however, the molecular formula requires 11 degrees of unsaturation, however one proton is left to assign. Therefore, the 7a and 10a oxygens were postulated to be the same, thus forming a five-membered furanone ring system. This assignment was confirmed after close examination of the CIGAR data. A very weak correlation was observed from the H-6 (δ_H 4.53) oxymethine proton to the C-10 (δ_C 93.6) sp^3 carbon. This $^4J_{CH}$ correlation could only exist if a five-membered ring was present, linking C-7 to C-10 and accounting for the 10th degree of unsaturation.

Carbon C-12 had to be quaternary, as defined by both the ^{13}C and HSQC NMR data. As no further carbon atoms were left to assign, position 12a was connected to N-1, forming a lactam ring. This accounted for the final proton assignment and the 11th degree of saturation. All atoms were now assigned and the complete structure for **6.16** was proposed (**Figure 6.40**).

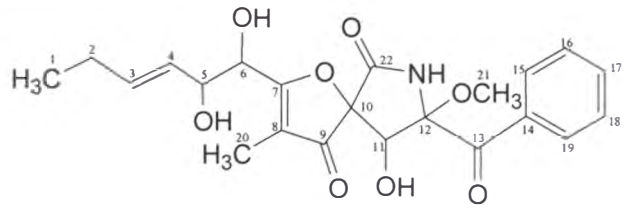

Figure 6.40: The proposed structure of **6.16**. This arbitrary numbering assignment is used in **Table 6.6**.

Table 6.6: The ^{1}H, ^{13}C, COSY and CIGAR NMR data for compound **6.16** (CD_3OD).

Position	$^{13}C\ \delta^{\S}$	$^{1}H\ \delta^{\xi}$	COSY	CIGAR
1	14.5 (CH_3)	1.01 (3H, t, 7.5)	H-2	C-3, C-2
2	22.2 (CH_2)	2.13-2.24 (2H, m)	H-1, H-3	C-4, C-3, C-1
3	137.3 (CH)	5.65 (1H, d, t, 7.0, 10.5)	H-4, H-2	C-5, C-4, C-2, C-1
4	128.7 (CH)	5.51 (1H, t, 10.5)	H-5, H-3	C-6, C-5, C-3, C-2
5	69.6 (CH)	4.71 (1H, t, 8.5)	H-6, H-4	C-7, C-6, C-4, C-3
6	72.9 (CH)	4.53 (1H, d, 6.5)	H-5	C-10(vw), C-8, C-7, C-5, C-4
7	188.8 (C)			
8	114.4 (C)			
9	199.3 (CO)			
10	93.6 (C)			
11	76.2 (CH)	4.58 (1H, s)		C-22, C-13, C-12, C-10, C-9
12	93.9 (C)			
13	197.0 (CO)			
14	135.2 (C)			
15	131.7 (CH)	8.38 (1H, d, 7.5)	H-16	C-19, C-17, C-13
16	129.5 (CH)	7.54 (1H, t, 7.5)	H-17, H-15	C-18, C-14,
17	134.8(CH)	7.68 (1H, t, 8.0)	H-18, H-16	C-19, C-15
18	129.5 (CH)	7.54 (1H, t, 7.5)	H-19, H-17	C-19, C-16
19	131.7 (CH)	8.38 (1H, d, 7.5)	H-18	C-17, C-15, C-13
20	5.8 (CH_3)	1.79 (3H, s)		C-9, C-8, C-7
21	52.5 (OCH_3)	3.37 (3H, s)		C-12
22	169.1 (CO)			

§ ^{13}C NMR spectra recorded at 125 MHz in CD_3OD. ^{13}C chemical shifts δ ppm from $\mathbf{C}D_3OD$ (49.3). ξ ^{1}H NMR spectra recorded at 500 MHz. ^{1}H chemical shift values δ ppm from $C\mathbf{H}_3OD$ (3.3) followed by number of protons, multiplicity and coupling constants (*J*/Hz).

A literature search[130,145] on the structure proposed for **6.16** identified this compound as pseurotin A, shown in **Figure 6.41** numbering assignment consistent with that reported in the literature. Pseurotin A (**6.16**), an antimicrobial secondary metabolite was isolated from the culture filtrates of *Pseudeurotium ovalis* STOLK

by Bloch *et al.*[211] The structure was determined from spectral data, chemical transformations and by X-ray analysis of the dibromo derivative.[212]

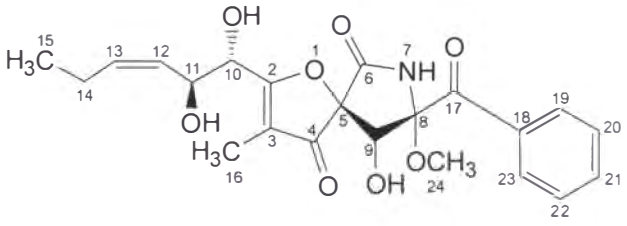

Figure 6.41: Numbering assignment and relative stereochemistry for the reported compound pseurotin A (**6.17**).[211-213]

However, direct comparison of the reported ^{13}C NMR data[213] with that obtained from the *Ulocladium* sp. (WS132) metabolite disclosed inconsistencies in assignments for carbons at C-2 and C-6. Reported data places C-2 at δ_C 167.3 and C-6 at δ_C 187.7 in the ^{13}C NMR spectrum, while C-2 and C-6 are assigned as δ_C 188.8 and 169.1, respectively, for the isolated compound. Although the ^{13}C NMR spectra were obtained in different solvents, $CDCl_3$ for the reported compound and CD_3OD for the isolated compound, carbons C-2 and C-6 were unambiguously assigned by CIGAR correlations from the H-11 and H-10 (δ_H 4.71 and 4.53, respectively) oxymethine protons to the C-2 (δ_C 188.8) quaternary carbon, while the C-6 carbon was assigned from an important CIGAR correlation from the H-9 (δ_H 4.58) oxymethine proton to the C-6 (δ_C 169.1) carbonyl carbon. On this basis, the literature assignments for C-2 and C-6 should be reversed.

The double bond stereochemistry for C-3/C-4 was established from the relative magnitude of the coupling constant between H-3 and H-4 protons. The coupling constant ($J_{3,4}$ = 10.5 Hz) was consistent with a (*Z*) configuration.[224] The relative stereochemistry of pseurotin A (**6.16**) was determined to be the same as that reported for pserotin A (**6.17**) on the basis that the chemical shift data, coupling constants (**Table 6.4**) and optical rotation data ($[\alpha]_D^{20}$ = -7° (*c* 0.5 MeOH)) closley matched that reported in the literature.[211,213] The absolute stereochemistry

of pseurotin A (**6.17**) was determined in the literature by X-ray crystal structure analysis of the 12,13-dibromopseurotin A derivative.[212]

Table 6.7: Comparison of the ^{1}H NMR chemical shift data for the isolated pseurotin A (**6.16**) (CD_3OD) and those reported for Pseurotin A (**6.17**) ($CDCl_3$).[214]

	Isolated pseurotin A (**6.16**)		Reported pseurotin A (**6.17**)	
Position	^{13}C δ §	^{1}H δ ξ	^{13}C δ †	^{1}H δ ‡
2	188.8 (C)		166.6 (C) ₸	
3	114.4 (C)		111.6 (C)	
4	199.3 (CO)		196.7 (CO)	
5	93 6 (C)		92.4 (C)	
6	169.1 (CO)		186.8 (CO) ₸	
8	93.9 (C)		91.1 (C)	
9	76.2 (CH)	4.58 (1H, s)	75.0 (CH)	4.41 (1H, s)
10	72.9 (CH)	4.53 (1H, d, 6.5)	72.0 (CH)	4.56 (1H, d, 3.8)
11	69.6 (CH)	4.71 (1H, dd, 6.5, 8.5)	68.3 (CH)	4.71 (1H, dd, 3.8, 8.8)
12	128.7 (CH)	5.51 (1H, dd, 8.5, 10.5)	128.4 (CH)	5.31 (1H, m)
13	137.3 (CH)	5.65 (1H, dt, 7.5, 11.0)	134.0 (CH)	5.62 (1H, dt, 11.3, 14.9)*
14	22.2 (CH_2)	2.13-2.24 (2H, m)	20.6 (CH_2)	2.1 (2H, m)
15	14.5 (CH_3)	1.01 (3H, t, 7.5)	14.1 (CH_3)	0.90 (3H, t, 7.0)
16	5.8 (CH_3)	1.79 (3H, s)	5.6 (CH_3)	1.65 (3H, s)
17	197.0 (CO)		196.4 (CO)	
18	135.2 (C)		133.6 (C)	
19	131.7 (CH)	8.38 (1H, d, 7.5)	130 2 (CH)	8.22 (1H, d, 7.2)
20	129.5 (CH)	7.54 (1H, t, 7.5)	128.4 (CH)	7.43 (1H, t, 7.5)
21	134.8(CH)	7.68 (1H, t, 7.5)	133.6 (CH)	7.57 (1H, t, 7.3)
22	129.5 (CH)	7.54 (1H, t, 7.5)	128.4 (CH)	7.43 (1H, t, 5.0)*
23	131.7 (CH)	8.38 (1H, d, 7.5)	130.2 (CH)	8.2-8.4 (1H, m)
24	52.5 (OCH_3)	3.37 (3H, s)	51.7 (OCH_3)	3.26 (3H, s)

§ ^{13}C NMR spectra recorded at 125 MHz in CD_3OD. ^{13}C chemical shifts δ ppm from $\mathbf{C}D_3OD$ (49.3). ξ ^{1}H NMR spectra recorded at 500 MHz. ^{1}H chemical shift values δ ppm from $C\mathbf{H}_3OD$ (3.3) followed by number of protons, multiplicity and coupling constant (*J*/Hz). † ^{13}C NMR spectra recorded at 100 MHz in $CDCl_3$. ^{13}C chemical shifts δ ppm from $\mathbf{C}DCl_3$ (77.0). ‡ ^{1}H NMR spectra recorded at 500 MHz. ^{1}H chemical shift values δ ppm from $C\mathbf{H}Cl_3$ (7.25) followed by number of protons, multiplicity and coupling constants (*J*/Hz). *Coupling constants reported for these protons do not match with those calculated from the ^{1}H NMR spectrum supplied in the online supporting information.[215] ₸These literature assignments should be revised on the basis of the CIGAR correlations observed in the assignment of structure **6.16**.

6.6: Biological Activity

All isolated compounds were subjected to the in-house anti-tumour assay system to assess their biological activity (P388), the results of which are shown in **Table 6.8**.

Table 6.8: The P388 activity for the compounds isolated from the organic extract of WS132.

COMPOUND	ACTIVITY (IC_{50} μg/mL)
6.6	1.0
6.7	> 12.5
6.9	>12.5
6.13	11.4
6.15	1.9
6.16	8.0

6.7: Concluding Remarks

In this section the aim was to isolate and identify the compounds responsible for the biological activity (P388) observed in the crude extract of the fungal isolate *Ulocladium* sp. (WS132) isolated from the Antarctic marine sponge *Mycale acerata.*

Six compounds were isolated as a direct result of bioassay-guided fractionation (HPLC microtitre plate P388 assay) of the crude extract. These included the three previously reported compounds trypacidin (**6.6**),[209,210] sulochrin-2'-*O*-methyl ether (**6.7**)[219,220] and pseurotin A (**6.16**),[211-216] along with the previously unreported compounds asterric acid-3'-*O*-methyl ether (**6.9**), methyl asterrate-3'-*O*-methyl ether (**6.13**) and methyl asterrate-4-*O*-acetyl-3'-*O*-methyl ether (**6.15**).

All the purified compounds were isolated by successive chromatographic steps. The initial reversed phase (C_{18}) flash column chromatography was followed by semi-preparative reversed phase (C_{18}) HPLC. Purity was assessed by analytical HPLC. Location of the biologically active 'peaks' of interest was maintained

throughout the purification process with the help of analytical reversed phase HPLC analysis.

Structural elucidation of all of the isolated compounds was achieved with the help of 1D and 2D NMR spectroscopic experiments, combined with high resolution mass spectrometry. The structural data obtained was directly compared to that reported in the literature. However, during the comparison of ^{13}C NMR chemical shift data published for pseurotin A (**6.15**) the assignment of carbons C-2 and C-6 were noted to be inconsistent with the experimental data obtained. The assignment made in the current work was consistent with data obtained independently by Ms Sonia van der Sar for the same compound isolated from the culture broth of a *Penicillium* sp. fungal isolate collected from a beach in Vancouver, Canada.[225] The chemical shift data from the NMR experiments unambiguously assigned these carbons.

Each of the purified compounds was submitted for biological activity assessment in-house. The compounds **6.6**, **6.13** **6.15** and **6.16** (IC_{50} of 1.0, 11.4, 1.9 and 8.0 μg/mL, respectively) were identified as being responsible for the biological activity located in the initial microtitre plate (P388) assay.

This body of work represents an expansion of the literature relating to the compounds isolated from the fungus *Ulocladium* sp. It also includes necessary corrections for structural data presented in previous publications.

6.8: Summary of Isolation

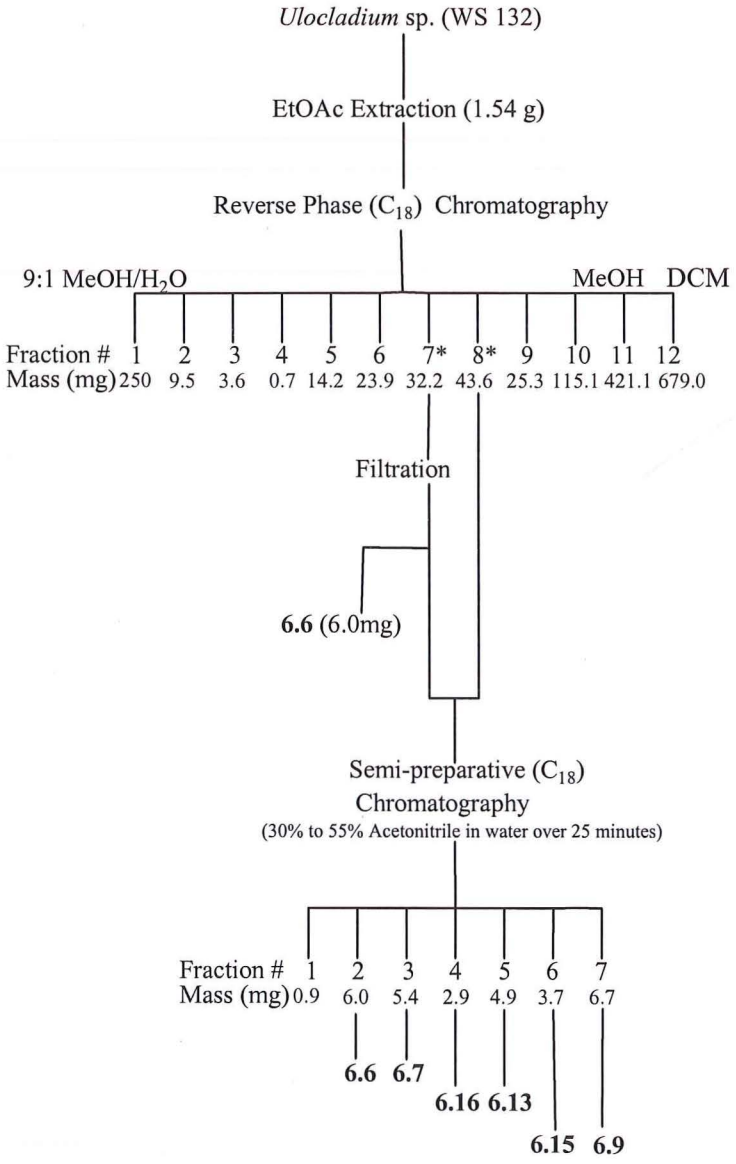

Scheme 6.1: Chromatographic purification summary of compounds isolated from the Antarctic marine sponge-derived fungus *Ulocladium* sp. *Fraction contains biologically active peak(s) of interest

CHAPTER 7

EXPERIMENTAL

7.1: General Methods

7.1.1: Nuclear Magnetic Resonance

The ^{1}H, 1DTOCSY, 2DTOCSY, COSY ROESY, NOESY, HSQC, and CIGAR NMR spectra were recorded on a Varian INOVA 500 NMR at 23 °C, operating at 500 MHz. The INOVA was equipped with a variable temperature and indirect broadband PFG (pulsed field gradient) 5 mm probe. The ^{13}C NMR spectra were recorded on a Varian UNITY 300 NMR spectrometer, at 23 °C, operating at 75 MHz. The UNITY was equipped with a variable temperature direct broadband 5 mm probe. Chemical shifts are expressed in parts per million (ppm) on the δ scale, and were referenced to the appropriate solvent peaks: $CDCl_3$ (0.1 μL pyridine)

referenced to $C\mathbf{H}Cl_3$ at δ_H 7.25 (^1H) and $\mathbf{C}HCl_3$ at δ_C 77.0 (^{13}C), CD_3OD referenced to $C\mathbf{H}_3OD$ at δ_H 3.3 (^1H) and $\mathbf{C}H_3OD$ at δ_C 49.3 (^{13}C) and DMSO-d_6 referenced to $CD_3(C\mathbf{H}D_2)SO$ at δ_H 2.60 (^1H) and $(CD_3)_2SO$ at δ_C 39.6 (^{13}C).

7.1.2: Mass Spectrometry

7.1.2.1: Electron Impact Mass Spectrometry

High Resolution Electron Impact Mass Spectra (HREIMS) were also obtained on a Kratos MS80RFA Mass Spectrometer, operating with a 4 kV accelerating potential, 70 eV, and a 250 ºC source temperature.

7.1.2.2: Electrospray Ionisation Mass Spectrometry

High Resolution Electrospray Ionisation Mass Spectra (HRESIMS) were obtained from a Micromass LCT spectrometer, with a probe voltage of 3200 V and temperature of 150 ºC. The nebuliser gas flow of 160 L/hr and desolvation gas flow of 520 L/hr, the source temperature was set at 80 ºC. The carrier solvent was 50 CH_3CN/H_2O at 20 μL/minutes (for direct injection mode). A 10 μL injection of sample was made from a 10 μg/mL solution.

Positive ESI mass spectra were recorded after addition of one of the following, formic acid, sodium iodide or caesium iodide to the sample prior to analysis. While negative ESI mass spectra were recorded after the addition of diethylamine to the sample.

7.1.2.3: Liquid Chromatography Electrospray Mass Spectrometry

Liquid Chromatography Mass Spectrometry (LCESIMS) samples were analysed with a Waters 2790 high pressure liquid chromatography (HPLC) system

equipped with a Waters photodiode array detector (PDA) coupled in parallel to a Micromass LCT mass spectrometer, as described above.

7.1.3: Chromatography

7.1.3.1: Flash Column Chromatography

All column chromatography was performed in glass columns or sintered glass funnels. Solvents used were of commercial grade distilled once in glass distillation apparatus, except for MeOH which was distilled twice. 'Flash' columns were run using positive N_2 (oxygen-free) pressure, while size exclusion columns were run at atmospheric pressure under gravity.

Reversed phase flash chromatography (RP) utilised Bakerbond (40 μm) octadecyl (C_{18}) packing. Samples were either dissolved in a minimum volume of solvent and loaded directly onto the column, or alternatively, adsorbed onto a plug of fresh C_{18} using a minimum volume of solvent which was removed under vacuum prior to the C_{18} plug being loaded onto the column. The standard elution profile consisted of column equilibration to 100 % H_2O, and then fractions were eluted with increasing concentrations of MeOH in steps of 10 % per fraction. Any material remaining on the column was washed off using combinations of MeOH and DCM (with TFA).

Size exclusion chromatography was carried out on Sephadex LH20 (Pharmacia Biotech AB) solid phase. Samples fractionated with Sephadex LH20 were dissolved in a minimal volume of solvent. Fractions were collected by automatic fraction collector LKB Bromma 2212 Helirac, based upon solvent volume.

Normal phase flash chromatography was performed on DIOL (40 μm APD) solid phase. Samples were either dissolved in a minimum volume of solvent and loaded directly onto the column, or alternatively, adsorbed onto a plug of fresh DIOL using a minimum volume of solvent which was removed under vacuum prior to the DIOL plug being loaded onto the column. The standard elution

profile consisted of column equilibration to 100 % Pet. ether, then fractions were eluted with increasing concentrations of DCM through to 100 % EtOAc in steps of 10 % per fraction. Any material remaining on the column was washed off using combinations of EtOAc, MeOH and water.

7.1.3.2: High Pressure Liquid Chromatography

Analytical High Pressure Liquid Chromatography (HPLC) was performed using a Shimadzu LC-10AD VP liquid chromatograph, with an SPD-M10A VP photodiode array detector. For reversed phase HPLC, a Phenomenex Prodigy C18 5-ODS (5μ, 250 x 4.6 mm) column was used with a flow rate of 1 mL/minute. The mobile phase solvents consisted of variable concentrations of CH_3CN (HPLC grade) and H_2O (Milli-Q). Some projects required the use of 0.05 % TFA in the H_2O.

All samples were filtered through 0.45 μm PTFE membrane filters before injection.

The standard gradient method comprised of the following solvent elution gradient; 2 minutes 10 % CH_3CN/H_2O, a linear gradient to 75 % CH_3CN/H_2O over 12 minutes, 75 % CH_3CN/H_2O isocratic for 10 minutes, a linear gradient to 100 % CH_3CN/H_2O over 2 minutes, 100 % CH_3CN/H_2O isocratic for 4 minutes then returned to 10 % CH_3CN/H_2O over 2 minutes, and finally re-equilibrated over an eight minute period.

Semi-preparative HPLC was performed on a Shimadzu LC-4A instrument equipped with a Hewlett Packard 3390A integrator. Reversed-phase HPLC chromatography was performed on Phenomenex Luna 5μ C18(2) (5μ, 250 x 10 mm)) column using a 5 mL/minute flow rate and variable concentrations of MeOH, CH_3CN (HPLC grade) and H_2O (milli-Q) with 0.05 % TFA added as required, as the mobile phase solvents.

7.1.4: Optical Rotation

Rotation values were obtained on a Perkin Elmer 341 polarimeter at 20 °C at a wavelength of 589 nm. The optical rotations were then calculated using the following equation:

$$[\alpha]_{\mathrm{D}}^{20} = \frac{\alpha}{LC}$$

Where L is the cell path length (dm) and C is the concentration (g/mL).

7.1.5: Media and Incubation Conditions

7.1.5.1: Fungal Isolation from Substrate

Sponge tissue was sliced into 5 mm cubes and placed onto the fungal-specific media which included oatmeal Emersons and Sabouraud agar. Media was incubated at 26 °C until cultures grew.

7.1.5.2: Difco™ Oatmeal Agar

Oatmeal agar is intended for the cultivating fungi, particularly for macrospore formation. Oatmeal is a source of nitrogen, carbon, protein and nutrients. Agar is the solidifying agent.

Approximate formula per litre consists of oatmeal (60.0 g) and agar (12.5 g).

Preparation of media was in accordance with the accompanying manufacturers directions.

7.1.5.3: Difco™ Emerson Agar

Emerson agar is used for culturing *Allomyces* and other fungi. The yeast provides a source of trace elements, vitamins and amino acids while the soluble starch provides starch for the hydrolysis, detoxification of metabolite byproducts and acts as a carbon source. Dipotassium phosphate is a buffer. Magnessium sulphate is a source of divalent cations and sulphate. Agar is the solidifying agent.

The agar (approximate per L) is made up of the following constituents: yeast extract 4.0 g, soluble starch 15.0 g, dipotassium phosphate 1.0 g, magnesium sulphate 0.5 g and agar 20.0 g.

Preparation of media was in accordance with the accompanying manufacturers directions.

7.1.5.4: Sabouraud Dextrose Agar in Seawater

Used for the cultivation isolation and identification of pathogenic fungi. This medium contains glucose and is especially suitable for dermatophytes. Its composition is 1/10 strength Dextrose agar (3.9 g Dextrose, 0.3 g Yeast, 9.0 g agar) in fresh filtered seawater (Cape Armitage, Antarctica, autoclaved).

Preparation of media was in accordance with the accompanying manufacturers directions.

7.1.5.5: ½ Sabouraud Dextrose Yeast (SDY) Broth Medium

The ½ SDY medium has been adapted by Nic Cummings, School of Biogical Sciences, University of Canterbury, as a general purpose medium used in the cultivation and isolation of fungi that grow more favourably in a liquid medium.

The medium consists of dextrose (10 g), polypeptone (5 g, BBL), yeast extract (1 g), distilled water (1 L).

Water (1 L) was boiled for 2 minutes, the ingredients were added and stired until dissolved. The medium solution was autoclaved at 121°C for 20 minutes. Medium was inoculated with spore suspension (10 mL) and incubated at 26°C for three weeks, or until visual inspection confirms that fungal growth is in the log phase.

7.1.5.6: Brown Rice Medium

The solid brown rice medium is an all purpose medium used for the cultivation and isolation of a variety of fungi. The Brown rice medium (Brown rice, 175 g; distilled water, 325 mL; K_2HPO_4, 0.25 g; yeast extract, 0.5 g) was prepared in square 2 L Nalgene® bottles. The mixture was then boiled in the microwave for 2-3 minutes, followed by sterilisation in the autoclave for 20 minutes at 121 °C. Medium was inoculated with 10 mL of spore suspension which was spread across the entire rice surface. Fungal samples were then incubated at 26 °C for three weeks. Visual inspection was used to determine when the growth cycle was at the log phase.

7.1.6: Biological Assays

7.1.6.1: The Anti-tumour assay

The anti-tumour assay[225] is the most sensitive assay for cytotoxicity. It consists of a 2-fold dilution series of the sample of interest incubated for 72 hours with P388 (murine leukaemia) cells. The concentration of sample required to reduce the P388 cell growth by 50 % (compared to control cells) is determined using the absorbance values obtained when the yellow MTT tetrazolium is reduced by

healthy cells to produce the purple coloured MTT formazan. The result is expressed as the IC_{50} (ng/mL).

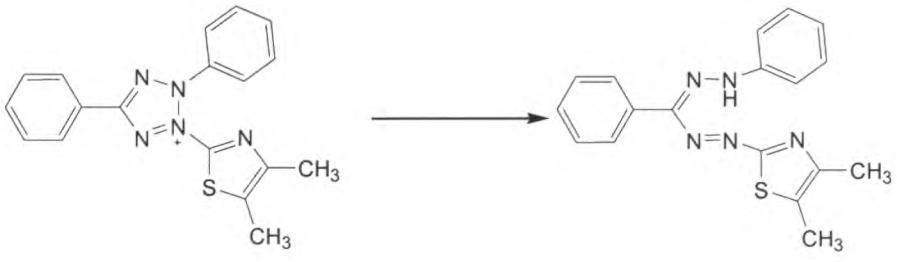

Tetrazolium salt MTT Formazan

Figure 7.1: Conversion of yellow MTT tetrazolium to purple MTT formazan by healthy P388 cells.

7.1.6.2: Microtitre Plate Collection/ P388 Assay

In order to identify the compounds responsible for the activity observed in the chemical pre-screening process, a small aliquot of the biologically active extract (250 μg) was subjected to analytical reversed phase (C18) HPLC chromatography and fractionated into a 96 well plate ('Master plate', 250 μL/well); flow rate was 1 mL/minute. Due to the inherent sensitivity of the polystyrene plates to high concentrations of acetonitrile (>75 %), the compounds that eluted from 25-30 and 31-35 minutes were collected in two vials, dried down and re-suspended in 250 µL of MeOH and added to wells 88 and 89 respectively. Eluant from the 'master plate' was transferred into dilution plates ('Daughter plates', 50 and 5 μL) and dried under vacuum in a centrifugal evaporator and submitted for P388 anti-tumour assay. Wells that possessed activity (C10-D11, coloured yellow) are related directly to the HPLC chromatogram (time in minutes), thus, activity can be assigned to the compound(s) that elute in that region of the chromatogram.

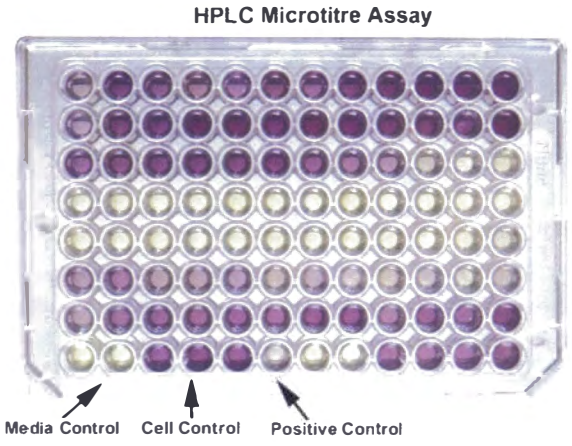

Figure 7.2: A 50 µL dilution microtitre daughter plate submitted for the P388 biological assay. Activity has been located in wells C10 to E11, represented by the yellow wells.

7.2: Work Described in CHAPTER 2

7.2.1: Extraction of New Zealand Marine Sponge Rhabderemia stelletta *(01MNP0729)*

Initial investigation of the sponge 01MNP0729 began by assessing of a portion of the crude extract in the P388 anti-tumour assay.

The frozen sponge sample (330 g) was thawed in MeOH (500 mL) and homogenised for three minutes. Before filtering through celite under vacuum, the residue was re-suspended and re-extracted a further three times using MeOH (3 × 300 mL), MeOH/DCM (1:1, 300 mL) and finally with DCM (300 mL). All filtrates were combined and the solvent was removed under vacuum. The crude extract was partitioned between EtOAc and H_2O (1:1, 500 mL). The organic and aqueous solvents were separated, collected and the solvent was removed from each fraction under vacuum to yield a thick yellow/brown and a thick brown gum respectively. Both fractions were analysed for biological activity using the P388 assay. Only the organic fraction (1.11 g) was cytotoxic (IC_{50} < 975 ng/mL). The aqueous layer (2.45 g) contained no significant cytotoxic activity (IC_{50} > 12500 ng/mL). Analysis of the organic extract by reversed phase (C_{18}) HPLC revealed a variety of polar and non-polar components.

7.2.2: Reversed Phase (C_{18}) Chromatography of the Organic Extract of the New Zealand Marine Sponge Rhabderemia stelletta *(01MNP0729)*

The EtOAc soluble fraction extract (1.11 g) was dissolved in a minimum volume of MeOH/DCM, adsorbed onto a plug of fresh C_{18} (2 g), and loaded onto a reversed phase flash chromatography column (30 mm x 300 mm) which had been packed with Bakerbond (C_{18}, 40 μm; 50 g) and equilibrated to 100 % H_2O. The column was eluted using a stepped solvent gradient of 100 % H_2O to 100 %

MeOH, increasing the MeOH concentration 10 % every fraction (25 mL). The column was finally eluted with combinations of DCM/MeOH (25 mL), increasing the DCM concentrations 20 % every fraction. The remaining material was washed from the column with MeOH/DCM (1:1, 0.1 % TFA, 100mL). Seventeen fractions were collected. All fractions were analysed for biological activity using the P388 assay. The biological activity was localised in fraction wjm12-312 which eluted with 4:1 DCM/MeOH (IC_{50} 2001 ng/mL, 79.4 mg). Fraction wjm12-312 was analysed by analytical reversed phase HPLC (C_{18}, no TFA) using microtitre plate collection P388 assay. The P388 activity indicated the peaks eluting between 27-32 minutes, were responsible for the observed activity.

7.2.3: Normal Phase (DIOL) Chromatography of Fraction wjm12-312

Fraction wjm12-312 (79.4 mg) was dissolved in a minimum volume of pet. ether and applied directly onto a normal phase (DIOL) flash chromatography column (15 mm x 150 mm, 15 g) equilibrated to 100 % pet. ether. The column was eluted with a stepped solvent gradient consisting of 100 % Pet. ether to 100 % DCM in 50 % steps, then 100 % DCM to 100 % EtOAc, increasing the EtOAc concentration 20 % every 7 mL collected. The column was finally eluted with combinations of 1:1 EtOAc/MeOH, 100 % MeOH (14 mL) and 9:1 MeOH/H_2O. A total of 12 fractions were collected. Odd numbered fractions were analysed for cytotoxic activity (P388). Fractions wjm12-701 to wjm12-703 (23.9 mg) were analysed by reversed phase (C_{18}) HPLC using the standard gradient method (see **Section 7.1.3**). Due to fraction complexity, further purification was deemed necessary in order to elucidate the biologically active compound(s).

7.2.4: Reversed Phase (C_{18}) Semi-preparative HPLC Chromatography of Fractions wjm12-701 to wjm12-703

Fractions wjm12-701 to wjm12-703 (30 mg) were combined in a minimum volume of MeOH and subjected to further purification by reversed phase (C_{18}) semi-preparative HPLC chromatography (Phenomenex Luna, 5μm C18, 250 x 10mm) using the conditions developed on the analytical HPLC column and scaled up by an appropriate factor (Flow rate 5 mL/minute, 91.5 % MeOH and 8.5 % H_2O, $\lambda = 230$ nm). Four fractions were collected as peaks eluted, and all fractions were analysed by ^1H NMR. The fractions that contained sufficient mass were subjected to the full suite of 2D NMR spectroscopic experiments and ESI mass spectrometry, leading to the elucidation of compounds **2.23** (6.5 mg), **2.24** (4.1 mg), **2.25** (2.8 mg) and **2.26** (2.5 mg) were elucidated. Purity was confirmed by re-injection on to the analytical reversed phase HPLC column. In order to obtain enough material for further structural elucidation (following degradation of compounds), the remaining portion of the frozen sponge material was processed.

7.2.5: Extraction and Chromatography of Remaining Sponge Material

The remainder of the frozen sponge sample (153 g) was exhaustively extracted using combinations of MeOH and DCM (4 x 500 mL) to yield 1.8 g of organic extract. The organic extract was partitioned between H_2O and EtOAc. The EtOAc fraction (450 mg) was re-dissolved in a minimum volume of EtOAc and adsorbed onto C_{18} (10 g). The solvent was removed under high vacuum and the adsorbed fraction loaded onto the top of a reversed phase (C_{18}) flash column (30 mm x 300 mm, 60 g) that was equilibrated to 100 % H_2O. The aqueous fraction from the partitioning was partially dried under vacuum and used as the first fraction of the column. The column was then eluted using a stepped solvent gradient from 100 % H_2O to 100 % MeOH, increasing the MeOH concentration 10 % every 30 mL, then 100 % MeOH to 100% DCM in 20 % steps from fractions 12 to 17. The column was finally eluted with 1:1 DCM/MeOH (0.05 %

TFA, 100 mL) followed by 100 % MeOH (0.05 % TFA, 100 mL). All fractions were examined for biological activity in the P388 assay. The activity was concentrated in fraction wjm12-1511 (IC_{50} = 5649 ng/mL, 30 mg).

7.2.6: Gel-permeation (LH-20) Chromatography of Fraction wjm12-1511

Fraction wjm12-1511 (30 mg) was subjected to further purification *via* LH-20 gel-permeation chromatography (40 g, 15 mm x 400 mm). The fraction was dissolved in a minimum volume of MeOH and applied directly to the top of the column. The column was eluted with 100 % MeOH. Nine fractions were collected (30 mL), and all fractions were analysed for biological activity. All nine fractions were found to be inactive. Analysis by re-injection on the analytical reversed phase (C_{18}) column confirmed the loss of activity as no peaks associated with the initial activity were detected. Further work on these fractions was abandoned at this point.

7.3: Work Described in CHAPTER 3

7.3.1: Extraction of Unidentified Antarctic Marine Sponge 02WM01-33

The frozen specimen 02WM01-33 (133 g) was thawed and extracted with combinations of MeOH and DCM (1:1, 500 mL). The extract was filtered through a bed of celite after homogenization and the solid material was re-suspended and extracted a further two times with MeOH and DCM (1:1, 250 mL). The solvent was removed under vacuum to yield a yellow extract (1.09 g). A small sample of this organic extract (250 µg) was analysed by reversed phase C18 HPLC microtitre plate analysis (P388 assay). Wells A4-A9 were identified to contain the biological activity (P388) as observed in the crude extract. This area of activity corresponded to the compounds eluting between 2.8 to 4.2 minutes in the HPLC chromatogram.

7.3.2: Reversed Phase (C_{18}) Flash Chromatography of the Organic Extract of 02WM01-33

The organic extract (1.1 g) was dissolved in a minimum volume of solvent (MeOH/DCM) and adsorbed onto a plug of fresh C_{18} (1 g) solid phase. The solvent was removed under vacuum and the C_{18} plug was loaded onto a reversed phase C_{18} flash chromatography column (30mm x 300 mm, 60 g), equilibrated to 100 % H_2O. Fractions were collected using the following solvent elution gradient system; 100 % H_2O to 100 % MeOH in steps of 10 % MeOH every 20 mL;, the remaining material was eluted from the column as fraction 12 (MeOH/DCM, 1:1). Odd numbered fractions were analysed by reversed phase (C_{18}) HPLC to identify the fractions that contained the compounds responsible for the activity as located by microtitre plate analysis (2.8 and 4.2 minutes). As a result fraction wjm20-203 was chosen for further purification.

7.3.3: Reversed Phase (C_{18}) Semi-preparative HPLC Chromatography of Fraction wjm20-203

Fraction wjm20-203 (32 mg) was further purified by reversed phase (C_{18}) semi-preparative HPLC chromatography (Phenomenex Luna, 5μm C18, 250 x 10mm) using a gradient solvent system of: 2minutes 5 % CH_3CN/H_2O, 20 minutes 36 % CH_3CN/H_2O, after the column was equilibrated back to 5 % CH_3CN/H_2O over 3 minutes; H_2O contained 0.05 % TFA (Flow rate 5 mL/minute, $\lambda = 230$ nm). Four fractions were collected as peaks eluted. Purity was confirmed by re-injection through the reversed phase (C_{18}) analytical HPLC. Fractions wjm20-203.2 (14 mg) and wjm20-203.4 (5.0 mg) were analysed by ^{1}H and ^{13}C NMR, and deemed to contain enough material for further 2D NMR experiments. HSQC and CIGAR NMR spectra were used to identify compounds **3.13** (14.0 mg) and **3.15** (5.0 mg).

7.4: Work Described in CHAPTER 4

7.4.1: Extraction of Antarctic Marine Sponge Suberites *sp. (02WM01-46)*

The frozen specimen 02WM01-46 (62 g) was thawed in a combination of MeOH/DCM (1:1, 500 mL). After substantial homogenisation (5 min) the extract was filtered through a bed of celite then the solid material was re-suspended and extracted twice with MeOH/DCM (1:1, 250 mL). The solvent was removed under reduced pressure to yield a green extract (248 mg). A small sample (250 μg) of the EtOAc soluble fraction of the organic extract was analysed by analytical reversed phase (C_{18}) HPLC chromatography microtitre plate analysis (see **Section 7.1.6.2**). The biological activity was attributed to the compound eluting at 7.8 minutes.

7.4.2: Reversed Phase (C_{18}) Vacuum Chromatography of the Organic Extract

The organic extract of 02WM01-46 (248 mg) was dissolved in a minimum volume of MeOH/DCM (3:1) and loaded onto a plug of fresh C_{18} solid phase (1.0 g). The solvent was removed under vacuum and the C_{18} plug was loaded onto a reversed phase (C_{18}) vacuum chromatography column (50 mm x 20 mm, 35 g) equilibrated to 100 % H_2O. The column was eluted with a solvent system consisting of 100 % H_2O to 100 % MeOH in steps of 10 % MeOH every 20 mL. The remaining material was eluted from the column as fraction 12 (MeOH/DCM, 1:1). Even numbered fractions were analysed by reversed phase (C_{18}) HPLC chromatography, to identify the fractions that contained the compounds responsible for the activity indicated by the P388 assay (microtitre plate). Based upon this analysis fractions wjm9-3204 to wjm9-3206 were combined for further purification.

7.4.3: Reversed Phase (C_{18}) Semi-preparative HPLC Chromatography of Combined Fractions wjm9-3204 to wjm9-3206

Fraction combination (wjm9-3204 to wjm9-3206) wjm9-3401 (12.4 mg) was subjected to further purification by reversed phase (C_{18}) semi-preparative HPLC chromatography (Phenomenex Luna, 5μm C18, 250 x 10mm) using a gradient solvent system of: 2 minutes 100 % H_2O, 15 minutes 36 % CH_3CN/H_2O, after which the column was equilibrated back to 100 % H_2O over 3 minutes (Flow rate 5 mL/minute, $\lambda = 254$ nm). Four fractions were collected as peaks eluted. Purity was confirmed by re-injection onto a reversed phase (C_{18}) analytical HPLC column. Fraction wjm9-3401.3 (4.5 mg) was analysed by ^{1}H and ^{13}C NMR, and deemed to contain enough material for further 2D NMR experiments. HSQC, CIGAR, Long range COSY and 1D NOSEY NMR spectra were used to elucidate compound **4.8** (4.5 mg).

7.5: Work Described in CHAPTER 5

7.5.1: Extraction of Antarctic Marine Sponge-derived Fungus Aspergillus *sp.(WS 76)*

The entire fungal culture WS 76 (500 mL) was homogenised for 5 minutes, ensuring complete maceration of the mycelial mat. This material was filtered through a bed of celite, re-suspended in EtOAc and repeatedly homogenised/extracted with 3 x 500 mL of EtOAc until no further colour was removed from culture. The organic extract was partitioned between EtOAc and H_2O (1:1, 500mL). The EtOAc soluble fraction (228.8 mg) was analysed by analytical reversed phase (C_{18}) HPLC chromatography (standard 10 % gradient, see **Experimental, Section 7.1.3**). Due to the modest level of P388 activity observed in the crude extract (IC_{50} 19750 ng/mL), 100 and 50 μL 'daughter plates' were submitted for P388 assay. Two areas of activity were identified, which corresponded to compounds eluting from 12.5 to 16.5 and 25 to 30 minutes of the HPLC chromatogram.

7.5.2: Normal Phase (DIOL) Chromatography of Organic Extract of Antarctic Marine Sponge-derived Fungus Aspergillus *sp. (WS 76)*

The EtOAc soluble fraction (228.8 mg) was dissolved in minimum volume of EtOAc and MeOH and adsorbed onto a solid plug of fresh DIOL (500 mg). The DIOL plug was loaded onto a DIOL flash chromatography column (15 mm x 150 mm, 15 g) equilibrated with 100 % pet. ether and was eluted with the following solvent gradient: 100 % pet. ether to 100 % DCM in 50 % steps, and then from 100 % DCM to 100 % EtOAc, increasing the EtOAc concentration 10 % every 5 mL collected for the next seven fractions. The column was finally eluted with combinations of 1:1 EtOAc/MeOH, 100 % MeOH (14 mL) and two fractions of 9:1 MeOH/H_2O. Seventeen fractions were collected. All fractions were analysed by reversed phase (C_{18}) analytical HPLC to locate the fractions that contained the active compounds as determined by microtitre plate analysis. Fractions wjm16-

703 (79 mg), wjm16-705 (15.6 mg), wjm16-708 (5.2 mg) and wjm16-710 (5.4 mg) were selected for further purification on this basis.

7.5.3: Reversed Phase (C_{18}) Semi preparative HPLC Chromatography of Fraction wjm16-703

Fraction wjm16-703 (78.6 mg) was subjected to further purification by reversed phase (C_{18}) semi-preparative HPLC chromatography (Phenomenex Luna, 5μm C18, 250 x 10mm) using a solvent system developed on the analytical HPLC and scaled by an appropriate factor (Flow rate 5 mL/min, 65 % CH_3CN and 25 % H_2O, λ = 330 nm). Two fractions were collected as peaks eluted, wjm16-703.1 and wjm16-703.2. Purity was confirmed by re-injection on to the analytical reversed phase HPLC using the standard 10 % gradient. Both fractions were analysed by ^{1}H NMR and contained sufficient mass suitable for COSY, HSQC and CIGAR 2D NMR spectroscopic experiments. Molecular mass was confirmed by ESI mass spectrometry; this led to the identification of compounds **5.32** (4.4 mg) and **5.34** (3.4 mg).

7.5.4: Reversed Phase (C_{18}) Semi-preparative HPLC Chromatography of Fraction wjm16-705

Fraction wjm16-705 (15.6 mg) was subjected to further purification by reversed phase (C18) semi-preparative HPLC chromatography (Phenomenex Luna, 5μm C18, 250 x 10mm) using an isocratic solvent system developed on the analytical HPLC and scaled by an appropriate factor (Flow rate 5 mL/minute, 65 % CH_3CN and 35 % H_2O, λ = 300 nm). Four fractions were collected as peaks eluted, wjm16-705.1 to wjm16-705.4. The purity of each fraction was confirmed by re-analysing *via* analytical reversed phase (C_{18}) HPLC using the standard 10 % gradient. All four fractions were analysed by ^{1}H NMR, to identify the fractions suitable for 2D NMR analysis. Fractions wjm16-705.2 (3.1 mg) and wjm16-705.3 (1.7 mg) were subsequently analysed by 2D NMR spectroscopy and mass spectrometry, where the compounds **5.35** (3.1 mg) were elucidated.

7.5.5: Reversed Phase (C_{18}) Semi-preparative HPLC Chromatography of Fraction wjm16-708

Fraction wjm16-708 (5.2 mg) contained predominantly one compound as indicated by reversed phase (C_{18}) analytical HPLC analysis. Purification of this fraction was achieved by reversed phase (C_{18}) semi-preparative HPLC chromatography (Phenomenex Luna, 5μm C18, 250 x 10mm) using an isocratic solvent system (Flow rate 5 mL/minute, 70 % CH_3CN and 30 % H_2O, λ = 300 nm). Two fractions were collected, however only fraction wjm16-708.1 (major peak of interest) contained enough material for further elucidation. Fraction purity was confirmed by re-injection onto an analytical reversed phase (C_{18}) HPLC column using the standard 10 % gradient. Compound **5.40** (3.3 mg) was structurally elucidated using 1D and 2D NMR spectroscopy and mass spectrometry.

7.5.6: Reversed Phase (C_{18}) Semi-preparative HPLC Chromatography of Fraction wjm16-710

Fraction wjm16-710 (2.5 mg) contained predominantly one compound by reversed phase analytical HPLC analysis. This fraction was subjected to further purification by reversed phase (C_{18}) semi-preparative HPLC chromatography (Phenomenex Luna, 5μm C18, 250 x 10mm) using an isocratic solvent system (Flow rate 5 mL/min, 70 % CH_3CN and 30 % H_2O, λ = 300 nm). One fraction was collected as the major peak eluted affording fraction wjm16-710.1. Purity was confirmed by analytical reversed phase (C_{18}) HPLC chromatography column using the standard 10 % gradient. The novel anthraquinone **5.41** (2.5 mg) was identified on the basis of HREI mass spectrometry, 1D and 2D NMR spectroscopy.

7.6: Work Described in CHAPTER 6

7.6.1: Extraction of Antarctic Marine Sponge-derived Fungus Ulocladium *sp. (WS 132)*

The solid rice culture (500 g) of WS 132 was extracted with solvent combinations consisting of EtOAc/DCM/MeOH (3:2:1, 500 mL). The extract was filtered through a bed of celite after homogenization; the solid material was re-suspended and extracted a further two times with the same solvent combinations. The solvent was removed under vacuum to yield a deep green extract (1.54 g).

7.6.2: Reversed Phase (C_{18}) Chromatography of the Organic Extract of the Marine Sponge-derived Fungus Ulocladium *sp (WS 76)*

A small portion of the organic extract was analysed by analytical reversed phase (C_{18}) HPLC chromatography. Fractions were collected in a microtitre plate (96 well). Dilution plates (100 and 50 µL) were submitted for biological activity assay (P388). The activity corresponded to the compounds eluting from 11.5 to 14.8 minutes.

The organic extract (1.54 g) was dissolved in a minimum volume of solvent (H_2O/MeOH, 9:1) and loaded onto a reversed phase (C_{18}) flash chromatography column (30 mm x 300 mm, 100 g). The column was equilibrated to the solvent mixture 90 % H_2O/10 % MeOH. Fractions were collected using the following solvent elution gradient: 90 % H_2O to 100% MeOH in steps of 10 % MeOH every 20 mL, the remaining material was eluted from the column as the final fraction, fraction 12 (MeOH/DCM, 1:1). All fractions were analysed by reversed phase (C_{18}) HPLC to locate the fractions that contained the peaks responsible for the observed activity. Fractions 23-1007 and 23-1008 were subsequently identified for further purification (IC_{50} 6 µg/mL).

7.6.3: Reversed Phase (C_{18}) Semi-preparative HPLC Chromatography of Fraction wjm23-1007 and wjm23-1008

Fractions 23-1007 (32.2 mg) and 23-1008 (43.6 mg) were combined in a minimum volume of MeOH. During storage at 4 °C, crystals dropped out of solution, so the fraction was filtered and the crystals (fraction 23-1007.xtl) were collected and analysed by 1D and 2D NMR spectroscopy and mass spectrometry. The purified compound trypacidin (**6.6**, 6.0 mg) was identified.

Fraction wjm23-1007-8, the supernatant, was further purified by reversed phase (C_{18}) semi-preparative HPLC chromatography (Phenomenex Luna, 5μ C18, 250 x 10mm) using a gradient solvent system of: 2 min 30 % CH_3CN/H_2O, 25min 55 % CH_3CN/H_2O, the column was equilibrated back to 30 % CH_3CN/H_2O over 5 minutes; the H_2O portion contained 0.05 % TFA (Flow rate 5 mL/min, λ = 210 nm). Seven fractions were collected as peaks eluted. Purity was confirmed by re-injection on the reversed phase (C_{18}) analytical HPLC column. Fractions wjm23-1007.1 (0.9 mg) wjm23-1007.2 (6.0 mg), wjm23-1007.3 (5.4 mg), wjm23-1007.4 (6.7 mg), wjm23-1007.5 (4.9 mg), wjm23-1007.6 (3.7 mg) and wjm23-1007.7 (3.9 mg) were analysed by ^{1}H NMR, however, only fractions three to seven were deemed to contain enough mass suitable for 2D NMR experiments. ^{1}H, ^{13}C and 2D NMR spectroscopy combined with ESI mass spectrometry were used to identify the purified compounds sulochrin-2'-*O*-methyl ether (**6.7**, 5.4 mg), asterric acid-3'-*O*-methyl ether (**6.9**, 6.7), methyl asterate-3'-*O*-methyl ether (**6.13**, 4.9 mg), methyl asterrate-4-*O*-3'-*O*-methyl ether (**6.15**, 3.7 mg) and pseurotin A (**6.16**, 2.9 mg).

REFERENCES AND NOTES

(1) Mann, J., *Chemical Aspects of Biosynthesis*; Davis, S. G., Ed.; Oxford Science Publications: Oxford, 1994; pp 1-3.

(2) Williams, D. H.; Stone, M. J.; Hauck, P. R.; Rahman, S. K., Why are secondary metabolites (natural products) biosynthesised? *J. Nat. Prod.*, **1989**, *52*, 1189-208.

(3) Sarma, A. S. D. T.; Muller, W. E. G., Secondary Metabolites from Marine Sponges. ed.; Berlin, (1993).

(4) Haefner, B., Drugs from the deep: marine natural products as drug candidates. *Drug Discovery Today*, **2003**, *8*, 536-544.

(5) Newman, D. J.; Cragg, G. M.; Snader, K. M., The influence of natural products upon drug discovery. *Nat. Prod. Rep.*, **2000**, *17*, 215-34.

(6) Kaufman, T. S.; Ruveda, E. A., The quest for quinine: Those who won the battles and those who won the war. *Angewandte Chemie, International Edition*, **2005**, *44*, 854-885.

(7) Woodward, R. B.; Doering, W. E., Total synthesis of quinine. *J. Am. Chem. Soc.*, **1945**, *67*, 860-74.

(8) Greenwood, B. M.; Bojang, K.; Whitty, C. J. M.; Targett, G. A. T., Malaria. *Lancet.*, **2005**, *365*, 1487-1498.

(9) Baldry, P. E., *The battle against bacteria: a fresh look; a history of man's fight against bacterial disease with special reference to the development of antibacterial drugs.*; Cambridge: 1976; p 1-13.

(10) Bugni, T. S.; Ireland, C. M., Marine-derived fungi: a chemically and biologically diverse group of micro-organisms. *Nat. Prod. Rep.*, **2004**, *21*, 143-163.

(11) Morin, R. B., Marvin, G., *Chemistry and biology of β-lactam antibiotics.*; New York : Academic Press: 1982; Vol. 1, pp 22-37.

(12) Levy, G. A., Neoral is superior to FK 506 in liver transplantation. *Transplant Proc.*, **1998**, *30*, 1812-1815.

(13) Elander, R. P., Industrial production of β-lactam antibiotics. *Appl. Microbiol. Biotechnol.* **2003**, *61*, 385-392.

(14) Bhat, S. V., Nagasampagi, Bhimsen A., Sivakumar, Meenakshi, Chemistry of natural products. Berlin; New York: Springer; New Delhi: Narosa Publishing House: 2005; pp 362-363.

(15) Barton, D., Sir, Comprehensive natural products chemistry. More, K., Ed., Elsevier: Amsterdam. 1999; Vol 8, pp 416-417.

(16) Blunt, J. W.; Copp, B. R.; Munro, M. H. G.; Northcote, P. T.; Prinsep, M. R., Marine natural products. *Nat. Prod. Rep.*, **2003**, *20*, 1-48.

(17) Urban, S.; Hickford, S. J. H.; Blunt, J. W.; Munro, M. H. G., Bioactive marine alkaloids. *Curr. Org. Chem.*, **2000**, *4*, 765-807.

(18) Blunt, J. W.; Copp, B. R.; Munro, M. H. G.; Northcote, P. T.; Prinsep, M. R., Marine natural products. *Nat. Prod. Rep.*, **2005**, *22*, 15-61.

(19) Blunt, J. W.; Copp, B. R.; Munro, M. H. G.; Northcote, P. T.; Prinsep, M. R., Marine natural products. *Nat. Prod. Rep.*, **2004**, *21*, 1-49.

(20) Faulkner, D. J., Marine natural products. *Nat. Prod. Rep.*, **2002**, *19*, 1-48.

(21) Faulkner, D. J., Marine natural products. *Nat. Prod. Rep.*, **2001**, *18*, 1-49.

(22) McClintock, J. B.; Baker, B. J., A review of the chemical ecology of Antarctic marine invertebrates. *American Zoologist*, **1997**, *37*, 329-342.

(23) Dietzman, G. R., *High throughput screening in drug discovery: The discovery of Bio-active substances*; Devlin, J. P., Ed.; Marcel Dekker Inc, 1997; pp 99-115

(24) Sader, H. S.; Streit, J. M.; Fritsche, T. R.; Jones, R. N., Antimicrobial activity of daptomycin against multidrug-resistant gram-positive strains collected worldwide. *Diagnostic Microbiology and Infectious Disease* **2004**, *50*, 201-204.

(25) Micklefield, J., Daptomycin structure and mechanism of action revealed. *Chemistry & Biology*, **2004**, *11*, 887-8.

(26) World Health Organisation. *Statistics by disease condition*, http://www.who.int/research/en/

(27) Sikora, K.; Advani, S.; Koroltchouk, V.; Magrath, I.; Levy, L.; Pinedo, H.; Schwartsmann, G.; Tattersall, M.; Yan, S., Essential drugs for cancer therapy: a World Health Organization consultation. *Annals of oncology: official journal of the European Society for Medical Oncology / ESMO*, **1999**, *10*, 385-90.

(28) Pauwels, B.; Korst, A. E. C.; Lardon, F.; Vermorken, J. B., Combined modality therapy of gemcitabine and radiation. *Oncologist*, **2005**, *10*, 34-51.

(29) Leszczyniecka, M.; Roberts, T.; Dent, P.; Grant, S.; Fisher, P. B., Differentiation therapy of human cancer: basic science and clinical applications. *Pharmacol. Ther.*, **2001**, *90*, 105-156.

(30) Bergmann, W.; Feeney, R. J., Marine products. XXXII. The nucelosides of sponges. I. *J. Org. Chem.*, **1951**, *16*, 981-7.

(31) Schwartsmann, G.; Brondani da Rocha, A.; Berlinck, R. G. S.; Jimeno, J., Marine organisms as a source of new anticancer agents. *Lancet Oncology*, **2001**, *2*, 221-225.

(32) UNAIDS/WHO. AIDS Epidemic Update: 2004.

(33) New Zealand Ministry of Health, AIDS NZ, *Issue 55*, Feburary 2005.

(34) De Clercq, E., Antiviral drugs in current clinical use. *Journal of Clinical Virology*, **2004**, *30*, 115-133.

(35) Watkins, B. M., Drugs for the control of parasitic diseases: current status and development. *Trends in Parasitology*, **2003**, *19*, 477-478.

(36) Ehrlich, J.; Bartz, Q. R.; Smith, R. M.; Joslyn, D. A., Chloromycetin, a new antibiotic from a soil actinomycete. *Science* (Washington, DC, United States) **1947**, *106*, 417.

(37) Wain, J.; Kidgell, C., The emergence of multidrug resistance to antimicrobial agents for the treatment of typhoid fever. *Transactions of the Royal Society of Tropical Medicine and Hygiene*, **2004**, *98*, 423-430.

(38) Wang, X.-W.; Li, J.-S.; Jin, M.; Zhen, B.; Kong, Q.-X.; Song, N.; Xiao, W.-J.; Yin, J.; Wei, W.; Wang, G.-J.; Si, B.-y.; Guo, B.-Z.; Liu, C.; Ou, G.-R.; Wang, M.-N.; Fang, T.-Y.; Chao, F.-H.; Li, J.-W., Study on the resistance of severe acute respiratory syndrome-associated coronavirus. *J. Virol. Methods*, **2005**, *126*, 171-177.

(39) *Systema Porifera: A guide to the classification of Sponges.* ed.; Hooper, J. N. A. and Van Soest, R. W. M., Eds.; Kluwer Academic/Plenum Publishers: 2002, Volumes. 1 & 2.

(40) Bewley, C. A.; Holland, N. D.; Faulkner, D. J., Two classes of metabolites from *Theonella swinhoei* are localized in distinct populations of bacterial symbionts. *Experientia*, **1996**, *52*, 716-22.

(41) Hickford, S. J. H., Chemistry Department, University of Canterbury, 2002, personal communication.

(42) Newman, D. J.; Cragg, G. M., Marine Natural Products and Related Compounds in Clinical and Advanced Preclinical Trials. *J. Nat. Prod.*, **2004**, *67*, 1216-1238.

(43) Rao, K. V.; Kasanah, N.; Wahyuono, S.; Tekwani, B. L.; Schinazi, R. F.; Hamann, M. T., Three new manzamine alkaloids from a common Indonesian sponge and their activity against infectious and tropical parasitic diseases. *J. Nat. Prod.* **2004**, *67*, 1314-1318.

(44) Gautschi, J. T.; Amagata, T.; Amagata, A.; Valeriote, F. A.; Mooberry, S. L.; Crews, P., Expanding the strategies in natural product studies of marine-derived fungi: a chemical investigation of *Penicillium* obtained from deep water sediment. *J. Nat. Prod.*, **2004**, *67*, 362-367.

(45) Oppenheimer, C. H., *Symposium on marine microbiology*. Chicago, 1963 p 769.

(46) Ravishankar, J. P.; Suryanarayanan, T. S., Influence of salinity on the activity of polyol metabolism enzymes and peroxidase in the marine fungus *Cirrenalia pygmea* (Hyphomycetes). *Indian Journal of Marine Sciences*, **1998**, *27*, 237-238.

(47) Kohlmeyer, J. K. and E., Marine Mycology: *The Higher Fungi.* Academic Press: New York, 1979.

(48) Blanchette, R. A.; Held, B. W.; Jurgens, J. A.; McNew, D. L.; Harrington, T. C.; Duncan, S. M.; Farrell, R. L., Wood-destroying soft rot fungi in the historic expedition huts of antarctica. *Appl. Environ. Microbiol.*, **2004**, *70*, 1328-1335.

(49) Grasso, S.; Bruni, V.; Maio, G., Marine fungi in Terra Nova Bay (Ross Sea, Antarctica). new microbiologica: *official journal of the Italian Society for Medical, Odontoiatric, and Clinical Microbiology (SIMMOC)*, **1997**, *20*, 371-6.

(50) Vetter, W.; Janussen, D., Halogenated Natural Products in Five Species of Antarctic Sponges: Compounds with POP-like Properties? *Environ. Sci. Technol.*, **2005**, *39*, 3889-3895.

(51) Seldes, A. M.; Deluca, M. E.; Gros, E. G.; Rovirosa, J.; San-Martin, A.; Darias, J., Steroids from aquatic organisms. XIX. New sterols from the antarctic sponge *Artemisina apollinis*., *Chem. Sci.*, **1990**, *45*, 83-6.

(52) Amsler, C. D.; Moeller, C. B.; McClintock, J. B.; Iken, K. B.; Baker, B. J., Chemical defenses against diatom fouling in Antarctic marine sponges. *Biofouling*, **2000**, *16*, 29-45.

(53) Ankisetty, S.; Amsler, C. D.; McClintock, J. B.; Baker, B. J., Further membranolide diterpenes from the Antarctic sponge *Dendrilla membranosa*. *J. Nat. Prod.*, **2004**, *67*, 1172-1174.

(54) Fontana, A.; Scognamiglio, G.; Cimino, G., Dendrinolide, a new degraded diterpenoid from the Antarctic sponge *Dendrilla membranosa*. *J. Nat. Prod.*, **1997**, *60*, 475-477.

(55) Manriquez, V.; San-Martin, A.; Rovirosa, J.; Darias, J.; Peters, K., Structure of membranolide, a diterpene from the antarctic sponge *Dendrilla membranosa*. *Acta Crystallogr, Sect C: Cryst. Struct. Commun.*, **1990**, *C46*, 2486-7.

(56) Molinski, T. F.; Faulkner, D. J., Metabolites of the antarctic sponge *Dendrilla membranosa*. *J. Org. Chem.*, **1987**, *52*, 296-8.

(57) Puliti, R.; Fontana, A.; Cimino, G.; Mattia, C. A.; Mazzarella, L., Structure of a keto derivative of 9,11-dihydrogracilin A. *Acta Crystallogr, Sect C: Cryst. Struct. Commun.* **1993**, *C49*, 1373-6.

(58) Wilkins, S. P.; Blum, A. J.; Burkepile, D. E.; Rutland, T. J.; Wierzbicki, A.; Kelly, M.; Hamann, M. T., Isolation of an antifreeze peptide from the Antarctic sponge *Homaxinella balfourensis*. *Cellular and Molecular Life Sciences*, **2002**, *59*, 2210-2215.

(59) Seldes, A. M.; Rovirosa, J.; San Martin, A.; Gros, E. G., Steroids from aquatic organisms. XII. Sterols from the Antarctic sponge *Homaxinella balfourensis* (Ridley and Dendy). *Comparative Biochemistry and Physiology, Part B: Biochemistry & Molecular Biology*, **1986**, *B83*, 841-2.

(60) Moon, B.; Baker, B. J.; McClintock, J. B., Purine and nucleoside metabolites from the Antarctic sponge *Isodictya erinacea*. *J. Nat. Prod.*, **1998**, *61*, 116-118.

(61) Moon, B.; Park, Y. C.; McClintock, J. B.; Baker, B. J., Structure and bioactivity of erebusinone, a pigment from the Antarctic sponge *Isodictya erinacea*. *Tetrahedron*, **2000**, *56*, 9057-9062.

(62) Butler, M. S.; Capon, R. J.; Lu, C. C., Psammopemmins (A-C), novel brominated 4-hydroxyindole alkaloids from an Antarctic sponge, *Psammopemma* sp. *Aust. J. Chem.*, **1992**, *45*, 1871-7.

(63) Jayatilake, G. S.; Baker, B. J.; McClintock, J. B., Rhapsamine, a cytotoxin from the Antarctic sponge *Leucetta leptorhapsis*. *Tetrahedron Lett.*, **1997**, *38*, 7507-7510.

(64) Diaz-Marrero, A. R.; Brito, I.; Dorta, E.; Cueto, M.; San-Martin, A.; Darias, J., Caminatal, an aldehyde sesterterpene with a novel carbon skeleton from the Antarctic sponge *Suberites caminatus*. *Tetrahedron Lett.*, **2003**, *44*, 5939-5942.

(65) Diaz-Marrero, A. R.; Brito, I.; Cueto, M.; San-Martin, A.; Darias, J., Suberitane network, a taxonomical marker for Antarctic sponges of the genus *Suberites*? Novel sesterterpenes from *Suberites caminatus*. *Tetrahedron Lett.*, **2004**; *45*, 4707-4710.

(66) Lee, H.-S.; Ahn, J.-W.; Lee, Y.-H.; Rho, J.-R.; Shin, J., New sesterterpenes from the Antarctic sponge *Suberites* sp. *J. Nat. Prod.*, **2004**, *67*, 672-674.

(67) Shin, J.; Seo, Y.; Rho, J.-R.; Baek, E.; Kwon, B.-M.; Jeong, T.-S.; Bok, S.-H., Suberitenones A and B: Sesterterpenoids of an unprecedented skeletal class from the Antarctic sponge *Suberites* sp. *J. Org. Chem.* **1995**, *60*, 7582-8.

(68) Ford, J.; Capon, R. J., Discorhabdin R: A new antibacterial pyrroloiminoquinone from two Latrunculiid marine sponges, *Latrunculia* sp. and *Negombata* sp. *J. Nat. Prod.*, **2000**, *63*, 1527-1528.

(69) Yang, A.; Baker, B. J.; Grimwade, J.; Leonard, A.; McClintock, J. B., Discorhabdin alkaloids from the Antarctic sponge *Latrunculia apicalis*. *J. Nat. Prod.*, **1995**, *58*, 1596-9.

(70) Jayatilake, G. S.; Baker, B. J.; McClintock, J. B., Isolation and identification of a stilbene derivative from the Antarctic sponge *Kirkpatrickia variolosa*. *J. Nat. Prod.*, **1995**, *58*, 1958-60.

(71) Perry, N. B.; Ettouati, L.; Litaudon, M.; Blunt, J. W.; Munro, M. H. G.; Parkin, S.; Hope, H., Alkaloids from the antarctic sponge *Kirkpatrickia varialosa*. Part 1: Variolin B, a new antitumor and antiviral compound. *Tetrahedron*, **1994**, *50*, 3987-92.

(72) Trimurtulu, G.; Faulkner, D. J.; Perry, N. B.; Ettouati, L.; Litaudon, M.; Blunt, J. W.; Munro, M. H. G.; Jameson, G. B., Alkaloids from the antarctic sponge *Kirkpatrickia varialosa*. Part 2: Variolin A and N(3')-methyl tetrahydrovariolin B. *Tetrahedron*, **1994**, *50*, 3993-4000.

(73) Perry, N. B.; Blunt, J. W.; McCombs, J. D.; Munro, M. H. G., Discorhabdin C, a highly cytotoxic pigment from a sponge of the genus *Latrunculia*. *J. Org. Chem.*, **1986**, *51*, 5476-8.

(74) Reyes, F.; Martin, R.; Rueda, A.; Fernandez, R.; Montalvo, D.; Gomez, C.; Sanchez-Puelles, J. M., Discorhabdins I and L, cytotoxic alkaloids from the sponge *Latrunculia brevis*. *J. Nat. Prod.*, **2004**, *67*, 463-465.

(75) Perry, N. B.; Blunt, J. W.; Munro, M. H. G.; Higa, T.; Sakai, R., Discorhabdin D, an antitumor alkaloid from the sponges *Latrunculia brevis* and *Prianos* sp. *J. Org. Chem.*, **1988**, *53*, 4127-8.

(76) Perry, N. B.; Blunt, J. W.; Munro, M. H. G., Cytotoxic pigments from New Zealand sponges of the genus *Latrunculia*: discorhabdins A, B and C. *Tetrahedron*, **1988**, *44*, 1727-34.

(77) Gunasekera, S. P.; Zuleta, I. A.; Longley, R. E.; Wright, A. E.; Pomponi, S. A., Discorhabdins S, T, and U, new cytotoxic

pyrroloiminoquinones from a deep-water Caribbean sponge of the genus *Batzella*. *J. Nat. Prod.* **2003**, *66*, 1615-1617.

(78) Antunes, E. M.; Copp, B. R.; Davies-Coleman, M. T.; Samaai, T., Pyrroloiminoquinone and related metabolites from marine sponges. *Nat. Prod. Rep.*, **2005,** 22, 62-72.

(79) Pinkert, A., Chemistry Department University of Canterbury, 2005, personal communication.

(80) Ahaidar, A.; Fernandez, D.; Perez, O.; Danelon, G.; Cuevas, C.; Manzanares, I.; Albericio, F.; Joule, J. A.; Alvarez, M., Synthesis of variolin B. *Tetrahedron Lett.*, **2003**, *44*, 6191-6194.

(81) Anderson, R. J.; Morris, J. C., Total synthesis of variolin B. *Tetrahedron Lett.*, **2001**, *42*, 8697-8699.

(82) Rinehart, K. L., Jr.; Gloer, J. B.; Hughes, R. G., Jr.; Renis, H. E.; McGovren, J. P.; Swynenberg, E. B.; Stringfellow, D. A.; Kuentzel, S. L.; Li, L. H., Didemnins: antiviral and antitumor depsipeptides from a caribbean tunicate. *Science*, **1981**, *212*, 933-5.

(83) Pettit, G. R.; Kamano, Y.; Herald, C. L.; Fujii, Y.; Kizu, H.; Boyd, M. R.; Boettner, F. E.; Doubek, D. L.; Schmidt, J. M.; et al., Antineoplastic agents. Part 247. The dolastatins. Part 18. Isolation of dolastatins 10-15 from the marine mollusc *Dolabella auricularia*. *Tetrahedron*, **1993**, *49*, 9151-70.

(84) Quinoa, E.; Adamczeski, M.; Crews, P.; Bakus, G. J., Bengamides, heterocyclic anthelmintics from a *Jaspidae* marine sponge. *J. Org. Chem.*, **1986**, *51*, 4494-7.

(85) Schwartz, R. E.; Hirsch, C. F.; Sesin, D. F.; Flor, J. E.; Chartrain, M.; Fromtling, R. E.; Harris, G. H.; Salvatore, M. J.; Liesch, J. M.; Yudin,

K., Pharmaceuticals from cultured algae. *Journal of Industrial Microbiology*, **1990**, *5*, 113-23.

(86) Trimurtulu, G.; Ohtani, I.; Patterson, G. M. L.; Moore, R. E.; Corbett, T. H.; Valeriote, F. A.; Demchik, L., Total Structures of Cryptophycins, Potent Antitumor Depsipeptides from the Blue-Green Alga *Nostoc* sp. Strain GSV 224. *J. Am. Chem. Soc.*, **1994**, *116*, 4729-37.

(87) Kobayashi, M.; Aoki, S.; Ohyabu, N.; Kurosu, M.; Wang, W.; Kitagawa, I., Arenastatin A, a potent cytotoxic depsipeptide from the Okinawan marine sponge *Dysidea arenaria*. *Tetrahedron Lett.*, **1994**, *35*, 7969-72.

(88) Mooberry, S. L.; Tien, G.; Hernandez, A. H.; Plubrukarn, A.; Davidson, B. S., Laulimalide and isolaulimalide, new paclitaxel-like microtubule-stabilizing agents. *Cancer Res.*, **1999**, *59*, 653-660.

(89) West, L. M.; Northcote, P. T.; Battershill, C. N., Peloruside A: a potent cytotoxic macrolide isolated from the New Zealand marine sponge *Mycale* sp. *J. Org. Chem.*, **2000**, *65*, 445-9.

(90) Gerwick, W. H.; Proteau, P. J.; Nagle, D. G.; Hamel, E.; Blokhin, A.; Slate, D. L., Structure of Curacin A, a Novel Antimitotic, Antiproliferative and Brine Shrimp Toxic Natural Product from the Marine Cyanobacterium *Lyngbya majuscula*. *J. Org. Chem.*, **1994**, *59*, 1243-5.

(91) Edler Michael, C.; Fernandez Annette, M.; Lassota, P.; Ireland Chris, M.; Barrows Louis, R., Inhibition of tubulin polymerization by vitilevuamide, a bicyclic marine peptide, at a site distinct from colchicine, the vinca alkaloids, and dolastatin 10. *Biochem. Pharmacol.*, **2002**, *63*, 707-15.

(92) Lindquist, N.; Fenical, W.; Van Duyne, G. D.; Clardy, J., Isolation and structure determination of diazonamides A and B, unusual cytotoxic metabolites from the marine ascidian *Diazona chinensis*. *J. Am. Chem. Soc.*, **1991**, *113*, 2303-4.

(93) Lindel, T.; Jensen, P. R.; Fenical, W.; Long, B. H.; Casazza, A. M.; Carboni, J.; Fairchild, C. R., Eleutherobin, a New Cytotoxin that Mimics Paclitaxel (Taxol) by Stabilizing Microtubules. *J. Am. Chem. Soc.*, **1997**, *119*, 8744-8745.

(94) D'Ambrosio, M.; Guerriero, A.; Pietra, F., Sarcodictyin A and sarcodictyin B, novel diterpenoidic alcohols esterified by (E)-N(1)-methylurocanic acid. Isolation from the Mediterranean stolonifer *Sarcodictyon roseum*. *Helv. Chim. Acta.*, **1987**, *70*, 2019-27.

(95) D'Ambrosio, M.; Guerriero, A.; Pietra, F., Isolation from the Mediterranean stoloniferan coral Sarcodictyon roseum of sarcodictyin C, D, E, and F, novel diterpenoidic alcohols esterified by (E)- or (Z)-N(1)-methylurocanic acid. Failure of the carbon-skeleton type as a classification criterion. *Helv. Chim. Acta.*, **1988**, *71*, 964-76.

(96) Proksch, P.; Edrada, R. A.; Ebel, R., Drugs from the seas - current status and microbiological implications. *Appl. Microbiol. Biotechnol.*, **2002**, *59*, 125-34.

(97) Long, P. F.; Dunlap, W. C.; Battershill, C. N.; Jaspars, M., Shotgun cloning and heterologous expression of the patellamide gene cluster as a strategy to achieving sustained metabolite production. *Chembiochem: a European Journal of Chemical Biology*, **2005**, *6*, 1760-5.

(98) Schmidt, E. W., From chemical structure to environmental biosynthetic pathways: navigating marine invertebrate-bacteria associations. *Trends in Biotechnology*, **2005**, *23*, 437-440.

(99) Park, B.-Y.; Min, B.-S.; Oh, S.-R.; Kim, J.-H.; Kim, T.-J.; Kim, D.-H.; Bae, K.-H.; Lee, H.-K., Isolation and anticomplement activity of compounds from *Dendropanax morbifera*. *Journal of Ethnopharmacology*, **2004**, *90*, 403-408.

(100) The complementary system plays a significant role in the host defense. The complement can be activated by a cascade mechanism of the classical pathway (CP), alternative pathway (AP), or the MBL/MASP (mannan binding lectin/MBL-associated serine protease pathway. These mechanisms control biological functions such as phagocytosis, immunomodulation. Therefore, modulation of complement activity should be useful in the therapy of inflammatory diseases.

(101) Perry, N. B.; Span, E. M.; Zidorn, C., Aciphyllal - a C34-polyacetylene from *Aciphylla scott-thomsonii* (Apiaceae). *Tetrahedron Lett.*, **2001**, *42*, 4325-4328.

(102) Sun, H. H.; Waraszkiewicz, S. M.; Erickson, K. L., C15-Halogenated compounds from the Hawaiian marine alga *Laurencia nidifica*. VI. The isomaneonenes. *Tetrahedron Lett.*, **1976**, *47*, 4227-30.

(103) Vanderah, D. J.; Schmitz, F. J., Marine natural products: isodactylyne, a halogenated acetylenic ether from the sea hare *Aplysia dactylomela*. *J. Org. Chem.*, **1976**, *41*, 3480-1.

(104) Higa, T.; Tanaka, J.; Kohagura, T.; Wauke, T., Bioactive polyacetylenes from stony corals. *Chem. Lett.*, **1990**, 145-8.

(105) Castiello, D.; Cimino, G.; De Rosa, S.; De Stefano, S.; Sodano, G., High molecular weight polyacetylenes from the nudibranch *Peltodoris atromaculata* and the sponge *Petrosia ficiformis*. *Tetrahedron Lett.*, **1980**, *21*, 5047-50.

(106) Cimino, G.; De Stefano, S., New acetylenic compounds from the sponge *Reniera fulva*. *Tetrahedron Lett.*, **1977**, 1325-8.

(107) Rotem, M.; Kashman, Y., New polyacetylenes from the sponge *Siphonochalina* sp. *Tetrahedron Lett.*, **1979**, *34*, 3193-6.

(108) Cimino, G.; Crispino, A.; De Rosa, S.; De Stefano, S.; Sodano, G., Polyacetylenes from the sponge *Petrosia ficiformis* found in dark caves. *Experientia.*, **1981**, *37*, 924-6.

(109) Ochi, M.; Ariki, S.; Tatsukawa, A.; Kotsuki, H.; Fukuyama, Y.; Shibata, K., Bioactive polyacetylenes from the marine sponge *Petrosia* sp. *Chem. Lett.*, **1994**, *1*, 89-92.

(110) Li, Y.; Ishibashi, M.; Sasaki, T.; Kobayashi, J. i., New bromine-containing unsaturated fatty acid derivatives from the Okinawan marine sponge *Xestospongia* sp. *J. Chem. Res. Synop.*, **1995**, *4*, 126-7.

(111) Dai, J.-R.; Hallock, Y. F.; Cardellina, J. H., II; Gray, G. N.; Boyd, M. R., Triangulynes A-H and triangulynic acid, new cytotoxic polyacetylenes from the marine sponge *Pellina triangulata*. *J. Nat. Prod.*, **1996**, *59*, 860-865.

(112) Kim, J. S.; Im, K. S.; Jung, J. H.; Kim, Y. L.; Kim, J.; Shim, C. J.; Lee, C. O., New bioactive polyacetylenes from the marine sponge *Petrosia* sp. *Tetrahedron*, **1998**, *54*, 3151-3158.

(113) Shin, J.; Seo, Y.; Cho, K. W.; Rho, J.-R.; Paul, V. J., Osirisynes A-F, highly oxygenated polyacetylenes from the sponge *Haliclona osiris*. *Tetrahedron*, **1998**, *54*, 8711-8720.

(114) Seo, Y.; Cho, K. W.; Rho, J.-R.; Shin, J.; Sim, C. J., Petrocortynes and petrosiacetylenes, novel polyacetylenes from a sponge of the genus *Petrosia*. *Tetrahedron*, **1998**, *54*, 447-462.

(115) Lim, Y. J.; Kim, J. S.; Im, K. S.; Jung, J. H.; Lee, C.-O.; Hong, J.; Kim, D.-k., New Cytotoxic Polyacetylenes from the Marine Sponge *Petrosia*. *J. Nat. Prod.*, **1999**, *62*, 1215-1217.

(116) Kim, J. S.; Lim, Y. J.; Im, K. S.; Jung, J. H.; Shim, C. J.; Lee, C. O.; Hong, J.; Lee, H., Cytotoxic Polyacetylenes from the Marine Sponge *Petrosia* sp. *J. Nat. Prod.*, **1999**, *62*, 554-559.

(117) Youssef, D. T. A.; Yoshida, W. Y.; Kelly, M.; Scheuer, P. J., Polyacetylenes from a Red Sea sponge *Callyspongia* species. *J. Nat. Prod.*, **2000**, *63*, 1406-1410.

(118) Aoki, S.; Matsui, K.; Tanaka, K.; Satari, R.; Kobayashi, M., Lembehyne A, a novel neuritogenic polyacetylene, from a marine sponge of *Haliclona* sp. *Tetrahedron*, **2000**, *56*, 9945-9948.

(119) Lim, Y. J.; Lee, C.-O.; Hong, J.; Kim, D.-k.; Im, K. S.; Jung, J. H., Cytotoxic polyacetylenic alcohols from the marine sponge *Petrosia* species. *J. Nat. Prod.*, **2001**, *64*, 1565-1567.

(120) Lim, Y. J.; Park, H. S.; Im, K. S.; Lee, C.-O.; Hong, J.; Lee, M.-Y.; Kim, D.-k.; Jung, J. H., Additional cytotoxic polyacetylenes from the marine sponge *Petrosia* species. *J. Nat. Prod.*, **2001**, *64*, 46-53.

(121) Nakao, Y.; Uehara, T.; Matunaga, S.; Fusetani, N.; Van Soest, R. W. M., Callyspongynic acid, a polyacetylenic acid which inhibits α-glucosidase, from the marine sponge *Callyspongia truncata*. *J. Nat. Prod.*, **2002**, *65*, 922-924.

(122) Nishimura, S.; Matsunaga, S.; Shibazaki, M.; Suzuki, K.; Harada, N.; Naoki, H.; Fusetani, N., Corticatic acids D and E, polyacetylenic geranylgeranyltransferase type I inhibitors, from the marine sponge *Petrosia corticata*. *J. Nat. Prod.*, **2002**, *65*, 1353-1356.

(123) Youssef, D. T. A.; Van Soest, R. W. M.; Fusetani, N., Callyspongamide A, a new cytotoxic polyacetylenic amide from the Red Sea sponge *Callyspongia fistularis*. *J. Nat. Prod.*, **2003**, *66*, 861-862.

(124) Lerch, M. L.; Harper, M. K.; Faulkner, D. J., Brominated polyacetylenes from the Philippines sponge *Diplastrella* sp. *J. Nat. Prod.*, **2003**, *66*, 667-670.

(125) Zhou, G.-X.; Molinski, T., Long-chain acetylenic ketones from the Micronesian sponge *Haliclona* sp. Importance of the 1-yn-3-ol group for antitumor activity. *Marine Drugs*, **2003**, *1*, 46-53.

(126) Braekman, J. C.; Daloze, D.; Devijver, C.; Dubut, D.; Van Soest, R. W. M., A new C-20 polyacetylene from the sponge *Callyspongia pseudoreticulata*. *J. Nat. Prod.*, **2003**, *66*, 871-872.

(127) Youssef, D. T. A.; Van Soest, R. W. M.; Fusetani, N., Callyspongenols A-C, new cytotoxic C22-polyacetylenic alcohols from a Red Sea sponge, *Callyspongia* species. *J. Nat. Prod.*, **2003**, *66*, 679-681.

(128) Nakao, Y.; Uehara, T.; Matsunaga, S.; Fusetani, N.; van Soest, R. W. M., Callyspongynic acid, a polyacetylenic acid which inhibits a-glucosidase, from the marine sponge *Callyspongia truncata*. [Erratum to document cited in CA137:76095]. *J. Nat. Prod.*, **2003**, *66*, 156.

(129) de Jesus, R. P.; Faulkner, D. J., Chlorinated acetylenes from the San Diego sponge *Haliclona lunisimilis*. *J. Nat. Prod.*, **2003**, *66*, 671-674.

(130) SciFinder Scholar Data Base, maintained by the Americian chemical Society, 2004 Edition.

(131) MarinLit, A database of marine natural product literature maintained by Blunt, J.W and Munro, M.H.G., Chemistry Department, University of Canterbury, 2005.

(132) Kemp, W., *Organic Spectroscopy*. ed.; Macmillan: Hong Kong: 1994; pp 152-153.

(133) Chamberlain, N. F., *The Practice of NMR Spectroscopy*. ed.; Plenum Press: New York and London, 1974; pp 75-91.

(134) Aoki, S.; Matsui, K.; Wei, H.; Murakami, N.; Kobayashi, M., Structure-activity relationship of neuritogenic spongean acetylene alcohols, lembehynes. *Tetrahedron*, **2002**, *58*, 5417-5422.

(135) Bianchi, L.; Orlandi, A.; Campione, E.; Angeloni, C.; Costanzo, A.; Spagnoli, L. G.; Chimenti, S., Topical treatment of basal cell carcinoma with tazarotene: A clinicopathological study on a large series of cases. *British Journal of Dermatology*, **2004**, *151*, 148-156.

(136) Guerriero, A.; D'Ambrosio, M.; Pietra, F.; Debitus, C.; Ribes, O., Pteridines, sterols, and indole derivatives from the lithistid sponge *Corallistes undulatus* of the Coral Sea. *J. Nat. Prod.*, **1993**, *56*, 1962-70.

(137) Cardellina, J. H., II; Meinwald, J., Leucettidine, a novel pteridine from the calcareous sponge *Leucetta microraphis*. *J. Org. Chem.* **1981**, *46*, 4782-4.

(138) Van Wagoner, R. M.; Jompa, J.; Tahir, A.; Ireland, C. M., A novel modified pterin from a *Eudistoma* species ascidian. *J. Nat. Prod.*, **2001**, *64*, 1100-1101.

(139) Inoue, S.; Okada, K.; Tanino, H.; Kakoi, H.; Ohnishi, Y.; Horii, N., New lumazines from the marine polychaete, *Odontosyllis undecimdonta*. *Chem. Lett.*, **1991**, 563-4.

(140) Pfleiderer, W.; *Tetrahedron Lett.*, **1984**, *25*, 1031.

(141) Zuleta, I. A.; Vitelli, M. L.; Baggio, R.; Garland, M. T.; Seldes, A. M.; Palermo, J. A., Novel pteridine alkaloids from the sponge *Clathria* sp. *Tetrahedron*, **2002**, *58*, 4481-4486.

(142) Nelson, M. E.; Loktionova, N.; Pegg, A. E.; Moschel, R. C., 2-Amino-O^4-benzylpteridines and O^4-benzylfolic acid: Potent inactivators of O^6-alkylguanine-DNA alkyltransferase and potential chemotherapy adjuvants. *J. Med. Chem.*, **2004**, *47*, 3887-3891.

(143) Pretch. E., B. P., Affolter. C., *Structure Determination of Organic Compounds: Tables of Spectral Data*. ed.; Springer-Verlag Berlin Heidelberg: 2000; pp 390-404.

(144) Debitus, C.; Cesario, M.; Guilhem, J.; Pascard, C.; Pais, M., Corallistine, a new polynitrogen compound from the sponge *Corallistes fulvodesmus*. *Tetrahedron Lett.*, **1989**, *30*, 1535-8.

(145) Laatsch, H., Antibase 2001: A Database for the Rapid Structure Identification of Microbial Metabolites. 2001, Wiley-VCH Verlag Berlin GmbH: Weinheim.

(146) ChemDraw Ultra, CambridgeSoft Corporation, Cambridge, USA, Version 7.0.1 Feburary 8, 2002.

(147) Devenish, S. R. A., Department of Chemistry, University of Canterbury, 2005, personal communication.

(148) Guella, G.; Mancini, I.; Zibrowius, H.; Pietra, F., Novel aplysinopsin type alkaloids from scleractinian corals of the family Dendrophylliidae of the Mediterranean and the Philippines. Configurational assignment criteria, stereospecific synthesis, and photoisomerization. *Helv. Chim. Acta.*, **1988**, *71*, 773-81.

(149) Mehta, N. B.; Diuguid, C. A. R.; Soroko, F. E., Potential anticonvulsants. 1. 5-Benzylhydantoins. *J. Med. Chem.*, **1981**, *24*, 465-8.

(150) Merritt, H. H.; Putnam, T. J. Landmark article Sept 17, 1938: *Sodium diphenyl hydantoinate in the treatment of convulsive disorders*. H. Houston Merritt and Tracy J. Putnam; United States, Feb 24, 1984; p 1062-7.

(151) Marton, J.; Enisz, J.; Hosztafi, S.; Timar, T., Preparation and fungicidal activity of 5-substituted hydantoins and their 2-thio analogs. *J. Agric. Food Chem.*, **1993**, *41*, 148-52.

(152) Harrington, P. M.; Jung, M. E., Stereoselective bromination of β-ribofuranosyl amide. Enantioselective synthesis of (+)-hydantocidin. *Tetrahedron Lett.*, **1994**, *35*, 5145-8.

(153) Tan, S. F.; Ang, K. P.; Jayachandran, H.; Fong, Y. F., Substituent effects in proton and carbon-13 nuclear magnetic resonance correlations of chemical shifts in para-substituted 5-(arylmethylene)hydantoins. *J. Chem. Soc., Perkin Transactions 2: Physical Organic Chemistry*, **1987**, *8*, 1043-5.

(154) Haruyama, H.; Takayama, T.; Kinoshita, T.; Kondo, M.; Nakajima, M.; Haneishi, T., Structural elucidation and solution conformation of the novel herbicide hydantocidin. *J. Chem. Soc., Perkin Transactions 1: Organic and Bio-Organic Chemistry*, **1991**, *7*, 1637-40.

(155) Aoki, S.; Ye, Y.; Higuchi, K.; Takashima, A.; Tanaka, Y.; Kitagawa, I.; Kobayashi, M., Novel neuronal nitric oxide synthase (nNOS) selective inhibitors, aplysinopsin-type indole alkaloids, from marine sponge *Hyrtios erecta. Chem. & Pharma. Bull.*, **2001**, *49*, 1372-1374.

(156) Guella, G.; Mancini, I.; Zibrowius, H.; Pietra, F., Aplysinopsin-type alkaloids from *Dendrophyllia* sp., a scleractinian coral of the family Dendrophylliidae of the Philippines. Facile photochemical (*Z*/*E*) photoisomerization and thermal reversal. *Helv. Chim. Acta.*, **1989**, *72*, 1444-50.

(157) Pettit, G. R.; Herald, C. L.; Leet, J. E.; Gupta, R.; Schaufelberger, D. E.; Bates, R. B.; Clewlow, P. J.; Doubek, D. L.; Manfredi, K. P.; *et al.*, Antineoplastic agents. 168. Isolation and structure of axinohydantoin. *Can. J. Chem.*, **1990**, *68*, 1621-4.

(158) Sosa, A. C. B.; Yakushijin, K.; Horne, D. A., Synthesis of Axinohydantoins. *J. Org. Chem.*, **2002**, *67*, 4498-4500.

(159) Inaba, K.; Sato, H.; Tsuda, M.; Kobayashi, J. i., Spongiacidins A-D, new bromopyrrole alkaloids from *Hymeniacidon* sponge. *J. Nat. Prod.*, **1998**, *61*, 693-695.

(160) Uemoto, H.; Tsuda, M.; Kobayashi, J. i., Mukanadins A-C, new bromopyrrole alkaloids from marine sponge *Agelas nakamurai. J. Nat. Prod.*, **1999**, *62*, 1581-1583.

(161) Chevolot, L.; Padua, S.; Ravi, B. N.; Blyth, P. C.; Scheuer, P. J., Isolation of 1-methyl-4,5-dibromopyrrole-2-carboxylic acid and its 3'-(hydantoyl)propylamide (midpacamide) from a marine sponge. *Heterocycles*, **1977**, *7*, 891-4.

(162) VanWagenen, B. C.; Larsen, R.; Cardellina, J. H., II; Randazzo, D.; Lidert, Z. C.; Swithenbank, C., Ulosantoin, a potent insecticide from the sponge *Ulosa ruetzleri*. *J. Org. Chem.*, **1993**, *58*, 335-7.

(163) Meanwell, N. A.; Roth, H. R.; Smith, E. C. R.; Wedding, D. L.; Wright, J. J. K., Diethyl 2,4-dioxoimidazolidine-5-phosphonates: Horner-Wadsworth-Emmons reagents for the mild and efficient preparation of C-5 unsaturated hydantoin derivatives. *J. Org. Chem.*, **1991**, *56*, 6897-904.

(164) Hocking, J. I. P. and A. D., Fungi and food spoilage. ed.; Blackie Academic, 1997: London, pp 489-507.

(165) Samson, R. A., Pitt, John I, Modern concepts in *Penicillium* and *Aspergillus* classification. ed.; Plenum Press: New York, pp 3-5.

(166) Kozakiewicz, Z., *Aspergillus* species on stored products. ed.; C.A.B. International, 1989: Wallingford, Oxon, UK, 1989.

(167) Smela, M. E.; Currier, S. S.; Bailey, E. A.; Essigmann, J. M., The chemistry and biology of aflatoxin B(1): from mutational spectrometry to carcinogenesis. *Carcinogenesis*, **2001**, *22*, 535-45.

(168) Moss, M. O., Risk assessment for aflatoxins in foodstuffs. *International Biodeterioration & Biodegradation*, **2002**, *50*, 137-142.

(169) Bunger, J.; Westphal, G.; Monnich, A.; Hinnendahl, B.; Hallier, E.; Muller, M., Cytotoxicity of occupationally and environmentally relevant mycotoxins. *Toxicology*, **2004**, *202*, 199-211.

(170) Cole, R. J.; Kirksey, J. W.; Dorner, J. W.; Wilson, D. M.; Johnson, J. C., Jr.; Johnson, A. N.; Bedell, D. M.; Springer, J. P.; Chexal, K. K.; *et al.*, Mycotoxins produced by *Aspergillus fumigatus* species isolated from molded silage. *J. Agric. Food Chem.*, **1977**, *25*, 826-30.

(171) Wick, E. L.; Wogan, G. N.; Asuo, T.; Buchi, G.; Abdel-Kadev, M. M.; Chang, S. B., The structures of aflatoxins B1 and G1. *J· Am. Chem. Soc*., **1965**, *87*, 882-6.

(172) Masri, M. S.; Haddon, W. F.; Lundin, R. E.; Hsieh, D. P. H., Aflatoxin Q1. Newly identified major metabolite of aflatoxin B1 in monkey liver. *J. Agric. Food Chem*., **1974**, *22*, 512-15.

(173) Holzapfel, C. W.; Steyn, P. S.; Purchase, I. F., Isolation and structure of aflatoxins M1 and M2. *Tetrahedron Lett*., **1966**, *25*, 2799-803.

(174) Diaz, S.; Dominguez, L.; Prieta, J.; Blanco, J. L.; Moreno, M. A., Application of a Diphasic Dialysis Membrane Procedure for Surveying Occurrence of Aflatoxin M1 in Commercial Milk. *J. Agric. Food Chem*., **1995**, *43*, 2678-80.

(175) Stubblefield, R. D.; Shotwell, O. L.; Shannon, G. M.; Weisleder, D.; Rohwedder, W. K., Parasiticol: new metabolite from *Aspergillus parasiticus*. *J. Agric. Food Chem*., **1970**, *18*, 391-3.

(176) Fischer, G.; Muller, T.; Ostrowski, R.; Dott, W., Mycotoxins of *Aspergillus fumigatus* in pure culture and in native bioaerosols from compost facilities. *Chemosphere*, **1999**, *38*, 1745-1755.

(177) Horak, R. M.; Vleggaar, R., Biosynthesis of verruculogen, a tremorgenic metabolite of *Penicillium verruculosum*. Stereochemical course of peroxide ring formation. *J· Chem. Soc., Chem. Commun*., **1987**, *20*, 1568-70.

(178) Brera, C.; Caputi, R.; Miraglia, M.; Iavicoli, I.; Salerno, A.; Carelli, G., Exposure assessment to mycotoxins in workplaces: aflatoxins and ochratoxin A occurrence in airborne dusts and human sera. *Microchem*., **2002**, *73*, 167-173.

(179) Scott, P. M.; Van Walbeek, W.; Kennedy, B.; Anyeti, D., Mycotoxins (ochratoxin A, citrinin, and sterigmatocystin) and toxigenic fungi in grains and other agricultural products. *J. Agric. Food Chem.*, **1972**, *20*, 1103-9.

(180) Li, Y.; Li, X.; Kim, S.-K.; Kang, J. S.; Choi, H. D.; Rho, J. R.; Son, B. W., Golmaenone, a new diketopiperazine alkaloid from the marine-derived fungus *Aspergillus* sp. *Chemical & Pharmaceutical Bulletin*, **2004**, *52*, 375-376.

(181) Lee, S. M.; Li, X. F.; Jiang, H.; Cheng, J. G.; Seong, S.; Choi, H. D.; Son, B. W., Terreusinone, a novel UV-A protecting dipyrroloquinone from the marine algicolous fungus *Aspergillus terreus*. *Tetrahedron Lett.*, **2003**, *44*, 7707-7710.

(182) Son, B. W.; Choi, J. S.; Kim, J. C.; Nam, K. W.; Kim, D.-S.; Chung, H. Y.; Kang, J. S.; Choi, H. D., Parasitenone, a new epoxycyclohexenone related to gabosine from the marine-derived fungus *Aspergillus parasiticus*. *J. Nat. Prod.*, **2002**, *65*, 794-795.

(183) Belofsky, G. N.; Jensen, P. R.; Renner, M. K.; Fenical, W., New cytotoxic sesquiterpenoid nitrobenzoyl esters from a marine isolate of the fungus *Aspergillus versicolor*. *Tetrahedron*, **1998**, *54*, 1715-1724.

(184) Capon, R. J.; Skene, C.; Stewart, M.; Ford, J.; O'Hair, R. A. J.; Williams, L.; Lacey, E.; Gill, J. H.; Heiland, K.; Friedel, T., Aspergillicins A-E: five novel depsipeptides from the marine-derived fungus *Aspergillus carneus*. *Org. & Biomol. Chem.*, **2003**, *1*, 1856-1862.

(185) Jiang, T.; Li, T.; Li, J.; Fu, H.-Z.; Pei, Y.-H.; Lin, W.-H., Cerebroside Analogues from Marine-Derived Fungus *Aspergillus flavipes*. *J. Asian Nat. Prod. Res.*, **2004**, *6*, 249-257.

(186) Tsukamoto, S.; Hirota, H.; Imachi, M.; Fujimuro, M.; Onuki, H.; Ohta, T.; Yokosawa, H., Himeic acid A: A new ubiquitin-activating enzyme inhibitor isolated from a marine-derived fungus, *Aspergillus* sp. *Bioorg. Med. Chem. Lett.*, **2005**, *15*, 191-194.

(187) Tsukamoto, S.; Miura, S.; Yamashita, Y.; Ohta, T., Aspermytin A: a new neurotrophic polyketide isolated from a marine-derived fungus of the genus *Aspergillus*. *Bioorg. Med. Chem. Lett.*, **2004**, *14*, 417-420.

(188) Hiort, J.; Maksimenka, K.; Reichert, M.; Perovic-Ottstadt, S.; Lin, W. H.; Wray, V.; Steube, K.; Schaumann, K.; Weber, H.; Proksch, P.; Ebel, R.; Mueller, W. E. G.; Bringmann, G., New natural products from the sponge-derived fungus *Aspergillus niger*. *J. Nat. Prod.*, **2004**, *67*, 1532-1543.

(189) Varoglu, M.; Crews, P., Biosynthetically diverse compounds from a saltwater culture of sponge-derived *Aspergillus niger*. *J. Nat. Prod.*, **2000**, *63*, 41-43.

(190) Lin, W.; Brauers, G.; Ebel, R.; Wray, V.; Berg, A.; Sudarsono; Proksch, P., Novel chromone derivatives from the fungus *Aspergillus versicolor* isolated from the marine sponge *Xestospongia exigua*. *J. Nat. Prod.*, **2003**, *66*, 57-61.

(191) ACDLabs 6.00, CNMR predictor, Advanced Chemistry Development Inc, Canada, 2002.

(192) Steyn, P. S.; Vleggaar, R.; Wessels, P. L.; Cole, R. J.; Scott, D. B., Structure and carbon-13 nuclear magnetic resonance assignments of versiconal acetate, versiconol acetate, and versiconol, metabolites from cultures of *Aspergillus parasiticus* treated with dichlorvos. *J. Chem. Soc. Perkin Trans. 1*, **1979**, *2*, 451-9.

(193) Holker, J. S. E.; Kagal, S. A.; Mulheirn, L. J.; White, P. M., Some new metabolites of *Aspergillus versicolo*r and a revised structure for averufin. *Chem. Commun., (London)*, **1966**, *24*, 911-13.

(194) Pusey, D. F. G.; Roberts, J. C., Mycological chemistry. XIII. Averufin, a red pigment from *Aspergillus versicolor*. *J. Chem. Soc. Abs.*, **1963**, 3542-7.

(195) Roffey, P.; Sargent, M. V.; Knight, J. A., Synthesis of some 1,3-benzodioxans and a revised structure for averufin. *J. Chem. Soc. [Section] C: Organic*, **1967**, *22*, 2328-31.

(196) Maebayashi, Y.; Horie, Y.; Yamazaki, M., Isolation of averufin dimethyl ether and 5,6-dimethoxysterigmatocystin from *Emericella foeniculicola*. *Mycotoxins*, **1985**, *21*, 36-7.

(197) Maskey, R. P.; Grun-Wollny, I.; Laatsch, H., Isolation, structure elucidation and biological activity of 8-*O*-methylaverufin and 1,8-*O*-dimethylaverantin as new antifungal agents from *Penicillium chrysogenum*. *J. Antibiot.*, **2003**, *56*, 459-463.

(198) Aucamp, P. J.; Holzapfel, C. W., Polyhydroxyanthraquinones from *Aspergillus versicolor*, *Aspergillus nidulans*, and *Bipolaris* sp. Their significance in relation to biogenetic theories on aflatoxin B1. *J. S. Afr. Chem. Inst.*, **1970**, *23*, 40-56.

(199) Castonguay, A.; Berger, Y., Synthesis of (+-)-averufanin, noraverufanin and bis-deoxyaverufanin. *Tetrahedron*, **1979**, *35*, 1557-63.

(200) Castonguay, A.; Brassard, P., C-Alkylation of 1,3-dihydroxyanthraquinones. Total synthesis of (+-)-averufin and (+-)-bipolarin. *Can. J. Chem.*, **1977**, *55*, 1324-32.

(201) Maes, C. M.; Steyn, P. S., Polyketide-derived fungal metabolites from Bipolaris sorokiniana and their significance in the biosynthesis of sterigmatocystin and aflatoxin B1. *J. Chem. Soc. Perkin Trans. 1*, **1984**, *5*, 1137-40.

(202) Beslija, S., The role of anthracyclines/anthraquinones in metastatic breast cancer. *Breast Cancer Research and Treatment*, **2003**, *81*, S25-S32.

(203) Pujol, I.; Aguilar, C.; Gene, J.; Guarro, J., In vitro antifungal susceptibility of *Alternaria* spp. and *Ulocladium* spp. *J Antimicrob Chemother*, **2000**, *46*, 337-338.

(204) Colakoglu, G., Airborne fungal spores at the Belgrad forest near the city of Istanbul (Turkey) in the year 2001 and their relation to allergic diseases. *J. Basic. Microbiol.*, **2003**, *43*, 376-84.

(205) Holler, U.; Konig, G.; Wright, A. D., A new tyrosine kinase inhibitor from a marine isolate of *Ulocladium botrytis* and new metabolites from the marine fungi *Asteromyces cruciatus* and *Varicosporina ramulosa*. *Euro. J. Org. Chem.*, **1999**, *11*, 2949-2955.

(206) Kameda, K.; Aoki, H.; Namiki, M.; Overeem, J. C., Alternative structure for botrallin, a metabolite of *Botrytis allii*. *Tetrahedron Lett.*, **1974**, *1*, 103-6.

(207) Sviridov, S. I.; Ermolinskii, B. S.; Belyakova, G. A.; Dzhavakhiya, V. G., Secondary metabolites from Ulocladium chartarum. Ulocladols A and B, novel terpenoidal phytotoxins. *Khim Prir Soedin* **1991**, (5), 642-8

(208) Ostenfeld Larsen, T.; Perry, N. B.; Andersen, B., Infectopyrone, a potential mycotoxin from *Alternaria infectoria*. *Tetrahedron Lett.*, **2003**, *44*, 4511-4513.

(209) Balan, J.; Kjaer, A.; Kovac, S.; Shapiro, R. H., The Structure of Trypacidin. *Acta. Chem. Scand.*, **1965**, *19*, 528-30.

(210) Balan, J.; Ebringer, L.; Nemec, P.; Kovac, S.; Dobias, J., Antiprotozoal antibiotics. II. Isolation and characterization of trypacidin, a new antibiotic, active against *Trypanosoma cruzi* and *Toxoplasma gondii*. *J. Antibiotics (Tokyo)*, **1963**, *16*, 157-60.

(211) Bloch, P.; Tamm, C.; Bollinger, P.; Petcher, T. J.; Weber, H. P., Pseurotin, a new metabolite of *Pseudeurotium ovalis* Stolk having an unusual hetero-spirocyclic system. *(Preliminary communication)*. *Helv. Chim. Acta.*, **1976**, *59*, 133-7.

(212) Weber, H. P.; Petcher, T. J.; Bloch, P.; Tamm, C., The crystal and molecular structure of 12,13-dibromopseurotin. *Helv. Chim. Acta.*, **1976**, *59*, 137-40.

(213) Bloch, P.; Tamm, C., Isolation and structure of pseurotin A, a microbial metabolite of *Pseudeurotium ovalis* Stolk with an unusual heterospirocyclic system. *Helv. Chim. Acta.*, **1981**, *64*, 304-15.

(214) Breitenstein, W.; Chexal, K. K.; Mohr, P.; Tamm, C., Pseurotin B, C, D, and E. Further new metabolites of *Pseudeurotium ovalis* Stolk. *Helv. Chim. Acta.*, **1981**, *64*, 379-88.

(215) Hayashi, Y.; Shoji, M.; Yamaguchi, S.; Mukaiyama, T.; Yamaguchi, J.; Kakeya, H.; Osada, H., Asymmetric Total Synthesis of Pseurotin A. *Organic Letters*, **2003**, *5*, 2287-2290.

(216) Wenke, J.; Anke, H.; Sterner, O., Pseurotin A and 8-O-demethylpseurotin A from *Aspergillus fumigatus* and their inhibitory activities on chitin synthase. *Biosci. Biotechnol. Biochem.*, **1993**, *57*, 961-4.

(217) Arison, B. H.; Wendler, N. L.; Taub, D.; Hoffsommer, R. D.; Kuo, C. H.; Slates, H. L.; Trenner, N. R., The delineation of griseofulvin and related systems by nuclear magnetic resonance spectroscopy. *J. Am. Chem. Soc.*, **1963**, *85*, 627-31.

(218) Inamori, Y.; Kato, Y.; Kubo, M.; Kamiki, T.; Takemoto, T.; Nomoto, K., Studies on metabolites produced by *Aspergillus terreus* var. *aureus*. I. Chemical structures and antimicrobial activities of metabolites isolated from culture broth. *Chem. Pharm. Bull.*, **1983**, *31*, 4543-8.

(219) Hargreaves, J.; Park, J.; Ghisalberti, E. L.; Sivasithamparam, K.; Skelton, B. W.; White, A. H., New chlorinated diphenyl ethers from an *Aspergillus* sp. *J. Nat. Prod.*, **2002**, *65*, 7-10.

(220) Shimada, A.; Shiokawa, C.; Kusano, M.; Fujioka, S.; Kimura, Y., Hydroxysulochrin, a tea pollen growth inhibitor from the fungus *Aureobasidium* sp. *Biosci. Biotechnol. Biochem.*, **2003**, *67*, 442-444.

(221) Curtis, R. F.; Hassall, C. H.; Jones, D. W.; Williams, T. W., Biosynthesis of phenols. II. Asterric acid, a metabolic product of Aspergillus terreus. *J. Chem. Soc. Abs.*, **1960**, 4838-42.

(222) Adeboya, M. O.; Edwards, R. L.; Lassoee, T.; Maitland, D. J.; Shields, L.; Whalley, A. J. S., Metabolites of the higher fungi. Part 29. Maldoxin, maldoxone, dihydromaldoxin, isodihydromaldoxin and dechlorodihydromaldoxin. A spirocyclohexadienone, a depsidone and three diphenyl ethers: key in the depsidone biosynthetic pathway from a member of the fungus genus *Xylaria*. *J. Chem. Soc., Perkin Trans. 1* **1996**, *12*, 1419-1425.

(223) Natori, S.; Nishikawa, H., Structures of osoic acids and related compounds; metabolites of *Oospora sulphurea-ochracea*. *Chem. Pharm. Bull.*, **1962**, *10*, 117-24.

(224) van der Sar, S. A., Department of Chemistry, University of Canterbury, Christchurch, 2005, personal communication.

(225) Ellis, G., Department of Chemistry, University of Canterbury, Christchurch, 2005, personal communication.